INTERACTIONS OF LUMINANCE, COLOR AND MOTION IN THE VISUAL SYSTEM

by

Eliot Robert Charles

B.S., Biology, Psychology (1984); M.S., Biology (1987)
University of Illinois, Urbana/Champaign

SUBMITTED TO THE DEPARTMENT OF BRAIN AND COGNITIVE SCIENCES IN PARTIAL FULFILLMENT OF THE REQUIREMENTS FOR THE DEGREE OF

DOCTOR OF PHILOSOPHY

at the

MASSACHUSETTS INSTITUTE OF TECHNOLOGY

February 1992

Signature of Author _____
Department of Brain and Cognitive Sciences
October 31, 1991

Certified by _____
Peter H. Schiller
Thesis Supervisor

Accepted by _____
Emilio Bizzi
Head, Department of Brain and Cognitive Sciences

INTERACTIONS OF LUMINANCE, COLOR AND MOTION IN THE VISUAL SYSTEM

by

Eliot Robert Charles

Submitted to the Department of Brain and Cognitive Sciences on October 31, 1991 in partial fulfillment of the requirements for the degree of Ph.D. in Neuroscience.

Abstract

Multiple analyses of a visual scene is a very appealing idea for the creation of a robust and reliable representation of the world. Convergent anatomical, physiological and clinical evidence suggests that the processing of visual attributes (color, motion, etc.) occurs independently using a limited or limited set of cues through extrastriate cortex and further, may be physically separate from each other either by dedicating subregions or whole visual areas for the separate analysis of each attribute. While it is clear that these areas are performing very different operations, it is possible that their functions have been underestimated. Cavanagh (1985; 1989) suggests that several of the independent channels relating to form perception need only extract two dimensional representations of the scene and that it is unlikely that processing up to the level of MT and V_4 is dedicated to this. Recent experiments also argue for a degree of anatomical and physiological convergence within visual cortex. Thus, by the time information reaches V_4 and MT it may already be integrated to represent a derived attribute (such as luminance and stereo discontinuities integrated to form an invariant representation of an edge) which undergoes higher-order analysis.

The experiments presented here are designed to challenge current notions of parallel processing in vision as well as provide evidence for integration of cues by single cells in extrastriate cortex. Using psychophysical methods in both behaving rhesus monkeys and human subjects, performance in stereoscopic depth and motion tasks were studied as a function of luminance contrast and wavelength information. As the amount of color information is increased, performance on each task improves at all luminance contrast levels. The results demonstrate that motion and depth perception are not solely reliant on luminance contrast but also have access to wavelength information. Physiological responses of cells in the lateral geniculate nucleus (LGN) and

extrastriate areas V_4 and MT were recorded in the paralyzed/anesthetized and alert monkeys respectively. The stimuli were defined by luminance, chrominance or motion or combinations of the three. The physiological experiments indicate that the activity in both magnocellular and parvocellular cells in the LGN is reduced but not abolished at isoluminance. This argues against a construct that attributes function to the magno channel based on deficits at isoluminance. It is also demonstrated that many cells in V_4 and MT are not solely reliant on wavelength and luminance information, respectively. Tuning properties of many MT cells do not change when isoluminant stimuli are used and many V_4 cells are tuned for orientation for stimuli defined by motion. These experiments show that early stages of vision exploit a variety of cues in the perception of many visual attributes. Integration of these cues occurs early in the processing of information and is essential for a rich representation of the world.

Thesis Supervisor: Peter H. Schiller
Professor of Neuroscience

Acknowledgements

First and foremost, I'd like to thank Dr. Nikos Logothetis, who contributed to this thesis in more ways than I could list. Needless to say, this thesis would not have realized without his help. I'd also like to thank my thesis advisor, Dr. Peter Schiller, for giving me the opportunity to produce this work and helping me develop many ideas.

Special gratitude to other members of my thesis committee, Dr. Patrick Cavanagh, Dr. Mriganka Sur and Dr. Richard Andersen for criticisms of this manuscript and consideration in the scheduling of the defense. I would also like to acknowledge Dr. Joe Malpeli for initiating my interest in this field and Drs. Charles Stromeyer, Tommy Poggio and Patrick Cavanagh for provoking interest in my thesis topic through their own research.

For providing the bulk of my education in the last six years, thanks to: R. Marty Bracewell, Alex Pouget, Bob Snowden, Sandeep Prasada, David and Amy Poeppel, Stephan Treue, Daphne Bavelier, Todd Holmes, Ken Moya and Dave Wilson.

Big Respect to my fellas for no intellectual discussions but the necessary 'deprogramming' sessions and global perspective: Eric, Jay, Woods, Russ, Nick and the triathlon boys from NY, Ron and Mike.

Special thanks to Jan Ellertsen, who shielded me from many of the problems of graduate student life at MIT. Thanks to my recent office mates, Ed and Kyoungmin for advice, tolerance in the final days, and taking care of my monkeys.

Lastly, I'd like to express my gratitude to my family, Anna Roe, Jong-On Hahm, and Terry Sullivan for their idealism, support and help in keeping me out of trouble.

Table of Contents

CHAPTER ONE

INTRODUCTION

Summary

Current ideas about the primate visual system suggest that much of the early processing occurs in parallel. Based predominantly on psychophysical studies using isoluminant color stimuli, it has been suggested that the M and P channels are the neural substrates for motion and color analysis, respectively. Additional psychophysical and physiological evidence do not support this viewpoint. Instead, it contends that the M and P pathways overlap in function. The experiments presented in this dissertation demonstrate that the pathways routed through MT and V_4 do not represent the physiological underpinnings of motion and color perception. Furthermore, information is integrated by the level of extrastriate cortex, creating a more robust and reliable visual system.

1.0 Introduction

Perception of a natural scene or object generally appears unified. Different attributes of an object however, are perceptually distinct in the sense that we perceive the size, shape, and color as qualitatively different properties and that these attributes are essential in the categorization of objects. Given the popular notion that these attributes are reliant on a limited set of cues (color is derived solely from wavelength information, for example) then we should be able to functionally divide these processes. There are convergent lines of evidence from psychophysics, anatomy and physiology that the primate visual system is indeed divided into several subprocesses. Perceptually distinct attributes such as color and motion however, do not appear to be organized into strictly parallel, independent channels.

2.0 Anatomy and Physiology

It has been claimed that the pathways involving different aspects of perception, most notably color and motion, are already segregated in the retina (Livingstone and Hubel, 1988; Zeki and Shipp, 1988; Shapley, 1990). These two pathways will be termed the P and M pathways for convenience and convention. Beginning with the ganglion cell layer in the retina, cells are classified by morphology, physiological properties, and projection zones (for a review, see Stone *et al.*,1979; Rodieck, 1979; Lennie, 1980; Shapley and Perry, 1986). The next stage of processing, the lateral geniculate nucleus (LGN), consists of two subdivisions whose cells reflect the physiological properties of

the ganglion cells in the retina, the parvocellular (pLGN) and magnocellular LGN (mLGN) layers. The pLGN contains a majority of cells that have color-opponent receptive fields whereas the mLGN cells do not have many color-selective receptive fields and as a result have been termed 'color-blind' (Ramachandran and Gregory, 1978; Livingstone and Hubel, 1987b). This assumption however, proves to be false as cells in both the mLGN (Schiller and Colby, 1983; Schiller *et al.*, 1990c) and the retinal ganglion cells projecting to this region (Lee *et al.*, 1988; 1989) respond to isoluminant stimuli. Lesions of the pLGN reveal that this region is essential for color perception and visual functions involving high spatial or low temporal frequency luminance information (Merigan, 1989; Schiller *et al.*, 1990a, 1990b). Magnocellular LGN lesions on the other hand produce deficits in motion perception and visual capacities requiring low spatial and high temporal frequency luminance information (Schiller *et al.*, 1990a, 1990b; Merigan and Maunsell, 1990). Either division has the capacity to process brightness, shape and stereoscopic depth information at low spatial frequencies (Schiller *et al.*, 1990a, 1990b) leading to the conclusion that early stages of the M and P pathways represent two systems that have considerable overlap in terms of function (Schiller and Logothetis, 1990).

Continuation and divergence of these two pathways in cortex have been revealed largely by physiological recordings in conjunction with cytochrome oxidase staining (Livingstone and Hubel, 1984). In V_1, densely staining cytochrome oxidase regions termed 'blobs' receive inputs from pLGN via $4C_\beta$

and possibly mLGN via $4C_{\alpha}$ (refer to figure 1.1). Cytochrome oxidase-poor regions, the interblobs, also receive inputs from the pLGN via $4C_{\beta}$. In addition, the magnocellular pathway continues predominantly in layer 4B of V_1 (Lund, 1973; Lund and Boothe, 1975). The blobs, interblobs, and layer 4B are claimed to be stages within pathways that separately process color, form, and motion and stereo information, respectively. The main evidence for this comes predominantly from single unit recordings in striate cortex, revealing that cells in each of these areas have different response characteristics (Livingstone and Hubel, 1984). Several investigators report that cells within the blob region are selective for color and that the majority of interblob cells are not (Livingstone and Hubel, 1984; Michael, 1987; Ts'o and Gilbert, 1988). Based on these collective findings it has been proposed that the unoriented blob cells (and all cells in the associated column) are responsible for the processing of color information. The oriented, non-wavelength selective interblob cells process form information. Finally, cells in 4B are believed to be processing motion since many of these cells are selective for direction of movement and are tuned for disparity (Dow, 1974; Livingstone and Hubel, 1984). Segregation of the M and P pathways is not complete, however (Lund and Boothe, 1975; Fitzpatrick *et al.*, 1985). Malpeli *et al.* (1981) find that subpopulations of both simple and complex cells receive inputs from both mLGN and pLGN, demonstrating convergence of these two pathways at the first stage of cortical processing.

Continuation of these subdivisions is seen in the extrastriate visual areas. Cytochrome oxidase 'thick stripes' in V_2 receive projections from layer 4B

(Livingstone and Hubel, 1987a) and project to area MT. Recording from cells in the thick stripes reveal that they are orientation selective and the majority are also selective for binocular disparity (Hubel and Livingstone, 1987). Densely staining 'thin stripes' in V_2 receive projections from the blobs and project to V_4 (Shipp and Zeki, 1985; DeYoe and Van Essen, 1985). Many of the cells in this area show color opponency and it is believed that none are orientation selective. The V_2 'pale stripes' receive input from the interblobs yet it is unclear where the next stage of processing occurs. These cells are also orientation selective and many are also end-stopped (Hubel and Livingstone, 1987). DeYoe and Van Essen (1985) in contrast, also report that some cells in the thin and interstripes are direction or orientation selective and some cells in the thick stripes are color selective, suggesting that segregation in V_2 may not be entirely complete.

At the next stages of the M and P pathways, MT and V_4, the two systems project to separate cortical areas leading to the parietal and temporal lobes (Ungerleider and Mishkin, 1982; Desimone and Ungerleider, 1989). With the divergence of theses two streams came the suspicion that MT and V_4 were specialized for analyzing different aspects of perception. Many studies implicate MT as being a significant area for the perception of motion. Dubner and Zeki (1971) first reported that cells in MT are selective for direction of motion which has been demonstrated many times since (Zeki, 1974a; Van Essen *et al.*, 1981; Baker *et al.*, 1981; Albright *et al.*, 1984; Felleman and Kaas, 1984; Mikami *et al.*, 1986; Saito *et al.*, 1986). Several laboratories also report

that cells in MT are tuned to a range of velocities of the stimulus (Baker *et al.*, 1981; Maunsell and Van Essen, 1983a; Felleman and Kaas, 1984; Mikami *et al.*, 1986; Rodman and Albright, 1987). In addition, when stimuli are presented beyond the classical receptive field, direction and velocity specific responses can also be elicited from surrounds of cells that are antagonistic to the responses in the classical receptive fields (Allman *et al.*, 1985; Tanaka *et al.*, 1986). Movshon *et al.* (1986) further implicated MT as an area specialized for motion by revealing a subpopulation of cells in MT that can respond to complex forms of motion which cells in V_1 are incapable of signalling. While cells in MT do respond to many components of motion, they have been found to be relatively unselective for stimulus form and wavelength (Albright *et al.*, 1984; Zeki, 1974a; Maunsell and Van Essen, 1983a).

Lesion studies confirm the hypothesis, put forward by physiological studies, that MT is involved in motion perception. Monkeys with ibotenic acid lesions have elevated thresholds for direction discrimination (Newsome and Pare, 1988) and detection of shearing motion and structure from motion (Andersen and Siegel, 1990) in dynamic random dot displays. Lastly, removal of the floor and banks of the superior temporal sulcus have only slight effects on pattern discrimination and no discernible effects on hue discrimination (Heywood and Cowey, 1987).

Pioneering studies in the extrastriate area V_4, Zeki proposed that this area is specialized for the analysis of color information (Zeki, 1973; Zeki, 1977). In his initial study, Zeki reports that every cell that he encountered in V_4 is

color coded. Some cells respond whenever the appropriate wavelength is used while others also require specific shapes or orientations. The percentage of color cells reported in V_4 has since decreased and remains controversial (Desimone *et al.*, 1985; Van Essen, 1985) but most agree that a majority of cells are wavelength selective: Schein *et al.* (1982) do report initially that only about 20 percent of the cells in V_4 are color-biased or color-opponent but later (Desimone *et al.*, 1985) this number increased to a "vast majority" or about two-thirds (Schein and Desimone, 1990).

In disagreement with the notion that V_4 is specialized for color analysis, several investigators indicate that V_4 also carries information about orientation and shape (Zeki, 1973; Desimone *et al*, 1985; Logothetis *et al.*, 1987; Desimone and Schein, 1987). Another indication that V_4 may be part of the form pathway is that one of the major outputs of V_4, inferotemporal cortex, contains many cells that selectively respond to complex patterns and faces (Richmond *et al.*, 1987; Gross *et al.*, 1972; Perrett *et al.*, 1982). Heywood and Cowey (1987) report elevated hue discrimination thresholds in V_4 lesioned animals and, in addition, also find that pattern and orientation discrimination is impaired. Our laboratory (Schiller *et al.*, 1988; Schiller and Logothetis, 1990) also find that color and form perception are impaired with V_4 lesions. When using identical stimuli however, parvocellular LGN lesions produce much more severe deficits in color discrimination than the V_4 lesions. This indicates that V_4 is not the only recipient of color information from the pLGN; other unidentified areas must be participating in color perception.

Other studies indicate that V_4 is involved in higher-order processes that are not directly tied to stimulus attributes. Several studies reveal that cells in V_4 are modulated by the attentional state of the animal in various behavioral tasks using visual stimuli (Mountcastle *et al.*, 1987; Spitzer *et al.*, 1988; Haenny and Schiller, 1988) and for visual and tactile stimuli (Haenny *et al.*, 1988). Lesion studies also indicate that complex processing occurs in this area. Weber and Fischer (1990) implicate V_4 in attention processes by showing that ibotenic lesions of V_4 affect saccadic latency. Moreover, Schiller and Lee (1991) argue that this area is involved in a form of learning, relating to patterns and relationships of objects across the visual field.

Furthermore, Desimone and Schein (1987) find that a fraction of the cells are direction selective, casting more doubt that this area is solely dedicated to processing color information. This may not be too surprising as connections between V_4 and MT have been demonstrated anatomically (Rockland and Pandya, 1979; Maunsell and Van Essen, 1983c; Ungerleider and Desimone, 1986). Physiologically, by inactivating parvo- and magnocellular LGN and recording from cells in V_4, Ferrera *et al.* (1990) find that V_4 receives substantial inputs from both pLGN and mLGN. Thus, because it receives M pathway input, V_4 cannot be considered to be representing the P pathway at the level of extrastriate cortex.

3.0 Psychophysics

Recently, psychophysicists have used isoluminant color stimuli, whose

contrast varies as a function of chrominance and not luminance, to test for independent processing of depth and stereopsis and color. An extensive review of the perceptual deficits at isoluminance can be found in Livingstone and Hubel (1987b). Basically, several aspects of perception are degraded under isoluminant conditions. Because no luminance information is available, deficits in perception must be due to the inability to use color information. Operating on the assumption that the 'color-blind' M pathway is inactive at isoluminance, perceptual functions that are degraded at isoluminance have been attributed to the M pathway. Lu and Fender (1972) report that stimuli defined by wavelength information cannot support the perception of depth. The results for figural and random dot stereograms are supported by others (Ramachandran *et al.* 1973; Comerford, 1974; Gregory, 1977; de Weert, 1979; de Weert and Sadza, 1983). Similarly, Ramachandran and Gregory (1978) report that motion perception is degraded under isoluminant conditions.

As discussed previously, cells in the mLGN are not silenced at isoluminance, making it difficult to assign function to the M pathway with the isoluminance arguments. Additional psychophysical evidence challenges the notion of segregated color and motion processing. Cavanagh *et al.* (1985) refined the work of Ramachandran and Gregory (1978) and found that the perception of motion is possible at isoluminance but over a narrower range of parameters than for a high luminance contrast. Thus, both luminance and chrominance can be analyzed in the perception of motion though color may provide only a weak input. Others have also found a color contribution to

motion perception (Papathomas *et al.,* 1989; Cavanagh and Anstis, 1991). Krauskopf and Farell (1991) find that when drifting isoluminant gratings are modulated along different cardinal directions, the gratings slip across each other. If however, the modulations are rotated by 45 degrees in color space the gratings cohere even though they are dissimilar in terms of hue. They interpret these results as evidence for separate mechanisms of motion analysis for each of the cardinal directions of color space. In addition, Stromeyer *et al.* (1990) measured thresholds for direction of motion of sinusoidal gratings. Like Krauskopf and Farell (1991), the stimuli were designed to modulate the activity of long and middle wavelength sensitive cones. For velocities up to 9 degrees/second, thresholds for chrominance modulation were lower than luminance modulation when both are expressed in the cone contrast metric. Thus, the motion system is more sensitive to a spectrally-opponent mechanism at low velocities.

Others have also found interdependence between color, motion, form and stereopsis: Ramachandran (1988) demonstrated that shape from shading information can be used to support motion perception. Lee (1970), and later Halpern (1991) used random dot displays to suggest that motion information can be used to feed stereoscopic depth processes. Monocularly, each display had a defined region in which the dots were moving and the edges of these regions are visible. When viewed binocularly the static images were uncorrelated and no depth is perceived. If the moving regions were horizontally displaced with respect to each other depth was perceived. Thus,

edge information is extracted from the motion cue and used to generate stereoscopic depth perception.

Many of the isoluminance experiments have only tested whether or not color can support motion or depth as opposed to simply providing an input. In many cases, the stimulus conditions determine whether or not specific aspects of perception are present at isoluminance. As a result, opposite conclusions have been reached regarding the segregation of color, motion and depth. By varying the amount of wavelength information in fixed luminance contrast stimuli, the relation between chrominance information and motion or depth may be demonstrated. Unfortunately, while psychophysics indicates that color does contribute to motion and depth under specific conditions, it is difficult to ascertain whether this contribution is carried by the M or P pathways or both.

4.0 Cortical Integration/Multiple Cue Hypothesis

The notion of separate parallel channels is an attractive idea for both physiology and computational vision. It allows us to divide vision into several subprocesses and treat each one independently. Unfortunately, while much has been invested into demonstrating that parallel processing exists, the preceding evidence indicates that the processing of color and motion are neither completely segregated nor do they likely correspond to the P and M pathways respectively. Furthermore, there are many criticisms of this segregation hypothesis. For example, these studies have revealed very little about the operations within a channel. Finding cells within the pLGN/V_4 pathway

responsive to stimuli with wavelength information reveals very little about how we recover the reflectance of a surface let alone what operations these cells are performing. Yet, functions such as color analysis have been proposed to be in a one to one relationship to cortical areas, subregions of an area, down to different classes of ganglion cells in the retina based simply a the cells' ability to discriminate wavelength differences. Whereas wavelength discrimination is necessary for color perception, it is not sufficient. Moreover, the issue of how we achieve a unified percept combining many aspects of perception is not addressed in the multiple map scheme. If one assumes separate, parallel processing, integration is necessarily ascribed to higher level areas where there will be convergence from these maps. In essence, concepts of parallel processing within early vision have been advanced to a point where considerable constraints have been imposed on theories of color perception and integration.

Computational vision (Marr, 1980; Gamble and Poggio, 1987; Poggio *et al.*, 1988; Bulthoff and Mallot, 1988) and psychophysics (Cavanagh, 1985; 1989) both recognize the advantage of cue integration. Consider the identification of edges, which is important for most early vision processes. Detection of a discontinuity may be difficult in one domain, yet relatively easy in another. For example, spectral information is more reliably linked to material changes in objects than luminance information (Rubin and Richards, 1981). Highlights, shading from surface orientation changes, and shadows will all produce changes in the luminance profile that do not correspond to material changes. If

there is cross-talk between modules, sparse or noisy data can be linked to other information to more reliably estimate discontinuities from the image data. Cavanagh argues that separate analyses need only extract two dimensional information of local size and orientation in each domain. The advantage being that the representation within each domain can be coded in the same way, providing a standardized image description. These modules may then be combined to form an invariant representation which can undergo higher-order processing. This makes the processing less dependent on the nature of the image data. Multiple cue integration makes the assumption that there are types of higher-order processing that are not dependent on the cue type. This, however, does not mean that each cue will be equally effective, as previous isoluminance experiments have demonstrated.

Recent examples from machine vision demonstrate that integration of different aspects of vision (i.e. color, stereo, motion, etc.) have been useful in the segmentation problem (Gamble and Poggio, 1987; Poggio *et al.*, 1988). By coupling Markov Random Fields corresponding to these different aspects, the investigators were able to segment an image quickly and reliably and also fill in regions where only sparse information exists. Bulthoff and Mallot (1988) describe the rules governing integration of cue types in the perception of depth. Using conflicting or cooperatively acting cues, they found that the various cues for depth have different strengths and are restricted in how they may be combined to enhance the perception of depth. For example, depth information from shading cannot support stereopsis by itself but can enhance the

perception of depth when combined with other cues. This facilitation demonstrates that different depth cues are integrated prior to depth perception in a nonlinear manner.

5.0 Goals of the Thesis

In order to establish a relationship between perceptually distinct aspects of vision and identified neural pathways one must combine psychophysics and physiology. Techniques developed in our laboratory allow testing both in humans and in trained behaving rhesus monkeys. Once a correlation, if any, is established, we can examine the neural responses within these identified pathways and compare them with the psychophysical results. Because psychophysical studies depend almost exclusively on data obtained from human subjects, it is very important to collect behavioral data from rhesus monkeys since single-unit physiology relies on animal models.

Based on the preceding evidence, specific predictions can now be made about the nature of early visual information processing. If the processing of individual attributes operates independently throughout the M and P pathways, color information should have little effect on cells within the M pathway. If cells within this pathway are not responsive to color information and are solely responsible for processing motion information, the perception of motion should be absent when using isoluminance color stimuli. Similarly, motion should not be a very effective cue for cells in the P pathway. If on the other hand, reliable two dimensional representations of the visual world can be

extracted by combinations of visual cues, then one might expect that the motion pathway, for instance, to be capable of responding to pure chromatic stimuli. If these cues are extracted and then integrated to form an invariant representation, motion and depth perception should be supported by using isoluminant color stimuli.

The experiments presented here are designed to challenge concepts of segregation and integration within the visual system. Psychophysical results are presented here for the role of color in stereoscopic depth and motion detection and discrimination tasks in humans and monkeys. Wavelength information was varied over a range of fixed luminance contrast values including isoluminance. In addition, physiological results are presented for the most anatomically and physiologically distinct stations within the proposed segregated pathways: pLGN, mLGN, V_4 and MT. This allows not only a comparison between the M and P pathways but also between early and later stages, where the pathways are believed to be more closely tied to function. Prior to the physiology experiments, behavioral isoluminance was established for each animal. The color space used in these experiments permit the comparison of color and luminance stimuli by defining them in terms of cone modulations. In an additional set of experiments, stimuli defined by motion are tested in V_4 to see if motion cues can be used by cells in this area.

REFERENCES

Albright, T.D., Desimone, R., and Gross, C.G. Columnar organization of directionally selective cells in visual area MT of the macaque. Journal of Neurophysiology 51:16-31, 1984.

Allman, J., Miezin, F., and McGuinness, E. Direction- and velocity-specific responses from beyond the classical receptive field in the middle temporal visual area (MT). Perception 14:105-126, 1985.

Andersen, R.A. and Siegel, R.M. "Motion processing in primate cortex." In: Signal and Sense: Local and Global Order in Perceptual Maps, eds. G.M. Edelman, W.E. Gall, and W.M. Cowan. Wiley, New York (1990).

Baker, J.F., Petersen, S.E., Newsome, W.T., and Allman, J.M. Visual response properties of neurons in four extrastriate visual areas of the owl monkey (*aotus trivirgatus*): A quantitative comparison of medial, dorsomedial, dorsolateral, and middle temporal areas. Journal of Neurophysiology 45:397-416, 1981.

Bulthoff, H.H. and Mallot, H.A. Integration of depth modules: Stereo and shading. Journal of the Optical Society of America A 5:1749-1758, 1988.

Cavanagh, P. "Local log polar frequency analysis in the striate cortex." In: Models of the Visual Cortex, eds D. Rose and V.G. Dobson, pp. 85-95. Wiley, New York, 1985.

Cavanagh, P. "Multiple analyses of orientation in the visual system." In: Neural Mechanisms of Visual Perception, eds D.M.K. Lam and C.D. Gilbert. Gulf Publishers, Houston, 1989.

Cavanagh, P. and Anstis, S. The contribution of color to motion in normal and color-deficient observers. Vision Research, in press (1991).

Cavanagh, P., Boeglin, J. and Favreau, O.E. Perception of motion in equiluminous kinematograms. Perception, 14:151-162, 1985.

Cavanagh, P., Tyler, C.W. and Favreau, O.E. Perceived velocity of moving chromatic gratings. Journal of the Optical Society of America, A, 1:893-899, 1984.

Comerford, J.P. Stereopsis with chromatic contours. Vision Research 14:975-982, 1974.

de Weert, C.M.M. Colour contours and stereopsis. Vision Research

19:555-564, 1979.

de Weert, C.M.M. and Sadza, K.J. "New data concerning the contribution of colour differences to stereopsis." In: Colour vision, ed. J.D. Mollon. Academy Press, London, pp. 553-562, 1983.

Desimone, R., and Schein, S.J. Visual properties of neurons in area V_4 of the macaque: Sensitivity to stimulus form. Journal of Neurophysiology 57:835-868, 1987.

Desimone, R., Schein, S.J., Moran, J., and Ungerleider, L.G. Contour, color and shape analysis beyond the striate cortex. Vision Research 25:441-452, 1985.

Desimone, R. and Ungerleider, L.G. Neural mechanisms of visual processing. In: Handbook of Neuropsychology, Vol. 2., eds F. Boller and J. Grafman. Elsevier Science Publishers (1989).

DeYoe, E.A. & Van Essen, D.C. Segregation of efferent connections and receptive field properties in the visual area V_2 of the macaque. Nature, 317:58-60, 1985.

Dow, B.M. Functional classes of cells and their laminar distribution in monkey visual cortex. Journal of Neurophysiology 37:927-946, 1974.

Dubner, R. and Zeki, S.M. Response properties and receptive fields of cells in an anatomically defined region of the superior temporal sulcus. Brain Research, 35:528-532, 1971.

Felleman, D.J. and Kaas, J.H. Receptive-field properties of neurons in middle temporal visual area (MT) of owl monkeys. Journal of Neurophysiology 52:488-513, 1984.

Ferrera, V.P., Nealy, T.A., and Maunsell, J.H.R. Magnocellular and parvocellular inputs to macaque area V_4. Investigative Ophthalmology and Visual Science Supplement 32:1117, 1991.

Fitzpatrick, D., Itoh, K., and Diamond, I.T. The laminar organization of the lateral geniculate body and the striate cortex in the squirrel monkey (*Saimiri scieurus*). Journal of Neuroscience 3:673-702, 1983.

Gamble, E. and Poggio, T. Visual integration and detection of discontinuities: The key role of intensity edges. A.I. Memo No. 970, Massachusetts Institute of Technology, 1987.

Gregory, R.L. Vision with isoluminant colour contrast: 1. A projection

technique and observations. Perception 6:113-119, 1977.

Gross, C.G., Rocha-Miranda, C.E., and Bender, D.B. Visual properties of neurons in inferotemporal cortex of the macaque. Journal of Neurophysiology 35:96-111, 1972.

Haenny, P.E., Maunsell, J.H.R. and Schiller, P.H. State dependent activity in monkey visual cortex. II. Retinal and extraretinal factors in V4. Experimental Brain Research 69:245-269, 1988.

Haenny, P.E. and Schiller, P.H. State dependent activity in monkey visual cortex. I. Single cell activity in V1 and V4. Experimental Brain Research 69:225-244, 1988.

Halpern, D.L. Stereopsis from motion-defined contours. Vision Research 31:1611-1617, 1991.

Heywood, C.A. and Cowey, A. On the role of cortical area V_4 in the discrimination of hue and pattern in macaque monkeys. Journal of Neuroscience 7:2601-2617, 1987.

Hubel, D.H. and Livingstone, M.L. Segregation of form, color, and stereopsis in primate area 18. Journal of Neuroscience 7:3378-3415, 1987.

Krauskopf, J. and Farell, B. Influence of colour on the perception of coherent motion. Nature 348:328-331, 1991.

Lee, B.B., Martin, P.R. and Valberg, A. The physiological basis of heterochromatic flicker photometry demonstrated in the ganglion cells of the macaque retina. Journal of Physiology (London) 404:323-347, 1988.

Lee, B.B., Martin, P.R. and Valberg, A. Nonlinear summation of M- and L-cone inputs to phasic retinal ganglion cells of the macaque. Journal of Neuroscience 9:1433-1442, 1989.

Lee, D.N. Binocular stereopsis without spatial disparity. Perception and Psychophysics 9:216-218, 1970.

Lennie, P. Parallel visual pathways: A review. Vision Research 20:561-594, 1980.

Livingstone, M.S. and Hubel, D.H. Anatomy and physiology of a color system in the primate visual cortex. Journal of Neuroscience 4:309-356, 1984.

Livingstone, M.S. and Hubel, D.H. Connections between layer 4B of area 17 and the thick cytochrome oxidase stripes of area 18 in the squirrel monkey. Journal of Neuroscience 7:3371-3377, 1987a.

Livingstone, M.S. and Hubel, D.H. Psychophysical evidence for separate channels for the perception of form, color, movement, and depth. Journal of Neuroscience 7:3416-3468, 1987b.

Livingstone, M. and Hubel, D. Segregation of form, color, movement, and depth: Anatomy, physiology, and perception. Science 240:740-749, 1988.

Logothetis, N.K., Voegels, R., and Schiller, P.H. Neuronal activity in V_1, V_2, and V_4 in Macaque Monkey Performing a Visual Matching Task. Society of Neuroscience Abstracts 13:624, 1987.

Lu, C. and Fender, D.H. The interaction of color and luminance in stereoscopic vision. Investigative Ophthalmology 11:482-490, 1972.

Lund, J.S. Organization of neurons in the visual cortex, area 17, of the monkey (*Macaca mulatta*). Journal of Comparative Neurology 147:455-475, 1973.

Lund, J.S. and Boothe, R.G. Interlaminar connections and pyramidal neuron organization in the visual cortex, area 17, of the macaque monkey. Journal of Comparative Neurology 159:305-334, 1975.

Malpeli, J.G., Schiller, P.H. and Colby, C.L. Response properties of single cells in monkey striate cortex during reversible inactivation of individual lateral geniculate laminae. Journal of Neurophysiology 46:1102-1119, 1981.

Marr, D. Vision. W.H. Freeman and Company, New York (1980).

Maunsell, J.H.R. and Van Essen, D.C. Functional properties of neurons in middle temporal visual area of the macaque monkey. I. Selectivity for stimulus direction, speed, and orientation. Journal of Neurophysiology 49:1127-1147, 1983a.

Maunsell, J.H.R. and Van Essen, D.C. The connections of the middle temporal visual area (MT) and their relationship to a cortical hierarchy in the macaque monkey. Journal of Neuroscience 3:2563-2586, 1983c.

Merigan, W.H. Chromatic and achromatic vision of macaques: Role of the P pathway. Journal of Neuroscience 9:776-783, 1989.

Merigan, W.H. and Maunsell, J.H.R. Macaque vision after magnocellular

lateral geniculate lesions. Visual Neuroscience 5:347-352, 1990.

Michael, C.R. Comparative studies of the color cells in layer IVC_b and in the blobs of the monkey's striate cortex. Society of Neuroscience Abstracts 13:2, 1987.

Mikami, A., Newsome, W.T., and Wurtz, R.H. Motion selectivity in macaque visual cortex. I. Mechanisms of direction and speed selectivity in extrastriate area MT. Journal of Neurophysiology 55:1308-1327, 1986.

Mountcastle, V.B., Motter, B.C., Steinmetz, M.A. and Sestokas, A.K. Common and differential effects of attentive fixation on the excitability of parietal and prestriate (V_4) cortical visual neurons in the macaque monkey. Journal of Neuroscience 7:2239-2255, 1987.

Movshon, J.A., Adelson, E.H., Gizzi, M.S., and Newsome, W.T. "The analysis of moving visual patterns." In: Pattern Recognition Mechanisms, eds. C. Chagas, R. Gattass, and G. Gross. Springer-Verlag, New York, pp. 117-151, 1986.

Newsome, W.T. and Pare, E.B. A selective impairment of motion perception following lesions of the middle temporal visual area (MT). Journal of Neuroscience 8:2201-2211, 1988.

Papathomas, T.V., Gorea, A. and Julesz, B. The strength of color and luminance in eliciting motion perception. Investigative Ophthalmology and Visual Science Supplement 30:388, 1989.

Perrett, D.I., Rolls, E.T., and Caan, W. Visual neurons responsive to faces in the monkey temporal cortex. Experimental Brain Research 47:329-342, 1982.

Poggio, T., Gamble, E.B. and Little, J.J. Parallel integration of vision modules. Science 242:436-440, 1988.

Poggio, T., Torre, V. and Koch, C. Computational vision and regularization theory. Nature 317:314-319, 1985.

Ramachandran, V.S. Perception of shape from shading. Nature 331:163-166, 1988.

Ramachandran, V. and Gregory, R. Does colour provide an input to human motion perception? Nature, 275:55-56, 1978.

Ramachandran, V.S., Madhusudran, R.V., and Vidysagar, T.R. The role

of contours in stereopsis. Nature 242:412-414, 1973.

Richmond, B.J., Optican, L.M., Podell, M., and Spitzer, H. Temporal encoding of two-dimensional patterns by single units in primate inferior temporal cortex. I. Response characteristics. Journal of Neurophysiology 57:132-146, 1987.

Rockland, K.S. and Pandya, D.N. Laminar origins and terminations of cortical connections of the occipital lobe in the rhesus monkey. Brain Research 179:3-20, 1979.

Rodieck, R.W. Visual pathways. Annual Review of Neuroscience 2:193-225, 1979.

Rodman, H.R. and Albright, T.D. Coding of visual stimulus velocity in area MT of the macaque monkey. Vision Research 27:2035-2048, 1987.

Rubin, J.M. and Richards, W.A. Color vision and image intensities: When are changes material? A. I. Memo No. 631, Massachusetts Institute of Technology, 1981.

Saito, H., Yukie, M., Tanaka, K., Hikosaka, K., and Iwai, E. Integration of direction signals of image motion in the superior temporal sulcus of the macaque monkey. Journal of Neuroscience 6:145-157, 1986.

Schein, S.J. and Desimone, R. Spectral properties of V_4 neurons in the macaque. Journal of Neuroscience 10:3369-3389, 1990.

Schein, S.J., Marrocco, R.T., and De Monasterio, F.M. Is there a high concentration of color-selective cells in area V_4 of monkey visual cortex? Journal of Neurophysiology 47:193-213, 1982.

Schiller, P.H., Charles, E.R. and Logothetis, N.K. The effect of V_4 and parvocellular lesions on primate vision. Investigative Ophthalmology and Visual Science Supplement 29:328, 1988.

Schiller, P.H. and Colby, C.L. The responses of single cells in the lateral geniculate nucleus of the rhesus monkey to color and luminance contrast. Vision Research 23:1631-1641, 1983.

Schiller, P.H. and Lee, K. The role of the primate extrastriate area V_4 in vision. Science 251:1251-1253, 1991.

Schiller, P.H. and Logothetis, N.K. The color-opponent and broad-band channels of the primate visual system. Trends in Neuroscience 13:392-398, 1990.

Schiller, P.H., Logothetis, N.K. and Charles, E.R. Functions of the colour-opponent and broad-band channels of the visual system. Nature 343:68-70, 1990a.

Schiller, P.H., Logothetis, N.K. and Charles, E.R. Role of the color-opponent and broad-band channels in vision. Visual Neuroscience 5:321-346, 1990b.

Schiller, P.H., Logothetis, N.K., Charles, E.R. and Hurlbert, A.C. Perceptual deficits and the activity of the color-opponent and broad-band pathways at isoluminance. Science 247:214-217, 1990c.

Shapley, R. Visual sensitivity and parallel retinocortical channels. Annual Review of Psychology, 41:635-658, 1990.

Shapely, R. and Perry, V.H. Cat and monkey retinal ganglion cells and their visual functional roles. Trends In Neuroscience 9:229-235, 1986.

Shipp, S. and Zeki, S. Segregation of pathways leading from area V_2 to areas V_4 and V_5 of macaque monkey visual cortex. Nature 315:322-325, 1985.

Spitzer, H., Desimone, R. and Moran, J. Increased attention enhances both behavioral and neuronal performance. Science 240:338-240, 1988.

Stone, J., Dreher, B., and Leventhal, A. Hierarchical and parallel mechanisms in the organization of visual cortex. Brain Research Reviews 1:345-394, 1979.

Stromeyer III, C.F., Eskew, Jr., R.T., and Kronauer, R.E. The most sensitive motion detectors in humans are spectrally-opponent. Investigative Ophthalmology and Visual Science Supplement 31:240, 1990.

Tanaka, K., Hikosaka, K., Saito, H., Yukie, M., Fukada, Y., and Iwai, E. Analysis of local and wide-field movements in the superior temporal visual areas of the macaque monkey. Journal of Neuroscience 6:134-144, 1986.

Ts'o, D. and Gilbert, C.D. The organization of chromatic and spatial interactions in the primate striate cortex. Journal of Neuroscience 8:1712-1727, 1988.

Ungerleider, L.G. and Desimone, R. Cortical connections of visual area MT in the macaque. Journal of Comparative Neurology 248:190-222, 1986.

Ungerleider, L.G. and Mishkin, M. Two cortical visual systems. In: Analysis

of Visual Behavior, eds D. Ingle, M.A. Goodale, R.J.W. Mansfield. MIT Press, Cambridge, MA (1982).

Van Essen, D.C. "Functional organization of primate visual cortex." In: Cerebral Cortex, eds. A. Peters and E.G. Jones. Plenum, New York, 1985.

Van Essen, D.C., Maunsell, J.H.R., and Bixby, J.L. The middle temporal visual area in the macaque: Myeloarchitecture, connections, functional properties, and topographic organization. Journal of Comparative Neurology 199:293-326, 1981.

Weber, H. and Fischer, B. Effect of a local ibotenic acid lesion in the visual association area on the prelunate gyrus (area V_4) on saccadic reaction times in trained rhesus monkeys. Experimental Brain Research 81:134-139, 1990.

Zeki, S.M. Colour coding in the rhesus monkey prestriate cortex. Brain Research 53:422-427, 1973.

Zeki, S.M. Functional organization of a visual area in the posterior bank of the superior temporal sulcus of the rhesus monkey. Journal of Physiology, London 236:549-573, 1974a.

Zeki, S.M. Colour coding in the superior temporal sulcus of rhesus monkey visual cortex. Proc. R. Soc. London Ser. B 197:195-223, 1977.

Zeki, S. Colour coding in the cerebral cortex: The reaction of cells in monkey visual cortex to wavelengths and colours. Neuroscience 9:741-765, 1983a.

Zeki, S. Colour coding in the cerebral cortex: The responses of wavelength-selective and colour-coded cells in monkey visual cortex to changes in wavelength composition. Neuroscience 9:767-781, 1983b.

Zeki, S. and Shipp, S. The functional logic of cortical connections. Nature 335:311-317, 1988.

FIGURES

Figure 1.1 Proposed visual pathways within the geniculo-cortical system. The pathways are segregated in the retina at the level of the retinal ganglion cells. P cells project to the pLGN and M cells project to the mLGN. These channels remain segregated at the input layers of striate cortex, $4C_{\beta}$ and $4C_{\alpha}$, respectively. The V_1 input layers project to the superficial layers where information is separated within the blob/interblob system. Cells in $4C_{\alpha}$ also project to layer 4B which in turn has a direct projection to MT, and an indirect projection via interblobs and thick stripes. Blob cells project predominantly to thin stripes in V_2 and then project to area V_4. 4B projects to both interblobs and blobs and this input is believed to be conveyed to both thin and interstripes.

Visual Pathways

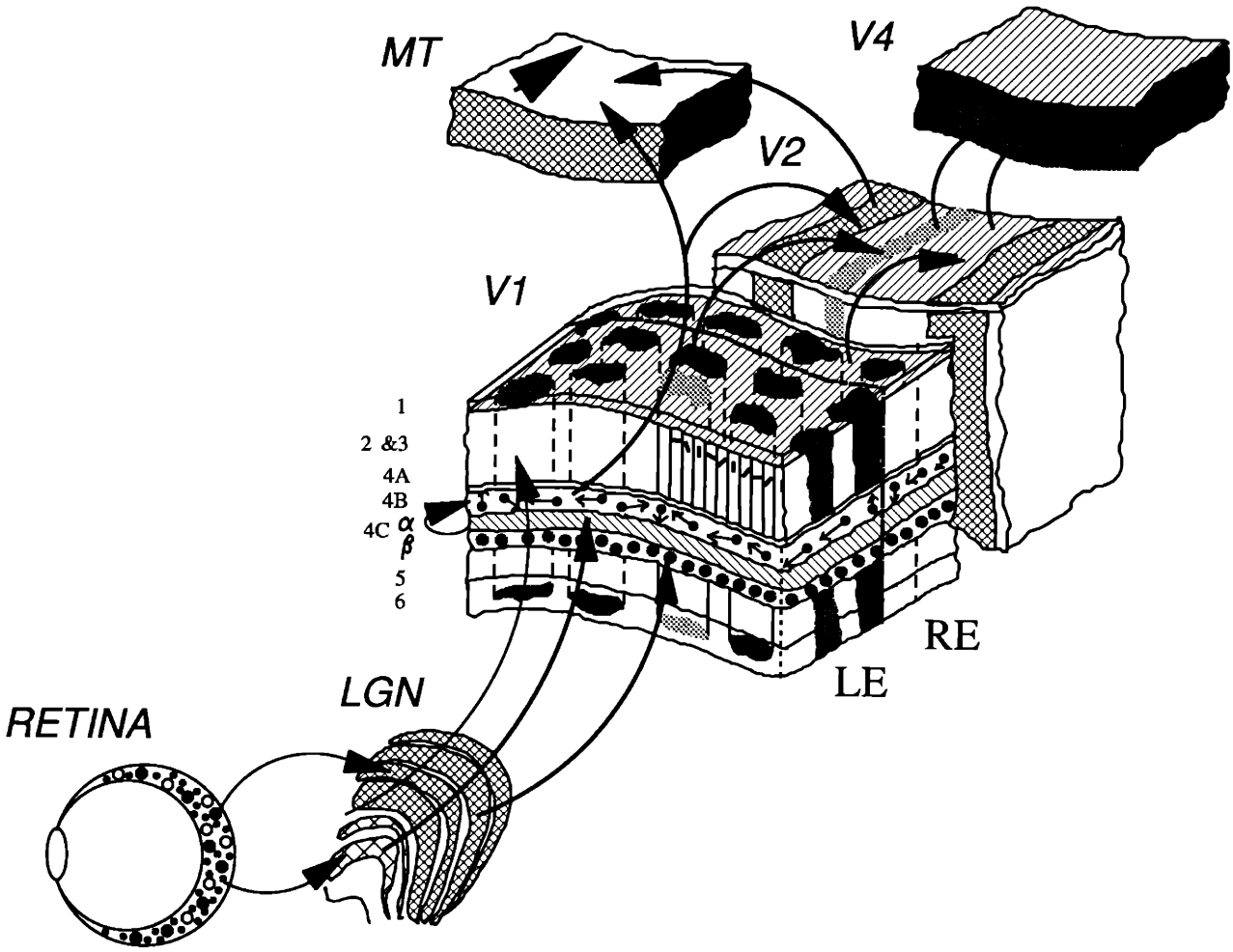

Figure 1.1

CHAPTER TWO

PSYCHOPHYSICS: 1) THE ESTABLISHMENT OF ISOLUMINANCE IN RHESUS MONKEYS; 2) THE CONTRIBUTION OF WAVELENGTH INFORMATION TO MOTION AND DEPTH PERCEPTION

Summary

Behavioral tests were performed on both human subjects and rhesus monkeys to determine isoluminance using the following methods: heterochromatic flicker photometry; stereoscopic depth detection; random dot motion detection; velocity discrimination; and the minimum motion technique. The results indicate that color vision between humans and monkeys are very similar. Heterochromatic flicker and the minimum motion method prove to be simple and accurate determinants of isoluminant values where depth and motion perception are degraded. Measurement of the velocity of the slow phase of optokinetic nystagmus indicate no reduction in gain at isoluminance. This suggests that the mLGN/MT pathway is functional at isoluminance. Introduction of wavelength information to stimuli in motion and stereo tasks reveal a contribution of color to stereopsis and motion perception. These findings are not consistent with current notions of information processing in the visual system.

1.0 INTRODUCTION

As mentioned in the previous chapter, it is proposed that vision is divided into several subprocesses. Information from different cues is believed to be segregated early within the visual processing of inferred attributes such as color, motion, form and depth. Anatomical, physiological and clinical evidence suggest a parallel organization of the visual system (Lennie, 1980; Van Essen and Maunsell, 1983; Maunsell, 1985; Livingstone and Hubel, 1988; DeYoe and Van Essen, 1988; Schiller, 1986). Two major pathways conveying qualitatively different information are the color-opponent (C-O) and the broad-band (B-B) channels. The cells in the initial stages of these two channels differ in many ways, among which the segregation of long-, middle- and short-wavelength cones into center and surround is the most important for this discussion. The former pathway begins with the color-opponent cells in the retina, continues through the parvocellular layers of the dorsal lateral geniculate nucleus (pLGN), and to segregated layers of the striate cortex. These layers project to identified subregions of extrastriate cortex including area V_4, an area that is thought to play a central role in the analysis of color and form. The B-B pathway starts with the retinal broad-band cells and projects to the magnocellular layers of the LGN. Magnocellular cells to some extent remain segregated through the striate cortex, and are the dominant input to the middle temporal visual area (MT) which is crucial in the processing of visual motion. The distinct physiological properties of the cells in

these pathways and their selectivity to visual cues led to the suggestion that one stimulus cue is represented in one pathway, and the processing within this pathway mediates the perception of a few visual attributes (Livingstone and Hubel, 1988). For example, motion and depth perception have been thought to be mediated by the activity of the broad-band pathway. Because the retinal broad-band cells do not spatially segregate different cone types (Wiesel and Hubel, 1966; Gouras, 1968; Gouras and Zrenner, 1981; Shapley and Perry, 1986; Derrington *et al.*, 1984), this channel is claimed to be sensitive only to luminance information.

In the same vein, the deterioration of motion and depth perception reported in psychophysical isoluminance experiments (Ramachandran and Gregory, 1978; Gregory, 1977; Lu and Fender, 1972) has been brought up as conclusive evidence for the complete inactivation of the broad-band pathway (Livingstone and Hubel, 1987, 1988; Livingstone, 1988). There are reports of a motion percept using isoluminant stimuli however, (Cavanagh *et al.*, 1984; Cavanagh *et al.*, 1985; Mullen and Baker, 1985; Derrington and Badcock, 1985; Cavanagh and Favreau, 1985) as well as the perception of depth with both figural and random dot stereograms (Comerford, 1974; de Weert and Sadza, 1983). In some cases though, it seems that the addition of color information is detrimental to perception (Cavanagh *et al.*, 1985; Ramachandran and Gregory, 1978). Is the broad-band system responsible for these deficits in perception at isoluminance?

One behavioral approach to examine this question is to look at eye

movements and see how they are affected when conditions of isoluminance are instantiated. It has been demonstrated that the broad-band pathway is crucial for the initiation of smooth pursuit eye movements and the programming of saccades elicited by moving stimuli. Cortical areas that are essential to motion analysis, such as the middle temporal visual area (MT) and the middle superior temporal area (MST), project to the pontine nuclei, which relay cortical inputs to the areas of the cerebellum that are concerned with pursuit eye movements (Lisberger *et al.*, 1987). Also, MT and MST contain cells that fire particularly when a moving target is tracked (Newsome *et al.*, 1988; Komatsu and Wurtz, 1988). Furthermore, ibotenic acid lesions of area MT induce deficits in oculomotor tasks that are based on visual motion processing (Newsome *et al.*, 1985; Dursteller *et al.*, 1987; Newsome and Wurtz, 1988).

If the decrement in the perception of motion under isoluminance conditions is the result of the inactivation of the broad-band channel, one might expect a drop in the gain of the eye tracking system during the optokinetic nystagmus (OKN) elicited by moving, isoluminant color gratings. In addition, if wavelength information confounds depth and motion processing, one would expect performance to diminish as color is increased in perceptual tasks.

The first part of this investigation establishes isoluminance using a variety of techniques in both humans and monkeys for direct comparison. These isoluminant values will later be used when investigating the responses of single cells of the color-opponent and broad-band systems at the level of the lateral geniculate nucleus and extrastriate cortex. The OKN response in

monkeys is then investigated under various luminance and chrominance contrast conditions using drifting gratings. Finally, stereoscopic depth and motion perception is examined over a range of luminance contrasts, including isoluminance, as a function of increasing color contrast.

2.0 MATERIALS AND METHODS

Five volunteer human subjects (EC, NL, SM, JS, AH) with normal or corrected vision and normal stereo and color vision, and 8 male and one female, juvenile rhesus monkeys (*Macaca mulatta*) were used to collect the data presented in this set of experiments. The animals were cared for in accordance with the National Institute of Health Guide for the Care and Use of Laboratory Animals and the guidelines of the Massachusetts Institute of Technology Committee on Animal Care.

All surgical procedures were accomplished under barbiturate anesthesia using sterile technique. The monkeys first learned to remain in the primate chair until they became used to the experimenter and to the laboratory conditions. Subsequently they underwent an eye-coil and head-post implantation surgery: A scleral search coil was implanted subconjunctivally (Judge *et al.*, 1980) and a stainless steel post to restrain the head was attached to the skull using stainless steel screws embedded in acrylic cement. The animals were then trained to perform the behavioral tasks.

2.1 Stimulus Presentation

The stimuli were generated by an Adage 3000 raster display system and presented on a Hitachi HM3619A color monitor. The monitor had a 1280 x 1024 spatial resolution, 0.31 mm dot pitch, 36 KHz horizontal scan frequency, and a self-convergence in-line gun. Misconvergence was minimized using a microcomputer (maximum deviation 0.1 mm within a central circle with diameter 14 inches). The bandwidth of the video amplifier was 45 MHz (10 nsec from 10% to 90% rise and fall time). The monitor was tested for phosphor and spatial independence, phosphor constancy and spatial homogeneity. To establish a linear relationship between the luminance of the colors and the color entries, a gamma correction was performed in software by recalculating the display-data values table. ABL (Automatic Brightness Level) adjustment was set to maximum to insure linearity for the higher intensities. Additional internal lookup tables were created to compensate for spatial inhomogeneities. Furthermore, the limited (45 Mhz) bandwidth of the video amplifier required a gun-dependent correction in the lookup table for high spatial frequency patterns. For example, when random dot patterns with a dot size less than 2x2 pixels were used, then for input values more than 0.75 (normalized to the maximum of each gun) a correction was required to reach the equivalent luminance value of a larger area. This correction was made by multiplying the lookup table values by 1.14 for the red, 1.33 for the green, and 1.11 for the blue gun. To avoid doming of the shadow-mask that would result in a desaturation of the colors, the monitor was always turned on at least 45 minutes before the begin of each experiment session.

The display colors were programmed in either direct R, G, and B terms or using the specifications of the standard color system introduced by the Commission Internationale de l'Eclairage (CIE). To create the transformation matrix for the RGB to CIE, or CIE to RGB conversions the monitor was first aligned to a white of D9300. The spectral energy distributions of the three phosphors (P22-R, P22-G, and P22-B with maximum energy at 625, 525 and 440 nm respectively) of the color monitors were then measured using a spectrometer and the resulting spectra were integrated with the CIE color-matching functions (Wright, 1931) to give CIE tristimulus values X, Y, and Z. From the tristimulus values, the CIE chromaticity values, x and y, were found to be: Red = (0.602, 0.353), Green = (0.284, 0.581) and Blue = (0.148, 0.067). The experiments were run in the low spatial resolution mode of the monitor (512 x 512 pixels), with a raster frequency of 60 Hz noninterlaced. The lookup tables and the digital to analog converters of the video control unit were 8 bits (256 levels). The stimuli were viewed from a distance of 57 cm.

The "amount" of color in the random dot stimuli was varied by changing the excitation purity of the colors. Figure 2.1 gives the definition of excitation purity. The triangle formed by joining the coordinates of the red (R), green (G) and blue (B) monitor phosphors lies within the space of all colors in the CIE chromaticity plane at one luminance; in this figure, 8 cd/m^2. The boundary of the CIE space represents pure monochromatic lights, a few of which are indicated. Luminance varies in the dimension perpendicular to the plane. The excitation purity (EP) of a color 'c' is the ratio of two distances: the first (Wc) is

the distance in the chromaticity plane between the coordinates of white (W) and the coordinates of c; the second (WC) is the distance along the same direction from white to the point 'C' where the continuation of the line Wc intersects the edge of the monitor color triangle. Increasing the EP of a color along the red phosphor line, for instance, changes its appearance from white (EP = 0%) to pink to red (EP = 100%). At a given EP value, the luminance of one of the colors was varied to change the luminance contrast. A combination of nine luminance contrasts and four excitation purity values were used in this study.

For the sinusoidal stimuli used in the velocity discrimination, direction of motion discrimination, and OKN experiments the saturation of a color was expressed as color contrast rather than excitation purity. Color contrast (figure 2.2) was defined as the ratio of the amplitude of the color change along the R-G axis of the CIE chromaticity diagram to the maximum change possible between the red and green phosphors each turned on by itself for a given luminance value represented by the overall size of the color triangle. The red/green gratings used throughout these experiments were generated by adding the red and green sine waves 180 degrees out of phase. When the amplitude of the modulation of the red and green were equal as defined by standard psychophysical tests such as flicker photometry, the red/green gratings were isoluminant since the luminous output of the monitor was gamma-corrected to ensure a linear relationship between color entries and luminance values. Amplitudes of the red/green modulations different from those psychophysically

defined as isoluminant result in luminance modulation (figure 2.3). Luminance contrast was expressed as the difference between the two amplitudes of the red and green modulations ($\mathbf{R}_{amp}$, $\mathbf{G}_{amp}$), divided by the mean luminances of the two wave forms ($\mathbf{R}_{mean}$, $\mathbf{G}_{mean}$). For the random dot patterns, contrast was given as the log difference between the luminance of the dots and the luminance of the background.

2.2 Chromatic Aberrations

Since the thin-lens equation is wavelength-dependent, the focal length varies as a function of wavelength and hence the constituent colors in a beam of white light are focused at different points on the optical axis. The axial distance between the focal points of two different colors is called axial (longitudinal) chromatic aberration. Another type of chromatic aberration is the lateral or transverse chromatic aberration which arise from the fact that the size of the retinal image varies with the color as well. The two effects are usually combined and can produce a substantial luminance contrast artifact in stimuli that are adjusted to be isoluminant. The reasoning goes as follows: an observer can only focus on one color at a time. For instance, in the case of two colors, say red and green, if the experimenter adjusts the intensity of red for a constant green intensity to make them isoluminant, the observer will attempt to reaccommodate to achieve maximum contrast (Wolfe and Owens, 1981). This observer-controlled contrast variation is the major effect of chromatic aberration. The lateral chromatic aberrations seem to be neurally corrected

since any attempt to correct them optically produces color fringes (Held, 1980). For the behavioral experiments, therefore, lateral chromatic aberrations will not be considered as a source of luminance artifacts. Since, however, the stimuli used in the psychophysical experiments were also used in paralyzed animal recordings from lateral geniculate nucleus both axial and lateral chromatic aberrations will discussed in the next sections.

2.21 Axial Chromatic Aberrations

The human eye suffers from axial chromatic aberration which has been shown to average approximately 1.75 D between 420 and 660 nm (Wald and Griffin, 1947; Bedford and Wyszeki, 1957). Correction of the axial chromatic aberration can be done with a number of achromatizing lenses (Bedford and Wyszeki, 1957; Powell, 1981; Lewis *et al.*, 1982; Howarth and Bradley, 1986). Even those lenses that do not introduce differential magnification, however, appear to 'create' a chromatic aberration (parallax) particularly when the lenses are not perfectly aligned (P. Cavanagh, personal communication). Furthermore, luminance artifacts by lateral chromatic aberration will be largest under conditions where the axial chromatic aberration has been corrected (Bradley *et al.*, 1989). In the experiments presented here there was no attempt to optically correct chromatic aberrations. A perfect alignment of achromatizing lenses in the case of monkey psychophysics is not realistic. Instead, low spatial frequency stimuli are used which, as is pointed out in the following paragraphs, produce no significant aberrations.

For the Hitachi monitor, the wavelengths with the most energy of the red and green phosphors were as follows: R = 627, G = 525 nm. For these wavelengths when the green is at zero diopters from the fixation, the red is estimated to be at -0.4 diopters (Howarth & Bradley, 1986). In the LGN physiological experiments, the stimuli were either flickering circular patches or red-green sinusoidal gratings of low spatial frequency (0.2 to 1.0 cpd). The stimuli used in these psychophysical experiments varied from 0.2 to 9 cpd. The relationship of maximum luminance artifact to the spatial frequency of the stimulus is expressed via the equation: contrast = $0.405(cpf)^2$ (Cavanagh and Anstis, 1989), where c is the chromatic aberration (difference of c diopters between the focal points for the two wavelengths), p is the pupil diameter and f is the spatial frequency in cpd. For a maximum possible pupil of 4 mm, the artificial contrast induced by chromatic aberrations is given in figure 2.4 for the spatial frequency range used in the present study. To evaluate a real color input to the motion and depth perception we compared the performance of the subjects at isoluminance with their performance in which achromatic stimuli had a contrast equivalent with that introduced by chromatic aberration. The luminance contrast produced by axial chromatic aberrations in the random dot patterns was predicted to be approximately 5%, a value that is well above detectability threshold. To ensure that the performance of the subjects in the stereoscopic depth and motion detection tasks was not based on such a luminance artifact, the random dot patterns were low-pass filtered to eliminate all frequencies above 3 cpd.

2.22 Lateral Chromatic Aberration

As mentioned earlier, the variation of lens power according to refractive index entails a corresponding variation of image size. This chromatic difference in magnification is known as lateral or transverse chromatic aberration. Le Grand (1967) showed that for a displacement of the optic axis of 5 degrees, a 340 nm spectrum spreads over 3 min of arc. In the Hitachi monitor there is a 100 nm difference between the peak wavelengths of the red and the green phosphors which would result in a displacement of less than 1 min of arc if one assumes that the system is linear. Since the displacement is much larger for the short wavelengths one expects a displacement much less than 1 min of arc. For two antiphase gratings of 100% color modulation this displacement causes a relative spatial shift that results in a pure luminance modulation even when the two gratings are isoluminant. Figure 2.5 illustrates the relation of luminance contrast due to transverse chromatic aberration to the spatial frequency of the stimulus. The dotted and thin solid lines shown in figure 2.5a represent luminance modulations of two different wavelengths. The thick black line represents the luminance contrast that results from lateral chromatic aberration. As can be seen in both 2.5a and 2.5b, the luminance artifact increases with the number of cycles. Like axial chromatic aberrations, luminance artifact in an isoluminant stimulus as the spatial frequency increases.

2.3 Data Collection

The experiments were under computer control (PDP 11/73) which presented the stimuli, collected the eye movements and delivered the juice reward. Eye movements were monitored with a scleral search coil method (Robinson, 1963) using the phase detection technique (Remmel, 1984). The eye position was sampled at 200 Hz.

2.4 Task Description

Rhesus monkeys were trained for the following tasks: 1) to detect a flickering stimulus; 2) to detect depth changes in random dot stereograms; 3) to detect a set of moving dots among a field of stationary dots; 4) to discriminate different motion velocities; 5) to discriminate different directions of motion; 6) to fixate before and after presentation of a moving grating designed to elicit optokinetic nystagmus. In the first four cases the task was to fixate a small bright white spot that appeared at the onset of each trial and then to locate the odd target that appeared randomly in one of 4 or 8 locations peripheral to the fixation point (figure 2.6). The specific tasks varied in certain details.

2.41 Chromatic Flicker Photometry

In both human subjects and monkeys the isoluminance point was first determined by heterochromatic flicker photometry (Rood, 1893; Allen, 1902; Judd, 1952). Generally, the procedure consists of a temporal alternation of two

spectral distributions at a low fixed rate. In this experiment the stimulus flickered between white and one of the primary colors, *i.e.* red, green or blue. A square waveform intensity modulation was used. Initially, data in a pilot experiment were collected from 5 human subjects. The intensity of the white was randomly selected among a set of 12 values and the subject adjusted the intensity of the primary color until minimum or no flicker was seen. Pressing a button would terminate the trial and start a new one in 1000 ms. The minimum flicker point was defined by a bracketing procedure.

Figure 2.7 shows the data collected in this preliminary session. The results are presented in this section, since they were basically used as a final test for the calibration of the monitor. Because the CIE defined luminance in accord with the requirement of linearity using the luminous efficiency function of the standard eye, which is based largely upon flicker photometry a linear relationship between the settings of the subjects and the values of the white would provide further evidence for the phosphor constancy and phosphor independence. As can be seen in figure 2.7 a clear linear relationship is evident for the whole range of red, green and blue values tested.

To use a common procedure for both humans and monkeys a four alternative forced choice (4AFC) method with constant stimuli was subsequently used to determine isoluminance points. Four stimuli, each subtending a visual angle of 2 degrees, were presented on a 5 cd/m^2 gray background one of which was flickering at 15 Hz between white and one of the phosphor primaries and the others had the average hue and brightness of the

two alternating lights. The task of the subject was to detect the flickering stimulus. There are two essential problems with this method, however. The first is the well known brightness enhancement effect (Bartley, 1938, 1941, and 1961); an intermittent light below the fusion point tends to look brighter than a steady light of the same luminance for frequencies of 2 to 20 cps. For an alternation frequency of 15 cps, a stimulus size of 3.5 degrees, and an average luminance of 5 to 15 cd/m^2 a brightness enhancement of up to 20% of the Talbot level of luminance can occur (Rabelo and Gruesser, 1961). The second is the hue shift of flickering lights to shorter wavelengths for flicker frequencies of 10 to 20 cps (Veringa, 1961). Both effects could be the basis for the discrimination for either the human subjects or the monkeys. To overcome this problem a method similar to the one described by De Valois *et al.* (1974) was used. First, all the stimuli were made to appear the same by having human subjects to perform a brightness or color matching task. Subjects had to adjust the hue and brightness of the nonflickering patch until it looked the same with the flickering stimulus. Using the values obtained from these matching tasks, small hue and intensity differences were then introduced among the various distractors so that the only remaining cue for the detection of the target stimulus was the flicker.

2.42 Stereoscopic Depth Perception at Isoluminance

For the depth discrimination task the subjects stereoscopically viewed Julesz-type (Julesz, 1964) random-dot stereograms; the target was a small

square in depth created by horizontally shifting a square area in one of the stereograms (figure 2.8). Disparities of 3.5 to 14 minutes of arc were used. The dot size in the random dot patterns was either 2x2 or 4x4 pixels. A spatial frequency filtered version of the random dot stereograms was also used to minimize chromatic aberrations by eliminating high spatial frequencies.

2.43 Random Dot Motion Detection

In the motion detection task the target was a small area of coherently moving dots in a larger array of stationary random dots (figure 2.9). All of the dots had the same intensity and the same color, red or green, on a green or red background respectively. Dot density was 50% and the dot size was either 2x2 or 4x4 pixels. A trial started with the fixation spot on a gray background of 5 cd/m^2. The same background was viewed during the intertrial period. After the subject or monkey had fixated the central spot the random dot pattern was presented. At the onset of the pattern a subset of the dots corresponding to a square of 1 to 2 degrees were drifting in one direction for up to 600 ms at a randomly selected location yielding the perception of a square. Within this time the subjects had to indicate the location of the moving dots, either by pressing one of the position buttons (humans) or by making a direct saccade to it (monkeys). Choice time (the time within which the subjects had to respond) was 600 ms for the monkeys and 800 ms for the human subjects.

2.44 Velocity Discrimination

In the velocity discrimination task four eccentrically placed drifting gratings were presented as shown in figure 2.10. Background luminance was 5 cd/m^2. Three of the targets were moving with a velocity of 5 deg/sec and one with 7 deg/sec or 3 deg/sec randomly intermixed. This velocity difference was well above just noticeable differences for velocity and at high luminance contrast the performance of the monkey was above 95%. The monkey was trained to saccade to the target having the odd velocity. The gratings were modulated both in their luminance and chrominance as described in section 2.11.

2.45 Direction of Motion Discrimination

The minimum motion stimulus was developed by Anstis and Cavanagh (1983) to deal with temporal or spatial variations at isoluminance and modified by Cavanagh *et al.* (1987) to minimize chromatic aberrations. A detailed description of the stimulus is given in Cavanagh *et al.* (1987). In the experiments presented here the stimulus consisted of four horizontal colored gratings presented in a repetitive sequence on a monitor (figure 2.11). The gratings are spatially superimposed, one grating at a time and each grating is displaced downwards by one-quarter cycle from the previous one. Two of these 4 gratings are modulated in both their chrominance and luminance as described in section 2.1 and will be referred to as the chromatic gratings. The other two gratings are composed by adding the sine waves in phase and will be referred to as the luminance gratings. The luminance gratings had the color

resulting from equal mixture of the two primaries and a 15% luminance contrast. In other words for the combination of red/green, red/blue and green/blue the luminance gratings were 15% contrast yellow, magenta and cyan respectively. The stimulus was viewed from a distance of 57 cm and subtended a visual angle of 2 degrees. Background luminance was 1 cd/m^2.

The direction of apparent motion of this stimulus depends on the modulation amplitude of the sine waves composing the chromatic gratings. In the case of red/green gratings, for example, when the red modulation is larger then the green, the darker green bars are associated with the darker yellow bars of the luminance grating and one perceives upward motion (figure 2.11a). Conversely, downward motion is perceived when the red bars become darker than the green bars (figure 2.11b). When the red and green bars are perceived equally bright, then neither of the colors will be consistently associated with the darker yellow bars of the luminance grating and no apparent motion is seen.

The monkeys were trained to perform a direction of motion discrimination task (figure 2.12). Each trial began with the appearance of a central fixation spot. After the monkey fixated it for 200 to 300 ms the minimum motion stimulus could be presented foveally or peripherally for 800 to 1200 ms. During the foveal presentation the fixation spot was turned off to allow eye movement responses to the moving grating. The stimulus was then replaced by a spot on the right and the left of the fixation spot. If the monkey perceived upward motion, he was required to make a saccade to the right spot;

a saccade to the left spot was required following the perception of downward movement.

In half of the trials the luminance gratings in the second and fourth frames were replaced by the chromatic gratings of the first and third frame shifted by a quarter-cycle. This produced 'real' apparent motion and was used to ensure proper reinforcement of the animal. The direction of motion in this case depends on the direction of phase shift which was randomized. In the other half of the trials the monkeys were rewarded for either response and these trials constituted the data for this study.

2.46 Gain of Optokinetic Nystagmus

To measure the optokinetic response of the monkeys to the drifting color gratings the animals were trained to fixate on a small central spot that was turned off for 1500 msec, then turned on at the same position, and subsequently moved rapidly the left or to the right of the fixation position. The monkey's task was to make a saccade to the new fixation position. Within these 1500 msec interval color gratings of various spatial frequencies and velocities were presented. The gratings subtended a visual angle of 20 degrees and usually elicited strong OKN responses.

3.0 RESULTS

3.1 Chromatic Flicker Photometry

Figure 2.13 shows color matching data obtained with red/white flicker

photometry for three human subjects (upper panels) and 3 monkeys (lower panels). Similar data were collected for green/white and blue/white. The target alternated between red and white at 15 Hz. White was set to 10 cd/m^2 and the luminance of the red was varied with 0.04 log unit steps. In each trial one of 11 preselected red luminance values was presented in random order. The performance of the monkey, expressed as the percent of trials in which the monkey correctly detected the flickering stimulus, was plotted against the luminance contrast. Luminance contrast was expressed as the logarithm of the ratio of red luminance to the luminance of the white. Each data point in figure 2.13 represents the average of 24 blocks, each block consisting of 40 presentations of the stimuli. The shaded area shows the confidence interval for a result different from chance on a given luminance contrast for significance at the 0.01 level (N=24, $t_{.01}[23] = 2.807$, low limit = 17%, high limit = 33%). Performance within this region is not significantly different from chance. The red luminance for which no flicker could be perceived, as indicated by the chance level performance, was 10 cd/m^2 for the subject NL, 10.9 cd/m^2 for EC and 10 cd/m^2 for JS. The lower panels show the same results for three of the tested monkeys. Here, the luminance of red that minimized flicker perception was 10 cd/m^2 for monkey 85-19, 9.1 cd/m^2 for 82-19, and 10.9 cd/m^2 for 86-5. Luminance equality as inferred by flicker photometry always obeys Abney's law; the method obeys the properties of reflexivity, additivity and transitivity. Therefore, from the equality of red and white luminance, and of green and white luminance it was possible to calculate the red/green isoluminance point.

One could theoretically have used red/green flicker directly to determine isoluminant red and green stimuli. Because of the slight misconvergence that inevitably remains in a monitor display, however, visible borders can be seen in the flickering stimulus when two individual phosphors are used in alternation. The effect is enhanced by the contribution of chromatic aberration and is particularly pronounced when small eye movements occur during the fixation period potentially providing an inadvertent cue for discrimination. Using an alternation of an individual phosphor type with white eliminates this problem by reducing the effects of any residual misconvergence. The results show that both humans and monkeys yield very similar heterochromatic matches and are in close agreement with the CIE standard observer.

3.2 Stereoscopic Depth Perception

Figure 2.14 shows data obtained from 3 humans and 3 monkeys in the stereoscopic depth detection task with 100% excitation purity. The results are displayed in terms of percent correct of responses to crossed or uncrossed disparity presentations of the stereoscopic target at each of the eleven luminance contrasts. The subjects had to indicate the position of the target (a square standing either behind or in front of the random dot background plane). The dot density was 50% and the dot size was 4x4 pixels (14 x 14 min of arc). The disparity of the two images was 7 min of arc. There was an obvious deterioration of the perceived depth close to and at isoluminance, as made evident by the poor performance of all subjects. As one can see from figure

2.14, however, all psychometric curves obtained in this tasks lie above chance level ($p = 0.01$, $N=36$, $t_{.01}[35] = 2.750$, low limit = 19%, high limit = 31%). A low pass filtered version of these stereograms was also used to minimize axial chromatic aberrations. The filter size was 8x8 pixels eliminating all spatial frequencies above 2.4 cpd. Similar results were obtained for 3.5 and 14 min of arc disparities and 2x2 pixels dot size patterns.

3.3 Random Dot Motion Detection

Figure 2.15 shows the data collected from 3 human subjects and 3 monkeys in the motion detection experiment. Dot density was 50% and the dot size was 2x2 pixels. Percent correct performance is plotted against the logarithm of the ratio of the luminance of the red dots to the luminance of the green background. Eleven luminance contrast values were used separated by 0.04 log units. The upper three panels are the data from human subjects. Here, each data point represents the average of 16 blocks, each block consisting of 24 presentations of the stimuli. The shaded area shows the confidence limits for chance performance for significance at the 0.01 level ($N=16$, $t_{.01}[15] = 2.943$, low limit = 15%, high limit = 35%). Green luminance was equal to 15 cd/m^2. The performance of subjects EC and NL dropped to minimum for a red of 15 cd/m^2. Subject JS had a minimum in performance for a red luminance of 15.7 cd/m^2. The lower three panels show the results for three of the tested monkeys. Green is again 15 cd/m^2. Performance minima were obtained at 15, 15, and 16.5 cd/m^2 respectively. All subjects performed above chance level in

this task when the excitation purity was 100 percent. Similar results were collected using patterns with 4x4 pixels dot size.

3.4 Velocity Discrimination

Figure 2.16 illustrates the results for two of the monkeys for the velocity discrimination experiment. Nine luminance contrast values with 0.04 log units increments and 2 chrominance modulations, 0 and 75% were used to collect the data shown in this figure. The spatial frequency of the gratings was 1.3 cpd. The green modulation had a luminance (100% modulation amplitude) of 13 cd/m^2. The filled circles show performance for gratings having a color modulation of 75% and the lower for color modulation of 0%. Confidence limits for a result different than chance are 16% and 34% (N=24, $t_{.01}[23] = 2.807$). It is evident that the performance of the monkey at isoluminance remains above chance levels for the 75% color modulation. This will be discussed further is sections 3.7 and 3.8.

3.5 Direction Discrimination Using the Minimum Motion Technique

3.51 Isoluminance Determined Through the Report of the Monkeys

Figure 2.17 shows the results of one typical session in which the monkey 87-45 reported motion direction for 9 luminance contrast values of the green grating combined with a red grating of 13 cd/m^2 amplitude at a spatial frequency of 0.7 cpd and a temporal frequency of 3.0 Hz. Each data point

represents the average of 10 blocks, each block consisting of 20 presentations of the moving gratings. It is important to emphasize that in none of the trials shown in figure 2.17 was the reward contingent on the monkey's report; the trials in which explicit motion was used were not relevant for, nor included in this analysis. The plot in this figure shows the percentage of trials in which the monkey reported seeing upward motion or downward motion. The lines through the data points represent the best fitting 5th order polynomials. The point where the two lines cross represents the point at which the monkey saw up 50% of the time and down 50% of the time; in other words there was no detectable motion, and the performance was at chance level. Accordingly, the green luminance value at which the two lines cross is an estimate of the isoluminant point. In this case the luminance of the green needed to null the motion percept when combined with the red luminance of 13.00 cd/m^2 was 12.80 cd/m^2 (red/green = 1.02). The confidence limits for a performance different from chance were from 43% to 57% for significance at the 0.05 level. Hence, for this monkey a 3.8% change in the isoluminance ratio was sufficient to elevate the performance above chance level indicating the high sensitivity of the method. Testing this animal with standard chromatic flicker photometry at 15 Hz gave a red/green ratio of 0.88. A red/green ratio of 0.99 was obtained from monkey 87-46 with the minimum motion stimulus while flicker photometry yielded a ratio of 0.92. The same paradigm was used to determine the isoluminance point when using red/blue or green/blue gratings of any of the above mentioned spatial and temporal frequencies.

3.52 Isoluminance Determined by OKN Reversals

When the drifting gratings were presented without the central fixation spot, they usually elicited an optokinetic response. The direction of the slow phase of this nystagmus for the various luminance contrast values used in this experiment was examined. Figure 2.18 illustrates the vertical eye position traces from 50 trials for three different luminance ratios. All of the eye traces are aligned on the time when the grating motion began. Figure 2.18a shows the eye movement responses for a high red/green luminance ratio (red = 13 cd/m^2, green = 5.84 cd/m^2). The plot shows that the tracking eye movements are consistently upward; as mentioned above this red/green ratio results to an upward apparent motion as perceived by human subjects and as reported by the trained animals. When the red/green ratio was balanced (red = 13 cd/m^2, green = 12.66 cd/m^2), and the impression of motion was minimal (the report of the monkey fell to chance levels) the gain of the nystagmic tracking was near zero (figure 2.18b). Crossing this isoluminant point reversed the direction of the optokinetic response of the monkey and for higher green luminance (red = 13 cd/m^2, green = 28.68 cd/m^2) only downward tracking was seen as shown in figure 2.18c.

Figure 2.19 shows the velocity of the smooth nystagmic eye movements for 9 different luminance ratios of 0.7 cpd gratings drifting at 3.0 Hz. The velocity of the smooth eye movement response is plotted as a function of the green luminance with a constant red luminance of 13 cd/m^2. Each data point represents the average eye velocity over 50 trials. As the red/green luminance

ratio decreases, the eye movement velocity decreases from high positive values, reverses sign and continues to negative values. The point at which the smooth eye movement velocity is 0 degrees per second is another representation of the red/green luminance ratio for which minimum motion occurs. In this case the green luminance value was 13.16 cd/m^2 for a red luminance of 13.00 cd/m^2.

3.53 Isoluminance Ratios for Different Spatial and Temporal Frequencies

Both the report of the monkeys and the reversals in the optokinetic responses were used to determine isoluminance ratios for different spatial and temporal frequencies. Four spatial frequencies, 0.5, 0.7, 1.1 and 2.2 cpd were combined with three temporal frequencies of 1, 3 and 7.5 Hz. The red in the red/green gratings was set to 13 cd/m^2, the green of the blue/green gratings was 12 cd/m^2, and the red in the red/blue gratings was 12 cd/m^2. In figure 2.20, the green luminance at which the perceptual choice was random for a constant red luminance of 13 cd/m^2 is shown as a function of spatial frequency for 3 temporal frequencies. The variation with spatial frequency was not statistically significant for either monkey. The effect of temporal frequency was, however, different in the two monkeys. For monkey 87-45 there was, on average, a 10% increase of the green intensity needed to null the motion when the temporal frequency increased from 1 Hz to 7.5 Hz. For monkey 87-46, on the other hand, the isoluminance ratio did not change significantly with increased temporal frequencies when the gratings were of low spatial frequency. For spatial frequencies above 1 cpd, however, there was a 7%

decrease in the amount of green needed to null the apparent motion when increasing the temporal frequency from 1 Hz to 7.5 Hz.

Figures 2.21 and 2.22 show the effects of spatial and temporal frequency on the chromatic matching between blue and green, and red and blue gratings for the two monkeys. No significant variation was found in the isoluminance ratios obtained for the three temporal frequencies tested. In contrast, there was a clear increase in the amount of the blue needed to match a given red or green value for higher spatial frequencies showing a decrease in the contribution of the blue component as spatial frequency increases.

As mentioned above, in all sessions isoluminance was defined by both the report of the monkeys and their eye movement responses to the drifting gratings. There was very close agreement between the values obtained by the two methods. Figure 2.23 compares the green luminance values obtained by the monkey's perceptual report and by the minimum pursuit velocity for red luminance of 13 cd/m^2 for all spatial and temporal frequencies tested. Each data point is the average of 50 measurements and represents a single combination of spatial and temporal frequency. The variation in the green luminance values reflects the variation in isoluminance ratios observed at different spatial and temporal frequencies. There is a significant correlation between the green luminance values obtained by the two behavioral measurements ($r = 0.81$ and $r = 0.82$, $p < 0.001$). Not only is there a significant correlation, but the slope of the function is also very close to 1.0 (the heavy diagonal lines in figures 2.23a and 2.23b) revealing a very close agreement

between the values obtained by the two methods.

3.54 Isoluminance Ratios for Parafoveal Stimulus Presentations

Isoluminance ratios for red/green, green/blue and red/blue gratings of 0.7 cpd spatial frequency and 3 Hz temporal frequency were also determined parafoveally (3 and 6 degrees eccentricity). Obviously, in this experiment only the behavioral report was relevant since the monkey had to fixate on a central fixation spot during the stimulus presentation. Both animals showed an increased error rate in the real motion condition in this task. Figure 2.24 shows the results for the monkey 87-45 for all three color combinations. There was a slight change in isoluminance points for the red/green gratings. Not surprisingly, however, there was a considerable elevation in the blue/green and blue/red ratio when the eccentricity was increased.

3.6 Optokinetic Responses to Drifting Isoluminant Gratings

Figure 2.25 shows a typical eye movement response to the drifting gratings. The upper trace shows the response of the eye to a leftward-moving grating, and the lower trace, the response to a rightward-moving grating. A computer algorithm was used to define the segments of OKN slow phase, and the mean slope of the regression lines within these limits defined the eye movement velocity. The gain was then computed as the ratio of eye to target velocity. Four different spatial frequencies (0.28, 0.38, 0.56, 1.12 cpd) and 4 velocities (2, 3, 7, 14 deg/sec) were used. The gratings were either of 78% color

contrast modulation (red-green gratings) or of 0% color modulation (yellow gratings modulated in intensity). Nine luminance contrast values were tested with the red-green gratings and 7 luminance contrast values with the yellow gratings. The mean luminance of the display was 22 cd/m^2.

Figure 2.26 shows the results obtained from one monkey for two spatial frequencies (0.56 and 0.28 cpd) and for 4 velocities. There is no decrement in the velocity gain of the OKN for low luminance contrast values for all velocities when using 0.56 cpd spatial frequency and only a slight change in the gain for low spatial frequency and high target velocities. Similar results are shown in figure 2.27 for another monkey. The velocity gain of the slow phase was considerably reduced, however, when gratings of zero chrominance modulation and luminance contrast lower than 10% were used as is shown in figure 2.28. Similar results were obtained from both human subjects tested with the same apparatus.

3.7 Contribution of Color Information to Movement Perception

As mentioned earlier, the perception of motion is compromised at and around isoluminance in some instances. It has been shown, however, that this decrement in the movement perception is not confined to isoluminant color stimuli. Campbell and Maffei (1981) and Thompson (1982) have shown that low spatial frequency achromatic sinusoidal gratings of low luminance contrast appear to drift slower than high contrast gratings. To study the effects of increasing color contrast in moving stimuli of low luminance contrast the

saturation of the stimuli was varied systematically for each of the eleven conditions used in the previous motion detection experiment. Four excitation purity values were used for each of the primary colors. Figure 2.29 shows the data collected from one human subject and one monkey for these 44 (11 x 4) conditions. Excitation purity was set to 0, 40, 80 and 100 percent. Shaded areas indicate the confidence limits for chance performance ($p = 0.01$), here 15% and 35% respectively. Both humans and monkeys exhibited substantially worse performance when achromatic stimuli were used for the low luminance contrast values. In the condition where no color information is available (0% purity), performance drops to near 10%. Performance less than chance level like the one in this task was observed in some animals that were extensively trained with catch trials. Animals that were planned to be used for studies with selective lesions were trained in sessions including catch trials to minimize guessing. In a catch trial only the fixation spot appeared and the monkey was rewarded for maintaining fixation. Animals trained in this way violated the 4AFC method since they maintained fixation in the trials that no stimulus was perceived. Two of the human subjects performed also at levels less than chance level for the motion detection and stereoscopic depth discrimination tasks. This is attributed to the short stimulus presentations (600 ms) that were used throughout these experiments.

As shown in figure 2.29 performance improves significantly with increasing color saturation. Performance at 40% excitation purity is significantly ($p = 0.01$) higher than at 0% purity, and performance at 100% is

higher than at 40% ($p = 0.01$). Similar results were obtained from the monkey 82-19 shown in the right panel. The equivalent luminance contrast for the performance measured at maximum color contrast was in average 12%. This contrast was significantly higher ($p = 0.05$) than the luminance contrast artifact expected from the chromatic aberrations as computed in section 2.2.

3.7 Contribution of Color Information to Stereoscopic Depth Perception

The effects of color saturation of the stimuli to stereoscopic depth perception were studied with red/green random dot patterns using 11 luminance contrast values and 4 excitation purity levels. Figure 2.30 shows the results for one humans subject and one monkey. Similar data were collected from another human subject and two other monkeys. The performance of all subjects dropped to chance or zero for achromatic stimuli close to isoluminance. As the purity of the color increased, increasing the effective contrast, the performance at isoluminance improved as well as other luminance contrast values. For 100% excitation purity level it reached the typical above-chance level shown in Figure 2.30. To insure that the improved performance was not an artifact due to chromatic aberrations (since the random dot patterns included frequencies up to 9 cpd) the experiment was repeated using a spatial frequency filtered version of the stereograms (figure 2.31). The images were blurred by covering the screen with an Ozolith neutral paper (no. 3). In either case, depth could be perceived for disparities as low as 7 min of arc.

3.9 Comparison of Luminance Ratios Among Tasks

Figure 2.32 is a plot of the luminance ratios at which minimum performance was measured against luminance contrast as defined for the standard observer. The data are pooled from three subjects and six monkeys in the flicker, motion, and stereoscopic depth detection tasks. The upper three panels show data form human subjects. The abscissa is the red value used as constant color in all tasks. The ordinate shows the green luminance for which minimum performance was obtained. The slope of the regression line gives the average color ratio at which minimum performance was observed. Correlation coefficients (r) and (r^2) are given. Vertical bars show the standard errors of the mean for 100 trials at each point. It can be seen that the red/green ratio for which motion and stereoscopic depth perception is degraded is very close to the isoluminance point as defined with flicker photometry (left hand upper panel). Similar results were shown for six monkeys in the lower three plots. As mentioned previously in section 3.5, luminance matches using minimum motion are also close to photometrically determined matches in monkeys (m= 0.93 for 87-46) and in humans (Anstis and Cavanagh, 1983).

4.0 DISCUSSION

The results of these experiments show that the performance of various psychophysical tests are comparable for humans and rhesus monkeys. This is in agreement with the study by De Valois *et al.* (1974) which compares spectral sensitivity between the two species and finds color vision to be very similar.

This permits the use of physiological studies to explain the underlying neural mechanisms for the psychophysical phenomena, which are collected almost exclusively from humans. Physiological experiments described in chapters 4 and 5 will also make use of the similarity in the creation of stimuli based on human cone fundamental data. In addition, the relative luminous-efficiency functions obtained in both species agree with the CIE standard observer. This is not particularly surprising since the CIE standard observer was originally based upon flicker photometry but is useful for confirming the procedures.

There is also close correspondence between isoluminance values for the different methods employed. Again, this is not trivial since Wagner and Boynton (1972) find that although isoluminance defined by minimally distinct borders and flicker photometry are comparable, they differ greatly from data generated by direct heterochromatic photometry. Depth and motion perception are degraded at isoluminant values that correspond to like values obtained by heterochromatic flicker photometry and the minimum motion technique. The well-established flicker photometry method and minimum motion technique can easily determine isoluminant values in behaving monkeys. In addition, the stimulus configurations for the two methods, a flickering spot of light and sinusoidal gratings, are very good for eliciting responses in the LGN and extrastriate areas V_4 and MT, respectively.

The minimum motion heterochromatic matching technique is especially useful for defining isoluminance for stimuli in behavioral and physiological studies in monkeys. With foveal stimulation, isoluminance can be determined

with monkeys trained solely in a fixation task by detecting the reversals in the smooth nystagmic eye movements elicited by the apparent motion. Since eye movements can be easily measured in non-human primates the reversals in the slow phase of nystagmus provide a simple and powerful means to determine isoluminance in monkeys without the considerable work involved in training the animal in a visual discrimination or matching task. Optokinetic nystagmus (OKN) has been used in the past as an objective indicator of defective color vision (Pitt, 1944; Moreland, 1975). Recently, Cavanagh *et al.*, (1984) recorded OKN elicited by the minimum motion stimulus in both normal and color-defective subjects, and Anstis *et al.* (1987) in infants. This study extends these observations to non-human primates providing a simple and accurate measure of isoluminance points that can be used in physiological experiments.

In agreement with Cavanagh *et al.* (1987), there was considerable variation of the isoluminance ratio when gratings of different spatial and temporal frequencies were tested. The data did not reveal a consistent relation between isoluminance points and temporal frequency, however, like the one found by the former investigators. These authors found that the amount of green required to equal the luminance of the red increases by 7 to 9 per cent as the temporal frequency increases. This was true for one of the monkeys tested in the present study, while the second monkey needed less green as the temporal frequency increased. This result does not support the idea that the temporal-frequency effect on the isoluminance points could be attributed to differences in temporal responses of the long- and medium-wavelength cones.

However, the lack of a consistent effect of the temporal frequency on the isoluminance point might be also the result of the four cycle stimulus that used in these experiments. Anstis and Cavanagh (1983) used a similar four-cycle stimulus and also found little effect of temporal frequency perhaps because of the broad frequency spectrum of the square wave temporal modulation in this stimulus. Finally, a consistent increase in the amount of blue needed to equate a red or green color was found as the spatial frequency or the eccentricity was increased.

The differences in isoluminance ratios raise some difficulties in experiments where cell activity is studied using equiluminant color patterns. Defining equiluminant colors by heterochromatic flicker photometry, usually at 15 Hz and with 2 x 2 or 10 x 10 degrees squares, can provide significantly different isoluminance ratios from those expected in grating stimuli moving with the cell's optimal spatial frequency and velocity. The difference is expected to be even higher when static stimuli are used. In the monkeys tested in this study this difference could reach 16% of the luminance of the constant color. Therefore, for gratings of spatial frequencies lower than 1 cpd this effect will cause significantly higher residual luminance contrast than the axial or transverse chromatic aberrations.

As mentioned earlier, the hypothesis of motion and stereopsis being processed exclusively by the broad-band magno channel (Livingstone and Hubel, 1987 and 1988) is mainly based on evidence from experiments with isoluminant stimuli. Isoluminant stimuli are thought to be invisible to the

broad-band system because this system does not segregate cone input in the retinal ganglion cell layer, showing no wavelength-dependent activity at either the retina or LGN levels (De Valois et al., 1966, 1977; Wiesel and Hubel, 1966; Krueger, 1977; Schiller and Malpeli, 1978; Nothdurft and Lee, 1982; Derrington et al, 1984). In addition, the perception of motion and depth have been shown to deteriorate greatly when the stimuli are made isoluminant to their background (Gregory, 1977; Ramachandran and Gregory, 1978; Lu and Fender, 1972; Cavanagh et al., 1984; Livingstone and Hubel, 1987, 1988, Livingstone, 1988). It seems temptingly obvious to assign the processing of a perceptual attribute that is ill-processed at isoluminance to the broad-band system, which is thought to be silenced under these conditions. This straightforward reasoning, however, is sound only if the stimuli causing a behavioral deficit selectively silence one major pathway leaving the other unaffected, a point will be resolved in the next chapter.

The psychophysical experiments presented here, however, argue against a construct that attributes stereopsis and depth perception to the broad-band channel based on this reasoning. All the tasks measuring behavioral performance had clear minima near or at isoluminance as measured by the CIE standard observer. Only in the case of heterochromatic flicker photometry however, did these minima fall within the confidence limits of the chance levels (figure 2.13). For the random dot stereopsis and motion tasks as well as velocity discrimination, performance did drop at values near isoluminance but in no case did the minima fall to chance (figures 2.14-2.16). These perceptual

attributes although compromised, are not abolished. Comparison of stimuli of various excitation purities reveals that color information is the source of this residual performance. As color information is added, performance for both stereoscopic depth and motion detection (figures 2.30, 2.31 and 2.29) increases over the entire range of luminance contrast values tested. As might be expected, performance only falls to chance levels when little or no color information is present. Thus, color does contribute to the perception of stereoscopic depth and motion, albeit perception is not as robust as comparable conditions with a large luminance contrast. These results are in agreement with recent psychophysical studies (Cavanagh *et al.*, 1984; Cavanagh *et al.*, 1985; Mullen and Baker, 1985; Derrington and Badcock, 1985; Cavanagh and Favreau, 1985). In addition, color can support stereopsis of simple figures (Comerford, 1974; de Weert and Sadza, 1983), motion of gaussian filtered spots (Poeppel and Logothetis, 1989) and simple line figures (Ramachandran and Gregory, 1978; Cavanagh *et al.*, 1985).

How is it that wavelength information can support motion and stereopsis in some cases and not others? It has been suggested that color information does not contribute to situations that rely on global processes to segment information (Ramachandran and Gregory, 1978; Cavanagh *et al.*, 1985). This implies that wavelength information is still not integrated at higher levels of visual processing. Another possible explanation is that high spatial frequency displays may be inappropriate for isoluminance experiments. While the color-opponent channel does convey high spatial frequency information (Schiller *et*

al., 1990; Merigan *et al.*, 1991), theoretical work suggests that red/green color-opponent cells are multiplexing information at different spatial frequencies (Ingling and Martinez-Uriegas, 1985). It is proposed that these cells are band-pass tuned for luminance contrast and low-pass for chromatic information. Indeed, Mullen (1985) finds that contrast sensitivity functions are low-pass for chromatic gratings and band-pass for monochromatic gratings with the intersection of these curves at about 0.5 cycles per degree. The motion and stereopsis tasks where color can support perception contain low spatial frequency information whereas many instances where motion and depth fail at isoluminance employ high spatial frequency displays. In addition, while high spatial frequency texture discrimination is not possible at isoluminance, texture segregation of low spatial frequency stimuli is possible (McIlhagga *et al.*, 1990). Random dot displays inherently contain some low spatial frequency information, however, and this may explain why color does contribute to the motion and stereopsis tasks presented in this section. Thus, isoluminance experiments are very sensitive to stimulus configurations and luminance artifacts. Many experiments compare stimuli with high luminance contrast to isoluminant ones without a systematic examination of color contribution. The interpretation of these results have been extended to suggest that color is not involved with many aspects of perception. Caution should be exercised when interpreting such isoluminance experiments.

The measurements of the slow phase of the optokinetic nystagmus also argue against attributing motion to the broad-band system based on

isoluminance. The drifting color gratings always elicited strong optokinetic responses in both humans and monkeys. The perceived velocity of the gratings slows dramatically when the subject maintains fixation during the grating presentation. Removal of the fixation spot to allow OKN responses, considerably decreases the "slowing" effect observed at isoluminance, indicating that the signal used by the oculomotor centers to initiate and maintain nystagmus can be made available to the centers mediating motion perception. Since the oculomotor system receives its information about motion primarily from the broad-band system, one would predict that the gain of the OKN would be severely reduced. This brings into contention the assumption that mLGN cells are silenced at isoluminance.

Analogous arguments can be made for high-resolution form perception (*e.g.* texture), which is believed to be carried by the parvo/color-opponent pathway (Merigan *et al.*, 1991). If the parvo channel is unimpaired under isoluminant conditions, texture perception should not be degraded at isoluminance. Ramachandran (1987), however, finds that high spatial frequency texture discrimination is severely impaired at isoluminance. Psychophysical measurements of texture perception as a function of luminance (Logothetis *et al.*, 1990) shows that this attribute is compromised at isoluminance in a manner similar to both motion and stereoscopic depth. Another example is a hyperacuity task (Morgan and Aiba, 1985). These authors reported that vernier acuity, another visual ability attributable to the high resolution parvo channel, is severely reduced at isoluminance.

Another line of evidence contradicting a strict association of visual attributes compromised at isoluminance to the broad-band system comes from the finding that some of these attributes are devastated after selective lesion of the parvocellular layers of LGN (Schiller *et al.*, 1990). Stereopsis, for instance, is a visual capacity that seems to require both channels in order to cover the whole spatial frequency range. High spatial frequency random dot stereograms cannot mediate depth perception in monkeys with selective parvocellular lesions. In contrast, perception of depth for these animals is unaffected for low spatial frequency stereograms (ibid). The preceding evidence suggests that isoluminance experiments cannot conclusively establish the underlying neural pathways for motion and stereoscopic depth perception.

The experiments presented in this chapter demonstrate that color information is utilized for the perception of motion and stereopsis since an increase in color contrast improves perceptual performance. These findings immediately imply that the operations underlying motion and stereoscopic depth perception are not simply luminance-based. In addition, since performance on the stereo and depth tasks increased at isoluminance with the addition of color, this input must be doing more than simply resolving ambiguities or "linking" features, a fact that is supported by Livingstone and Hubel (1987).

REFERENCES

Allen, F. Persistence of vision in colour-blind subjects. Physical Reviews 15:193-225, 1902.

Anstis, S. and Cavanagh, P. "A minimum motion technique for judging equiluminance." In: Colour Vision: Physiology and Psychophysics, ed. J.D. Mollon and L.T Sharpe. Academic Press, London (1983).

Anstis S.M., Cavanagh, P., Maurer, D. and Lewis, T. Optokinetic technique for measuring infant's responses to color. Applied Optics 27:1510-1516, 1987.

Bartley, S.H. Subjective brightness in relation to flash rate and the light-dark ratio. Journal of Experimental Psychology 23:313-319, 1938.

Bartley, S.H. Vision, Van Nostrand, New York (1941).

Bartley, S.H. "A clarification of some of the procedures and concepts involved in dealing with the optic pathway." In: The Visual System: Neurophysiology and Psychophysics, eds. R. Jung and H. Kornhuber. Springer-Verlag, Berlin (1961).

Bedford, R.E. and Wyszecki, G. Axial chromatic aberration of the human eye. Journal of the Optical Society of America 47:564-565, 1957.

Bradley, A., Thibos, L. and Zhang, X. Luminance artifacts in the retinal images of isoluminant color-modulated stimuli: Effect of correcting axial chromatic aberration. Investigative Ophthalmology and Visual Sciences Supplement 30:507, 1989.

Campbell, F.W. and Maffei, L. The influence of spatial frequency and contrast on the perception of moving patterns. Vision Research 21:713-721, 1981.

Cavanagh, P. and Anstis, S. The contribution of color to motion in normal and color-deficient observers. Vision Research (in press).

Cavanagh, P., Boeglin, J. and Favreau, O.E. Perception of motion in equiluminous kinematograms. Perception, 14:151-162, 1985.

Cavanagh, P. and Favreau, O.E. Color and luminance share a common motion pathway. Vision Research 25:1595-1601, 1985.

Cavanagh, P., MacLeod, D.I.A. and Anstis, S.M. Equiluminance: Spatial and temporal factors and the contribution of blue-sensitive cones. Journal of the Optical Society of America A 4:1428-1438, 1987.

Cavanagh, P., Tyler, C.W. and Favreau, O.E. Perceived velocity of moving chromatic gratings. Journal of the Optical Society of America, A, 1:893-899, 1984.

Comerford, J.P. Stereopsis with chromatic contours. Vision Research 14:975-982, 1974.

De Valois, R.L., Abramov, E. and Jacobs, G.H. Analysis of response patterns of LGN cells. Journal of the Optical Society of America 56:966-977, 1966.

De Valois, R.L., Morgan, H.C., Polson, M.C., Mead, W.R. and Hull, E.M. Psychophysical studies of monkey vision: I. Macaque luminosity and color vision tests. Vision Research 14:53-67, 1974.

De Valois, R.L., Snodderly, Jr., D.M., Yund, E.W. and Hepler, N.K. Responses of macaque lateral geniculate cells to luminance and color figures. Sensory Processes 1:244-259, 1977.

de Weert, C.M.M. and Sadza, K.J. "New data concerning the contribution of colour differences to stereopsis." In: Colour vision, ed. J.D. Mollon. Academy Press, London, pp. 553-562, 1983.

Derrington, A.M. and Badcock, D.R. The low level motion system has both chromatic and luminance inputs. Vision Research 25:1874-1884, 1985.

Derrington, A.M., Krauskopf, J. and Lennie, P. Chromatic mechanisms in lateral geniculate nucleus of macaque. Journal of Physiology 357:241-265, 1984.

DeYoe, E.A. and Van Essen, D.C. Concurrent processing streams in monkey visual cortex. Trends in Neuroscience 11:219-226, 1988.

Dursteller, M.R., Wurtz, R.H. and Newsome, W.T. Directional pursuit deficits following lesions of the foveal representation within the superior temporal sulcus of the macaque monkey. Journal of Neurophysiology 57:1262-1287, 1987.

Gouras, P. Identification of cone mechanisms in monkey ganglion cells. Journal of Physiology 199:533-547, 1968.

Gouras, P. and Zrenner, E. Color Vision: A review from a

neurophysiological perspective. Progress in Sensory Physiology 1:139-179, 1981.

Gregory, R.L. Vision with isoluminant colour contrast: 1. A projection technique and observations. Perception 6:113-119, 1977.

Held, R. "The rediscovery of adaptability in the visual system: Effects of extrinsic and intrinsic chromatic dispersion." In: Visual Coding and Adaptability, ed. S. Harris. Erlbaum, Hillsdale, NJ (1980).

Howarth, P.A. and Bradley, A. The longitudinal chromatic aberration of the human eye, and its correction. Vision Research 26:361-366, 1986.

Ingling, Jr, C.R. and Martinez-Uriegas, E. The spatiotemporal properties of the r-g x-cell channel. Vision Research 25:33-38, 1985.

Judd, D.B. (1952) In: CIE (Commission Internationale de l'Eclairage) Proceedings, 12th Session. Stockholm, 1951 1:11, 1952.

Judge, S.J., Richmond, B.J. and Chu, F.C. Implantation of magnetic search coils for measurement of eye position: An improved method. Vision Research 20:535-538, 1980.

Julesz, B. Binocular depth perception without familiarity cues. Science 45:356-362, 1964.

Komatsu, H. and Wurtz, R.H. Relation of cortical areas MT and MST to pursuit eye movements. I. Localization and visual properties of neurons. Journal of Neurophysiology 60:580-603, 1988.

Krueger, J. Stimulus dependent colour specificity of monkey lateral geniculate neurones. Experimental Brain Research 30:297-311, 1977.

Le Grand, Y. Form and Space Vision, transl. M. Millodot and G.G. Heath. Indiana Press University, Bloomington (1967).

Lennie, P. Parallel visual pathways: A review. Vision Research 20:561-594, 1980.

Lewis, A.L., Katz, M. and Oehrlein, C. A modified achromatizing lens. American Journal of Optometry and Physiological Optics 59:909-911, 1982.

Lisberger, S.G., Morris, E.J., and Tychsen, L. Visual motion processing and sensory-motor integration for smooth pursuit eye movements. Annual Review of Neuroscience 10:97-129, 1987.

Livingstone, M.S. Art, illusion and the visual system. Scientific American 258:78-85, 1988.

Livingstone, M.S. and Hubel, D.H. Psychophysical evidence for separate channels for the perception of form, color, movement, and depth. Journal of Neuroscience 7:3416-3468, 1987.

Livingstone, M. and Hubel, D. Segregation of form, color, movement, and depth: Anatomy, physiology, and perception. Science 240:740-749, 1988.

Logothetis, N.K., Schiller, P.H., Charles, E.R. and Hurlbert, A.C. Perceptual deficits and the activity of the color-opponent and broad-band pathways at isoluminance. Science 247:214-217, 1990.

Lu, C. and Fender, D.H. The interaction of color and luminance in stereoscopic vision. Investigative Ophthalmology 11:482-490, 1972.

Maunsell, J.H.R. "Physiological evidence for two visual subsystems." In: Matters of intelligence, ed. L. Vaina, 1985.

McIlhagga, W., Hine, T., Cole, G.R. and Snyder, A.W. Texture segregation with luminance and chromatic contrast. Vision Research 30:489-495, 1990.

Merigan, W.H., Katz, L.M. and Maunsell, J.H.R. The effects of parvocellular lateral geniculate lesions on the acuity and contrast sensitivity of macaque monkeys. Journal of Neuroscience 11:994-1001, 1991.

Moreland, J.D., Kogan, D. and Smith, S.S. "Optokinetic nystagmus: An objective indicator of defective color vision. In: Color deficiencies III. International Symposium: Modern Problems of Ophthalmology, eds. Basel and Karger. Amsterdam (1975).

Morgan, M.J. and Aiba, T.S. Positional acuity with chromatic stimuli. Vision Research 25:689-695, 1985.

Mullen, K.T. The contrast sensitivity of human color vision to red-green and blue-yellow chromatic gratings. Journal of Physiology 359:381-400, 1985.

Mullen, K.T. and Baker, C.L. A motion aftereffect from an isoluminant stimulus. Vision Research 25:685-688, 1985.

Newsome, W.T. and Wurtz R.H. Probing visual cortical function with discrete chemical lesions. Trends in Neuroscience 11:394-400, 1988.

Newsome, W.T., Wurtz, R.H., Dursteller, M.R., and Mikami, A. Deficits in visual motion processing following ibotenic acid lesions of the middle temporal visual area of the macaque monkey. Journal of Neuroscience 5:825-840, 1985.

Newsome, W.T., Wurtz, R.H., and Komatsu, H. Relation of cortical areas MT and MST to pursuit eye movements. II. Differentiation of retinal from extraretinal inputs. Journal of Neurophysiology 60:604-620, 1988.

Nothdurft, H.C. and Lee, B.B. Responses to coloured patterns in the macaque lateral geniculate nucleus: Analysis of receptive field properties. Experimental Brain Research 48:55-65, 1982.

Pitt, F.H.G. The nature of normal trichromatic and dichromatic vision. Proceedings of the Royal Society (London) B132: 101-117, 1944.

Poeppel, D.E. and Logothetis, N.K. Chrominance information can be used by the oculomotor system to program saccades to moving targets. Investigative Ophthalmology and Visual Sciences Supplement 30:112, 1989.

Powell, I. Lenses for correcting chromatic aberration of the eye. Applied Optics 20:4152-4155, 1981.

Rabelo, C. and Gruesser, O.J. Die Abhaengigkeit der subjectiven Helligkeit intermittierender Lichtreize von der Flimmerfrequenz (Bruecke-Effekt, "brightness enhancement"): Untersuchungen bei verschiedener Leuchtdichte und Feldgroesse. Psychol. Forsch., 26:299-312, 1961.

Ramachandran, V. "Visual perception of surfaces: A biological theory." In: The Perception of Illusory Contours, eds. S. Petry and G.E. Meyer. Springer, New York (1987).

Ramachandran, V. and Gregory, R. Does colour provide an input to human motion perception? Nature 275:55-56, 1978.

Remmel, R.S. An inexpensive eye movement monitor using the scleral search coil technique. IEEE Trans. Biomed. Engineering. Vol. BME-31, No. 4:388-389, 1984.

Robinson, D.A. A method of measuring eye movement using a scleral search coil in a magnetic field. IEEE Trans. Biomed. Electronics. 10:137-145, 1963.

Rood, O.N. On a photometric method which is independent of color. American Journal of Science 46:173-176, 1893.

Schiller, P.H. The central visual system. Vision Research 26:1351-1386, 1986.

Schiller, P.H., Logothetis, N.K. and Charles, E.R. Functions of the colour-opponent and broad-band channels of the visual system. Nature 343:68-70, 1990.

Schiller, P.H. and Malpeli, J.G. Functional specificity of lateral geniculate nucleus laminae of the rhesus monkey. Journal of Neurophysiology 41:788-797, 1978.

Shapley, R. and Perry, V.H. Cat and monkey retinal ganglion cells and their visual functional roles. Trends in Neuroscience 9:229-235, 1986.

Thompson, P. Perceived rate of movement depends on contrast. Vision Research 22:377-380, 1982.

Van Essen, D.C. and Maunsell, J.H.R. Hierarchical organization and functional streams in the visual cortex. Trends in Neuroscience 63:370-375, 1983.

Veringa, F. Enige natuurkundige aspecten van het zien vangemoduleerd lcht. Thesis. Amsterdam, The Netherlands (1961).

Wald, G. and Griffin, D.R. The change in refractive power of the human eye in dim and bright light. Journal of the Optical Society of America 37:321-366, 1947.

Wagner, G. and Boynton, R.M. Comparison of four methods of heterochromatic photometry. Journal of the Optical Society of America 62:1508-1515, 1972.

Wiesel, T.N. and Hubel, D.H. Spatial and chromatic interactions in the lateral geniculate body of the rhesus monkey. Journal of Neurophysiology 29:1115-1156, 1966.

Wolfe, J.M. and Owens, D.A. Is accommodation colorblind? Focusing chromatic contours. Perception 10:53-62, 1981.

FIGURES

Figure 2.1 Luminance and color characteristics of the stimuli used in this study. Definition of excitation purity. The color triangle **BGR** of the display monitor in CIE space is illustrated. Any given combination of the monitor gun values will display a color with CIE coordinates confined within this triangle. The R, G, B vertices represent the points in CIE space of the monitor color primaries; that is, the color of each gun when turned on alone. A color can be defined either in the CIE space or directly in the RGB system. Transformations between the two systems require a fourth reference point, the coordinates of the monitor white (**W**) adjusted to D9300 for the monitor used in this study. The excitation purity of a color **c** ($\mathbf{EP_c}$) is the ratio of the distance (**Wc**) in the chromaticity plane between the coordinates of white (**W**) and the coordinates of **c** to the distance (**WC**) along the same line from white to the point **C** defined by the intersection of this line with the boundary of the CIE triangle.

Figure 2.2 Definition of color contrast for sinusoidal gratings. For the grating stimuli used in the velocity discrimination experiment the color saturation is expressed as color contrast rather than excitation purity. Color contrast (**C**) for these red/green gratings is defined as the ratio of the amplitude (**d**) of the color change along the red-green line of the CIE chromaticity diagram to the maximum change possible between the red and green phosphors (**D**) of our display. The red/green gratings were generated by adding two red and green sine waves 180° out of phase.

Figure 2.3 Definition of luminance contrast. Luminance contrast was expressed as the difference between the two amplitudes of the red and green modulations ($\mathbf{R_{amp}}$, $\mathbf{G_{amp}}$), divided by the mean luminances of the two wave forms ($\mathbf{R_{mean}}$, $\mathbf{G_{mean}}$). For the texture and random dot patterns contrast was given as the log difference between the luminance of the dots or textures and the luminance of the background.

Figure 2.4 Luminance contrast artifacts due to axial chromatic aberrations. Luminance contrast induced by axial chromatic aberration is plotted versus the spatial frequency of the stimulus. The shaded area indicates the spatial frequencies mainly used in these experiments. For an isoluminant pattern containing up to 2 cpd the luminance contrast induced by the observer controlled reaccommodation is approximately 4%.

Figure 2.5 Luminance contrast artifacts due to lateral chromatic aberrations. **A)** The dotted and thin black lines represent two different wavelengths modulated 180 degrees out of phase. The thick black line represents the resulting luminance artifact. As more cycles of the stimulus are displayed, more luminance artifact is introduced. **B)** Calculated lateral chromatic

aberration as a function of spatial frequency for a fixed area.

Figure 2.6 Time course of an experimental trial. Each trial begins with the appearance of a fixation spot at the center of the screen. In the discrimination paradigm shown in the upper panel, 4 stimuli, one of which is the target, appear in the periphery after the monkey fixates on the fixation spot for 200 to 400 ms. The task for the monkeys is to locate the target with a single direct saccade to it within a choice time of 300 to 600 ms. Human subjects responded by depressing the appropriate button on a push-button box. The location of the buttons on the box corresponded to the location of the targets on the screen. In the detection paradigm, illustrated in the lower panel, after a 300 ms fixation the fixation spot is turned off and a target appears in one of 4 locations in the periphery. The task is to detect the target by making a single saccade to it. Saccades to other locations or pressing of the wrong button abort the trial. The squares with dashed lines indicate the electronic windows defining the boundaries of correct fixation or target localization. Trials are separated by a 2 sec intertrial interval. The lightly shaded lines represent eye movement traces.

Figure 2.7 Flicker photometry data from 5 human subjects collected by adjusting the intensity of the variable color through a potentiometer. A linear relationship between the values of the variable color (one of the primary colors in this experiment) and of the constant color (white in this experiment) can be seen over the whole range of the tested intensities. Both constant and variable color luminances are given as a percent of the maximum possible luminance for each color. A small deviation from the linearity was found only for the maximum value of the blue color.

Figure 2.8 Random dot stereograms. Dot density was 50% and dot size was 4x4 pixels (14 x 14 min of arc). A low pass filtered version of these stereograms was also used to minimize axial chromatic aberrations. The shaded square region indicates the set of dots that were shifted to give disparities from 3.5 to 14 min of arc.

Figure 2.9 Random dot motion stimulus. The small shaded square area indicates the region within which the display was scrolled yielding the perception of locally drifting dots.

Figure 2.10 Velocity discrimination stimulus. Four drifting gratings were presented one of which (large arrow) was drifting with a different velocity.

Figure 2.11 A) The minimum motion stimulus: Four gratings, two chromatic and two luminance gratings, were displayed sequentially in the same location of the screen. Each grating is displaced downwards by one-quarter cycle from the previous one, and it represents the sum of two sinusoidal modulations (e.g. red and green) at 100% contrast. The luminance gratings were of a 15% contrast. The lighter shading in the figure means more luminous color,

regardless of whether it is red, green or yellow. The direction of the apparent motion depends on the relative amplitudes of the sinusoidal luminance modulation of the two colors composing the chromatic gratings. When the red modulation is higher than the green modulation (brighter red bars) then upward motion will be seen as indicated by the arrows. Conversely, higher green modulation yields downward perceived motion. When both colors have equal luminance no association can be made between the light or dark bars of the luminance gratings and the colors in the chromatic gratings; subsequently, no consistent motion will be seen. **B)** Color and luminance contrast of the stimuli: The color gratings were generated by adding the two sine waves (could be red and green, or green and blue, or red and blue) 180° out of phase. Here we use the red/green gratings as an example. The same definitions hold also for the other combinations. Color contrast (C) for the red/green gratings was defined as the ratio of the amplitude (d) of the color change along the red-green line of the CIE chromaticity diagram to the maximum change possible between the red and green phosphors (D) of our display for a given luminance value represented by the overall size of the color triangle. Different amplitudes of the red and green modulations (thin solid sine waves) result in a luminance modulation indicated by the thick solid sine wave. Luminance contrast (L) was expressed as the difference between the two amplitudes of the red and green (R_{amp}, G_{amp}), divided by the mean luminances of the two wave forms (R_{mean}, G_{mean}).

Figure 2.12 Description of a single trial in the motion discrimination task used to determine isoluminance points. Each trial began with the appearance of a central fixation spot. After the monkey fixated it for 200 to 300 ms the minimum motion stimulus was presented foveally (upper series of displays; no fixation spot during grating presentation) or peripherally (lower series of displays; fixation spot is always present). The stimulus was replaced first by the initial fixation spot (third display) and subsequently by two spots on the right and the left of the fixation spot (fourth display). Perception of upward motion was signaled by a saccade to the right spot; a saccade to the left spot was required following the perception of downward movement.

Figure 2.13 Isoluminance defined through heterochromatic flicker photometry. Percent correct is plotted as a function of the contrast which is defined as the log difference of the luminance of the two colors. Data from individual subjects are shown in separate panels. Each data represents the average of 24 blocks, each block consisting of 40 presentations of the stimuli. The shaded area shows the confidence interval for a result different from chance on a given luminance contrast for significance at the 0.01 level. Stimulus is a 2x2 degree square flickering at 15 Hz between a gray of 10 cd/m2 and a red varying with 0.04 log unit steps. Color purity was 100%. The upper panels show the performance of three human subjects and the lower panels are data from three rhesus monkeys. When the luminance contrast is zero, as defined with a photometer the performance of all subjects falls to a minimum.

Figure 2.14 Stereoscopic depth perception at isoluminance. Conventions as in figure 2.7. Each data represents the average of 36 blocks each block consisting of 24 presentations. Depth perception is deteriorated but not abolished at isoluminance.

Figure 2.15 Motion perception at isoluminance. Results from three human subjects and three monkeys. Conventions as in figure 2.13. Here, however, each data point represents the average of 16 blocks, each block consisting of 24 presentations of the stimuli.

Figure 2.16 Velocity discrimination at isoluminance. Performance is plotted against nine luminance contrast values (0.04 log units increments) and 2 chrominance modulations (0 and 75%). The spatial frequency of the gratings was 1.3 cpd. Green had a luminance (100% modulation amplitude) of 13 cd/m2. The filled circles show performance for gratings having a color modulation of 75% and the lower for color modulation of 0%. The shaded area shows the confidence interval for chance level performance. Each data represents the average of 24 blocks. It is evident that the performance of the monkey at isoluminance remains above chance levels. At isoluminance there is a consistent decrement in performance. For colored gratings, however, the performance remains above chance levels for all luminance contrast values.

Figure 2.17 The plot in this figure shows the percent of the trials in which the monkey reported seeing upward motion (solid circles) or downward motion (solid squares). Standard error bars are shown. The lines through the data points represent the best fitting 5th order polynomials. The point where the two lines cross represents the point at which the monkey saw up 50% of the time and down 50% of the time; in other words there was no detectable motion, and the performance was at chance level. Accordingly, the green luminance value at which the two lines cross is an estimate of the isoluminant point. In this case the luminance of the green needed to null the motion percept when combined with the red luminance of 13.00 cd/m^2 was 12.80 cd/m^2.

Figure 2.18 Vertical eye position traces for trials in which the red/green luminance ratio was high (A), for trials in which the red/green ratio was low (C) and for trials in which the red/green ratio was 1.0 (B). All of the eye traces are aligned on the time when the grating motion began. In the top panel, it is evident that the smooth nystagmic eye movements are consistently upward; this is a red/green ratio for which the apparent motion is upward. When the red/green luminance ratio was balanced (middle panel), and the monkey's report fell to chance levels, the gain of pursuit was near zero. Crossing this isoluminant point reverses the direction of the optokinetic response of the monkey and for higher green luminance only downward eye movements were seen (bottom panel).

Figure 2.19 Velocity of the slow phase of the nystagmus for different

luminance ratios for gratings of 0.7 cpd drifting at 3.0 Hz. The results are plotted as a function of the green luminance for a 13 cd/m^2 red luminance. Each data point represents the average eye velocity over 50 trials. The vertical bars indicate the standard errors. As the red/green luminance ratio decreases, the eye velocity decreases from high positive values, reverses sign and continues to negative values. The point at which the eye velocity is 0.0 represents in another way the red/green isoluminance ratio.

Figure 2.20 **A)** The amplitude of the green luminance at which the perceptual choice was random for a constant red luminance of 13 cd/m^2 as a function of spatial frequency for 3 temporal frequencies for the monkey 87-45. Each data point represents the average of 10 measurements. The vertical bars are the standard errors. **B)** Similar to figure 2.20a except for monkey 87-46.

Figure 2.21 **A)** The amplitude of the blue luminance at which the perceptual choice was random for a constant green luminance of 12 cd/m^2 as a function of spatial frequency for 2 temporal frequencies for the monkey 87-45. Each data point represents the average of 10 measurements. The vertical bars are the standard errors. **B)** Similar to figure 7A except for monkey 87-46.

Figure 2.22 **A)** The amplitude of the blue luminance at which the perceptual choice was random for a constant red luminance of 12 cd/m^2 as a function of spatial frequency for 2 temporal frequencies for the monkey 87-45. Conventions like figures 2.20 and 2.21. **B)** Similar to figure 2.22a except for monkey 87-46.

Figure 2.23 **A)** Scatter plot of the green luminance at which the zero crossing of the eye movement velocity occurred as a function of the green luminance at which the monkey's perceptual choice of motion direction was at chance level. All the data were collected with a constant red luminance value of 13.0 cd/m^2. Each data point is the average of 50 measurements and represents a single combination of spatial and temporal frequency. The variation in the green luminance values reflects the variation in isoluminance observed at different spatial and temporal frequencies. A significant correlation ($r = 0.814$) was found between the green luminance values obtained by the two behavioral measurements. The heavy diagonal line represents the regression line between the eye movement defined and report defined isoluminance ratios. The slope of the line was 0.80. **B)** Similar to 2.23a but for monkey 87-46 ($r = 0.82$ and slope = 1.06).

Figure 2.24 Isoluminance ratios for red/green, green/blue and red/blue gratings of 0.7 cpd spatial frequency and 3 Hz temporal frequency for 0, 3 and 6 degrees eccentricities.

Figure 2.25 Typical eye movement response to the drifting gratings. The upper trace shows the response of the eye to a leftward moving grating, and

the lower trace, the response to a rightward moving grating. The velocity of the slow phase of OKN was determined as the mean slope of the regression lines within the limits illustrated by the dashed parallelograms. Gain was then computed as the ratio of eye to target velocity.

Figure 2.26 OKN velocity gain as a function of luminance contrast for chromatic gratings (monkey 85-19). Each data represents the mean of 20 trials. The small vertical bars indicate the standard deviation. Data were collected for a combination of 2 spatial frequencies and 4 drift velocities. Nine contrast values ranging from 0 to 25% luminance contrast were tested. No systematic variation of the OKN gain over the tested contrast values was measured as one can see in all 8 plots.

Figure 2.27 OKN velocity gain as a function of luminance contrast for chromatic gratings (monkey 82-19). Conventions as in Figure 2.26. A small decrement in the OKN gain was measured only for drift velocity of 14 deg/sec.

Figure 2.28 OKN velocity gain as a function of luminance contrast for achromatic gratings (monkey 85-19). Conventions as in Figure 2.26. There is a significant decrement in the OKN gain for luminance contrast less than 10%.

Figure 2.29 The contribution of color to motion perception. Percent correct is plotted as a function of the contrast which is defined as the log difference of the luminance of the two colors. Each data represents the average of 24 blocks, each block consisting of 40 presentations of the stimuli. The shaded area shows the confidence interval for a result different from chance on a given luminance contrast for significance at the 0.01 level. The results from a human subject are shown on the left and from a macaque monkey on the right panel for different excitation purity levels. As shown in the inset, different line styles indicate different purity levels. At isoluminance there is a consistent decrement in performance for all purity levels. As the purity of the color increases, however, increasing the effective contrast the performance at isoluminance improves.

Figure 2.30 The contribution of color to stereoscopic depth perception. Conventions as in figure 2.27. Each data represents the average of 36 blocks each block consisting of 24 presentations. At isoluminance there is a consistent decrement in performance for both filtered and unfiltered images. As the purity of the color increases, however, increasing the effective contrast the performance at isoluminance improves.

Figure 2.31 Similar to figure 2.28 but for low-pass filtered images. Seven luminance contrast values were tested, 0.08, 0.12 and 0.16 log units from isoluminance for the two humans subjects (left panel) and 0.08, 0.16 and 0.24 log units from isoluminance for one monkey. Conventions as in figure 7.

Figure 2.32 Pooled data from three subjects and six monkeys in the flicker, motion, and stereoscopic depth detection tasks. The upper three panels show data form human subjects. The abscissa is the red value used as constant color in all tasks. The ordinate shows the green luminance for which minimum performance was obtained. The slope of the regression line gives the average color ratio at which minimum performance was observed. Correlation coefficients (r) and (r^2) are given. Vertical bars show the standard errors of the mean for 100 trials at each point. It can be seen that the red/green ratio for which motion and stereoscopic depth perception is degraded is very close to the isoluminance point as defined with flicker photometry (left hand upper panel). Similar results were shown for six monkeys in the lower three plots.

Excitation purity (EP)

$$EP_c = \frac{Wc}{WC} \times 100$$

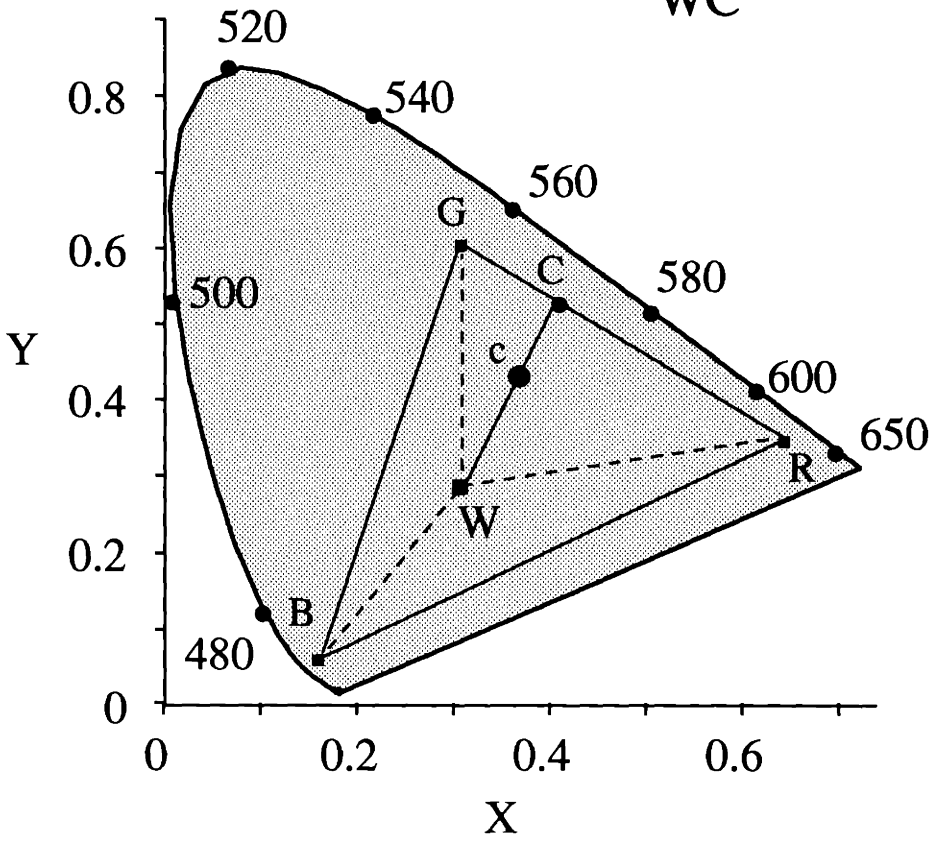

Figure 2.1

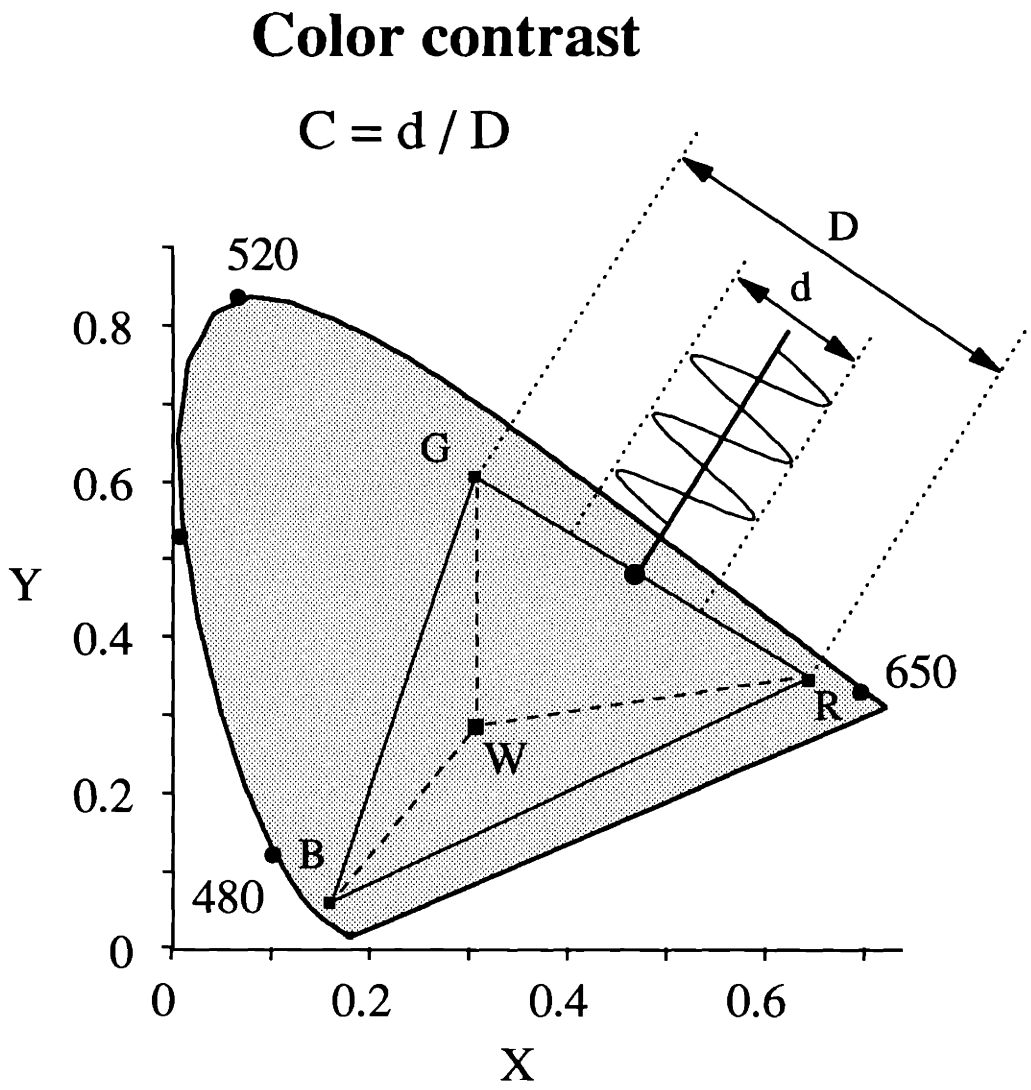

Figure 2.2

Luminance contrast

$$L = \frac{R_{mod} - G_{mod}}{R_{mean} + G_{mean}}$$

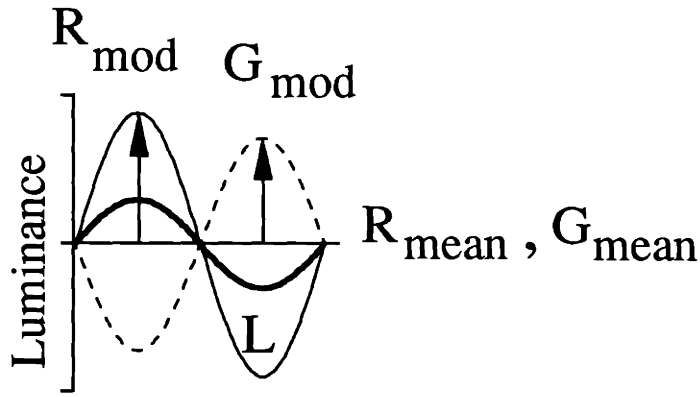

Figure 2.3

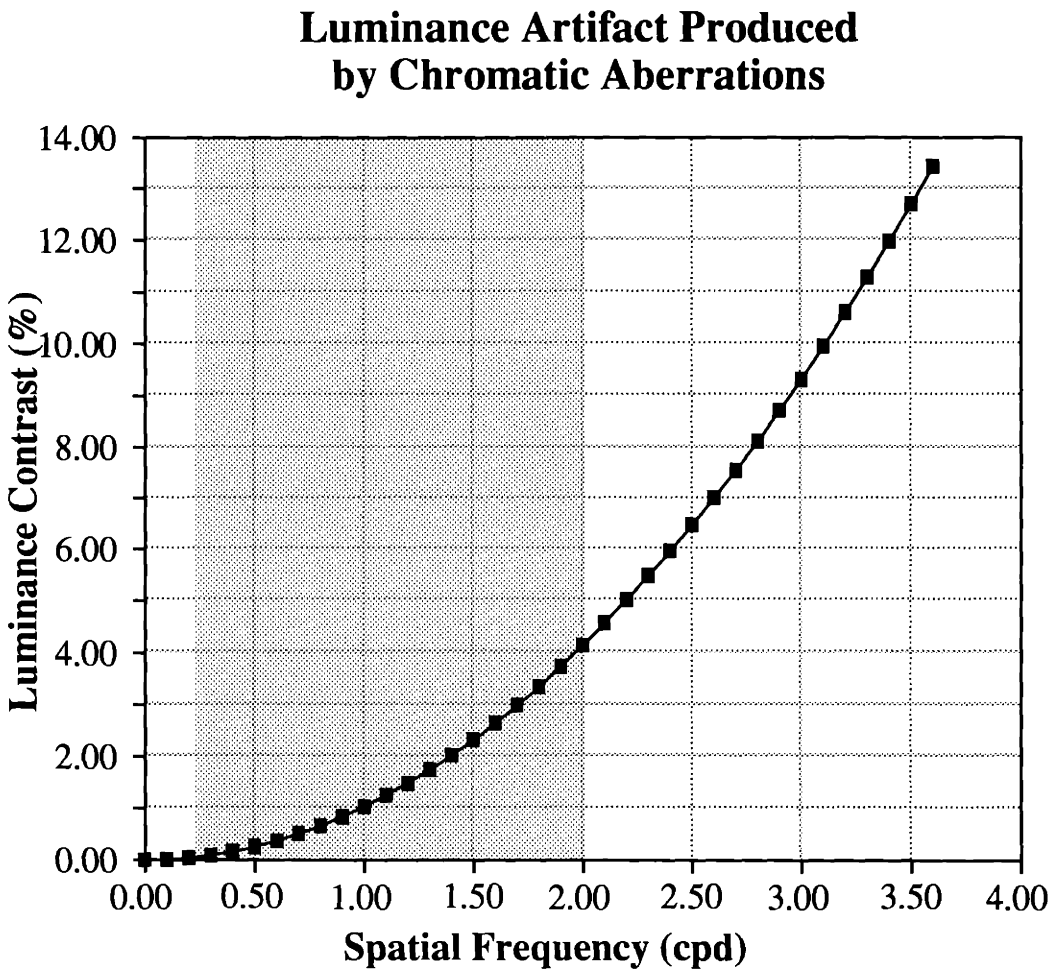
Luminance Artifact Produced
by Chromatic Aberrations
Luminance Contrast (%)
14.00
12.00
10.00
8.00
6.00
4.00
2.00
0.00
0.00
0.50
1.00
1.50
2.00
2.50
3.00
3.50
4.00
Spatial Frequency (cpd)

Figure 2.4

Luminance Artifacts Due to Lateral Chromatic Aberrations

A.

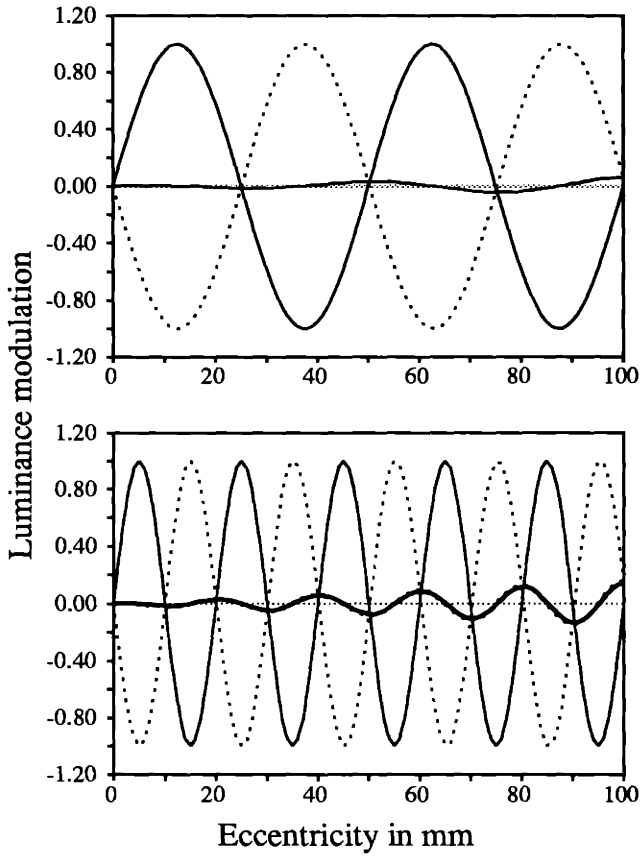

B.

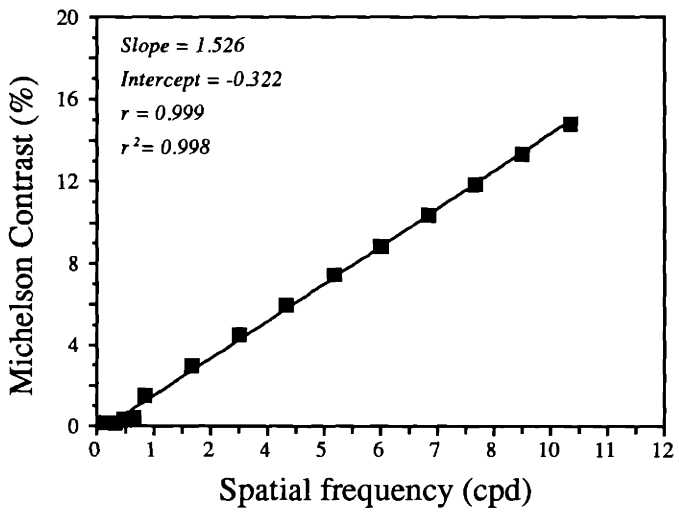

Figure 2.5

A. **DISCRIMINATION**

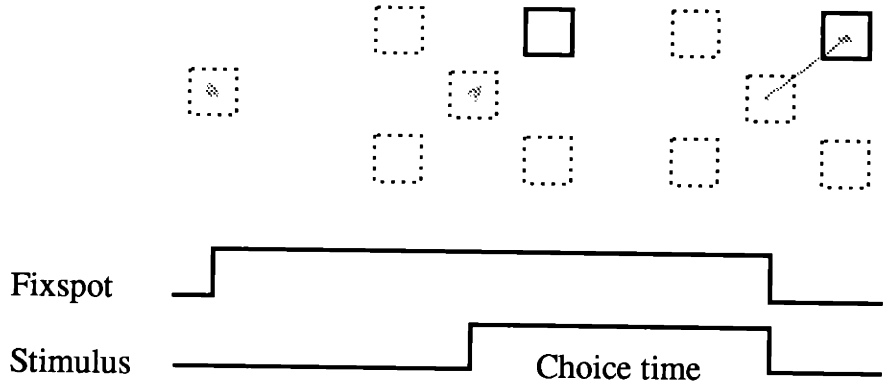

B. **DETECTION**

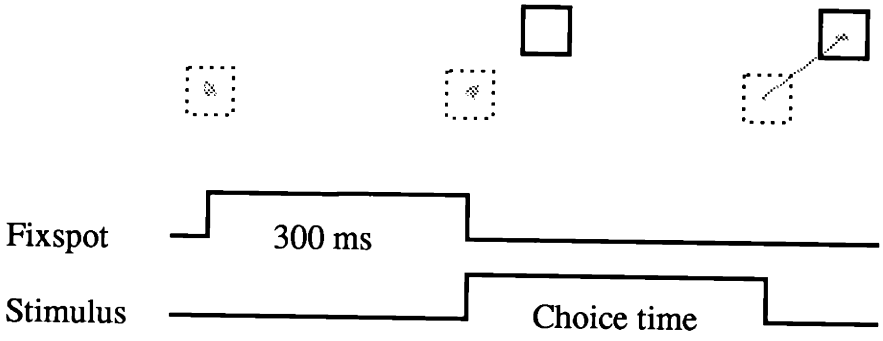

Figure 2.6

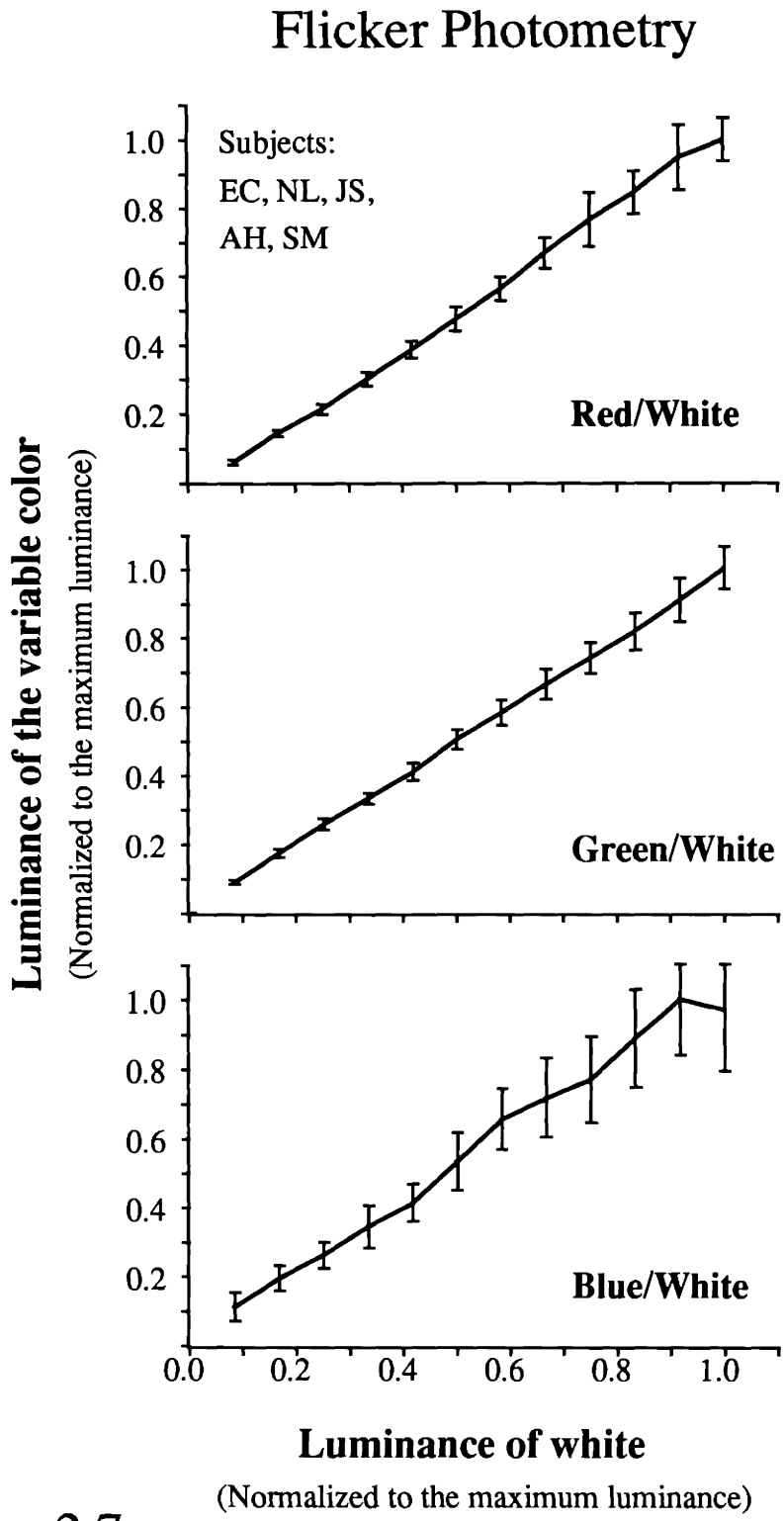
Flicker Photometry
Subjects:
EC, NL, JS,
AH, SM
Red/White
Green/White
Blue/White
1.0
0.8
0.6
0.4
0.2
0.0
0.2
0.4
0.6
0.8
1.0
Luminance of the variable color
(Normalized to the maximum luminance)
Luminance of white
(Normalized to the maximum luminance)

Figure 2.7

Random Dot Stereopsis

Figure 2.8

Random Dot Motion Detection

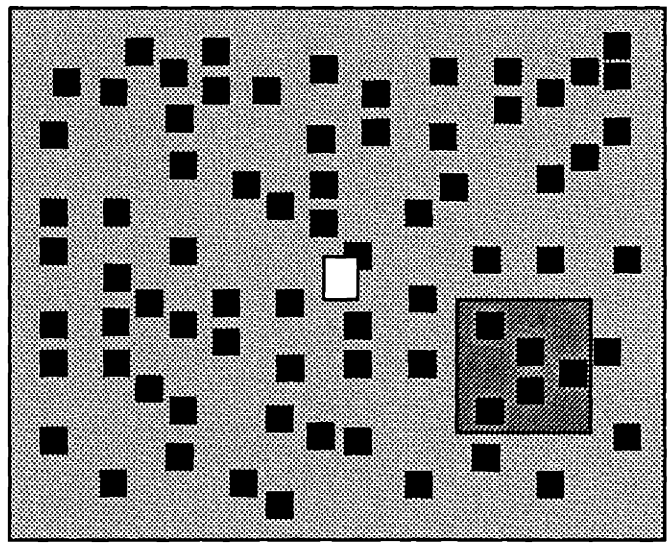

Figure 2.9

Stimuli For The Velocity Discrimination Task

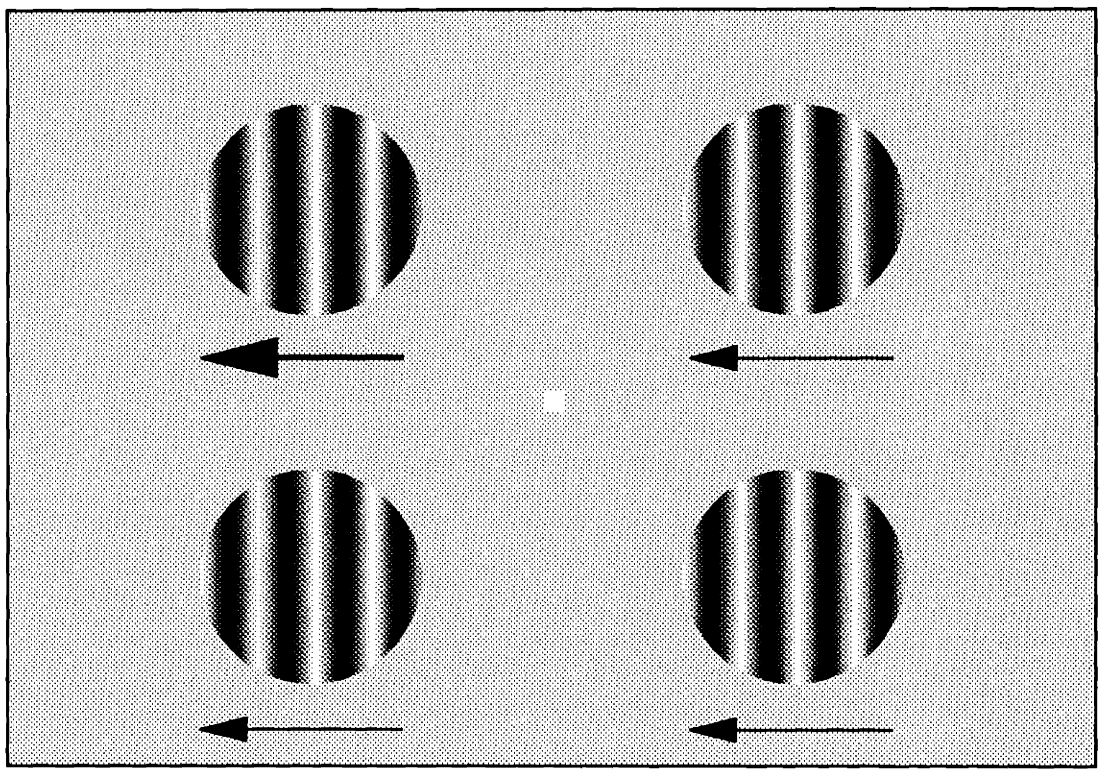

Figure 2.10

Minimum Motion Stimulus

A. Upward apparent motion

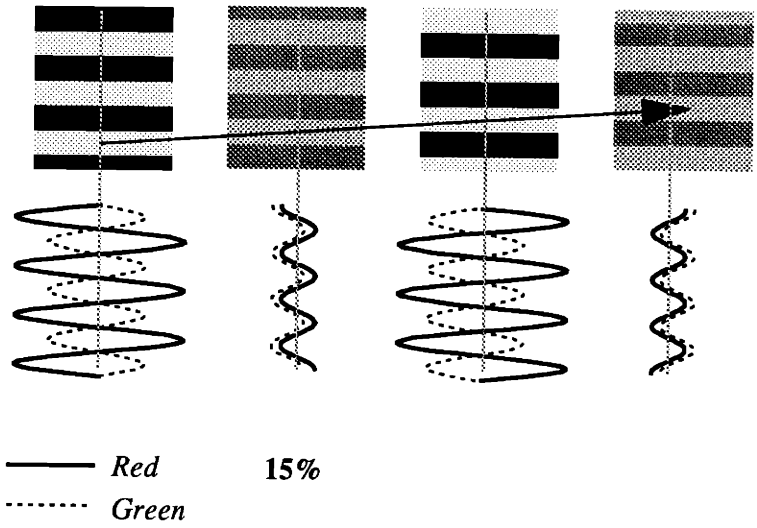

B. Downward apparent motion

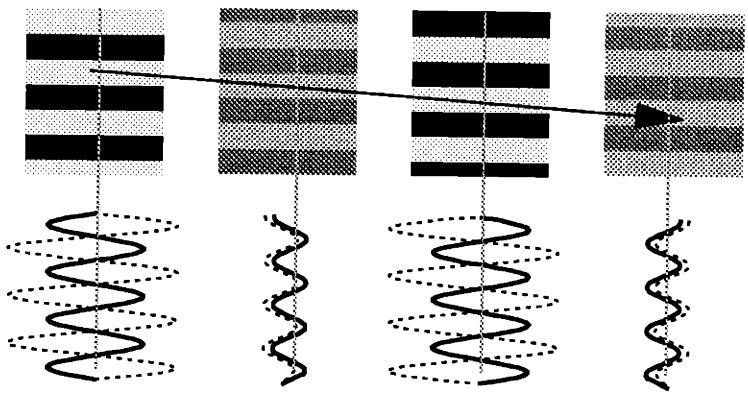

Figure 2.11

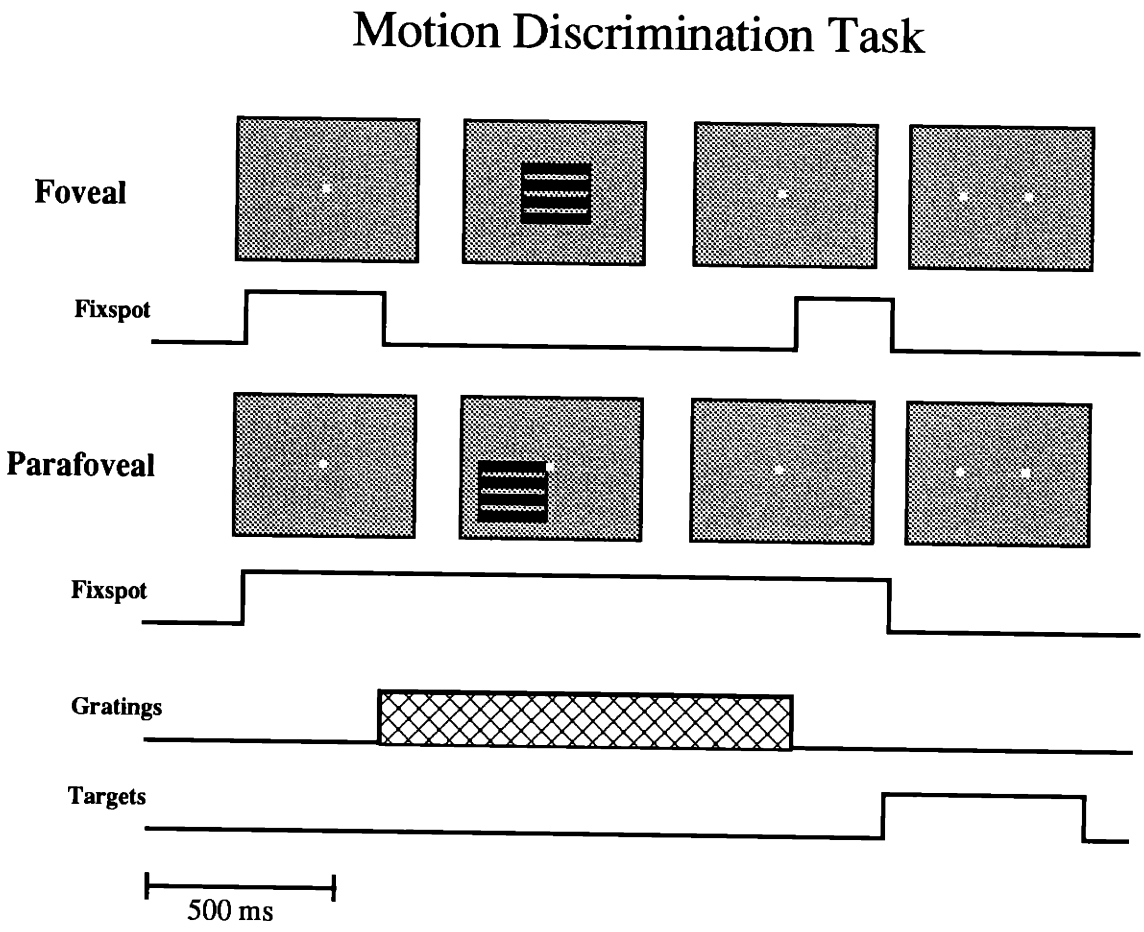
Motion Discrimination Task
Foveal
Fixspot
Parafoveal
Fixspot
Gratings
Targets
500 ms

Figure 2.12

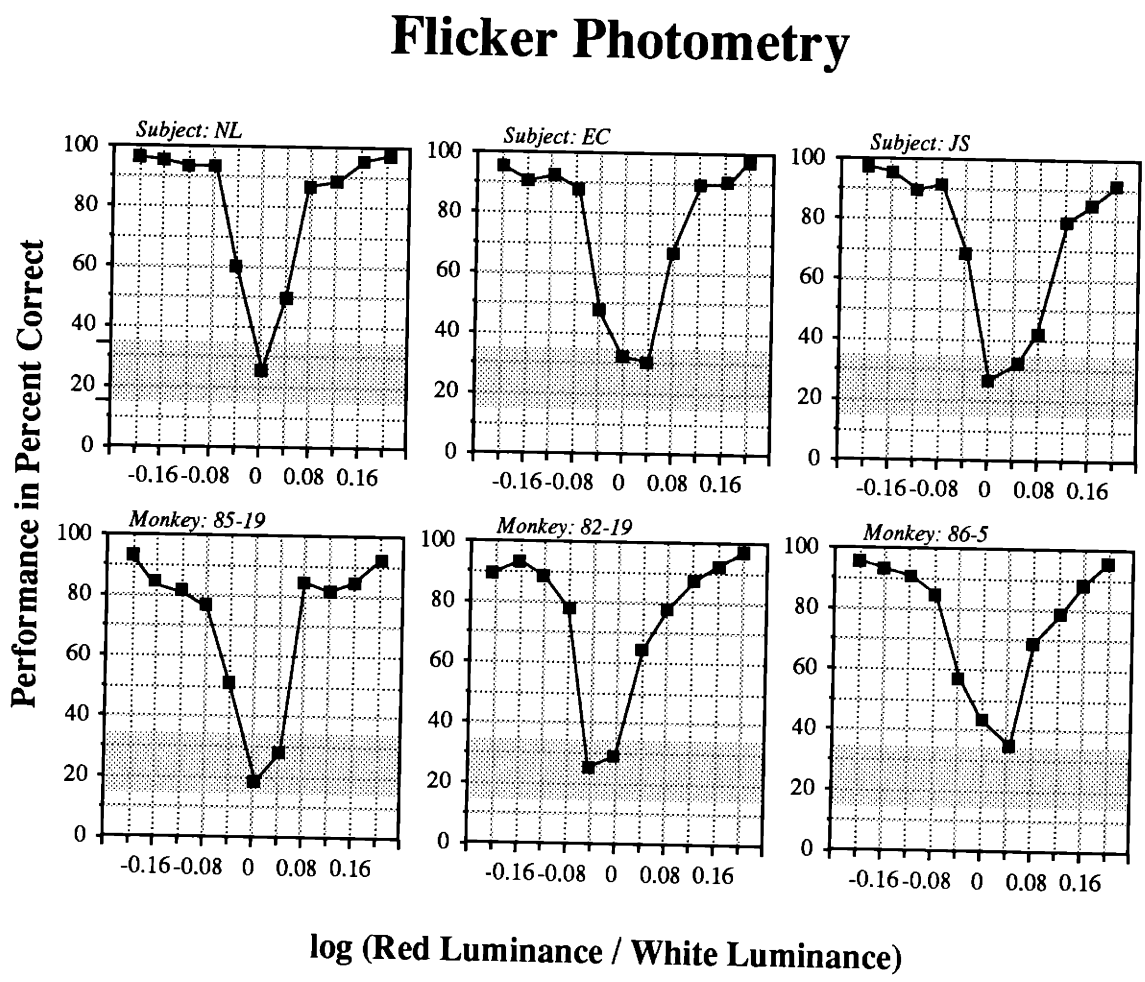
Flicker Photometry
Subject: NL
Subject: EC
Subject: JS
Monkey: 85-19
Monkey: 82-19
Monkey: 86-5
Performance in Percent Correct
100
80
60
40
20
0
-0.16 -0.08 0 0.08 0.16
log (Red Luminance / White Luminance)

Figure 2.13

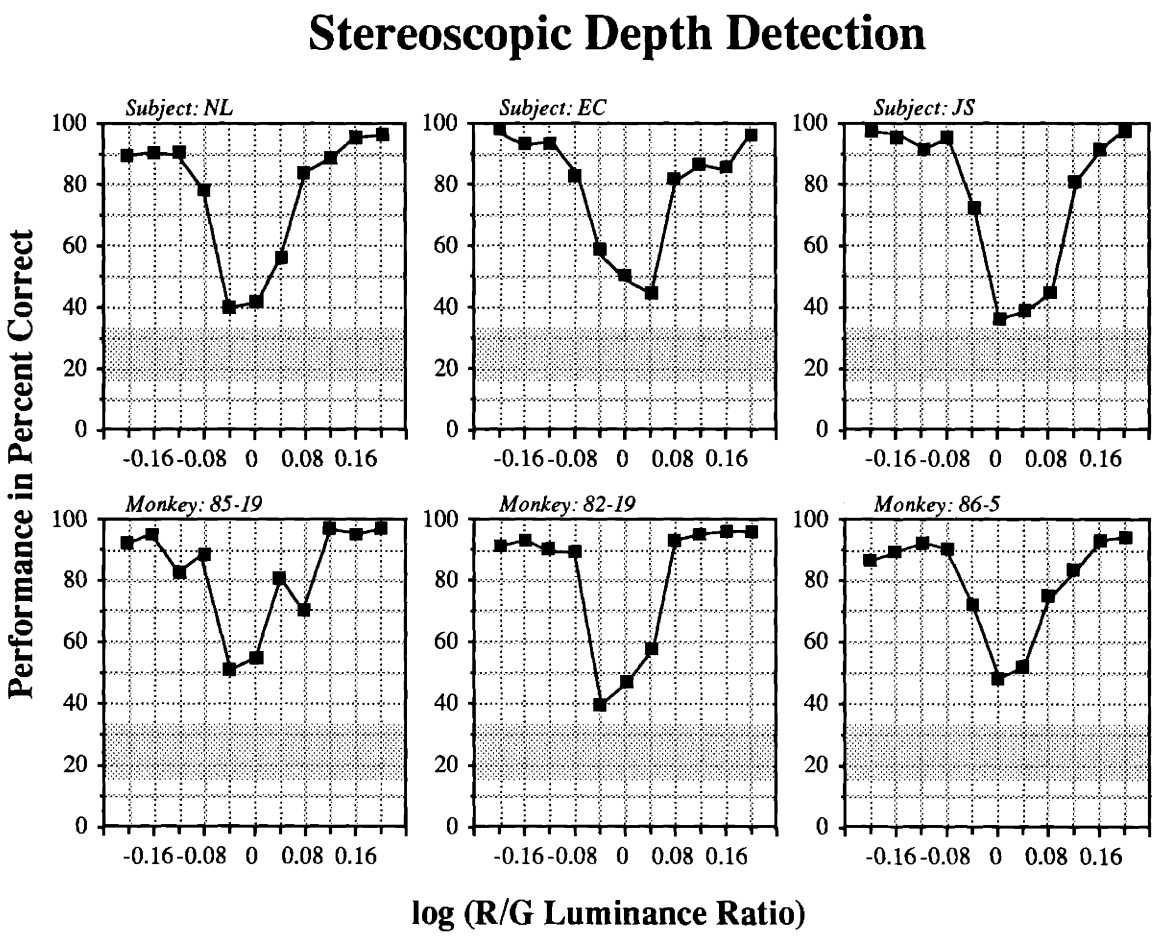
Stereoscopic Depth Detection
Subject: NL
Subject: EC
Subject: JS
Monkey: 85-19
Monkey: 82-19
Monkey: 86-5
Performance in Percent Correct
log (R/G Luminance Ratio)
100
80
60
40
20
0
-0.16 -0.08 0 0.08 0.16

Figure 2.14

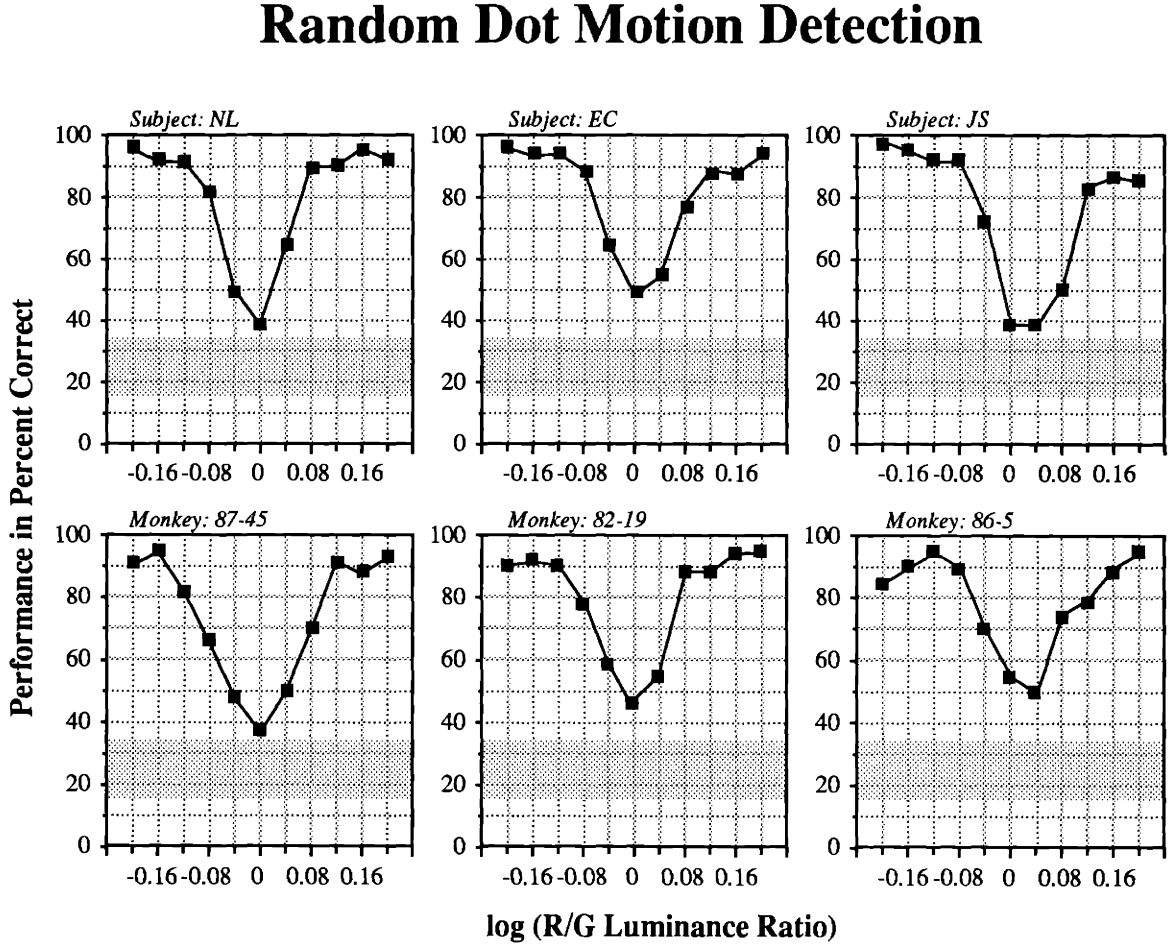
Random Dot Motion Detection
Subject: NL
Subject: EC
Subject: JS
Monkey: 87-45
Monkey: 82-19
Monkey: 86-5
Performance in Percent Correct
log (R/G Luminance Ratio)
100
80
60
40
20
0
-0.16 -0.08 0 0.08 0.16

Figure 2.15

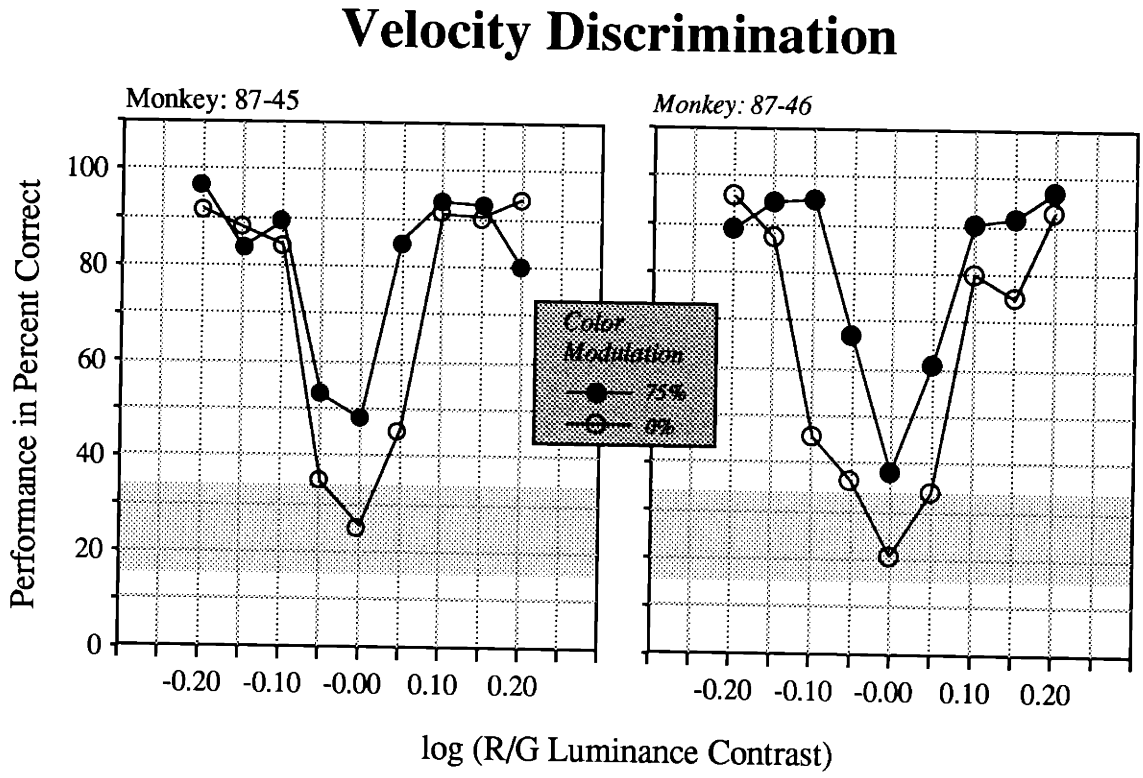
Velocity Discrimination
Monkey: 87-45
Monkey: 87-46
Performance in Percent Correct
100
80
60
40
20
0
-0.20
-0.10
-0.00
0.10
0.20
Color Modulation
75%
0%
log (R/G Luminance Contrast)

Figure 2.16

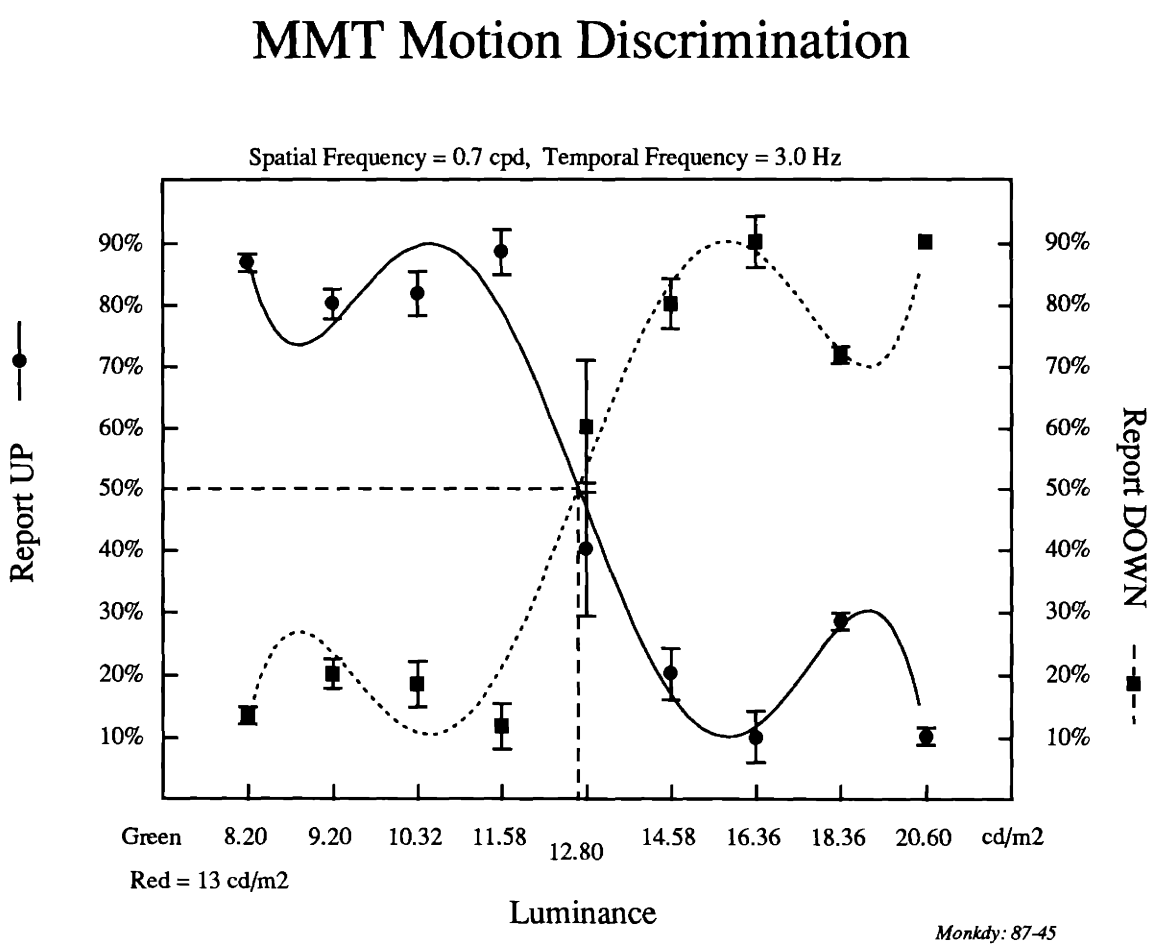
MMT Motion Discrimination
Spatial Frequency = 0.7 cpd, Temporal Frequency = 3.0 Hz
Report UP
Report DOWN
90%
80%
70%
60%
50%
40%
30%
20%
10%
Green
8.20
9.20
10.32
11.58
12.80
14.58
16.36
18.36
20.60
cd/m2
Red = 13 cd/m2
Luminance
Monkdy: 87-45

Figure 2.17

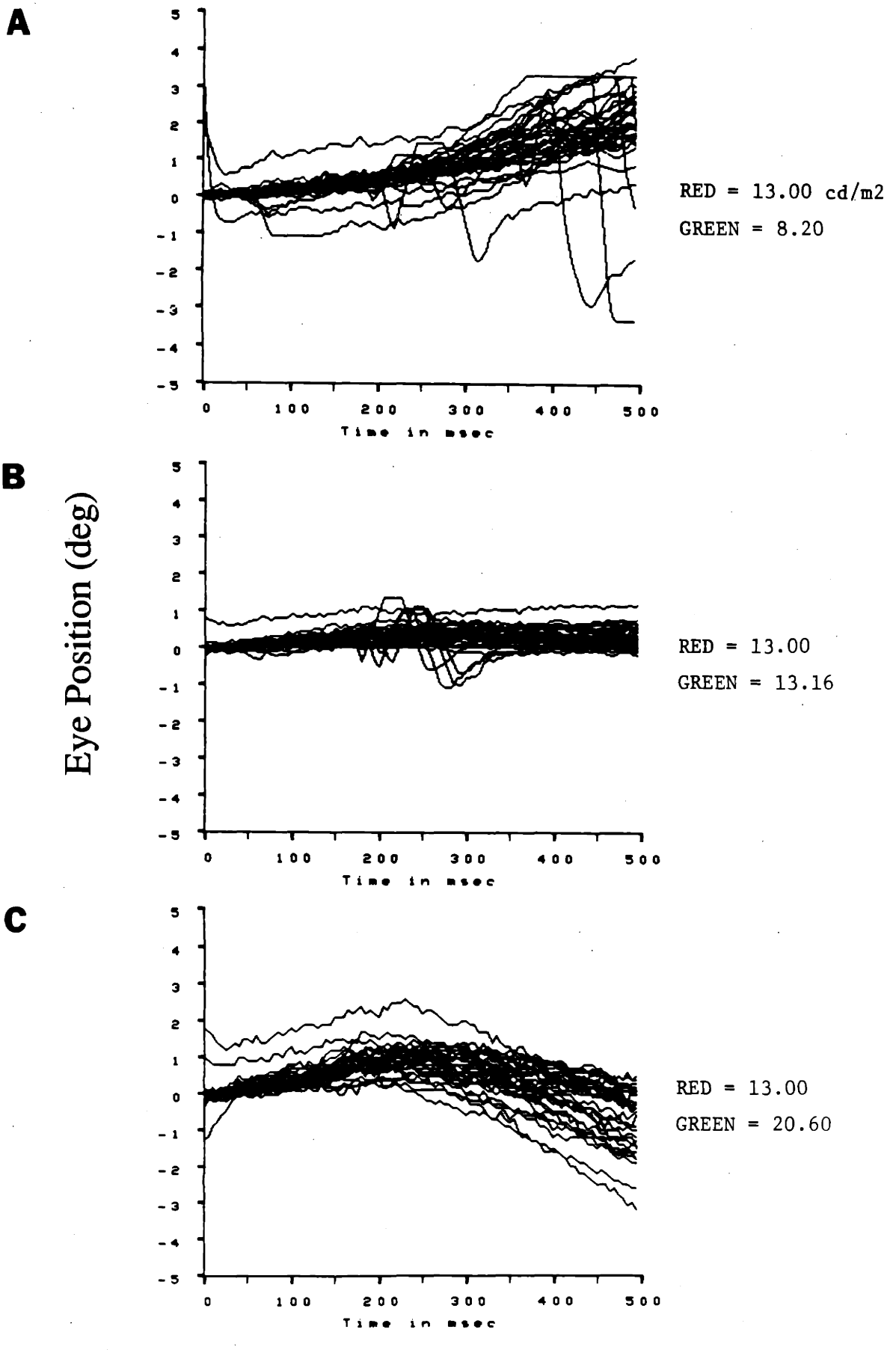
A
B
C
Eye Position (deg)
5
4
3
2
1
0
-1
-2
-3
-4
-5
0
100
200
300
400
500
Time in msec
RED = 13.00 cd/m2
GREEN = 8.20
RED = 13.00
GREEN = 13.16
RED = 13.00
GREEN = 20.60

Slow Phase of OKN During Minimum Motion Stimulus

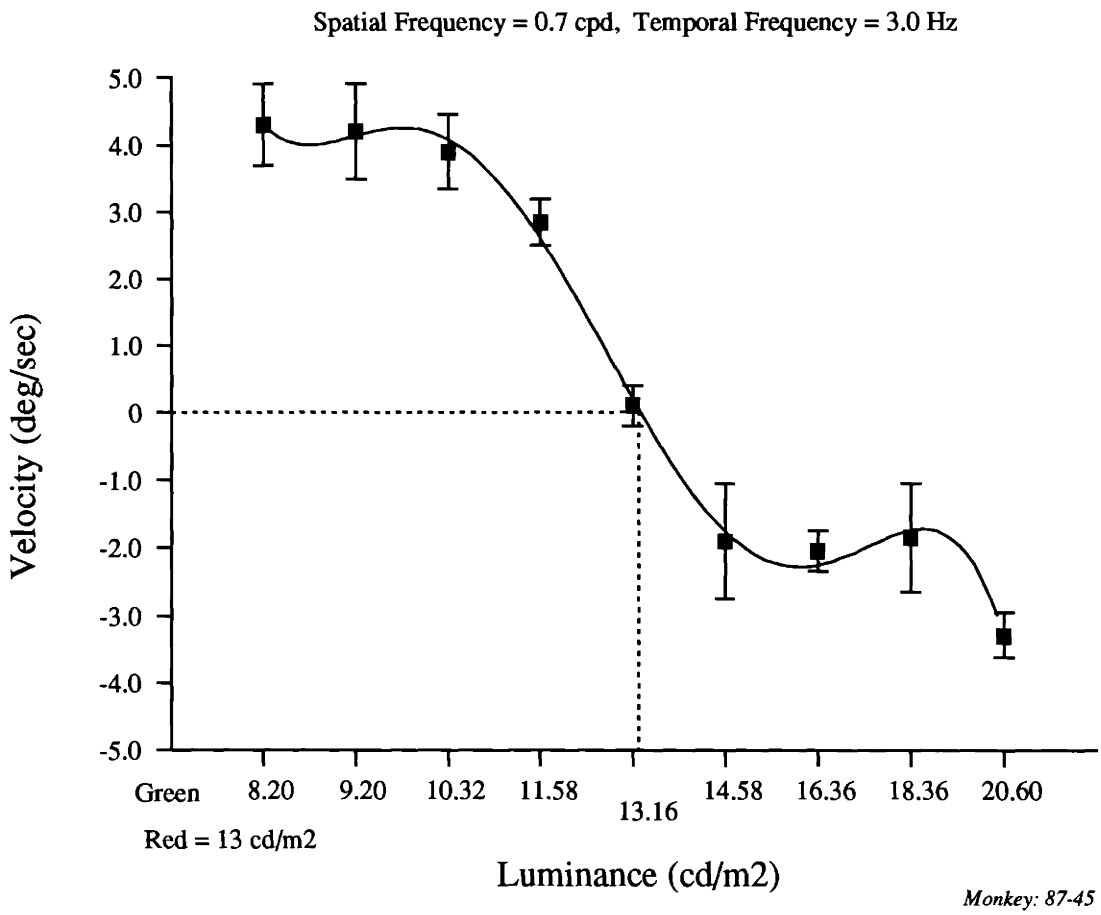

Figure 2.19

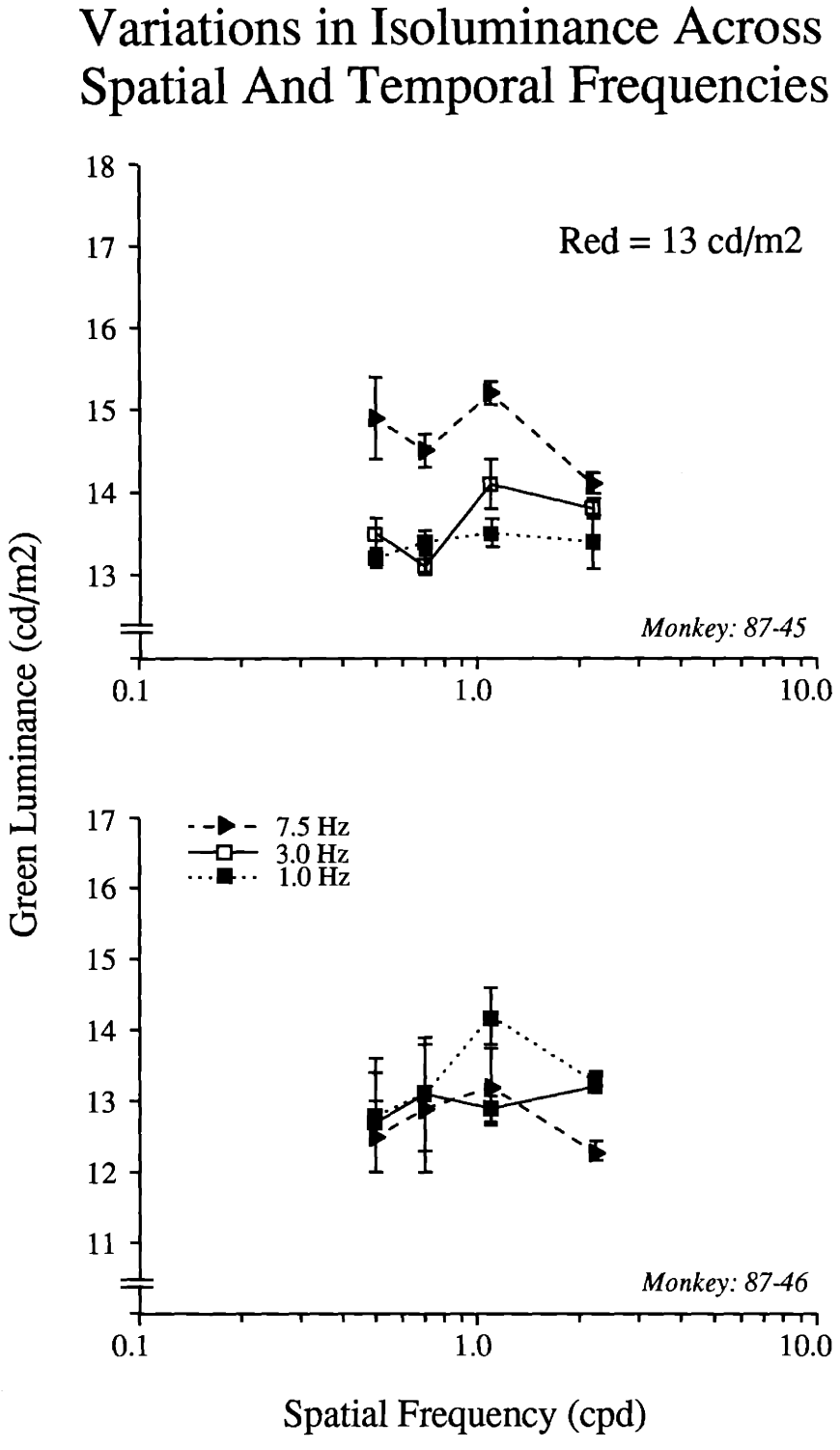
Variations in Isoluminance Across
Spatial And Temporal Frequencies
Red = 13 cd/m2
Monkey: 87-45
Monkey: 87-46
7.5 Hz
3.0 Hz
1.0 Hz
Green Luminance (cd/m2)
Spatial Frequency (cpd)
18
17
16
15
14
13
12
11
0.1
1.0
10.0

Figure 2.20

Spatial and Temporal Frequency Variations For Blue/Green Stimuli

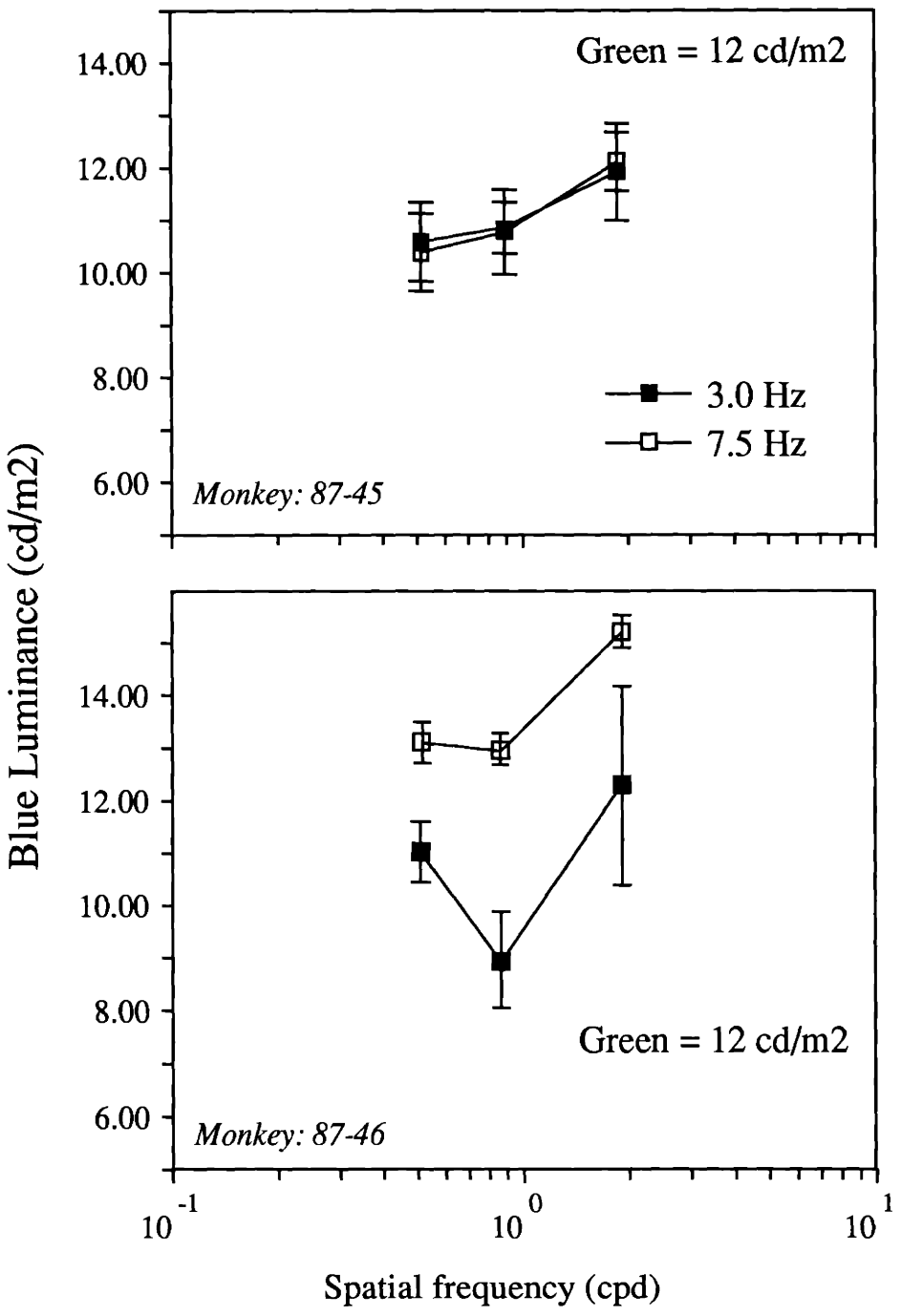

Figure 2.21

Spatial and Temporal Frequency Variations For Red/Blue Stimuli

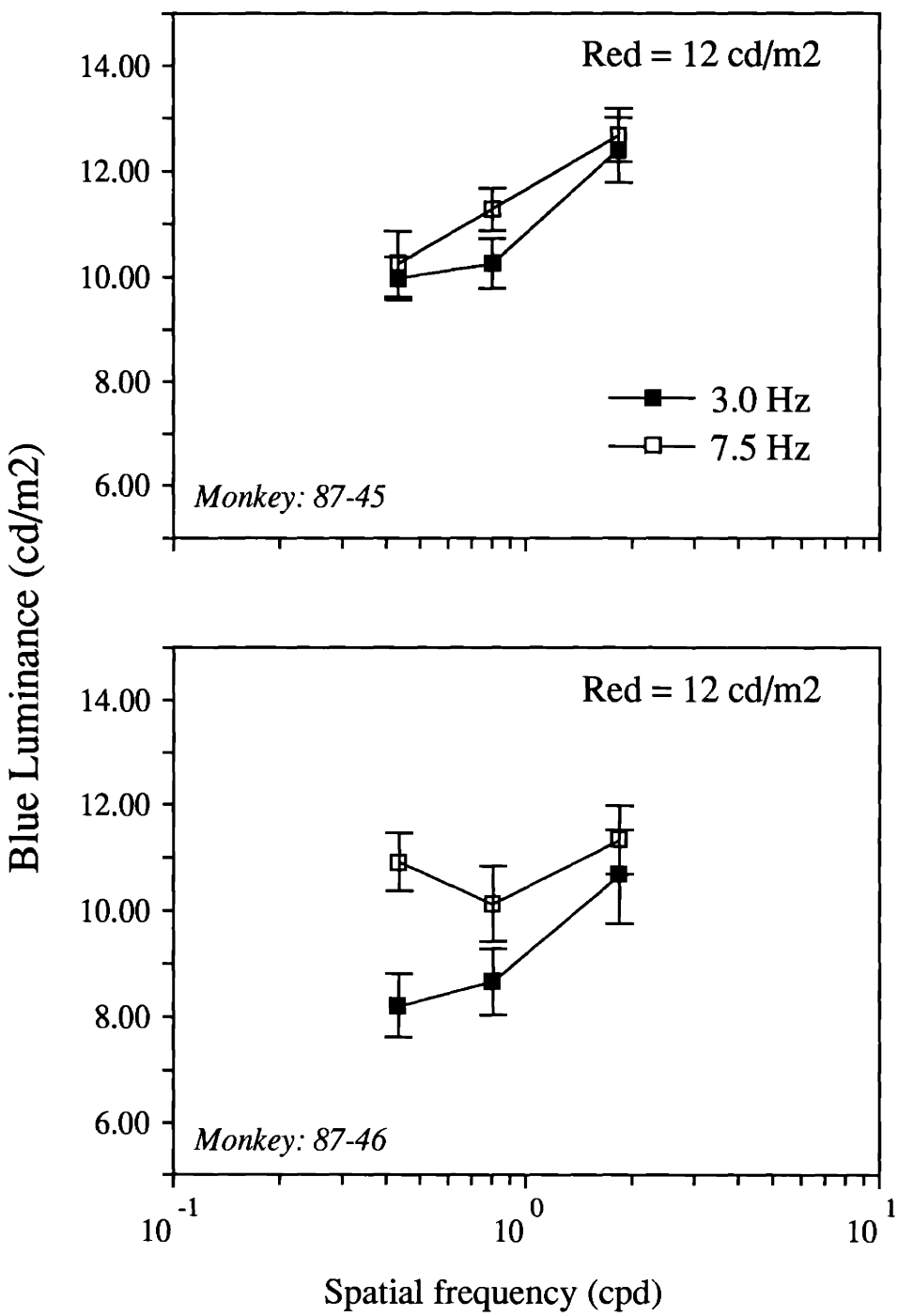

Figure 2.22

Isoluminance Determined by Eye Movements vs. Report

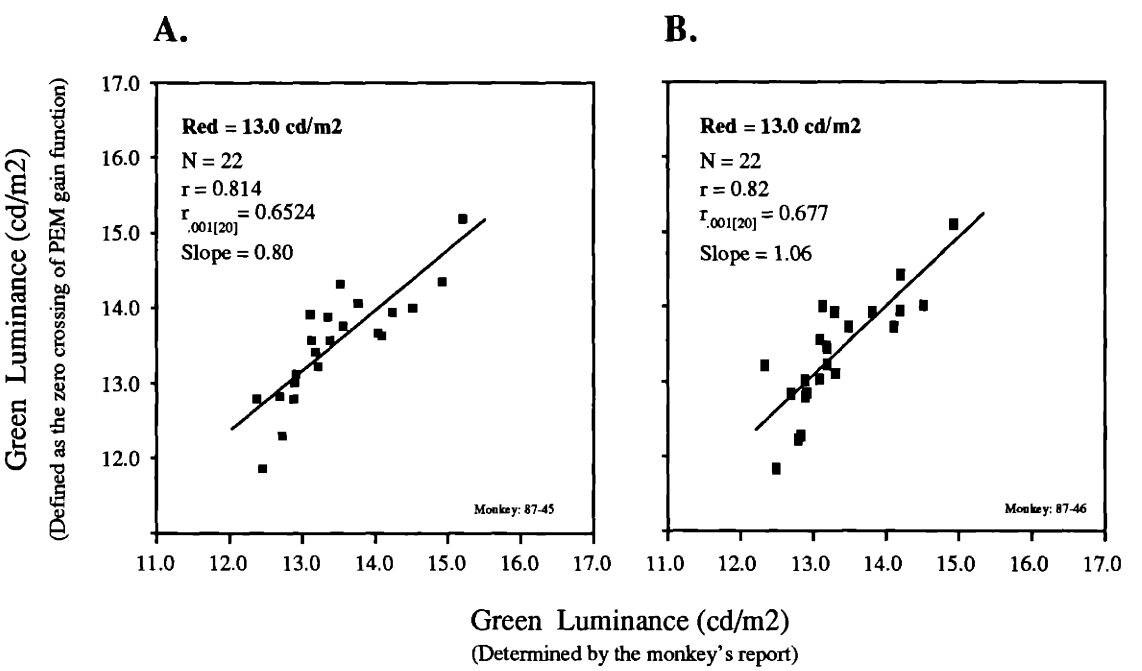

Figure 2.23

Isoluminance Variations With Eccentricity

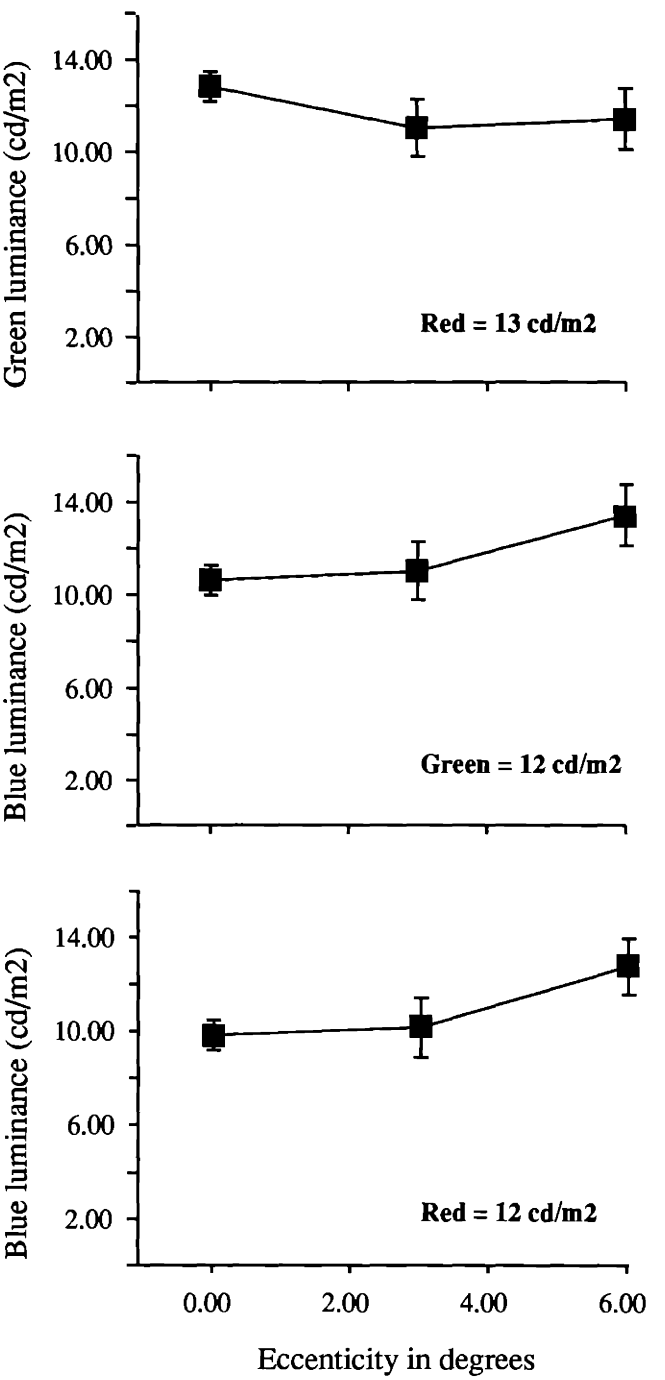

Figure 2.24

Measurement of Slow Phase Optokinetic Nystagmus

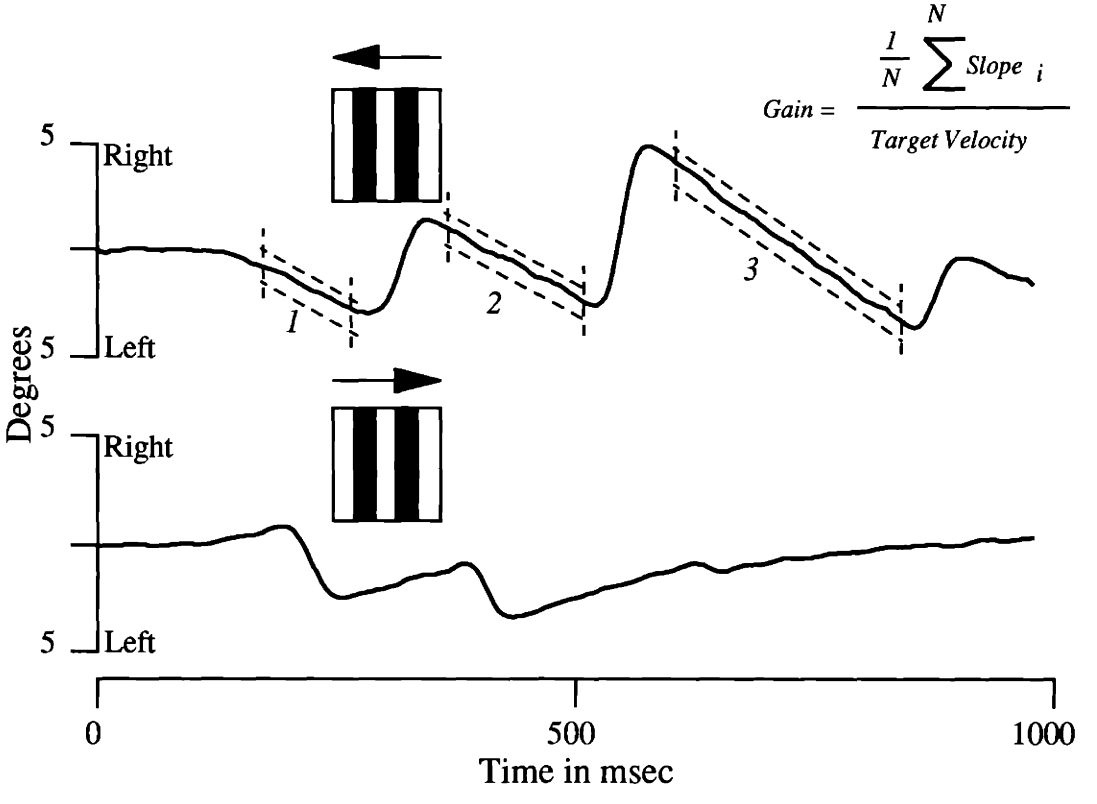

Figure 2.25

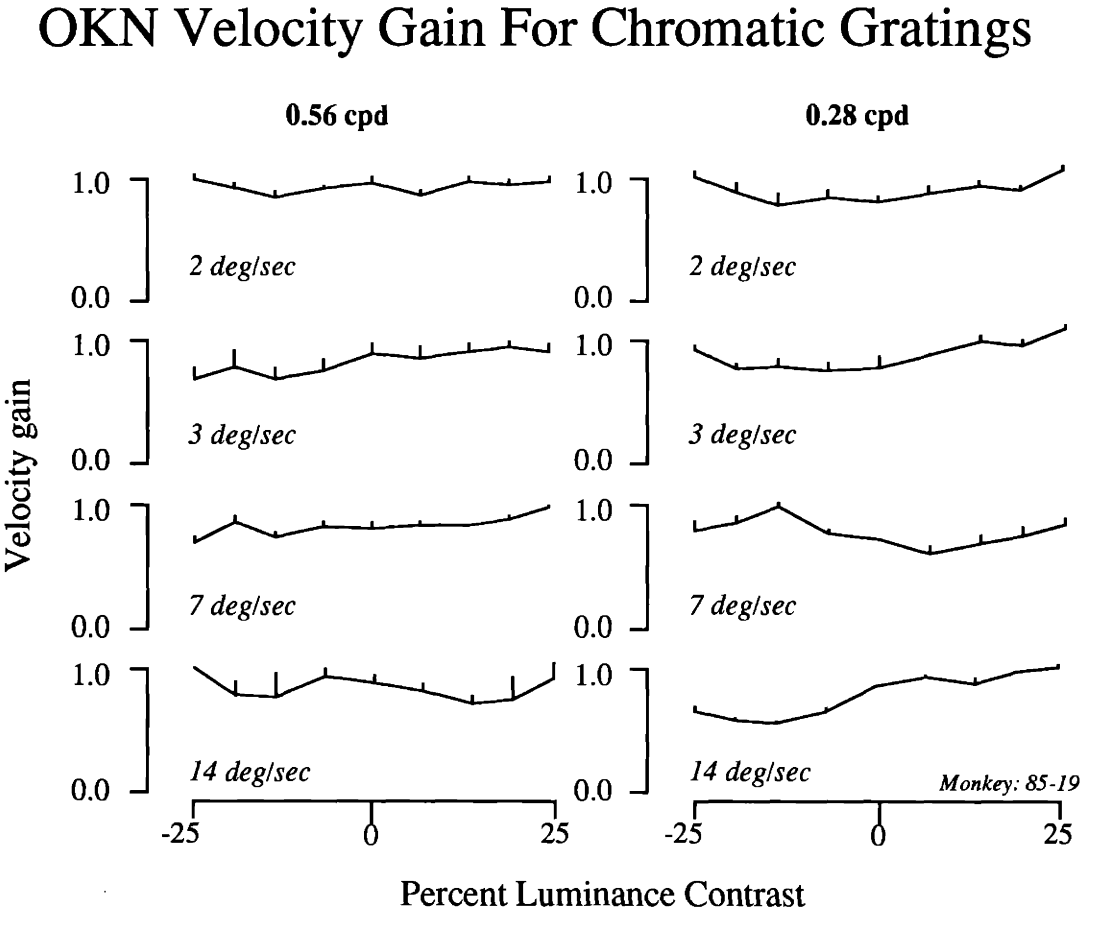
OKN Velocity Gain For Chromatic Gratings
0.56 cpd
0.28 cpd
1.0
0.0
2 deg/sec
3 deg/sec
7 deg/sec
14 deg/sec
Velocity gain
-25
0
25
Percent Luminance Contrast
Monkey: 85-19

Figure 2.26

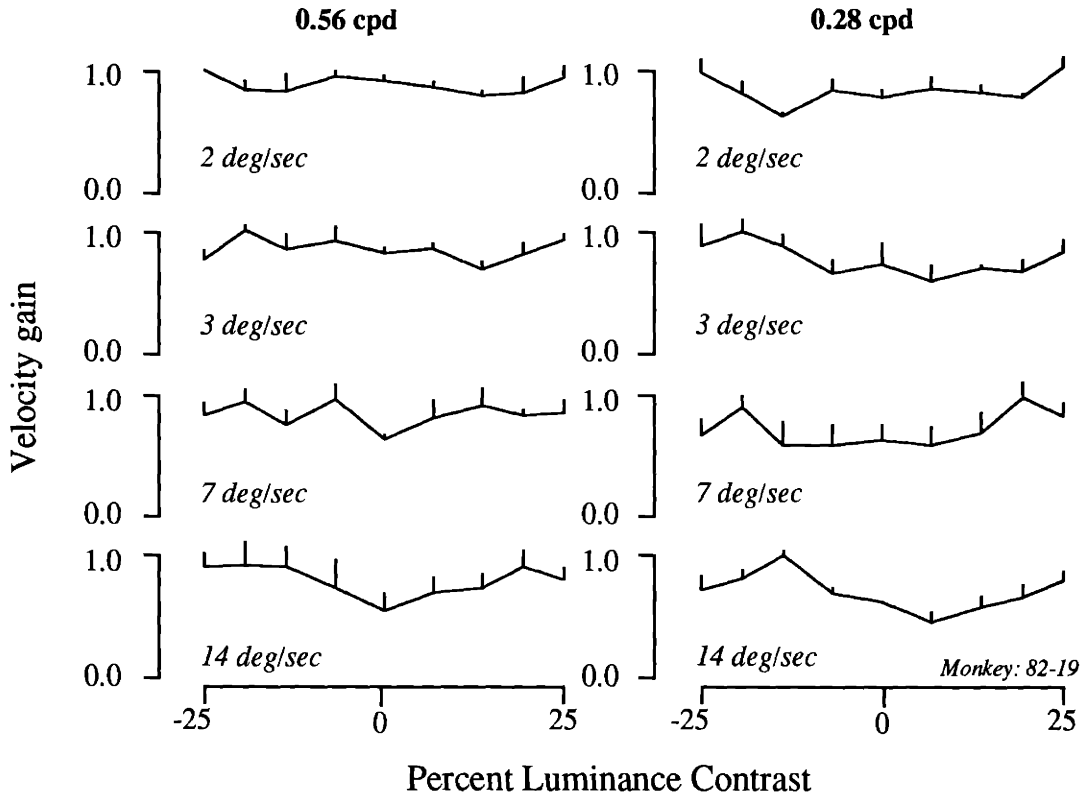
OKN Velocity Gain For Chromatic Gratings
0.56 cpd
0.28 cpd
1.0
0.0
2 deg/sec
3 deg/sec
7 deg/sec
14 deg/sec
Velocity gain
-25
0
25
Percent Luminance Contrast
Monkey: 82-19

Figure 2.27

OKN Velocity Gain For Achromatic Gratings

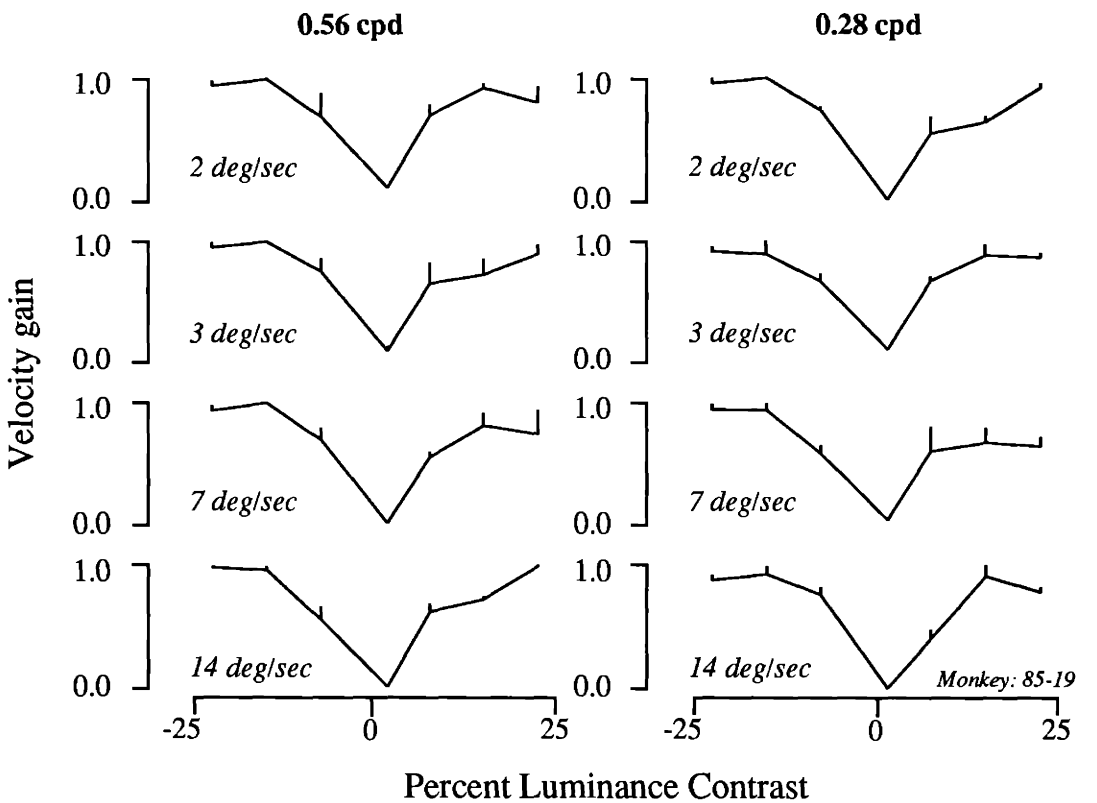

Figure 2.28

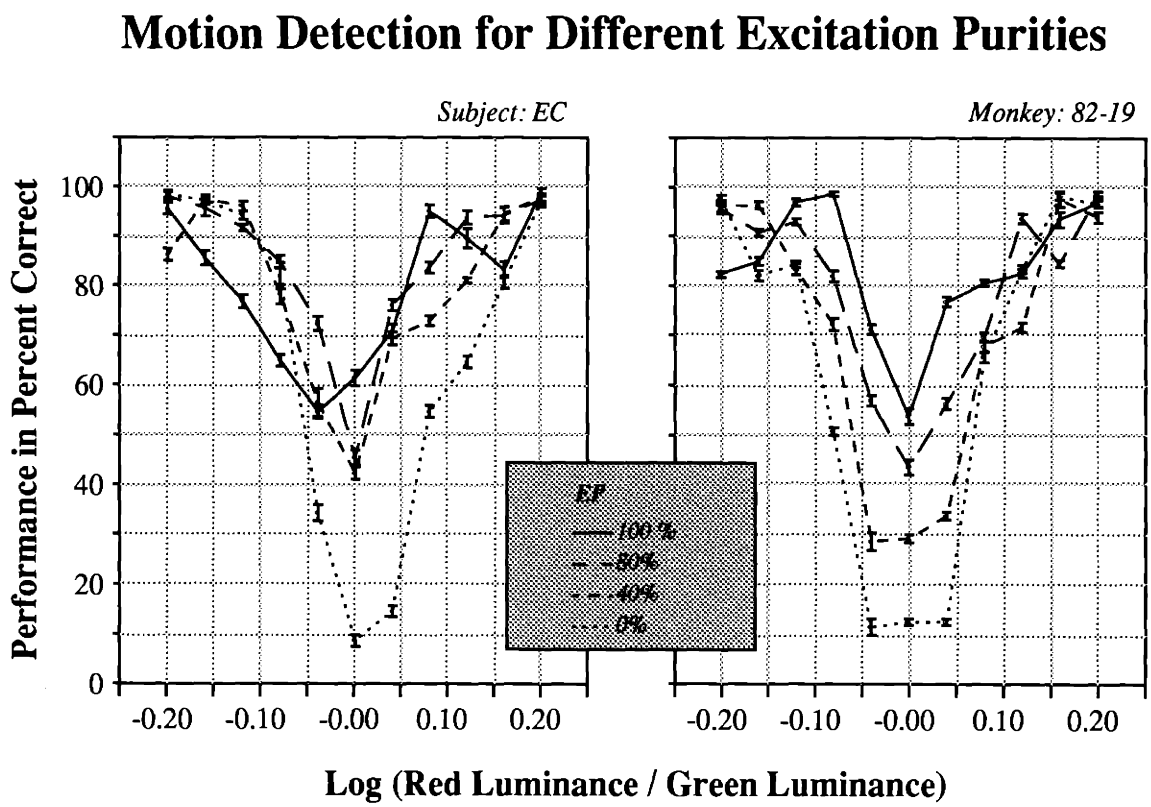
Motion Detection for Different Excitation Purities
Subject: EC
Monkey: 82-19
Performance in Percent Correct
100
80
60
40
20
0
-0.20
-0.10
-0.00
0.10
0.20
EP
100%
80%
40%
0%
Log (Red Luminance / Green Luminance)

Figure 2.29

Stereo Depth Detection for Different Excitation Purities

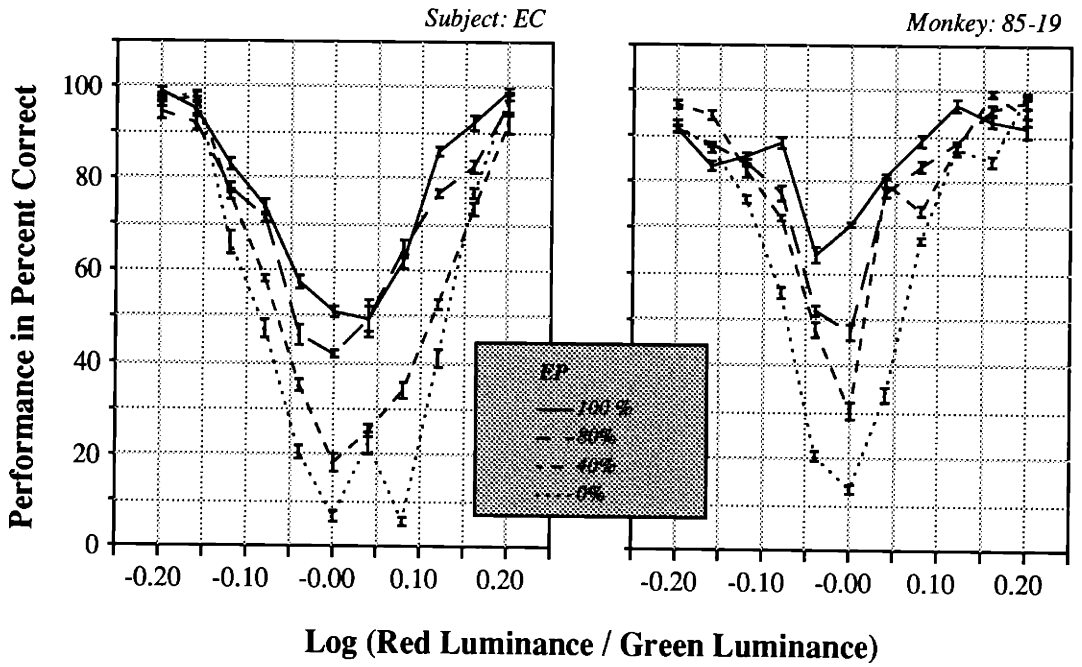

Figure 2.30

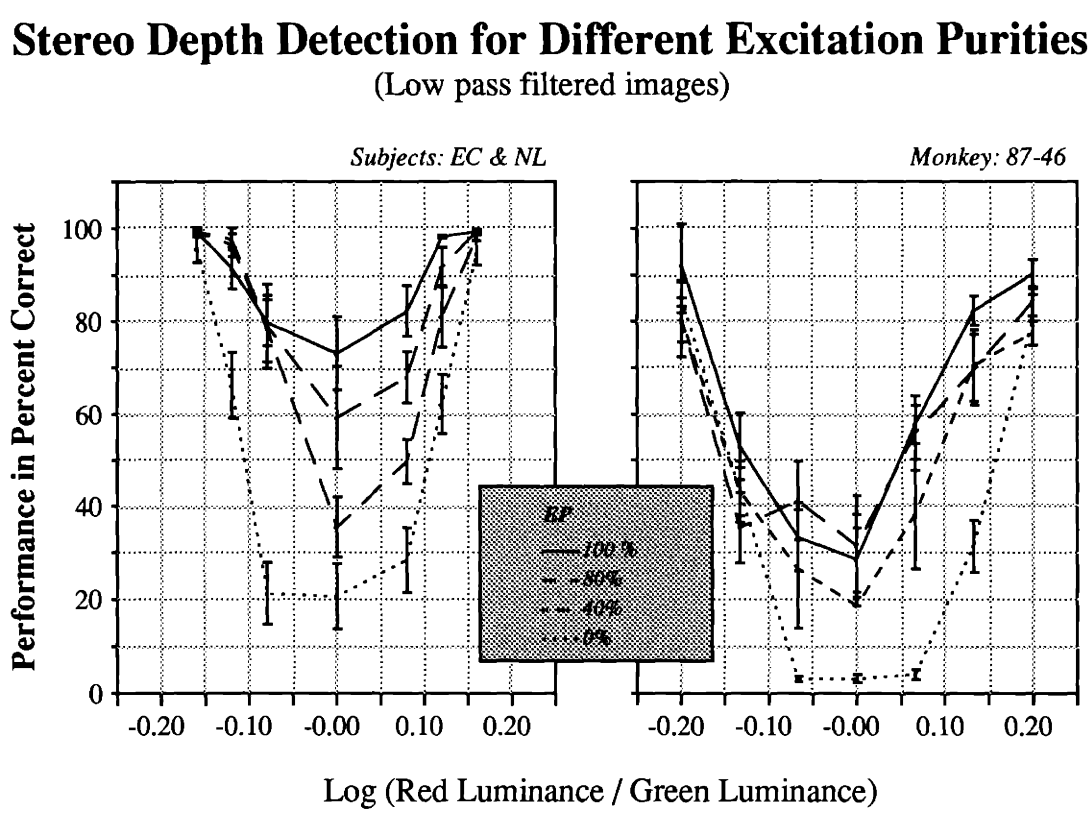
Stereo Depth Detection for Different Excitation Purities
(Low pass filtered images)
Subjects: EC & NL
Monkey: 87-46
Performance in Percent Correct
100
80
60
40
20
0
-0.20
-0.10
-0.00
0.10
0.20
-0.20
-0.10
-0.00
0.10
0.20
RP
100 %
80%
40%
0%
Log (Red Luminance / Green Luminance)

Figure 2.31

Pooled Isoluminance Ratios

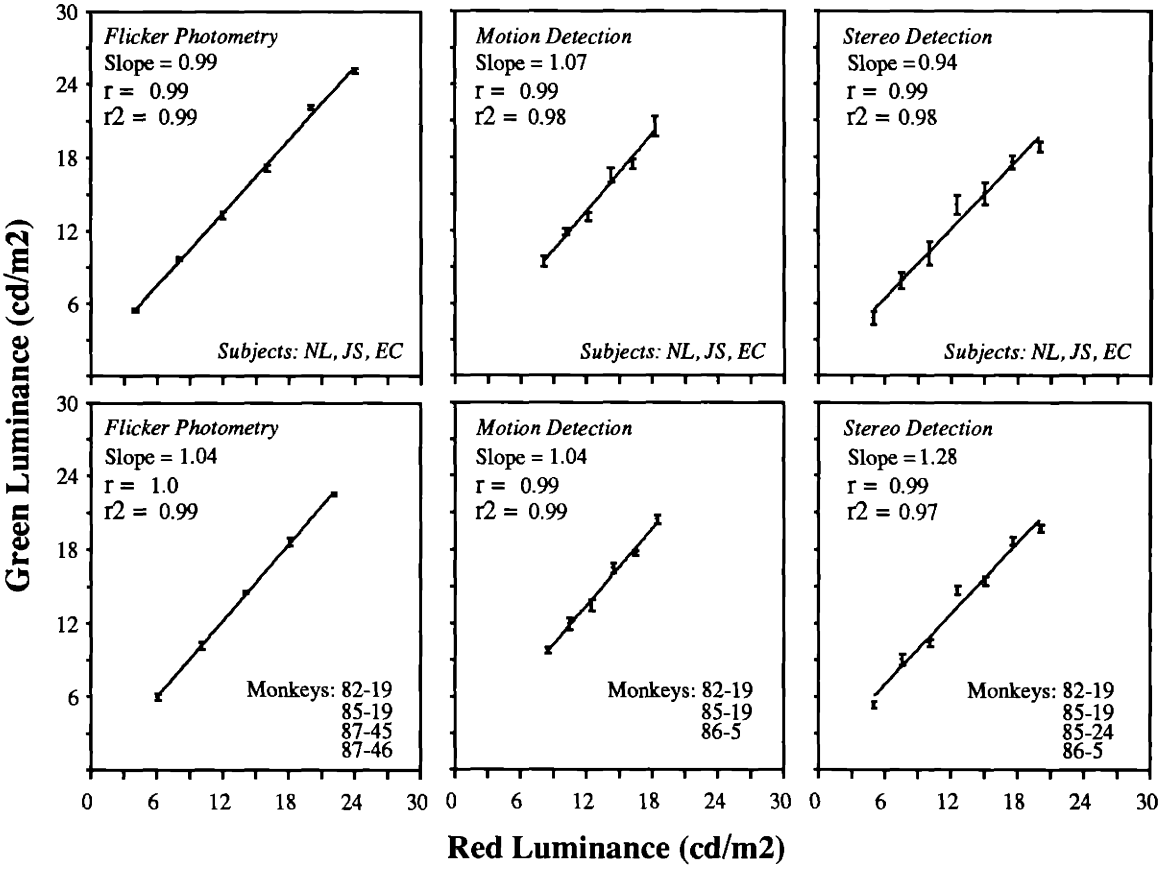

Figure 2.32

CHAPTER THREE

PHYSIOLOGY: ACTIVITY IN THE PARVO- AND MAGNOCELLULAR LAYERS OF THE DORSAL LATERAL GENICULATE NUCLEUS AS A FUNCTION OF CHROMINANCE AND LUMINANCE

Summary

Single and multiple unit recordings were made from the dorsal lateral geniculate nucleus of paralyzed, anesthetized rhesus monkeys. The stimuli consisted of either small red/green flickering spots of light or drifting sinusoidal gratings 180 degrees out of phase. Achromatic stimuli of the same luminance contrast were also presented for comparison.

Cells in the mLGN were active throughout the entire range of luminance contrasts, including isoluminance. For a range of low luminance contrasts however, the overall activity of the magno cells decreased and the residual firing occurred at each light exchange. While the pLGN as a whole was not silenced, the individual cells exhibited a broad range of behavior. Cells with high color selectivity always responded to the preferred wavelength, even if the luminance was very low compared to the non-preferred wavelength. At the other end of the continuum, parvo cells that were not color selective could be silenced at luminance contrasts near isoluminance. For the majority of cells a luminance contrast ratio could be found that would null the activity of that particular cell. These results indicate that activity in both divisions of the LGN are affected at isoluminance yet neither is silenced. Since the magno channel remains active at isoluminance it is inaccurate to ascribe functions to this channel based on perceptual deficits at isoluminance.

1.0 INTRODUCTION

In the introductory chapter it was pointed out that the bulk of retinal ganglion cells could be divided into two major classes. Cells with large dendritic trees and relatively sparse branching have been labelled P_α (Perry and Cowey, 1981) or M cells. Cells with smaller, branching dendritic fields were classified as the P_β or P cells. The P cells project to the parvocellular layers of the lateral geniculate nucleus (pLGN) and the M cells to the magnocellular layers (mLGN) (Leventhal *et al.*, 1981; Perry *et al.*, 1984). Evidence also suggests that these two populations remain segregated to some extent through extrastriate cortex (Livingstone and Hubel, 1984; Maunsell, 1990). The two sets of ganglion cells and their counterparts have distinct physiological properties (Wiesel and Hubel, 1966; Gouras, 1968; Schiller and Malpeli, 1978; DeMonasterio, 1978). Most (about 80%) of the cells in the pLGN are spectrally opponent, meaning that information from long-, middle- and short-wavelength selective cones are segregated by the center and surround mechanisms. These cells have, on average, a slower conduction velocity, lower contrast sensitivity and smaller receptive fields than cells in the mLGN. The pLGN cells will also give a sustained response to an appropriate visual stimulus; they continue to fire for the duration of the stimulus presentation. On the other hand, mLGN cells produce transient responses to stimuli, have higher conduction velocities, higher contrast sensitivity, and larger receptive fields. In general, mLGN cells are not believed to segregate information from different cones classes and thus, are not selective for color.

Because of the physiological differences between these two classes of cells, many have proposed that they are subserving different aspects of perception. Some investigators have used lesion studies to determine the roles of the pLGN and mLGN channels in vision (Schiller, 1990; Merigan, 1990; Merigan and Maunsell, 1990). Others have ascribed certain functions to these channels based on isoluminance experiments (Ramachandran and Gregory, 1978, Livingstone and Hubel, 1987) as discussed in the previous chapter. In these experiments, it is proposed that the magno system is responsible for aspects of perception that are absent when only wavelength information is available. The underlying assumption is that cells in the magnocellular layers of the LGN are unresponsive to isoluminant stimuli since these cells do not segregate wavelength information. Psychophysical experiments in the preceding chapter revealed a color input to motion and depth perception and that the slow phase portion of optokinetic nystagmus is unaffected at isoluminance. While this evidence suggests that mLGN cells are not silenced at isoluminance, it is not unequivocal. It is conceivable that something other than the magno pathway is carrying this information.

In order to 'silence' a cell, inputs from different cone classes must be summed linearly. At some r/g luminance ratio depending on the weighting of the signals, the response to each cone class is equal. To silence a channel, one would expect that this ratio be identical within the population of cells as well as equivalent to the behaviorally determined isoluminance. By recording physiological responses over a range of luminance contrasts including

isoluminance in mLGN and pLGN, one can determine if these two conditions are met. In order to draw comparisons to the behavioral data, it is necessary to match the stimuli for the physiology study in chrominance, luminance and configuration to the psychophysical studies.

2.0 MATERIALS AND METHODS

2.1 Subjects

Three male and three female rhesus monkeys (*Macaca mulatta*), weighing between 4 and 8.5 kg at the time of the recordings, were used for this study. One of these animals was used for extensive psychophysical testing, together with the monkeys used in the previous chapter. The animals were cared for in accordance with the National Institutes of Health Guide for the Care and Use of Laboratory Animals and the guidelines of the Massachusetts Institute of Technology Committee on Animal Care.

2.2 Surgery and Recording

All surgical procedures were carried out under anesthesia using sterile technique. The animal was initially restrained with an intramuscular dose of ketamine (10 mg/kg) and prepared for surgery. Induction of surgical anesthesia was accomplished with a dose of pentobarbital (15mg/kg) followed by an initial dose of analgesic (Butorphenol, 0.05-0.1 mg/kg) and an antibiotic (Tribrissen, 0.11 ml/kg) which was also given the day prior to the surgery. Somatic responses were tested particularly during surgical manipulations and

before making incisions or placing the animal in the stereotaxic head holder. The sites of incision and the contact points were infiltrated with local anesthetic (2% lidocaine) and a small (6 mm diameter) craniotomy was made above one of the lateral geniculate bodies. Mydriasis and cycloplegia were achieved by instillation of a drop of scopolamine (hyoscine) in the acute experiments or a drop of tropicamide (mydriacyl) for the reversible procedures. The corneas were protected with clear contact lenses wetted with allergan solution. The lenses were selected to optimally focus the eyes on a tangent screen 150 cm away. The monkey was then paralyzed with 0.08 mg/kg/min (induction duration about 1 minute) of vecuronium bromide (Norcuron) in dextrose-lactated Ringer's solution and artificially respirated at 21-30 strokes per minute at a tidal volume adjusted to keep the end-tidal CO_2 within the range of 4-4.5%.

2.3 Maintenance and Recording

Reversible procedures never lasted more than 8 hrs from the induction of anesthesia. In the acute experiments, recordings were usually obtained over a period of two and a half days. During both procedures the stage of surgical anesthesia was monitored continuously to detect any signs of discomfort or pain. Maintenance of paralysis was accomplished with a perfusion rate of 0.003 mg/kg/min. Anesthesia was maintained with a 70-30% mixture of N_20 and O_2 supplemented with 5 to 8 mg/kg/hr sufentanil. To insure adequate anesthesia, cortical activity (electroencephalogram), heart rate

(electrocardiogram), blood pressure (sphigmometry), body temperature and expired CO2 were monitored constantly and recorded every 10 minutes. The EEG was recorded from electrodes on the skull and EKG was monitored with a 3 leads cardiac monitor (Physio Control VSM 3). Desychronization of EEG or high frequency waveforms show inadequate anesthesia. Stage III surgical anesthesia (Slatter, 1985) is characterized by less periodic large slow waves. Prolonged desychronization of the EEG was countered by intramuscularly administrating additional sufentanil. Body temperature was measured by a rectal thermistor and kept at 37°. Respiration rate was adjusted as needed to insure a end-tidal CO_2 of 4.5%. During the long lasting acute procedures the eye lenses were removed every 6-8 hrs the eyes washed with sterile water and the quality of the optic media was checked. Every 12 hrs the contact lenses were removed and the eyes kept closed for about 2 hrs.

Extracellular action potentials were recorded from single isolated units or small groups of neurons (multi-unit recordings) using glass coated platinum-iridium electrodes. The electrodes had exposed tips of 10 to 20 micrometers and impedance of 1 to 10 Mohm at 1 KHz. The electrodes were placed in a stainless steel guard tube and advanced with a hydraulic microdrive. Most electrode penetrations were made within 15 degrees of the fovea, which was identified with a reverse ophthalmoscope. Recordings were restricted almost in the medial portion of the LGN to assure of reaching the magnocellular laminae. Magnocellular and parvocellular classification as well as individual laminae were identified by the progression of receptive field position, eye dominance,

receptive field size, and response properties of the cells (see Schiller and Colby, 1983 for details). Receptive fields were hand-plotted using either a hand-held gun or a joystick-controlled CRT that generated various stimuli. Single and multiple-unit recordings were amplified, bandpass filtered, discriminated conventionally and sampled at 10 kHz.

2.4 Stimulus Description

Initial experiments were carried out using a computer-controlled diode that emitted red or green light of known luminance values. Further experiments used a raster display system that was controlled by another PDP 11\73. These stimuli had identical chrominance and luminance profiles to stimuli used in the behavioral experiments. For the light-emitting diodes (LEDs) the CIE coordinates were x = .475, y = .528 for the red and x = .054, y = .592 for the green. To insure that an isoluminance point for a cell would not be missed due to sampling frequency, the luminance of each LED could be adjusted continuously by means of a variable resistor in the current source circuit. Once determined, the luminance of the red LED was fixed at 14.75 cd/m^2 and the luminance of the green LED varied from 1.41-54.5 cd/m^2 in 0.02 log unit steps. For the Hitachi monitor using an Adage raster display system, the dominant wavelengths and CIE chromaticity coordinates were R = 627 nm and x = 0.602, y = 0.353; and G = 525 nm and x = 0.84, y = 0.581. Luminances of the red and green stimuli for the monitor were lower on average than the LEDs, falling within a range of 1-25 cd/m^2. Background illumination for both

stimulus sources was 5 cd/m^2. Details of the calibration of the raster display system can be found elsewhere (Logothetis, 1991). For the initial experiments using flickering stimuli, the red and green lights were modulated at temporal frequencies ranging from 1-30 Hz using a square-wave function. Typically, the flicker rate corresponded to frequencies used for the heterochromatic flicker photometry experiments described in chapter 2.

Four types of stimuli were used to drive the LGN cells: Flickering stimuli restricted to the centers of the receptive fields; counter-flickering stimuli in the center and surround (a red circle in the center and surrounded by a green annulus exchanged with a green center and red surround); counter-flickering checkerboard patterns; and moving square and sine wave gratings. Both the checkerboards and the gratings covered the entire receptive fields. All four sets of stimuli could be varied in terms of the red and green luminance values. Chromatic versus achromatic stimuli of equivalent luminance contrast were also tested.

2.5 Histology

During and at the conclusion of an acute experiment, electrolytic marker lesions were placed in the LGN by passing current through the electrode. The animals were sacrificed with an overdose of sodium pentothal (250-400 mg/kg) and perfused transcardially with heparinized saline, followed by a 4% paraformaldehyde solution, then, in some cases, a 4% paraformaldehyde/10% sucrose solution. The LGN was then blocked, sectioned at 40 microns, mounted

and stained with cresyl violet. Electrode penetrations were then reconstructed and laminar position for each cell was compared to the physiological properties.

3.0 RESULTS

3.1 Magnocellular LGN

We recorded from 161 cells in the lateral geniculate nucleus. Sixty-six pLGN cells and 41 mLGN cells were held long enough for detailed, quantitative analysis. In addition, we collected multiple unit data from 79 sites in pLGN and mLGN. Figure 3.1 shows the response of an mLGN off-cell to flickering stimuli presented in the center of the receptive field over a range of luminance values. The luminance contrast of the red and green stimuli (log(lum. red/lum. green) is listed for each set of responses. The cell fires strongly to the offset of the brighter of the two colors when the luminance contrast is high. At the intermediate values when the luminance contrast between the red and green is reduced, the magno cell also fires to the offset of the less bright stimulus. At some red/green luminance contrast, the magno cell shows a balanced response (i.e. the appearance of a secondary excitatory peak) to both red and green but at no luminance contrast is the cell silenced. The second excitatory peak would usually be present over a range of 0.1 log contrast. This second harmonic response increases monotonically and is maximal when the response was balanced. Taken at log luminance contrast steps larger than 0.1, the balance point was approximated by taking the luminance contrast ratio at which the

appearance of a second excitatory peak was observed. No incidence of nulling the response at any luminance contrast was found for any of the mLGN cells examined.

The balance point for magno cells were distributed over a narrow range (Figure 3.2) of luminance contrasts. All mLGN cells could be balanced within a range of 8% luminance contrast. In addition, the distribution was not centered on the red/green luminance contrast of zero which was determined to be the isoluminant point both behaviorally and by a photometer.

The variation of the balance point in the mLGN cells is sufficient to suggest that the magno system as a whole is not compromised at isoluminance. This is further demonstrated in figure 3.3. This figure shows multiple-unit data in mLGN consisting of 5 to 7 on- and off-center cells. For a population of cells, the decrement in response at isoluminance is not substantial. Instead, the magno system signals chrominance changes at all luminance contrasts.

3.2 Parvocellular LGN

Cells in the parvocellular layers exhibited a broad range of responses. Figure 3.4 shows the responses of a pLGN cell that is selective for long wavelengths. This cell fires solely for the red stimulus over the entire range of luminance contrasts shown. The strength of the response is proportional to the luminance of the red stimulus. Cells were tested over a wide range of luminances, at least six-fold in either direction. At the extreme ends of the range the strongly wavelength-selective cells did become unresponsive to the

stimuli, but this may not have been a nulling of the response as much as reducing the luminance of the preferred color to levels below the resolution of the pLGN cone inputs. More importantly, this cell did not respond to the green at any luminance level tested. Figure 3.5 represents the responses of a pLGN cell that did not show a strong wavelength selectivity. Like mLGN cells, this cell responded to the color that had the higher luminance value. When the luminance contrasts are near zero, however, as defined by a calibrated photometer, the cell fails to signal the wavelength exchange of the stimulus. We obtained similar responses from cells using the other stimulus configurations. The only difference was a slight shift in the isoluminance point however the response profile to luminance contrast remained unchanged. The responses of these two parvo cells exemplify extreme ends of a range of responses seen in pLGN. We found a broad distribution of wavelength selectivities and red/green luminance contrasts where cells would fail to signal the light exchange. This is demonstrated in figure 3.6. This figure shows the distribution of LGN cells as a function of the luminance contrasts at which parvo cells do not signal the red/green exchange. Luminance values are taken in 0.15 log unit steps. The parvo cells show a continuous distribution over the entire range of luminance contrasts tested as one might expect from the variability in wavelength selectivity.

3.3 Comparison of Chromatic and Achromatic Stimuli

In another series of experiments, the responses of mLGN cells were

compared between chromatic and achromatic stimuli. Figure 3.7 shows the responses of one mLGN cell to a chromatic and achromatic stimulus stimulating the center of the receptive field. Again, one luminance value was held constant while the other was varied. The left column is the response of the cell to a red and green flickering stimulus in the same spatial location with a variety of luminance contrasts. The stimuli used here are identical to the ones described previously except luminance contrasts for each histogram are taken in equal log steps of 0.05. The response of the cell is similar to that of the magno cell shown in figure 3.1. The right column of histograms are the same magno cell's responses to stimuli that are identical to those in the left column with the exception that these stimuli do not contain any chromatic information. These stimuli flicker between two gray levels varying only in luminance except when the log contrast is zero, in which case the stimulus appears as a single gray level. The log luminance contrasts used in this experiment are identical to those values used in chapter 2 describing the perception of motion and stereopsis for achromatic and chromatic stimuli of different excitation purity levels. The psychophysical data demonstrate that performance is improved with the addition of chrominance information for these two tasks. Figure 3.7 shows that for extreme luminance contrasts, the cell responds similarly for the both the chromatic and achromatic stimuli. At the intermediate luminance contrast levels, however, the magno cell responded to each red/green exchange and demonstrated a balanced response at -0.05. For the achromatic stimulus on the other hand, the cell responds only to the

onset of the brighter stimulus and this response is diminished as the luminance contrast is reduced. These responses are representative of the responses seen in all mLGN cells for these experiments. In addition, we found no changes discharge rates for different flicker frequencies tested, including the behaviorally relevant flicker frequency (1, 5, 10, 15 Hz).

Figure 3.8 displays the transient response (burst) of the pooled responses of 6 mLGN cells for each of the stimulus conditions over a wider range of contrasts. The open squares show the response of the cell to the onset of the red stimulus in the lower graph and gray level 1 in the upper (stimulus 2). The filled circles show the response to green and gray level 2 (stimulus 1). The intersection of the curves for stimulus one and stimulus two cross near a luminance contrast of zero for both the chromatic and achromatic flicker for this cell. By definition then, the best balance for these cells is near zero. For the chromatic flicker, however, this crossover point is at a higher firing rate. Thus, the cells are more active at zero luminance contrast when chrominance information is present. Indeed, at all luminance contrasts the cells respond better for the chromatic flicker condition.

4.0 DISCUSSION

These results show that there is no universal isoluminance point for either class of cells in the LGN. Parvocellular LGN cells exhibit a broad range of wavelength selectivity. Some cells are strongly selective for wavelength. For these cells the red/green luminance contrast deviates from the photometrically

determined value of zero considerably. Other pLGN cells show very little color selectivity. The luminance contrasts at which the red/green light exchange is no longer signalled is close to zero for these cells. The distribution of these red/green luminance contrasts for the entire population of pLGN cells sampled covers the entire range of luminance ratios that were tested. This range extended from a red luminance that was over six times the green luminance to one-tenth the green luminance.

The cells in the mLGN remain active for all luminance contrasts. These cells predominantly respond to the stimulus with the higher luminance value. For a narrow luminance contrast range of about 0.1 log units the magno cells have a second excitatory peak. At some luminance contrast the strength of the second excitatory peak is equal to the fundamental transient excitation. The range of contrasts which magno cells show the secondary excitatory peak is much narrower than the range at which red/green exchanges were not signalled in parvo cells.

The LGN physiology results confirm previous results from this laboratory. Schiller and Colby reported that pLGN cells that lack well-defined wavelength selectivity could be made unresponsive to red/green exchanges at certain contrast ratios (Schiller and Colby, 1983). In addition, magno cells respond at all ratios and exhibit the balanced response. The distribution of cells for the luminance contrasts are also similar to the distributions seen in figures 3.2 and 3.6. Derrington, Krauskopf, and Lennie also found cells in the mLGN that do not summate cone inputs linearly and thus respond at each

chrominance shift comparable to the second excitatory peaks (Derrington *et al.*, 1984). They were unable to obtain a balanced response however, possibly because their modulation of chromaticity was not as large as ours. Lee and colleagues also found a second excitatory peak when recording from phasic cells (Lee *et al.*, 1988; 1989a,b). Lee *et al.* find that the response near isoluminance is directly related to the degree that M- and L- cones are stimulated out of phase. Lee found that if the stimuli are reduced to 0.5 degrees, however, 'residual flicker' is present at high luminance levels yet disappears at low luminance levels. Assuming a pupil diameter of 5 mm, conversion of his units in trolands would give values of 2.25, 7.15, and 71.46 cd/m^2 (Lee *et al.*, 1988). In our experiments using LED's, the red luminance was fixed at 14.75 cd/m^2 which is within the photopic range, and the stimuli were approximately 0.13 degrees. For these conditions a second excitatory peak was observed for the all mLGN cells. The differences in results may be attributed to the low luminance levels (2.25 cd/m^2) which may not be sufficient to drive the cone inputs or the differences in the wavelengths tested: 627 nm/525 nm vs. 440 nm/white (Lee *et al.*, 1990).

Not only is the magno system able to signal changes in pure chrominance information but there is evidence that some mLGN cells have differential cone inputs to center and surround. Wiesel and Hubel classified a cell type (IV) that have a sustained suppression of maintained firing for long wavelengths in the surround portion of the receptive field (Wiesel and Hubel, 1966). Derrington, Krauskopf, and Lennie found that a much larger population

of magno cells have differential cone inputs to their center and surround regions (Derrington et al., 1984). This suggests that the receptive fields have a degree of spectral opponency with respect to center and surround.

In the previous chapter discussing psychophysics, the isoluminance point was determined using flicker photometry. This isoluminance point did not vary significantly from isoluminance as defined by a calibrated photometer. In addition, monkeys were tested for random-dot motion detection, stereopsis, and pattern perception under various luminance contrast and chrominance conditions. The perceptual deficits in these tasks mainly occurred at the psychophysically-defined isoluminance point. The physiology experiments used stimuli that were identical to those in the flicker photometry experiments with the exception of size. The size of the stimuli, however, did not vary more than one degree from the psychophysical stimuli. As we are interested in the response of the mLGN and pLGN as a population, the size of the stimuli should not affect these results. The results of the physiological studies then, are a reflection of the activity in the LGN that occurs during perception in the behavioral tasks. In addition, the previous chapter demonstrates that chrominance information can enhance the perception of motion and stereopsis. The physiological evidence supports these findings. Magno cells respond to light exchanges at all luminance contrasts if chrominance information is present. At low luminance contrast when chrominance information is absent, the cells fail to respond to the light exchanges.

On the other hand, Cavanagh and Anstis (1991) suggest that neither the

second harmonic response at isoluminance nor the variability in balance point in magno cells is sufficient to explain a color contribution to motion. Using opposed motion in color and luminance gratings, Cavanagh and Anstis find that color can make a significant contribution to motion. When a counterflickering red/green sinusoidal grating (introduced to generate a second harmonic response) was combined with a luminance grating in quadrature phase no motion was observed, suggesting no contribution of the second harmonic response. Also, by modelling uniform, singly and doubly peaked distributions of isoluminance points where units have compressive, linear or expansive response functions, interunit variability predicts that a color contribution to motion will be maximal at isoluminance and falls to zero at higher luminance contrasts. Their data however, show that while there may be a small contribution due to variability, the color equivalent contrast does not drop to zero at high luminance contrast. These results suggest that neither a second harmonic response in magno cells nor variations in individual isoluminance points are sufficient to account for the contribution of color to motion. Instead, it is suggested that a color contribution to motion may be mediated by the color-opponent pathway. The source of this opponent color signal to the motion system is not clear from these results.

Both the mLGN and pLGN as entire systems remain active for all luminance contrast ratios. In the magno system, cells respond at all luminance contrasts. Even the balanced response that could be interpreted as a loss of polarity information is not centered on the behaviorally determined

isoluminance point for the system. In addition, the range which magno cells have this balanced response is large in comparison to the range which any individual magno cell shows a second excitatory peak. This is well demonstrated by the mLGN multi-unit data which shows that the cells are active at all the luminance contrast ratios. Perceptual deficits at isoluminance are not due to the failure of the 'color-blind' magno system. This evidence suggests that the magno channel may in fact be contributing to color perception. The parvo system as a whole also responds at all luminance contrasts. There are luminance contrasts where individual parvo cells do not signal the light exchange but these values cover a very broad range. It is inappropriate then, to assume that perceptual deficits at isoluminance can be attributed to the failure of either the entire magno or parvo system. It is important to stress, however, that both systems are compromised over a wide range of luminance ratios. A substantial portion of the parvo system will no longer respond to a wavelength exchange at any given luminance ratio. In addition, the magno system responds with a second excitatory peak, the effects of which remain unclear. By the same argument then, because both systems are affected at isoluminance, it is inappropriate to suggest that perceptual deficits can be attributed to one channel exclusively. The data suggest that processing of stimulus attributes cannot be strictly divided at the level of the LGN into the magno and parvocellular systems. There is additional evidence that the parvo system is involved in stereopsis. Discrete lesions in the pLGN produce perceptual deficits in a random-dot stereogram task in the lesioned

area of visual space (Schiller *et al.*, 1990). Thus, it may be more appropriate to discuss the processing of attributes in terms of the color, motion, form, depth, etc. channels rather than the P and M pathways. Focus could then shift to the contributions of various subdivisions to these channels and interaction between different channels at early stages of visual processing.

REFERENCES

Cavanagh, P. and Anstis, S. The contribution of color to motion in normal and color-deficient observers. Vision Research, in press.

DeMonasterio, F.M. Properties of concentrically organized X and Y ganglion cells of macaque retina. Journal of Neurophysiology 41:1394-1417, 1978.

Estevez, O. and Spekreijse, H. The "silent substitution" method in visual research. Vision Research 22:681-691, 1982.

Gouras, P. Identification of cone mechanisms in monkey ganglion cells. Journal of Physiology (London), 199:533-547, 1968.

Lee, B.B., Martin, P.R. and Valberg, A. The physiological basis of heterochromatic flicker photometry demonstrated in the ganglion cells of the macaque retina. Journal of Physiology (London) 404:323-347, 1988.

Lee, B.B., Martin, P.R. and Valberg, A. Sensitivity of macaque retinal ganglion cells to chromatic and luminance flicker. Journal of Physiology (London) 414:223-243, 1989a.

Lee, B.B., Martin, P.R. and Valberg, A. Nonlinear summation of M- and L-cone inputs to phasic retinal ganglion cells of the macaque. Journal of Neuroscience 9:1433-1442, 1989.

Leventhal, A.G., Rodieck, R.W. and Dreher, B. Retinal ganglion cells in the old world monkey: Morphology and Central Projections. Science 213:1139-1142, 1981.

Livingstone, M.S. and Hubel, D.H. Anatomy and physiology of a color system in the primate visual cortex. Journal of Neuroscience 4:309-356, 1984.

Logothetis, N. Use of a color monitor in vision research: Calibration and color programming. (In preparation).

Maunsell, J.H.R., Nealy, T.A. and DePriest, D.D. Magnocellular and parvocellular contributions to responses in the middle temporal visual area (MT) of the macaque monkey. Journal of Neuroscience 10:3323-3334.

Merigan, W.H. Chromatic and achromatic vision of macaques: Role of the P pathway. Journal of Neuroscience 9:776-783, 1989.

Merigan, W.H. and Maunsell, J.H.R. Macaque vision after magnocellular lateral geniculate lesions. Visual Neuroscience 5:347-352, 1990.

Perry, V.H. and Cowey, A. The morphological correlates of X- and Y-like retinal ganglion cells of monkeys. Experimental Brain Research 43:226-228, 1981.

Perry, V.H., Oehler, R. and Cowey, A. Retinal ganglion cells that project to the dorsal lateral geniculate nucleus in the macaque monkey. Neuroscience 12:1101-1123, 1984.

Ramachandran, V. and Gregory, R. Does colour provide an input to human motion perception? Nature, 275:55-56, 1978.

Schiller, P.H. and Colby, C.L. The responses of single cells in the lateral geniculate nucleus of the rhesus monkey to color and luminance contrast. Vision Research 23:1631-1641, 1983.

Schiller, P.H. and Malpeli, J.G. Functional specificity of LGN laminae of the rhesus monkey. Journal of Neurophysiology 41:788-797, 1978.

Schiller, P.H., Logothetis, N.K. and Charles, E. Functions of the colour-opponent and broad-band channels of the visual system. Nature 343:68-70, 1990.

Slatter, D.H. Textbook of Small Animal Surgery. W.B. Saunders, 1985.

Wiesel, T.N. and Hubel, D.H. Spatial and chromatic interactions in the lateral geniculate body of the rhesus monkey. Journal of Neurophysiology, 29:1115-1156, 1966.

FIGURES

Figure 3.1. The responses of an mLGN off-cell to red/green flickering stimuli of various luminance contrasts. Stimuli were approximately 0.13 degrees presented in the center of the receptive field. The mLGN off-cell responds predominantly to the higher luminance. At one ratio, however, (0.2) it exhibits a second excitatory peak. Histograms had binwidths of 20 msec.

Figure 3.2. Distribution of mLGN cells that gave a second excitatory peak (balanced response) as a function of log luminance contrast. The mLGN cells were distributed over a narrow range and were not centered on the psychophysically and photometrically determined isoluminance point of 0.0.

Figure 3.3. Multi-unit data consisting of 5-7 mLGN on- and off-centered cells. At no luminance contrast, including the behaviorally determined isoluminance point, are the magno cells silenced. Identical responses were obtained with drifting sinusoidal gratings. Histograms had binwidths of 20 msec.

Figure 3.4. The responses of a pLGN cell to red/green flickering stimuli of various luminance contrasts. Stimuli were approximately 0.13 degrees presented in the center of the receptive field. This cell has a strong selectivity for the long wavelengths. It responds only to the red throughout the entire luminance contrast range. Histograms had binwidths of 20 msec.

Figure 3.5. The responses of another pLGN cell to red/green flickering stimuli of various luminance contrasts. Stimuli were approximately 0.13 degrees presented in the center of the receptive field. The cell has a sustained response to the red stimulus when the luminance contrast of red to green (log R/G) is high. At low luminance contrast (0.0) the cell does not signal the red/green exchange. Histograms had binwidths of 20 msec.

Figure 3.6. Distribution of pLGN cells that did not signal the red/green light exchange as a function of log luminance contrast. The pLGN cells were distributed over the entire range of log luminance contrasts tested.

Figure 3.7. Comparison of the responses of an mLGN cell to a chromatic and achromatic stimulus. The stimuli were identical including luminance contrasts but the stimulus on the right contained chromatic information (red and green). For low luminance contrasts the cell continues to respond to the chromatic stimulus but fails to respond to the achromatic stimulus. This is in good agreement with our psychophysical data that compare chromatic and achromatic stimuli.

Figure 3.8. The pooled responses of six mLGN cells for chromatic and achromatic flicker. Only the transient portion of the response is measured in these graphs. In this case, the cells show a balanced response to both stimuli

at a luminance contrast near zero. The cells respond to the chromatic stimuli with more spikes per bursts at all luminance contrast levels than to the achromatic stimuli.

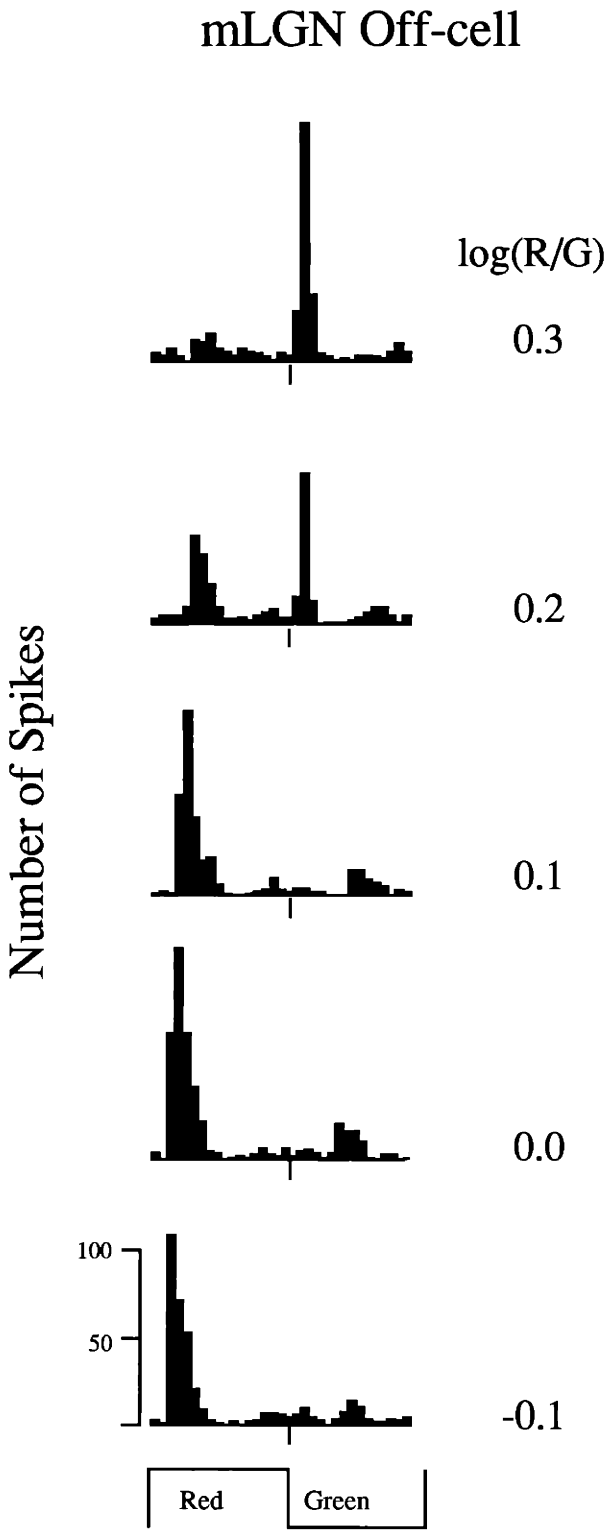
mLGN Off-cell
log(R/G)
0.3
0.2
0.1
0.0
-0.1
Number of Spikes
100
50
Red
Green

Figure 3.1

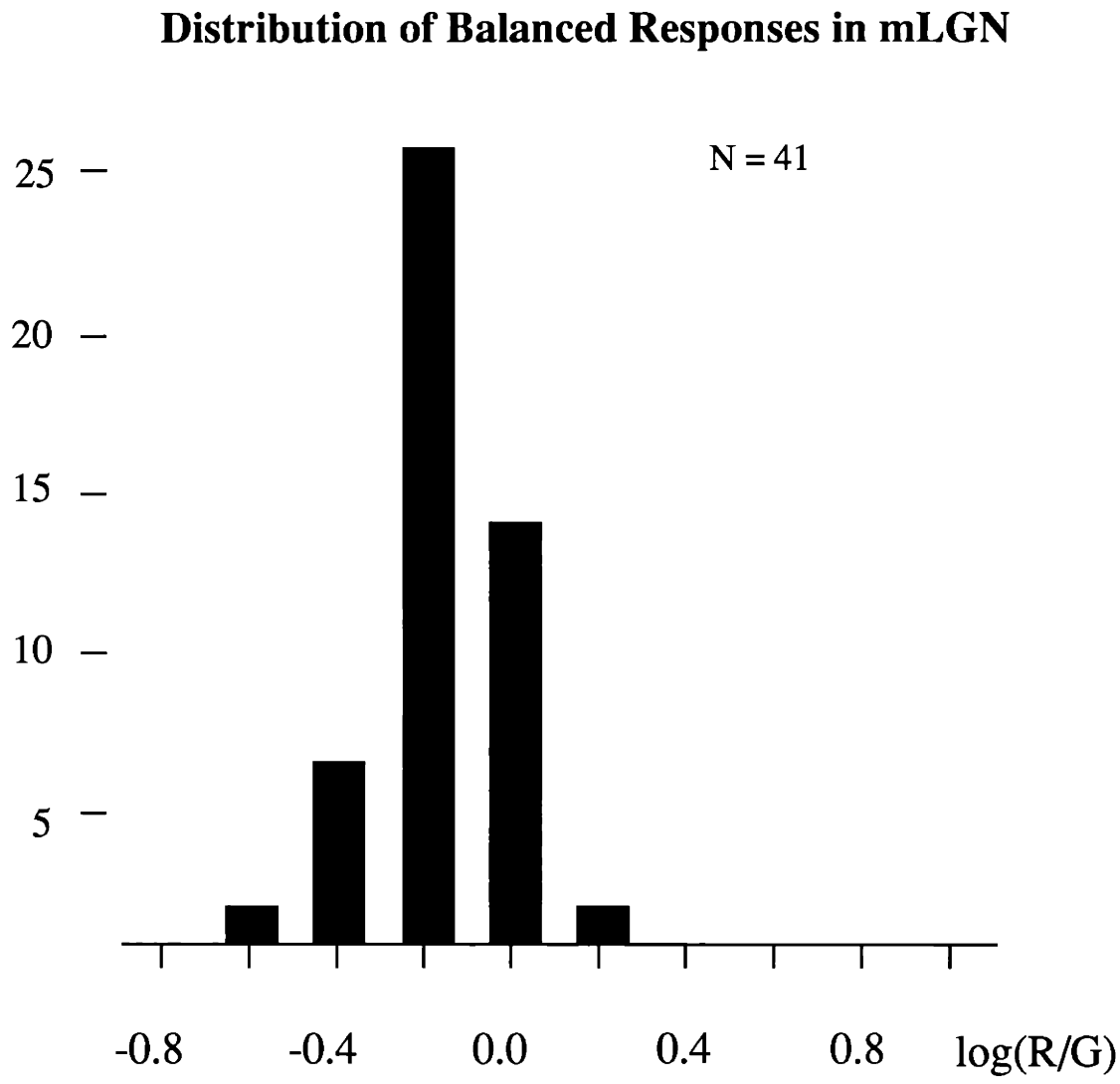
Distribution of Balanced Responses in mLGN
N = 41
25
20
15
10
5
-0.8
-0.4
0.0
0.4
0.8
log(R/G)

Figure 3.2

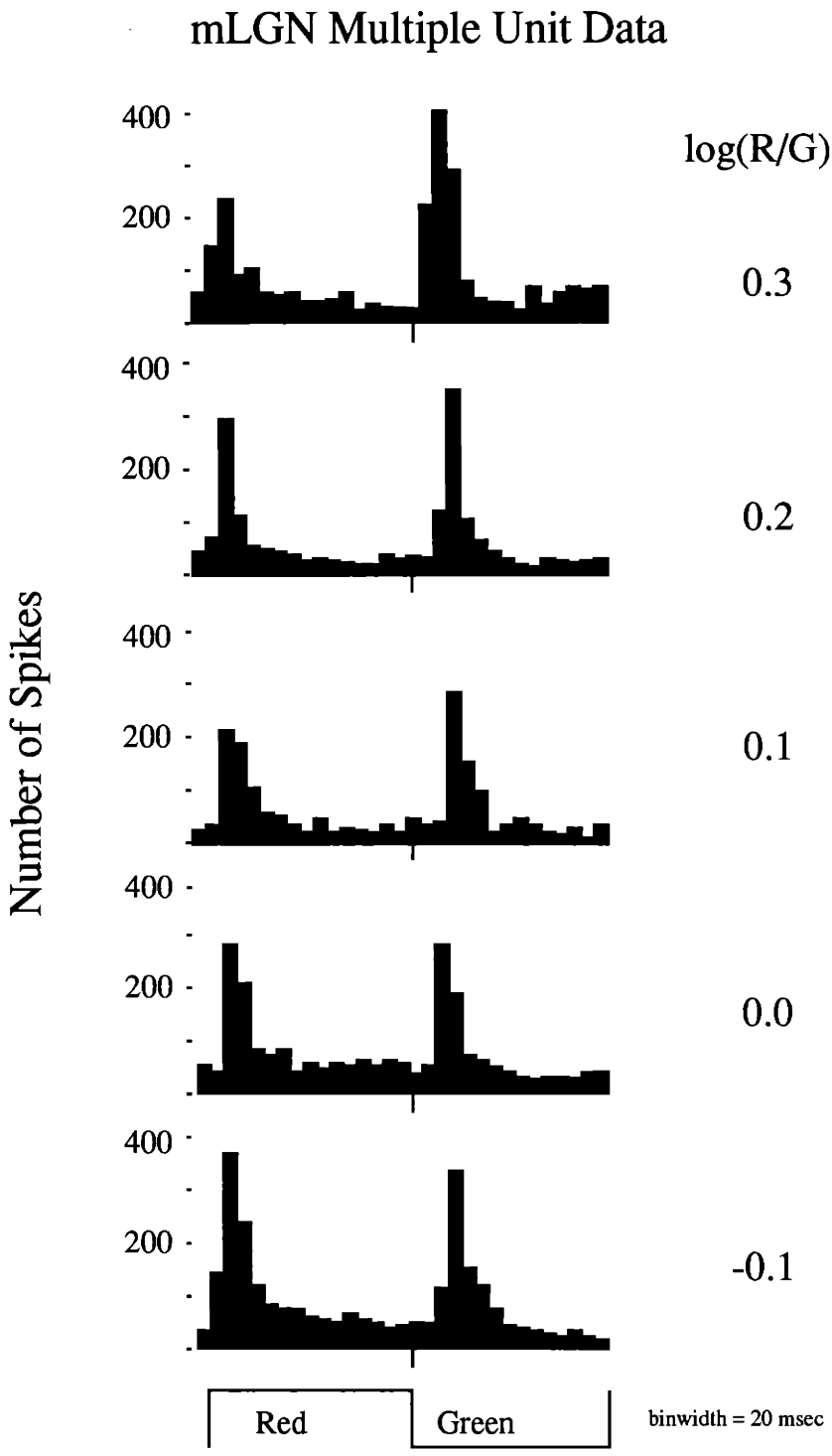
mLGN Multiple Unit Data
Number of Spikes
400
200
log(R/G)
0.3
0.2
0.1
0.0
-0.1
Red
Green
binwidth = 20 msec

Figure 3.3

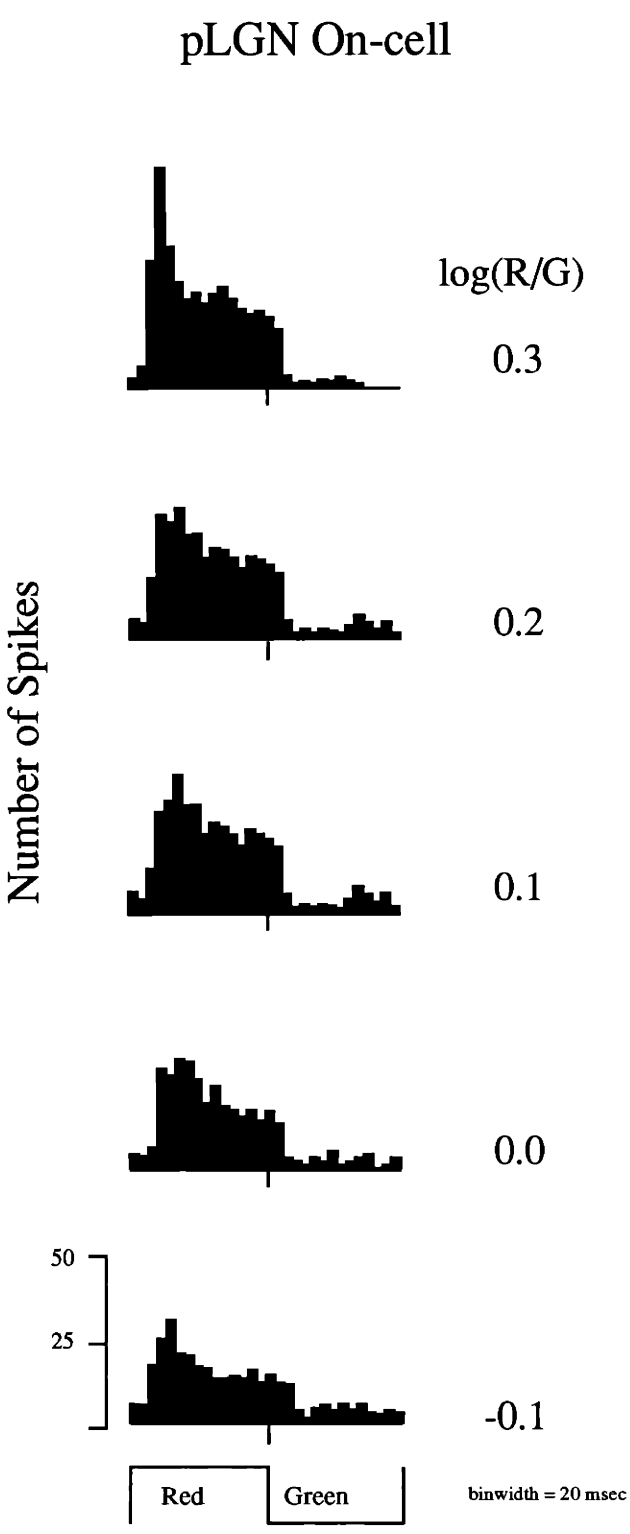
pLGN On-cell
log(R/G)
0.3
0.2
0.1
0.0
-0.1
Number of Spikes
50
25
Red
Green
binwidth = 20 msec

Figure 3.4

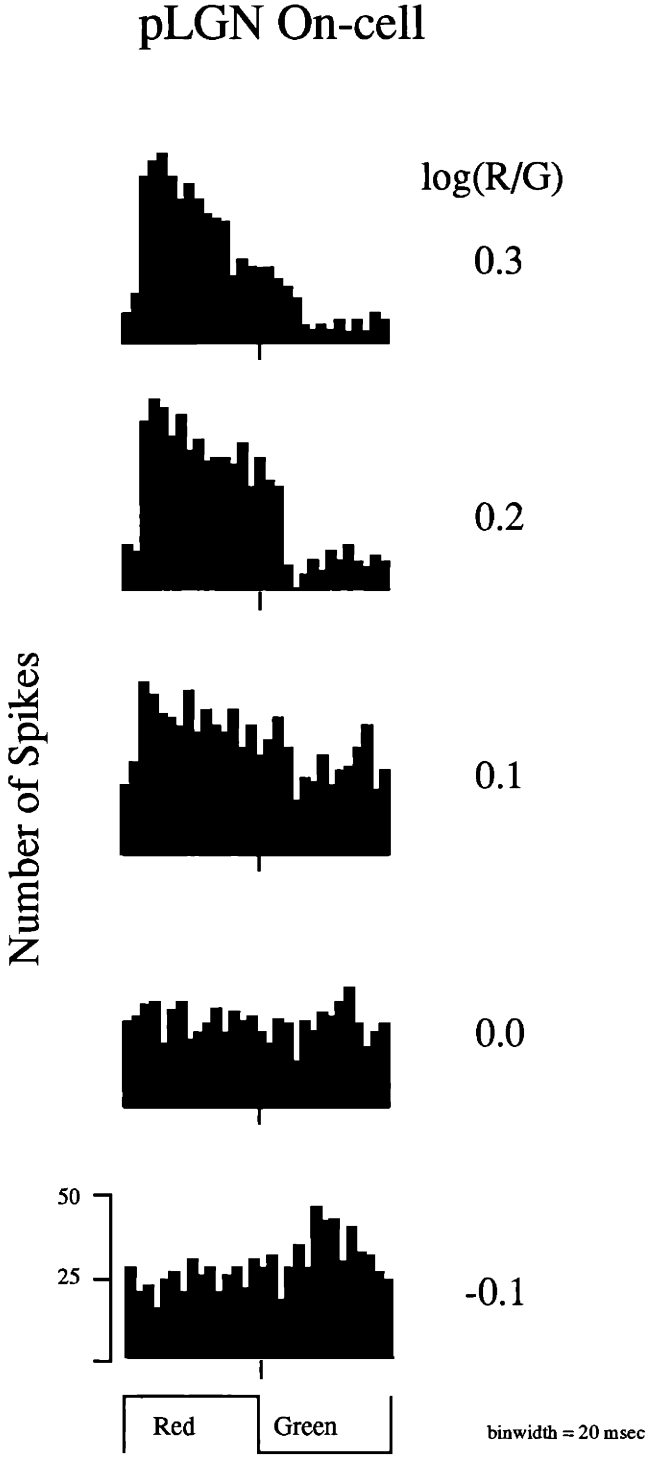
pLGN On-cell
log(R/G)
0.3
0.2
0.1
0.0
-0.1
Number of Spikes
50
25
Red
Green
binwidth = 20 msec

Figure 3.5

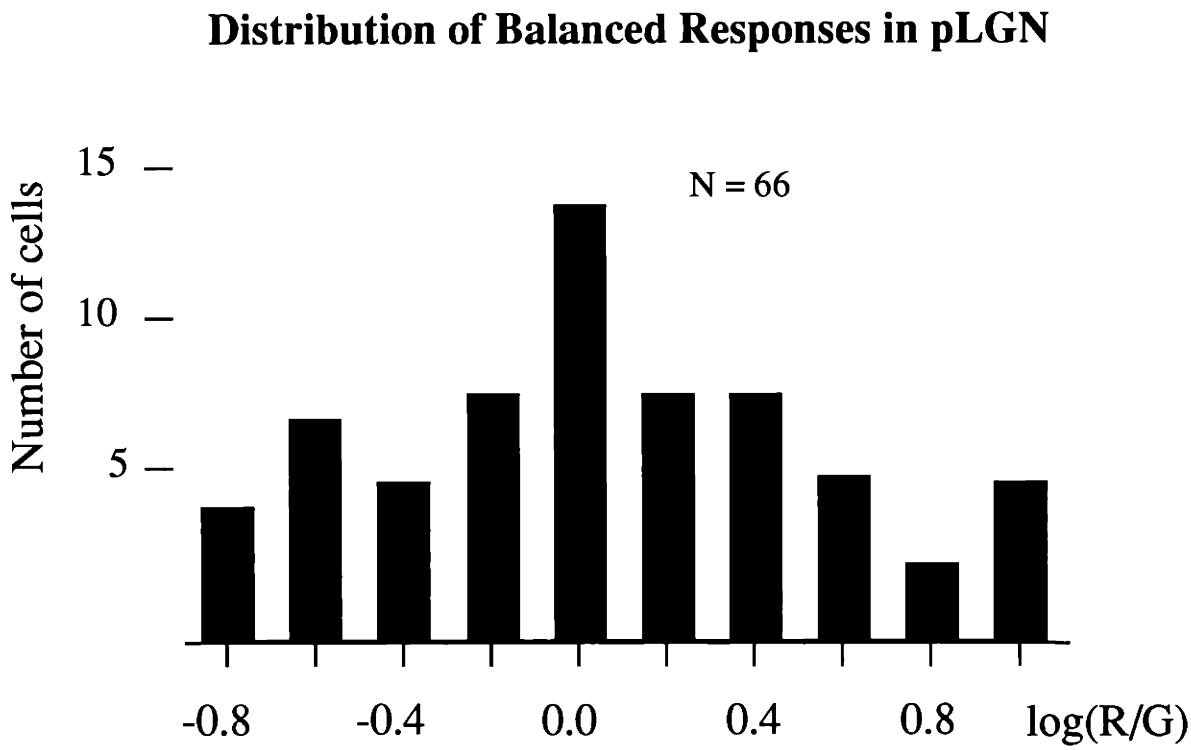
Distribution of Balanced Responses in pLGN
Number of cells
15
10
5
N = 66
-0.8
-0.4
0.0
0.4
0.8
log(R/G)

Figure 3.6

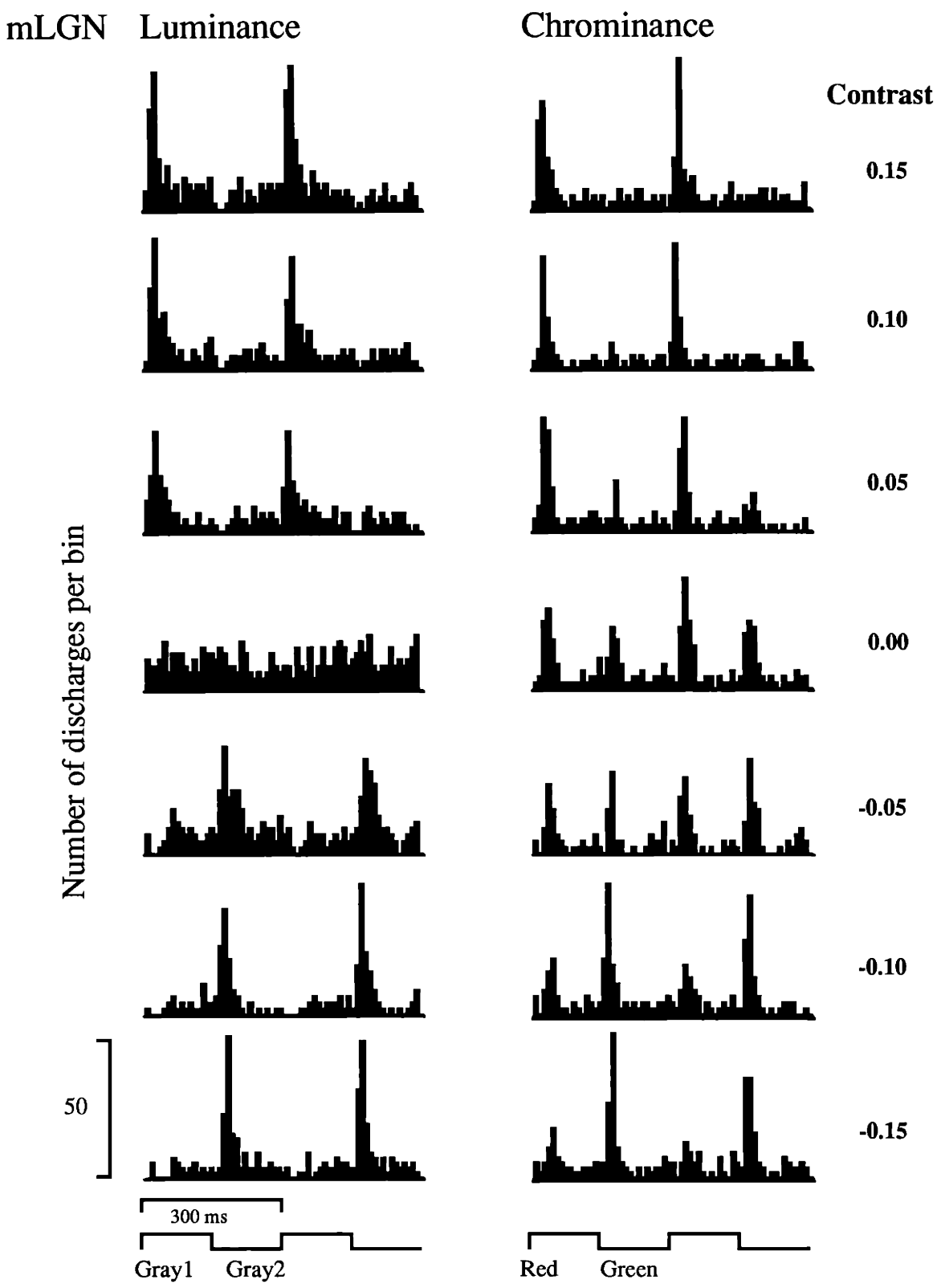
mLGN
Luminance
Chrominance
Contrast
0.15
0.10
0.05
0.00
-0.05
-0.10
-0.15
Number of discharges per bin
50
300 ms
Gray1
Gray2
Red
Green

Figure 3.7

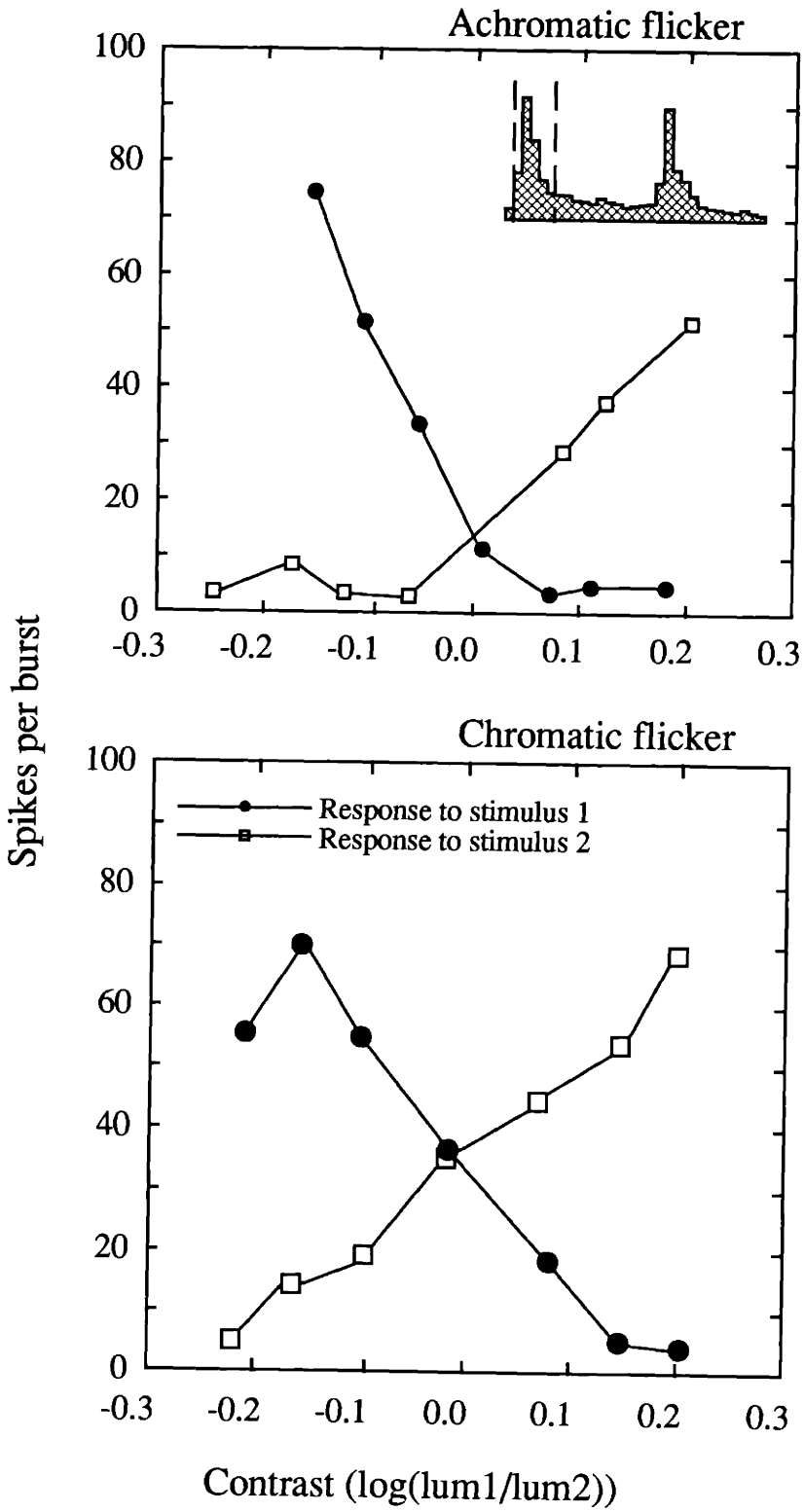
Achromatic flicker
100
80
60
40
20
0
-0.3
-0.2
-0.1
0.0
0.1
0.2
0.3
Chromatic flicker
Response to stimulus 1
Response to stimulus 2
Spikes per burst
Contrast (log(lum1/lum2))

Figure 3.8

CHAPTER FOUR

TUNING PROPERTIES OF CELLS IN AREA MT AS A FUNCTION OF CHROMINANCE AND LUMINANCE

Summary

We studied the ability of cells responsible for movement perception to use color and luminance information. Single unit recordings were obtained from the middle temporal area (MT) in alert rhesus monkeys. The stimuli consisted of counterphased sine wave gratings that varied in their luminance and chromatic content and were restricted to the central 20 degrees of visual field. The stimuli were expressed in terms of L and M cone modulations (Stromeyer *et al.*, 1985). Contrast sensitivity functions were obtained for luminance and isoluminant color conditions and tuning properties were measured for direction and velocity and compared for each contrast configuration.

MT cells respond well to red\green and to blue\yellow isoluminant stimuli. For directionally tuned cells, neither the degree of tuning nor the preferred direction were altered by isoluminant stimuli. For velocity tuning on the other hand, the optimal response shifted towards lower velocities for many of the cells when using isoluminant stimuli. The cells do however, remain tuned to velocity. These results demonstrate that MT is capable of processing information based on differences in wavelength as well as luminance. This is consistent with the concept of an invariant representation of discontinuities within motion analysis.

1.0 INTRODUCTION

The perception of movement is of such importance to image processing that it is considered to be a fundamental property of vision like color or stereopsis (Nakayama, 1985). By analyzing displacements within a visual image over time, spatial relationships between objects can be determined: Relative depth of objects (motion parallax), three-dimensional shape (structure from motion), and image segmentation (figure-ground segregation) can all be recovered from motion information. In addition, stabilization of moving objects or the visual environment during self-motion also depend on visual motion signals. The importance of movement perception in vision is reflected by the existence of several cortical areas that appear to be dedicated to motion analysis.

Recently, there has been some controversy over the kind of information that can be used for motion analysis (Livingstone and Hubel, 1987; 1988; Ramachandran and Gregory, 1978). Specifically, it has been claimed the motion system is unresponsive to color cues (*i.e.* information provided by differences in wavelength). This is supported by psychophysical evidence that shows that under conditions where only color cues are available, the perception of movement is degraded (Ramachandran and Gregory, 1978; Livingstone and Hubel, 1987). In addition, there is physiological evidence that area MT receives input predominantly from the magnocellular subdivision of the lateral geniculate nucleus (mLGN) (Maunsell *et al.*, 1990). The center/surround organization of cells in the mLGN are not spatially segregated by cone type

(DeMonasterio, 1978) and thus have no overt color selectivity. This has lead to the suggestion that pathways involving the mLGN (M pathway) and parvocellular LGN (P pathway) are the neural substrates for the psychophysical luminance and chrominance pathways respectively (Shapley, 1990) and are believed to operate independently (Livingstone, 1984) in the early stages of these pathways.

On the other hand, integration of different types of information increases the robustness and reliability of the visual system; an idea that has also been applied to machine vision (Poggio *et al.*, 1988). Psychophysical experiments in chapter two as well as data from other experiments (Lee, 1970; Ramachandran, 1988; Cavanagh, 1989) suggest that information from different cues, particularly wavelength and luminance, are integrated to some extent. Indeed, there is a contribution of color to motion perception (Logothetis *et al.*, 1990; Stromeyer *et al.*, 1990; Krauskopf and Farell, 1991; Dobkins and Albright, 1991; Cavanagh, 1991). The physiology described in chapter three demonstrates that cells in both the parvocellular and magnocellular LGN are capable of signalling changes in wavelength information and that activity in both the P and M channels are reduced at isoluminance. This argues against ascribing function to the P and M channels based on a 'silenced' M channel at isoluminance. The LGN physiology suggests that color information may have an input to motion through either LGN pathway: residual activity may occur at isoluminance due to interneuronal variability in the isoluminance point or second harmonic responses seen in mLGN cells. It is also possible that motion

perception at isoluminance is mediated by a chromatic, opponent-color mechanism. Activity at the level of LGN is not likely to reveal the nature of this color input to movement perception.

Lying in the posterior bank and floor of the superior temporal sulcus, the middle temporal (MT) area is one of the most extensively studied visual cortical areas that has been associated with motion processing. Dubner and Zeki (1971) first reported that cells in MT are selective for direction of motion which has been demonstrated many times since (Zeki, 1974; Van Essen *et al.*, 1981; Baker *et al.*, 1981; Albright *et al.*, 1984; Felleman and Kaas, 1984; Mikami *et al.*, 1986; Saito *et al.*, 1986). Several laboratories also report that cells in MT are tuned to a range of speeds of the stimulus (Baker *et al.*, 1981; Maunsell and Van Essen, 1983; Felleman and Kaas, 1984; Mikami *et al.*, 1986; Rodman and Albright, 1987). Monkeys with ibotenic acid lesions have elevated thresholds for direction discrimination (Newsome and Pare, 1988) and detection of shearing motion and structure from motion (Andersen and Siegel, 1990) in dynamic random dot displays. In this series of experiments, tuning properties of cells in area MT are measured using luminance and color stimuli to determine if the color contribution to motion is mediated by area MT.

2.0 MATERIALS AND METHODS

2.1 Subjects

One juvenile (88-52) and two adult (87-45, 87-46) male rhesus monkeys weighing between 2.8 and 8.5 kg at the time of recordings were used for this

study. All three animals were used for the psychophysical experiments described in chapter two and as a result, isoluminance was well established for each animal. The animals were cared for in accordance with the National Institutes of Health Guide for the Care and Use of Laboratory Animals and the guidelines of the Massachusetts Institute of Technology Committee on Animal Care.

2.2 Training and Recording

The animals were initially fitted with collars and restrained in primate chairs to familiarize them with the experimenter and laboratory conditions. Subsequently they underwent an eye-coil and head-post implantation surgery: A scleral search coil is surgically attached to the conjunctiva (Judge *et al.*, 1980) to monitor eye movements (Robinson, 1963) and a stainless post is attached to the skull to eliminate head movements. The animals were then trained to perform a fixation task described in figure 4.1. To receive an apple juice reward, the animal had to maintain fixation on a small spot in the center of the monitor for a period of two to three seconds. During this fixation period, a visual stimulus, either a bar or sinusoidal grating, would appear in the visual field for receptive field plotting or data collection. Data was collected prior to the appearance of the stimulus to determine the spontaneous level of activity. In order to reduce the transient response to onset of the stimulus, the grating was ramped on over a period of 100 msec. After the period of plotting the stimulus would disappear and the monkey would then make a saccade to a

laterally displaced target, signifying the end of the trial.

When the animals were sufficiently trained, they underwent a recording chamber implantation surgery. One animal received an open cylinder chamber (Evarts, 1966) while the other two received a ball and socket chamber. The latter consisted of a ball and socket joint implanted to the skull with a guide tube passing through the center of the joint. The ball and socket chambers were implanted so penetrations were roughly perpendicular to area MT. This approach simplified locating suitable recording sites because of the topographic organization of the area. In addition, the upper layers could be accurately determined since the electrode passed through area MST and the superior temporal sulcus immediately prior to MT.

Etched platinum\iridium wires coated in glass were used for these recordings. Signals were amplified (BAK Electronics, Inc., A-1B) and band-pass filtered (Krohn-Hite, 3750) before being sent to a window discriminator (Mentor, N-750) to isolate individual cells. The signal was then split and sent to a PDP 11/73 for data collection, an oscilloscope (Hitachi, VC-6020) and an audio monitor (Grass, AM8). Recording sessions typically lasted four to six hours.

2.3 Stimulus Presentation

The entire experiment with the exception of stimulus presentation was controlled by a PDP 11/73 (Digital). The stimuli were generated by an Adage 3000 raster display system and, in later experiments by an IBM/Pepper SGT

Plus graphics system (Number Nine Computer Corp.).

When an individual MT cell was isolated, the receptive field was hand-plotted with a high contrast white bar using a computer-controlled joystick. The extent of the receptive field was delineated and stored using the bar stimulus. All of the subsequent stimuli consisted of sine wave gratings that were confined to the excitatory receptive fields. Brief tuning curves (2-3 trials per condition) were taken but not saved to get an indication of the degree of tuning for contrast, direction and velocity. Most of the data files varied along one of these parameters while the others were optimized. Typically ten trials were taken for each condition within a file unless the isolation was compromised. In some cases the files varied along two parameters (i.e. contrast and velocity or contrast and direction) and the results were consistent with tuning files presented in sequential order.

As described in chapter two, chromatic aberrations produce considerable luminance artifacts at higher spatial frequencies. For this reason, the majority of sinusoidal gratings had spatial frequencies below 4 cycles/degree (see chapter 2, section 2.2). For stimuli of 2 cycles/degree or higher special consideration was taken to insure that the results were not artifactual due to chromatic aberrations. At higher spatial frequencies there was concern for truncations in the calculated values for the sine wave gratings. These experiments were run using a spatial frequency filtered version of the stimulus (Ozolith neutral paper no. 3) which was designed to remove high spatial frequencies that may have been introduced by errors in the calculations. In addition, the majority of cells

in MT did not respond to luminance gratings of contrast equivalent to the calculated worst-case artifact for a 4 cyc/deg grating.

2.4 Von Kries Color Space

The Von Kries color space was used to generate and represent the contrast of the stimuli (Von Kries, 1899; Stromeyer *et al.,* 1985; Stromeyer *et al.*, 1987). The stimuli are expressed as a function of individual cone class modulation (AC component), normalized to the excitation due to the steady state, background illuminant (DC component). There are several advantages of using this space: First, because the principal axes are expressed as long-, middle- and short-wavelength cone excitations, stimuli representing the cardinal directions of color as well as luminance modulation are easily expressed. Defining stimuli in terms of cone excitation also allows for the comparison of cell responses to luminance and chrominance. A given set of equivalent cone modulations can produce either luminance or chromatic gratings depending on the spatial phase of the modulation. Lee *et al.* (1989) has shown that the response of mLGN cells at isoluminance is directly dependent on this degree of antiphase cone modulation. Finally, because the axes of the space are represented as the change in cone excitation over total excitation, the space is independent over a large range of luminance values (Weber's Law).

Figure 4.2 illustrates the configuration of the stimuli used for one animal (87-45) in this space. The horizontal, or 0 degree axis represents the

rate of quantal absorption of the L cones to the stimulus (ΔL) normalized to the rate of quantal absorption due to the background adaptation level (L). The vertical, or 90 degree axis similarly represents the rate of quantal absorption for the M cones normalized to the adaptation level. The vectors represent the spatial (or temporal) modulation of the drifting sinusoidal gratings. For these experiments the modulation was constant around the mean so the vectors are symmetric. The mean level for M- and L-cone modulation was a yellow with a luminance level of 35 cd/m^2. The CIE coordinates were x = 0.459 and y = 0.463. Vectors along the vertical axis stimulate the M cone without affecting the L cones. Inset A shows the modulation of cone excitation (M cones, solid line; L cones, broken line) along this axis over space. In this case the M cones are modulated sinusoidally while the rate of quantal absorption of the L cones remains constant. For both the M and L cones the mean rate of quantal absorption is the same and equivalent to the rate at the background illumination. An identical profile would be seen for vectors along the horizontal axis if the solid line referred to the L cones.

For this particular animal, modulation along the 45 degree axis shown in inset B produces an equivalent rate of quantal absorption at all spatiotemporal points forming a light/dark yellow luminance grating. For each cone class the cone excitation is varying sinusoidally and with the same phase with respect to the other. Stimuli presented along this axis will be referred to as "inphase" or "luminance" modulation. The representation in cone excitation space can be converted to standard Michelson contrast by dividing the 45

degree vector by the square root of two. Vectors along the -45 degree axis shown in inset C also create sinusoidally varying absorption rates of equal amplitude but the modulation is 180 degrees out of phase. For these stimuli the net quantal catch is constant and the same as the adaptation level. Thus, the luminance is constant and the stimuli appear as red/green sinusoidal gratings. These stimuli will be referred to as "antiphase" or "chrominance" modulation or "isoluminant" stimuli when relevant.

2.5 Comparison to Color Space Proposed by MacLeod and Boynton

The color space defined by MacLeod and Boynton (1979) has been used in recent physiological experiments to determine the chromatic properties of neurons (Derrington *et al.,* 1984; Lennie *et al.,* 1990). The primary difference between this space and the one described in the previous section is the location of the mean adaptation level in CIE space. The MacLeod and Boynton space uses a mean level that is close to equal energy white (x = 0.311, y = 0.336) whereas in the space used in these experiments the mean level is closer to yellow (x = 0.459, y = 0.463). There are several distinct advantages of using the Von Kries space. First, greater cone modulations can be achieved. As Cavanagh (1991) points out, one can only achieve a modest modulation of color in cone space with monitor phosphors (about 30%) whereas a luminance modulation of 100% is easily achieved. Unlike the MacLeod and Boynton space, the Von Kries space is not modulating around a white point and can achieve a higher degree of cone contrast. This is due to the mean adaptation

level of the Von Kries space falling closer to the edge of the triangle defined by the monitor phosphors in CIE space. In addition, modulating the L and M cones on the axis that passes through equal energy white (orthogonal to L-M modulation) also does not take full advantage of the usable color space. As mentioned above, Lee *et al.,* (1989) showed that the response of mLGN cells at isoluminance was dependent of the degree of antiphase L and M cone stimulation. Using the MacLeod and Boynton space, Lennie *et al.,* (1990) were only able to modulate M cones by 7.4% whereas we were able to achieve modulations near 20% for both L and M. For the yellow mean level, the Weber-Fechner fractions are approximately equal for both L and M cones which also contributes to a larger degree of modulation (Stromeyer *et al.*, 1985; 1987). In addition, Stromeyer *et al.* measured detection threshold of flashing (1985) and flickering stimuli (1987) on adaptation fields of different wavelengths. They found that detection thresholds were lowest when using a yellow adapting field. Further evidence indicates that a yellow field of this magnitude will enhance the detection of chromatic stimuli (Cole *et al.*, 1990), suggesting that this stimulus configuration may be the most appropriate for detecting an opponent-color mechanism in MT.

2.6 Data analysis

Figure 4.3 describes how cell activity was defined for the majority of analysis. For each trial the spike train was convolved with a gaussian function generating a spike density function (MacPherson and Aldridge, 1979). The

mean level of activity, or spontaneous rate, was computed during the time period in which the monkey was fixating prior to the appearance of the stimulus. Excitation and inhibition levels were taken as the activity that was two standard deviations above or below this mean level of activity. Integration of these shaded portions of the curve then represent the total excitation and inhibition of the cell. Fast Fourier transforms (Brigham, 1988) were applied to the data to determine if responses at isoluminance were a result of harmonic distortion.

Direction tuning was measured at 22.5 degree intervals beginning with upwards motion along the vertical axis. To obtain a measure of direction selectivity, cell activity is represented in polar coordinates with the sum of the vectors having a length equal to the cell activity (either excitation or inhibition) and a direction equal to the tested stimulus direction over a block of trials. Let us assume that R_i represents the spike activity value for a given stimulus direction, θ_i, where $\theta_i = (i \times 22.5)$. These vectors can be decomposed into x and y components:

$$SumY = \sum_{i=0}^{15} (R_i \cos\theta_i)$$

$$SumX = \sum_{i=0}^{15} (R_i \sin\theta_i)$$

The vector length is also normalized to the cell activity:

$$SumAct = \sum_{i=0}^{15} R_i$$

To obtain the direction index, DI, then:

$$DI = \frac{\sqrt{SumX^2 + SumY^2}}{SumAct}$$

This represents the sum of cell activity for the tested directions. Note that because inhibition of the firing rate is assigned a negative value, the direction index can have a value greater than one. This index of direction tuning is not like the commonly used measure (Mikami *et al.*, 1986; Saito *et al.*, 1989):

$$DI' = 1 - \left(\frac{response_{nulldirection}}{response_{preferreddirection}}\right)$$

The former index includes responses that do not fall on the preferred axis, and thus, includes a measure of the width of the direction tuning.

The preferred direction (θ_m), of the cell in degrees is calculated as:

$$\theta_m = ArcTan\left(\frac{SumY}{SumX}\right) x \frac{180}{\Pi}$$

Thus, the preferred direction, like DI, is a weighted sum of the responses in all tested directions, and does not necessarily correspond to the tested direction

giving the maximal response.

Two ranges of values were used to determine the velocity tuning for each cell depending on the optimal spatial frequency. For higher spatial frequencies, velocities of 0.5, 1, 2, 4, 8, 12, 16, and 20 degrees/sec were used. For lower spatial frequencies 1, 3, 7, 15, 20, 25, 30, and 35 degrees/sec were used.

For some of the data analysis, the mean firing rate and standard error for each condition was calculated trial by trial. Using a two-tailed T-test, it could be determined if two populations of responses were significantly different. The formula used was:

$$t = \frac{\bar{X}_1 - \bar{X}_2}{\sqrt{\frac{(se_1^2 * (n_1 - 1) + se_2^2 * (n_2 - 1))}{n_1 + n_2 - 2} (\frac{1}{n_1} + \frac{1}{n_2})}}$$

Where $\bar{X}_1$ and $\bar{X}_2$ are the mean firing rates for the two populations, n_1 and n_2 are the number of trials for each condition and se_1 and se_2 are the standard errors. This method was used to compare responses to isoluminant color stimuli to responses to stimuli of various luminance contrasts.

2.7 Histology

At the completion of data collection marker lesions were placed in MT and the animal (87-46) received an overdose of sodium pentothal. Following transcardial perfusion with heparinized saline and 4% paraformaldehyde, the

tissue was blocked and stored in a 30% sucrose/paraformaldehyde solution. The tissue was sectioned at 40 microns and alternate sections were stained for either cell bodies (cresyl violet) or myelin (Gallyas, 1979, modified by Maunsell, personal communication). Histological verification of recordings sites has not been completed on the other two animals (87-45, 88-52) because of continuing experiments.

3.0 RESULTS

I collected data from 195 cells from 4 hemispheres of 3 monkeys. Due to the duration of stimulus presentation, however, not all conditions are tested in each cell.

3.1 Response to Isoluminant Color Stimuli

All MT cells responded to isoluminant color gratings[1]. Figure 4.4 shows the responses of one MT cell to moving isoluminant color and luminance gratings. The gratings for each condition had identical velocities, directions and spatial frequencies. The top row represents the cell activity to sinusoidal gratings in which L and M cones are modulated 180 degrees out of phase with respect to each other (*i.e.* antiphase modulation represented as inset C in Figure 4.2). The lower row ($\Delta L/L+\Delta M/M$) is the response to sinusoidal gratings in which the L and M cones are modulated inphase (inset B in Figure 4.2) to produce a luminance grating. Each column of histograms depicts a different level of cone modulation (2, 4, 8, 16%, from left to right). For each column the

degree of cone modulation is identical, only the spatial phase with respect to each cone class is shifted. As is typical for all cells in MT, the response to the stimuli increases as cone modulation is increased. For this cell, the largest response is to a luminance grating with a 16% L and M cone modulation. This also corresponds to 22.63% in conventional Michelson contrast. This cell also fires to the higher contrast gratings modulated in antiphase. Under these conditions the response to the isoluminant grating is considerably less than the luminance grating at 16% cone contrast. This however, is not the case for all cells. Figure 4.5 are histograms of the responses of another cell to gratings of the same cone contrasts. Like the previous cell, the response increases as cone modulation is increased. This cell however, responds better to the isoluminant color gratings when luminance and isoluminance are expressed in equivalent cone contrasts. This cell is also more sensitive than the previous cell, having a noticeable response at 4% cone modulation. Figure 4.6 shows the responses of another cell that also responds well to an isoluminant color grating. For the given stimulus configuration, the cell also responds better to the high contrast grating modulated in antiphase.

Figure 4.7 is a three-dimensional representation of cell activity to moving sinusoidal gratings composed of modulations along several axes of the color space (inset). For convention, modulation of $\Delta M/M$ will be designated as the zero degree axis. A luminance grating would then roughly be the forty-five degree axis and isoluminance would be -45 degrees, depending on the animal's isoluminance point. In addition to luminance and isoluminant L and M

modulated gratings, the cell was tested for modulations of single cone classes, ΔL/L and ΔM/M (90 and 0 degree axes, respectively). Activity is measured as the average spike discharge for the duration of the stimulus. This cell responds well to each individual cone class modulation, and like the previous cell, gives a larger response to antiphase modulation (-45 degree axis) than to inphase modulation (45 degree axis).

Figure 4.8 compares the responses of 175 MT cells to high contrast luminance and isoluminant L- and M-cone modulated moving gratings. All stimulus conditions other than the spatial phase of the cone modulations were held constant. For each cell, the response of the cell to a sinusoidal luminance grating (inphase modulation), excitation or inhibition as defined in the methods section, is plotted against the response to the isoluminant color grating (antiphase modulation). Almost all the cells respond to both luminance or isoluminant color gratings. The slope of the linear regression analysis is 0.8841, and the amount of scatter is low (R^2 = 0.859). Thus, cells in area MT are very active under isoluminant conditions when cone modulation is high. For a subpopulation of cells, a two-tailed t test was administered to determine if the responses to luminance and isoluminance color gratings were significantly different (figure 4.9). The two independent sample t test is a means for testing a hypothesis of equality of means, requiring a trial-by-trial analysis of the cell activity. For both conditions, the criterion level (t_{18}) was 2.101 at a significance level of 0.05. When comparing the responses between 8% L- and M-cone modulation inphase and 8% modulation antiphase, 10 out of

49 cells reached criterion, and are thus considered to be significantly different at the $\alpha = 0.05$ level. Six of these ten did not respond as well to the isoluminant grating while the other four responded better. For 80% of the cells, there was no significant difference between responses to luminance and isoluminant color gratings. On the other hand, when comparing an 8% antiphase color grating to a 2% cone modulation luminance grating, 45% of the cells are considered to be significantly different at the $\alpha = 0.05$ level. In this case however, all of the cells that fail the equality hypothesis have a $t > 2.101$ meaning that they all respond significantly better to the isoluminant color grating than to the 2% inphase modulation grating.

In chapter 3 a frequency-doubled response at isoluminance in magnocellular LGN cells was described and has been well-documented elsewhere (Schiller and Colby, 1983; Derrington *et al.*, 1984; Lee *et al.*, 1989; Logothetis *et al.*, 1990). Since Maunsell *et al.* (1990) find that MT receives input predominantly from mLGN, it may be that responses at the second harmonic are responsible for the activity of MT cells at isoluminance. To test this the spike density functions were analyzed for the power spectrum distribution in the frequency domain. Figure 4.10 shows the contributions of the first and second Fourier components for cell activity at isoluminance. We have previously shown (Charles and Logothetis, 1990) that the second harmonic components of some MT cells increase with increasing chromatic contrast but that this response is only a fraction of the total activity. This is supported by figure 4.10. Activity at the first and second components are

normalized to the total activity at isoluminance. For most of the cells, the first and second fourier components make up less than ten percent of the response. Some cells do have a large contribution from the second harmonic but this is still less than half of the total response. Thus, although MT receives a heavy input from mLGN, a frequency-doubled response does not constitute the majority of activity at isoluminance.

3.2 Directional Tuning of Cells in MT

Figure 4.11 shows the distribution of 59 cells using the directional index described in section 2.5 and summarized in the inset. Direction tuning was tested using drifting sinusoidal gratings of optimal spatial frequency and velocity. The grating consisted of a luminance grating of 65% Michelson contrast. Over half of the cells tested had an index of less than 0.2 but many cells have an index greater than 0.3. As mentioned previously, this measure of directional tuning is not equivalent to the conventional measure of tuning, (1 - null direction/pref. direction). Figure 4.12 shows two examples of cells with low indices of direction. Part A is a polar plot of the cell activity (r) for the direction tested (Θ_i). Also included in the figure is the resultant vector, (DI, Θ_m) represented as the black line beginning at the origin. The directional index for this cell is 0.11 when summing the activity over all the tested directions. If one measures direction tuning by comparing activity on the axis of preferred direction however, the index becomes 0.5. Part B shows an example of another cell which also is not very directional (DI = 0.06). The lower portion of the

figure shows the raster displays of spike activity for each of the directions listed above. Below the rasters are the spike density functions of the corresponding activity. The solid vertical line indicates when the grating begins to move and the dotted vertical line marks when the stimulus disappears. As mentioned before, the stimulus fades in gradually in an attempt to reduce the transient response to the appearance of the stimulus. Still, there is a substantial response to the appearance of the grating which is seen as the area under the spike density function to the left of the solid black line. While the spontaneous activity is relatively low, this cell responds well for all directions tested. The preferred direction of this cell is 339 degrees however it is clear that the cell is not very directional. Thus, it should be noted that using this method of directional tuning the preferred direction, Θ_m, will not be reliable when the DI is low.

Figure 4.13 displays the direction tuning for one MT cell. Like the previous figure, r is the firing rate in spikes per second and Θ is the direction of motion of the grating. The left plot is the direction tuning for an antiphase L and M cone modulation of 16% while the right is an inphase modulation of the same cone modulation. The direction indices (SI) and preferred directions (Θ_m) are given in the lower left corners of each plot. As described in section 3.1, the cell responds as well to the isoluminant L and M modulated grating as to the luminance modulated grating. Upon visual inspection one can see that the cell responds similarly to different directions of motion for both conditions. This is verified by the quantitative analyses of the tuning for both the direction

index (DI = 0.47 and 0.43) and preferred direction (Θ_m = 95.28 and 102.96 degrees).

The next figure, 4.14, plots the direction index for a luminance grating that elicited the best response against the DI for an antiphase modulated grating (R/G Isoluminance) that also elicited the maximal response. Spatial frequency and velocity were fixed for both conditions for all cells. The plot shows that there is a fair amount of variability (R^2 = 0.56) and that for many cells with a low direction index to a luminance grating (less than 0.3), many of the cells show a sharper tuning for the luminance grating. For cells with a DI > 0.3 for luminance however, all cells retain a high degree of directionality for when tested with an isoluminant color grating. The slope of the linear regression analysis is 0.9563, suggesting that overall, the degree of directionality of cells in MT is unaffected at isoluminance.

It is obvious to next address whether there is a change in the preferred direction. As mentioned previously, the preferred direction, Θ_m, becomes less meaningful as the directional index decreases. If one assumes a given amount of variability in the response of the cell, the preferred direction becomes more random as the DI decreases. Thus, it is necessary to include some measure of the DI when looking at the preferred direction. In figure 4.15, the direction index, determined from a high contrast luminance grating, is plotted against changes in the preferred direction for luminance and isoluminant color gratings. Like cells in the previous figure, spatial frequency and drift rate were held constant while inphase and antiphase modulation values were

chosen to produce maximal excitation. Over seventy percent of the cells had a shift in the preferred direction of less than 22.5 degrees, which was the interval for which direction was tested. As one might predict, most of the cells with a $\Delta\Theta_m$ > 22.5 degrees had a low direction index. The preferred direction changed very little for all but one of the cells with a DI > 2.5. Thus the direction tuning for highly directional cells is not affected by isoluminance.

In addition to holding luminance constant and varying cone modulation, chromatic contrast was fixed and luminance was varied. Chromatic content was expressed as color contrast (see figure 2.2), defined as the ratio of the amplitude of the color change along the R-G axis of the CIE chromaticity diagram to the maximum change possible between the red and green phosphors. The red/green gratings were generated by adding the red and green sine waves 180 degrees out of phase. In this case modulation of the red (CIE = 0.602, 0.303; dom λ = 625 nm) and green phosphors (CIE = 0.284, 0.581; dom λ = 525 nm) was 100%. Nine luminance contrasts, generated by varying the luminance of the green sine wave while holding the red sine wave fixed, varied up to 18% Michelson luminance contrast. Figure 4.16 shows representative responses to these stimuli. Negative contrast values refer to a red luminance greater than the green luminance. Like conditions in which cone modulation is held constant, the preferred direction, DI and firing rate change very little over the various contrasts. This was typical for cells that exhibited direction tuning.

3.3 Velocity Tuning of MT Cells

In addition to determining direction tuning for luminance and isoluminant color gratings, several of the cells were also tested over a range of velocities for luminance and isoluminant conditions. Many of the cells exhibited a shift in the preferred velocity. Figure 4.17 shows the velocity tuning for one cell for a luminance grating and red\green and blue\yellow isoluminant gratings. The raster displays on the right represent the occurrence of action potentials for each velocity listed (1.0, 3.0, 7.0, 15.0, 20.0, 25.0, 30.0, 35.0 deg/sec). Underneath each raster display is the corresponding spike density function described in the methods section[2]. On the left are the mean spikes per second for each velocity. For the luminance grating the response of the cell increases monotonically, reaching a peak at 30 deg/sec. Underneath are the velocity tuning curves for red/green isoluminance (L and M cone antiphase modulation) and blue/yellow isoluminant gratings. For the isoluminant conditions, the cell responded optimally at 15-20 deg/sec and gave little to no response to a grating drifting at the optimal velocity for the luminance grating. It must be pointed out that the gratings are not at equivalent cone contrasts. The velocity tuning for the luminance grating is taken at a much higher cone contrast level than either the red/green or blue/yellow gratings. The luminance contrast is much higher than the contrast of the red/green grating when both are expressed in terms of cone modulations. Spatial frequency as well as other stimulus conditions, however, are held constant suggesting that the difference in stimulus conditions does show a shift in the cell's tuning for either the preferred velocity or the temporal frequency.

The next two figures show the responses for one cell modulated along different vectors for two different temporal frequencies. In this case the stimulus configurations in the two figures were fixed except for velocity and were not chosen to provide the optimal response. Unlike the cell in the previous figure, the same cone modulations were used for luminance and isoluminant color gratings. Figure 4.18 shows the response of the cell to various gratings modulated at 16.5 Hz. Notice that the responses to stimuli along the -45 degree vector (isoluminance) are appreciably lower than all of the comparable luminance conditions when using this very high temporal frequency. (It is also interesting that the responses to the individual cone class modulations are as large as the L and M cone inphase-modulated gratings). The next figure, 4.19, shows the responses of the same cell under identical conditions using a temporal frequency of 3.3 Hz. Under these conditions the response at isoluminance is considerably larger and more in agreement with the results presented in section 3.1. Thus, the velocity tuning of many cells in MT are shifted to lower velocities when using red/green isoluminant color stimuli.

3.4 Response to Blue/Yellow Isoluminant Stimuli

Tuning curves were obtained for a small number of cells (n = 14) using isoluminant blue/yellow gratings. Figure 4.20 compares the excitation and inhibition for a luminance (45% L and M inphase modulation) grating to the activity of a blue/yellow isoluminant grating. Unlike an antiphase L and M

cone modulated grating, all but one cell responded worse to the Blue/Yellow grating than the luminance grating. These data are however, not expressed in terms of equivalent cone contrast (see discussion). The slope of the linear regression is low (0.1) and the variability is high ($R^2 = 0.01$) but the graph is representing sum activity, *i.e.* the amount of activity that is two standard deviations above the level of spontaneous activity. If cells were not driven by the blue/yellow isoluminant grating, all the points would fall on the x axis.

The data also suggests that direction tuning is similar for luminance and the blue/yellow isoluminant gratings. Figure 4.21 plots the direction index calculated for cells using a luminance grating versus the direction index for the B/Y isoluminance grating. Although the sample is small, there is nothing to suggest that the direction index is different for the two conditions. Figure 4.22 shows the change in preferred angle as a function of direction index for these same cells. Like the comparison between L and M cone modulation inphase to antiphase modulation, when the direction index is higher than 0.25, the preferred direction does not change much for the blue/yellow grating. Finally, the bottom row of figure 4.17 shows that there may be a shift in the velocity tuning similar to that seen in the L and M cone antiphase modulated stimuli.

Figures 4.23 and 4.24 show tuning of two cells that summarize the findings for area MT. The tunings for contrast, velocity and direction are displayed for L and M cone inphase-modulated gratings (luminance) and antiphase-modulated gratings (R\G) in the left and right columns respectively. The cell shows high contrast sensitivity to the luminance grating, responding at

4.75% contrast. By comparison, the cell responds to the two higher isoluminant values tested (5.98, 8.46%) but the mean spike activity is lower than the comparable luminance grating. In the case of velocity, the cell responds best to the three highest velocities tested (12, 16 and 20 deg/sec) for luminance condition but the best response is shifted downwards for the R\G grating (4-16 deg/sec). The bottom set of figures show that the cell remains directional with the same preferred direction when using isoluminant conditions. Figure 4.24 includes responses to blue/yellow isoluminant color gratings (B\Y). For this cell the mean spikes per second are the same for a 47.5% luminance contrast grating and the 8.46% L and M cone antiphase-modulated (R\G) grating. The response to the blue/yellow grating is somewhat less than the others. Although the cell is not well tuned for velocity, the shape of the tunings for the luminance and isoluminant color grating look comparable as are the direction tuning curves. Figure 4.25 shows similar data for another cell that also shows a shift in velocity. This cell however, did show a difference in direction tuning. The cell was bidirectional for the luminance grating but was very directional for the isoluminant R\G condition (as well as the B\Y condition, not displayed here). This was the only cell that did show a shift from bidirectional tuning to unidirectional tuning.

4.0 DISCUSSION

4.1 Responses at Isoluminance

It is clear from figures 4.3-4.7 that cells in area MT respond to

isoluminant color stimuli. These results are consistent with other physiology experiments that find MT cells responsive to isoluminant color stimuli (Dobkins and Albright, 1991; Saito *et al.*, 1989). One would predict that slope of the regression for figure 4.8 to be very low or zero if cells in MT were not capable of responding to color information. Figure 4.8 shows that MT cells can respond almost as well to an isoluminant color stimuli as luminance stimuli when certain conditions are met: For the stimuli used in these experiments, cone modulation is equated for the luminance and chromatic stimuli so the only difference between the two is the phase of modulation. If instead one uses stimuli that the monitor is capable of producing, comparisons would be between a 100% luminance modulation and a 30% chrominance modulation (Cavanagh and Anstis, 1991) reflecting the limits of the monitor phosphors more than the biological system. Using equivalent cone modulations, MT cells respond almost as well to isoluminant red/green stimuli as luminance stimuli as seen by the slope of the regression in figure 4.8 (slope = 0.88). Saito *et al.* (1989) find that about 50% of the cells are silenced at isoluminance and the rest have reduced activity. The discrepancy in results may be due to differences in the stimulus configurations. In addition, cells in area MT are largely a homogeneous population in terms of response magnitude when comparing luminance and chromatic stimuli ($R^2 = 0.86$). This suggests that M and L cone inputs to receptive field structure are similar for all cells in MT.

Lee *et al.* (1989) found that when stimuli are antiphase modulated with respect to M and L cone excitation, mLGN cells respond to isoluminant stimuli.

Similar results are found for area MT. The isoluminant stimuli described in these experiments produced much better responses than isoluminant color stimuli that produced little antiphase modulation of M and L cone excitation. It was shown also in chapter three that the activity of mLGN cells at isoluminance consists of responses at twice the alternation rate of the stimulus. The isoluminance ratio of this "frequency-doubled" response also varies slightly from cell to cell. In addition, many cells in parvocellular LGN that do exhibit nulls are silenced at luminance ratios that are not centered on behavioral isoluminance.

A frequency-doubled signal is not reflected in the activity of MT cells at isoluminance. Figure 4.10 shows that the majority of cells have a first and second harmonic contributions of less than ten percent of the total activity. This however, does not imply that the second harmonic responses seen at the level of the mLGN are not responsible for activity in MT at isoluminance. The activity of mLGN cells at isoluminance may be redistributed within the frequency domain by the time the signals reach MT. It is also possible that nulls in activity may have been missed due to individual variation in isoluminance points for cells in MT. This is ruled out since many cells were tested using a fixed chromatic contrast over a range a luminance contrasts (0.05-0.01 log steps) and no null was observed (see figure 4.16). Spatial or temporal frequency variations or variations in isoluminance across the visual field cannot explain these results either. Behavioral isoluminance was tested across the visual field using stimulus configurations that were identical to the

ones used in the recordings for each animal (Logothetis and Charles, 1990). Finally, contrast sensitivity functions for luminance stimuli show that the calculated luminance artifacts due to chromatic aberrations are not large enough to produce responses, given the spatial frequencies used in these experiments.

4.2 Relation to Psychophysical Data

The data are consistent with findings in chapter two. As chromatic information was added to a motion task, performance improved. For low luminance contrasts, cells in area MT fire more as chromatic contrast (antiphase modulation) is increased and are thus able to signal motion. Psychophysical experiments by Cavanagh and Anstis (1991) also support the physiological data. They test for a color contribution to motion using an opposed, drifting gratings paradigm. Luminance and chrominance gratings with the same spatial and temporal frequencies are superimposed and drift in opposite directions. By adjusting the luminance of one grating, at some point the two gratings appear to flicker in counterphase, indicating the gratings have equivalent contrasts. The authors find that red/green and blue/yellow color gratings require luminance contrasts on the order of 4-12% to null motion, suggesting a color contribution to motion. When measured in terms of multiple of contrast threshold, luminance and chrominance contributed equally to motion. This is in agreement with other work (Stromeyer *et al.*, 1990) that finds that humans are more sensitive to chromatic stimuli for low temporal

frequency motion detection when luminance and chrominance are expressed in terms of cone modulation.

Krauskopf and Farell (1990) also have evidence for a color input to the motion system. Based on earlier work by Adelson and Movshon (1982) they superimpose two sinusoidal gratings and drift them obliquely. If the two gratings are similar, the pattern coheres and one sees a moving plaid moving in a direction that is a vector sum of the components. If the two gratings are not similar, the two gratings appear to slip past one another in the directions of the components. Using identical spatial and temporal frequencies, Krauskopf and Farell modulate the gratings along the cardinal directions of the MacLeod and Boynton color space. These axes consist of one luminance and two isoluminant chromatic axes. One chromatic axis corresponds to the difference in the excitations of the L and M cones, and the other to the difference in the excitations of the S and the sum of the L and M cones (S/L+M). They find that when gratings are modulated along orthogonal cardinal directions, the gratings appear to slip past one another. They suggest that motion is analyzed by independent mechanisms along these cardinal directions of color space. While this rests on the assumption that lack of coherence implies independent motion mechanisms, motion signals within the isoluminant plane are clearly integrated in the absence of luminance information to achieve coherent motion.

4.3 Direction Tuning at Isoluminance

The direction tuning of MT cells does not change when using isoluminant color gratings. Although there is variability in the direction indices between luminance and red/green isoluminant conditions ($R^2 = 0.56$, figure 4.14) the direction indices are comparable for the population (slope of the regression = 0.96). In addition, there is little change in the preferred direction between luminance and isoluminant color gratings when cells are tuned (DI > 2.5) for direction (figure 4.15). The measure of directionality takes into account the sharpness of the tuning rather just looking along the preferred axis. The circular statistical analysis (DI) fails to describe tuning however, if cells are orientation tuned as in figure 4.25. A cell that is sharply tuned for orientation fires equally well to opposite directions of motion. This cell will produce a direction index that would be the same as a cell that fires equally to all directions. Upon visual inspection of the tuning curves, no changes between pan- or bidirectional cells were seen.

Dobkins and Albright (1990) and Saito *et al.* (1989) also find that cells in MT retain their directional tuning. Saito *et al.* (1989) however, find that in cells that continue to respond at isoluminance (about 50%) the response is reduced by 30-90%, and thus reduces direction tuning by a similar factor. Psychophysical experiments suggest that the direction of movement is not affected by using isoluminant stimuli. In chapter two, optokinetic nystagmus (OKN) was elicited by moving sinusoidal gratings. The directions of these eye movements were consistent with OKN's using gratings of luminance contrast, suggesting that direction of movement is preserved at isoluminance. Other

experiments that investigate motion (Cavanagh *et al.,* 1984; 1985; Poeppel and Logothetis, 1989) do not report errors in direction at isoluminance either. Derrington and Badcock (1985) are able to generate motion aftereffects using isoluminant color gratings. When aftereffects are induced, the motion aftereffect differs from adaptation to a luminance grating in magnitude only, not direction. However when multiples of contrast thresholds are compared, motion discrimination is higher than detection levels for isoluminant color gratings but not for luminance gratings (Lindsey and Teller, 1990; Cavanagh and Anstis, 1991). Thus, the visual system is more sensitive to the appearance of color gratings than to their motion. This is not to suggest that color has little contribution to motion. Detection of the chromatic stimuli is not even likely governed by the same mechanism. To the contrary, Stromeyer *et al.*, (1990) find that motion discrimination thresholds are about four times lower for chromatic stimuli than for luminance stimuli as mentioned in section 4.2.

4.4 Velocity Tuning at Isoluminance

Some cells in MT show a shift in preferred velocity towards lower values when using isoluminant stimuli (figure 4.17). For this cell the cone modulations for the luminance grating was much higher than the isoluminant red/green grating (47.5 vs. 16%). While there is a shift in the preferred velocity the stimuli are not compared in a meaningful way and the result may be due to differences in the effective contrast of the stimuli, not color and luminance (Campbell and Maffei, 1981). Figures 4.18 and 4.19 show the responses of one

where modulations were equivalent as were all other conditions with the exception of velocity. When using the lower velocity (3.3 Hz), the response to vectors along the isoluminance axis is much greater than when using the higher velocity (16.5 Hz).

Cavanagh *et al.*, (1984; 1985) first reported a reduction in the perceived velocity in drifting isoluminant color gratings at low spatial frequencies in comparison to gratings with substantial luminance contrast. Unlike the slowed motion seen in low luminance contrast achromatic gratings (Thompson, 1982), Cavanagh *et al.* (1984) find that the addition of chromatic information reduces the velocity further. This argues for perceived velocity being the weighted sum of luminance and chrominance components, depending on effective contrast. The chromatic information signals a lower velocity, and as the weight of this information increases, the grating slows. Troscianko and Fahle (1988) come to a different conclusion. They find that reaction time latencies for isoluminant color gratings can be imitated using either achromatic low contrast stimuli or high contrast stimuli with spatial uncertainty introduced. This is taken as evidence that luminance and chrominance information are handled by the same system and that the perceived velocity will depend only on the effective contrast of the stimulus. Cavanagh and Anstis (1991) point out that velocity estimates cannot simply rely on effective contrast. Accurate estimates of velocity are made for low (1-5%) contrast as well as high contrast gratings. In addition, an isoluminant color grating appears to move much slower than a 12% luminance contrast grating although the two have equivalent effective

contrasts, as determined by the opposed motion paradigm. Cavanagh and Anstis instead argue that in directionally selective units, velocity signals must be disambiguated from the contrast of the stimulus. They propose that a second type of nondirectional unit is necessary to recovery velocity. If the nondirectional unit is more sensitive to contrast or responds better at isoluminance, the contrast of the stimulus will be overestimated and the contribution of velocity in the directional unit will be underestimated, resulting in a reduction in perceived velocity. In this chapter it is demonstrated that directional units in area MT respond almost as well to isoluminant color stimuli and that little energy (usually less than 10%) is contained in the second harmonic component. On the other hand, cells in mLGN have a frequency-doubled response for stimuli at isoluminance (chapter 3). Making no assumptions regarding the origin of responses of MT cells at isoluminance (see section 4.6) it is possible that these are the neural substrates for velocity estimation.

4.5 Blue/Yellow Isoluminant Stimuli in MT

Although the data is limited, it appears that MT cells respond to isoluminant blue/yellow gratings. Like the L and M cone antiphase modulated gratings, the cells also have the same tuning properties for direction and velocity as the luminance modulated gratings. This is not surprising since the blue/yellow stimulus produces considerable modulation of the L and M cones in antiphase. For this stimulus, $\Delta L/L = 0.07$; $\Delta M/M = 0.09$; $\Delta S/L+M = 0.42$. These

data reemphasize that the response of MT cells depends on the degree of antiphase cone modulation not the perceived difference in hue. Qualitative hue differences may be detected by entirely different mechanisms. This difference in cone modulation likely explains the reduced response to the blue/yellow grating in comparison to the luminance grating. Cavanagh and Anstis (1991) find similar psychophysical results for using the opposed motion stimulus described above. A red/green grating (0.5 c/deg, 2 Hz) has an equivalent luminance contrast of 12% whereas a blue/yellow grating under the same conditions produces an 8% equivalent contrast. When using a green/purple stimulus that falls on the tritanopic confusion line and modulates the S/L+M cone signal, a 4% equivalent luminance contrast is seen. The higher equivalent contrast of the blue/yellow grating is attributed to the additional modulation of L and M cones.

There is also physiological evidence for a S/L+M cone contribution to area MT (Charles *et al.*, 1991). A bright yellow field was superimposed on a sinusoidal modulation of the blue phosphor of the monitor. This reduced the contribution of the blue phosphor to less than 0.5% luminance contrast, effectively restricting modulation to the blue-sensitive cones. Under these conditions we find that most MT cells respond to this S cone stimulus. Since cells in MT also fire to L and M cone antiphase modulated gratings, these findings do not support the notion of independent motion mechanisms for the two chromatic cardinal directions of color space. It does however support an opponent-color input to motion analysis at the level of MT.

4.6 Opponent-color Input to MT

These experiments demonstrate that cells in area MT are responsive to stimuli that are defined solely by wavelength. In addition, the cells remain tuned for direction and velocity, although tuned to lower velocities in many cases. This evidence indicates that MT has access to color information. Recent psychophysics also argues for a opponent-color input to motion, *i.e.* information that is not conveyed by the luminance channel (Cavanagh *et al.*, 1984; Derrington and Badcock, 1985; Logothetis *et al.*, 1990; Krauskopf and Farell, 1990; Cavanagh and Anstis, 1991). What is the nature of this input? There does not seem to be a conclusive answer to this yet. Chapter 3 provided evidence that mLGN cells are active at isoluminance, responding at each wavelength exchange. Established anatomical connections between V_4 and MT may also be the source of a color input (Rockland and Pandya, 1979; Maunsell and Van Essen, 1983c; Ungerleider and Desimone, 1986).

Dobkins and Albright (1990) investigate the nature of the color input to the motion system. They use red/green sinusoidal gratings that reverse in contrast with each shift in phase. This provides two sources of border information. For each contrast reversal, a polarity-contrast border shift in position by 45 degrees or less, for borders that maintain the color contrast the phase shift is larger than 135 degrees. When luminance contrast is present in the stimulus, humans follow motion that preserves the luminance and chrominance polarity. At isoluminance, small phase shifts produce motion in the direction that corresponds to using polarity-changing borders. In this case,

the small phase shifts provide a distance cue for edge correspondence and color information is discarded. For larger phase shifts the distance cue is weaker and color information is used and facilitates correspondence.

Cavanagh and Anstis (1991) find that signalling at polarity-changing borders, likely conveyed by the M pathway, are not responsible for the color input to motion in their stimulus. By introducing a luminance lure into the opposed drifting grating paradigm, they are able to show that phase lag, second harmonic distortion, and interunit variability in their stimulus cannot account for the color input to motion. They also argue that any signals due to these effects will be attenuated because of the combination of On and Off mLGN signals in cortex. The data presented in this chapter does not support a color contribution to motion being mediated by the mLGN either, though it is not ruled out. Responses at the second harmonics contribute only roughly 10% of the total activity at isoluminance although it was pointed out previously that this energy could be redistributed. Krauskopf and Farell argue for separate motion analysis for the three cardinal directions of color space. If these three directions fed into a common motion mechanism, one would expect gratings along different cardinal directions to cohere. This however, is not supported by physiological data that suggests that cells in MT respond to red/green isoluminant stimuli and isolated blue cone stimuli (Charles *et al.*, 1991).

1) It is conceivable that MT cells have nulls that are close but not centered on isoluminance, similar to the balanced response of some mLGN cells. To insure that MT cells did not have nulls coinciding with behavioral isoluminance, cells were tested with a range of nine luminance contrasts centered on isoluminance. Luminance contrast steps were 0.05 or 0.01 log units and chromatic contrast (red/green) was fixed and high for all values (see section 3.2). MT cells were active for all values tested. This is also represented in figure 4.16.

2) Because the displays of the spike density functions are normalized to the maximum value within a block of trials, the area underneath each curve is only comparable within each condition, not between them. This is a problem for display purposes only and in no way affects the analysis.

REFERENCES

Adelson, E.H. and Movshon, J.A. Phenomenal coherence of moving gratings. Nature 300:523-525, 1982

Albright, T.D., Desimone, R., and Gross, C.G. Columnar organization of directionally selective cells in visual area MT of the macaque. Journal of Neurophysiology 51:16-31, 1984.

Andersen, R.A. and Siegel, R.M. "Motion processing in primate cortex." In: Signal and Sense: Local and Global Order in Perceptual Maps, eds. G.M. Edelman, W.E. Gall, and W.M. Cowan. Wiley, New York (1990).

Baker, J.F., Petersen, S.E., Newsome, W.T., and Allman, J.M. Visual response properties of neurons in four extrastriate visual areas of the owl monkey (*aotus trivirgatus*): A quantitative comparison of medial, dorsomedial, dorsolateral, and middle temporal areas. Journal of Neurophysiology 45:397-416, 1981.

Brigham, E.O. The Fast Fourier Transform and its Applications. Prentice Hall, Englewood Cliffs, New Jersey (1988).

Campbell, F.W. and Maffei, L. The influence of spatial frequency and contrast on the perception of moving patterns. Vision Research 21:713-721, 1981.

Cavanagh, P. "Multiple analyses of orientation in the visual system." In: Neural Mechanisms of Visual Perception, eds D.M.K. Lam and C.D. Gilbert. Gulf Publishers, Houston, 1989.

Cavanagh, P. and Anstis, S. The contribution of color to motion in normal and color-deficient observers. Vision Research (in press).

Cavanagh, P., Boeglin, J. and Favreau, O.E. Perception of motion in equiluminous kinematograms. Perception, 14:151-162, 1985.

Cavanagh, P., Tyler, C.W. and Favreau, O.E. Perceived velocity of moving chromatic gratings. Journal of the Optical Society of America, A, 1:893-899, 1984.

Charles, E.R. and Logothetis, N.K. MT responses to drifting low contrast homochromatic and heterochromatic gratings. Investigative Ophthalmology and Visual Science Supplement 31:238, 1990.

Charles, E.R., Logothetis, N.K. and Cavanagh, P. The response of cells in area

MT to stimulation of blue-sensitive cones. Society of Neuroscience Abstracts 17:440, 1991.

Cole, G.R., Stromeyer III, C.F. and Kronauer, R.E. Visual interactions with luminance and chromatic stimuli. Journal of the Optical Society of America, A 7:128-140, 1990.

DeMonasterio, F.M. Properties of concentrically organized X and Y ganglion cells of macaque retina. Journal of Neurophysiology 41:1394-1417, 1978.

Derrington, A.M. and Badcock, D.R. The low level motion system has both chromatic and luminance inputs. Vision Research 25:1879-1884, 1985.

Derrington, A.M., Krauskopf, J. and Lennie, P. Chromatic mechanisms in lateral geniculate nucleus of macaque. Journal of Physiology 357:241-65, 1984.

Dobkins, K.R. and Albright, T.D. What happens if it changes color when it moves? Investigative Ophthalmology and Visual Science Supplement 32:823, 1991.

Dubner, R. and Zeki, S.M. Response properties and receptive fields of cells in an anatomically defined region of the superior temporal sulcus. Brain Research, 35:528-532, 1971.

Eisner, A. and MacLeod, D.I.A. Flicker photometric study of chromatic adaptation: Selective suppression of cone inputs by colored backgrounds. Journal of the Optical Society of America 71:705-718, 1981.

Evarts, E.V. Methods for recording activity of individual neurons in moving animals. Methods in Medical Research 11:241-250, 1966.

Felleman, D.J. and Kaas, J.H. Receptive-field properties of neurons in middle temporal visual area (MT) of owl monkeys. Journal of Neurophysiology 52:488-513, 1984.

Gallyas, F. Silver staining of myelin by means of physical development. Neurological Research 1:203-209, 1979.

Krauskopf, J. and Farell, B. Influence of colour on the perception of coherent motion. Nature 348:328-331, 1990.

Lee, B.B., Martin, P.R., and Valberg, A. Nonlinear summation of M- and L-cone inputs to phasic retinal ganglion cells of the macaque. Journal of Neuroscience 9:1433-1442, 1989.

Lindsey, D.T. and Teller, D.Y. Motion at isoluminance: Discrimination/detection ratios for moving isoluminant gratings. Vision Research 30:1751-1761, 1990.

Livingstone, M.S. and Hubel, D.H. Anatomy and physiology of a color system in the primate visual cortex. Journal of Neuroscience 4:309-356, 1984.

Livingstone, M.S. and Hubel, D.H. Psychophysical evidence for separate channels for the perception of form, color, movement, and depth. Journal of Neuroscience 7:3416-3468, 1987.

Livingstone, M. and Hubel, D. Segregation of form, color, movement, and depth: Anatomy, physiology, and perception. Science 240:740-749, 1988.

Logothetis, N.K., Schiller, P.H., Charles, E.R. and Hurlbert, A.C. Perceptual deficits and the activity of the color-opponent and broad-band pathways at isoluminance. Science 247:214-217, 1990.

MacLeod, D.I.A. and Boynton, R.M. Chromaticity diagram showing cone excitation by stimuli of equal luminance. Journal of the Optical Society of America 69:1183-1186, 1979.

MacPherson, J.M. and Aldridge, J.W. A quantitative method of computer analysis of spike train data collected from behaving animals. Brain Research 175:183-187, 1979.

Maunsell, J.H.R., Nealy, T.A. and DePriest, D.D. Magnocellular and parvocellular contributions to responses in the middle temporal visual area (MT) of the macaque monkey. Journal of Neuroscience 10:3323-3334, 1990.

Maunsell, J.H.R. and Van Essen, D.C. Functional properties of neurons in middle temporal visual area of the macaque monkey. I. Selectivity for stimulus direction, speed, and orientation. Journal of Neurophysiology 49:1127-1147, 1983.

Maunsell, J.H.R. and Van Essen, D.C. The connections of the middle temporal visual area (MT) and their relationship to a cortical hierarchy in the macaque monkey. Journal of Neuroscience 3:2563-2586, 1983.

Mikami, A., Newsome, W.T., and Wurtz, R.H. Motion selectivity in macaque visual cortex. I. Mechanisms of direction and speed selectivity in extrastriate area MT. Journal of Neurophysiology 55:1308-1327, 1986.

Nakayama, K. Biological image motion processing: A review. Vision Research 25:625-660, 1985.

Newsome, W.T. and Pare, E.B. A selective impairment of motion perception following lesions of the middle temporal visual area (MT). Journal of Neuroscience 8:2201-2211, 1988.

Poeppel, D.E. and Logothetis, N.K. Chrominance information can be used by the oculomotor system to program saccades to moving targets. Investigative Ophthalmology and Visual Sciences Supplement 30:112, 1989.

Poggio, T., Gamble, E.B. and Little, J.J. Parallel integration of vision modules. Science 242:436-440, 1988.

Ramachandran, V. and Gregory, R. Does colour provide an input to human motion perception? Nature, 275:55-56, 1978.

Robinson, D.A. A method of measuring eye movements using a scleral search coil in a magnetic field. IEEE Transactions in Biomedical Electrons 10:137-145, 1963.

Rockland, K.S. and Pandya, D.N. Laminar origins and terminations of cortical connections of the occipital lobe in the rhesus monkey. Brain Research 179:3-20, 1979.

Rodman, H.R. and Albright, T.D. Coding of visual stimulus velocity in area MT of the macaque monkey. Vision Research 27:2035-2048, 1987.

Saito, H., Yukie, M., Tanaka, K., Hikosaka, K., and Iwai, E. Integration of direction signals of image motion in the superior temporal sulcus of the macaque monkey. Journal of Neuroscience 6:145-157, 1986.

Saito, H., Tanaka, K., Isono, H., Yasuda, M. and Mikami, A. Directionally selective response of cells in the middle temporal area MT of the macaque monkey to the movement of equiluminous opponent color stimuli. Experimental Brain Research 75:1-14, 1989.

Schiller, P.H. and Colby, C.L. The responses of single cells in the lateral geniculate nucleus of the rhesus monkey to color and luminance contrast. Vision Research 23:1631-1641, 1983.

Shapley, R. Visual sensitivity and parallel retinocortical channels. Annual Review of Psychology 41:635-658, 1990.

Stromeyer III, C.F., Cole, G.R., and Kronauer, R.E. Second-site adaptation in the red-green chromatic pathways. Vision Research 25:219-237, 1985.

Stromeyer III, C.F., Cole, G.R., and Kronauer, R.E. Chromatic suppression of

cone inputs to the luminance flicker mechanism. Vision Research 27:1113-1137, 1987.

Stromeyer III, C.F., Eskew, Jr., R.T., and Kronauer, R.E. The most sensitive motion detectors in humans are spectrally-opponent. Investigative Ophthalmology and Visual Sciences Supplement 31:240, 1990.

Thompson, P. Perceived rate of movement depends on contrast. Vision Research 22:377-380, 1982.

Troscianko, T. and Fahle, M. Why do isoluminant stimuli appear slower? Journal of the Optical Society, A 5:871-880, 1988.

Ungerleider, L.G. and Desimone, R. Cortical connections of visual area MT in the macaque. Journal of Comparative Neurology 248:190-222, 1986.

Van Essen, D.C., Maunsell, J.H.R., and Bixby, J.L. The middle temporal visual area in the macaque: Myeloarchitecture, connections, functional properties, and topographic organization. Journal of Comparative Neurology 199:293-326, 1981.

von Kries, J. Ueber die anomalen trichromatischen farbensysteme. Z. Sinnesphysiol. 19:63-69, 1899.

Zeki, S.M. Functional organization of a visual area in the posterior bank of the superior temporal sulcus of the rhesus monkey. Journal of Physiology, London 236:549-573, 1974.

FIGURES

Figure 4.1. Description of a trial during MT recordings. Time progresses from left to right. The trial begins with the appearance of a small fixation spot in the center of the monitor which the animal must foveate. Data collection begins after foveation and spontaneous activity is recorded. A sinusoidal grating is then ramped on over a period of 100 msec within the receptive field and then begins drifting with a fixed velocity. After the data collection period, a laterally displaced target appears to signal the end of the trial. If the animal fails to hold fixation during any point during the trial is aborted.

Figure 4.2 Description of the color space used to define the luminance and chrominance stimuli. The sinusoidal gratings are modulated around a mean level defined in CIE coordinates in the upper left. This is a saturated yellow background. Axes of the space are changes in individual cone excitation normalized to the cone excitation due to the mean level. M cone modulation is represented on the Y axis and L cone modulation is on the X axis. All modulation vectors used in these experiments were equal around the mean. Inset A represents modulation of the M cones while the excitation of the L cones remains constant at the mean level. Inset B represents equal modulation of both M and L cones with the same phase (inphase modulation). Modulation approximately along this 45 degree axis represents luminance modulation of the stimulus. Modulation along the -45 degree axis (inset C) represents excitation of M and L cones 180 degrees out of phase (antiphase modulation). In one animal modulation along this axis represented isoluminance. Individual variation in isoluminance determined behaviorally will shift the angle of this axis slightly.

Figure 4.3 Definition of cell activity. Individual spike trains were convolved with a gaussian function to produce spike density functions. Spike density functions were aligned to the onset of the stimulus and summed. The portion of the function prior to the onset determined the mean spontaneous activity level. We defined excitation as the area under the curve that was two standard deviations above the mean level (shaded area). Similarly, inhibition is the area integrated under the curve two standard deviations below the mean level (cross-hatched area). Inhibition was assigned negative values.

Figure 4.4 MT cell activity for antiphase and inphase cone modulation. The top row consists of histograms of the response to an L and M cone antiphase modulated sinusoidal gratings ($\Delta L/L-\Delta M/M$). The bottom row are histograms for L and M cones modulated inphase ($\Delta L/L+\Delta M/M$). Cone contrasts are equal for each column and increase from left to right (2, 4, 8, and 16%). Binwidths are 5 msec and there are ten trials for each condition. This cell responds well to a 16% luminance grating (bottom right) but also shows increased firing to the isoluminant color grating as cone contrast is increased.

Figure 4.5 MT cell activity for antiphase and inphase cone modulation. This cell is more sensitive to luminance and chrominance contrast than the previous cell (figure 4.4). It also fires more to the antiphase modulated gratings than the inphase gratings at all cone modulation levels.

Figure 4.6 MT cell activity similar to the previous figure. This cell also responds better to L and M antiphase modulated gratings than the inphase gratings. The response to the luminance grating appears to saturate at 8% contrast.

Figure 4.7 MT cell activity represented in cone modulation space. The inset shows vectors of L and M cone modulation which are identical to those shown in figure 4.2. This figure shows this same space rotated 45 degrees clockwise into the page with the addition of activity represented on the Z axis. Cell responses increase as cone modulation increases along all vectors tested. This cell fires slightly worse to the inphase luminance grating.

Figure 4.8 Population data comparing the MT cell responses to L and M cone inphase modulation to equivalent antiphase modulation. Values for the linear regression analysis are in the lower right corner. Sum Activity values represent either the excitation or inhibition values for the response. Since ten trials were collected for each condition, the firing rate can be approximated by dividing sum activity by 10. Note that the slope of the regression is 0.88 indicating that MT cells fire almost as well at isoluminance when L and M cone contrast is equated and modulated in antiphase. In addition, the population is not widely distributed (R^2 =0.859).

Figure 4.9 Test of equality for responses to an 8% L and M cone antiphase modulated grating and 8 and 2% inphase modulated gratings. Eighty percent of the 8% antiphase vs. 8% inphase cases meet the two-tailed t test at an α = 0.05. For the responses of an 8% antiphase grating (isoluminant) versus a 2% inphase grating (luminance) 44% of the cases are rejected, all having a $t >$ 2.101 demonstrating that these cells fire significantly better to the isoluminant grating.

Figure 4.10 Contribution of first and second harmonics to activity at isoluminance. Fourier analysis was applied to the spike trains resulting from responses to isoluminant color gratings. First and second fourier components were divided by the total activity. The majority of cells had first and second harmonic contributions of less than ten percent. All had contributions less than fifty percent.

Figure 4.11 Distribution of directionally tuned cells in MT. Inset describes index for direction tuning (see section 2.5 also). This index takes into account the responses at the non-preferred directions, giving an indication of the breadth of the tuning.

Figure 4.12 Examples of two cells with relatively low direction indices (SI). Figure 4.12a shows the response of a cell in polar coordinates with r = spike rate and θ = direction tested. This cell prefers a downward moving grating and has a DI = 0.11. The solid line represents the computed direction tuning. If a direction tuning index using 1 - (non-preferred/preferred) had been used, the index would be close to 0.5. Figure 4.12b shows the responses of another cell tested for direction tuning in polar coordinates. Underneath are the raster displays and spike density functions for each direction. The solid line in the spike density functions represent the initiation of moving grating. The cell responds to the appearance of the stimuli in some directions prior to movement thus showing a degree of orientation selectivity. This portion of the response is not included in the direction tuning analysis and is reflected by the low DI (0.06) since the cell responds well to motion in all directions.

Figure 4.13 Comparison of direction tuning for luminance and red/green isoluminant gratings for one cell. On the right is the response of an MT cell to a luminance grating (inphase) tested for the 16 directions listed. For this condition the cell has a direction index of 0.43 and preferred direction of 103 degrees. On the left is an isoluminant color grating (antiphase) tested for the same directions. Direction tuning changes very little using the L and M cone antiphase modulated grating (DI = 0.47, θ_m = 95 degrees).

Figure 4.14 Comparison of direction indices determined by L and M cone inphase (luminance) and antiphase (R/G isoluminance) modulated gratings. The slope of the linear regression is 0.956, indicating that the direction index does not change much when using an isoluminant stimulus. R^2 = 0.56, however, so there is variability in the degree of tuning seen in the two conditions.

Figure 4.15 Change in preferred direction as a function of direction index. The preferred direction was computed for responses to inphase and antiphase modulated gratings and plotted against the direction index determined using a luminance grating. The data are represented in this way because the determination of the preferred direction is more reliable with higher direction indices. Over seventy percent of the cells have a change in preferred direction less than 22.5 degrees, the interval for which directions were tested. As expected, those cells with a large change in preferred direction had low directional indices. The solid line represents the power function regression analysis.

Figure 4.16 Direction tuning tested for nine luminance contrasts. For this set of experiments, the red phosphor modulation is constant and the green phosphor modulation is varied from low (-18.0) to high (18.0). Thus, luminance contrast is varied over a range centered on photometrically-defined isoluminance while the color contrast (figure 2.2) is fixed. At no luminance contrast is the cell silenced and further direction tuning does not change as a

function of luminance contrast.

Figure 4.17 Velocity tuning for an MT cell. Velocity tunings for eight velocities (1, 3, 7, 15, 20, 25, 30, and 35 deg/sec) tested with a luminance, red/green and blue/yellow isoluminant color gratings. On the left are histograms of mean firing rate and on the right are the raster displays and spike density functions of each condition. For the sinusoidally modulated luminance grating the tuning is centered on 30 degrees/second. For the isoluminant color gratings the tuning shifts to lower velocities. It should be noted that for this cell the cone modulations are not equivalent between conditions and the luminance grating has a much higher degree of cone modulation than either of the isoluminant color gratings.

Figure 4.18 Three-dimensional plot of an MT cell's activity in cone modulation space. The representation is identical to figure 4.7. When the sinusoidal grating is drifted very rapidly (temporal frequency of 16.5 Hz), the cell does not respond well to the antiphase modulated grating.

Figure 4.19 Three-dimensional plot of the same cell as in figure 4.18 with a slower drift rate. In this case the grating drifts with a temporal frequency of 3.3 Hz. All other conditions are identical to those in the previous figure. Under these conditions the cell responds much better to the isoluminant color grating.

Figure 4.20 Comparison of responses of MT cells for luminance and blue/yellow isoluminant gratings. Isoluminance was defined photometrically and cone contrast is not equated between the two conditions. Unlike L and M cone antiphase grating responses (figure 4.8) slope of the linear regression (solid line) is only 0.1 but the y intercept is 199.5. Even though the sample is small, MT cells do respond to blue/yellow isoluminant gratings.

Figure 4.21 Comparison of direction indices using luminance and blue/yellow isoluminant gratings. Although the sample is small (N = 9), it appears that the direction index does not change much for blue/yellow isoluminant gratings. These results are similar to those seen in figure 4.14. The solid line represents the linear regression analysis.

Figure 4.22 Change in preferred direction as a function of direction index. The change in preferred direction is computed from luminance and blue/yellow isoluminant grating conditions and plotted as a function of the direction index determined using a luminance grating. Like the results of figure 4.15, direction tuning changes very little when the direction index is high.

Figure 4.23 Contrast, velocity and direction tuning for one MT cell summarizing results for stimuli with L and M cones modulated inphase (luminance) and in antiphase (R/G). Histograms represent the mean firing rate

in response to drifting sinusoidal gratings. In the case of contrast, the cell fires better in the isoluminant condition as cone modulation is increased. There is a slight shift in the preferred velocity towards lower values for the isoluminant condition. Direction tuning changes very little for the isoluminant color grating.

Figure 4.24 Data for another cell showing various tunings similar to figure 4.23. The blue/yellow isoluminant grating condition is also included in the contrast condition. For contrast tuning, an 8.46% L and M cone antiphase-modulated grating (R/G) fires as much as a 47.5% inphase (luminance) modulated grating. The cell fires somewhat less to the blue/yellow isoluminant grating. No differences are seen between conditions in the velocity tuning for the cell. There are also no changes in the direction tuning of the cell.

Figure 4.25 Tuning curves for another cell, similar to figure 4.24. Contrast tuning shows increasing response with increased cone modulation. Velocity tuning shows a slight shift towards slower velocities for the antiphase modulated grating. For this cell there is a shift in direction tuning. The cell is bidirectional when tested with a luminance grating but is unidirectional when tested with the isoluminant color grating (R/G). This was the only cell that exhibited this behavior.

Trial Description

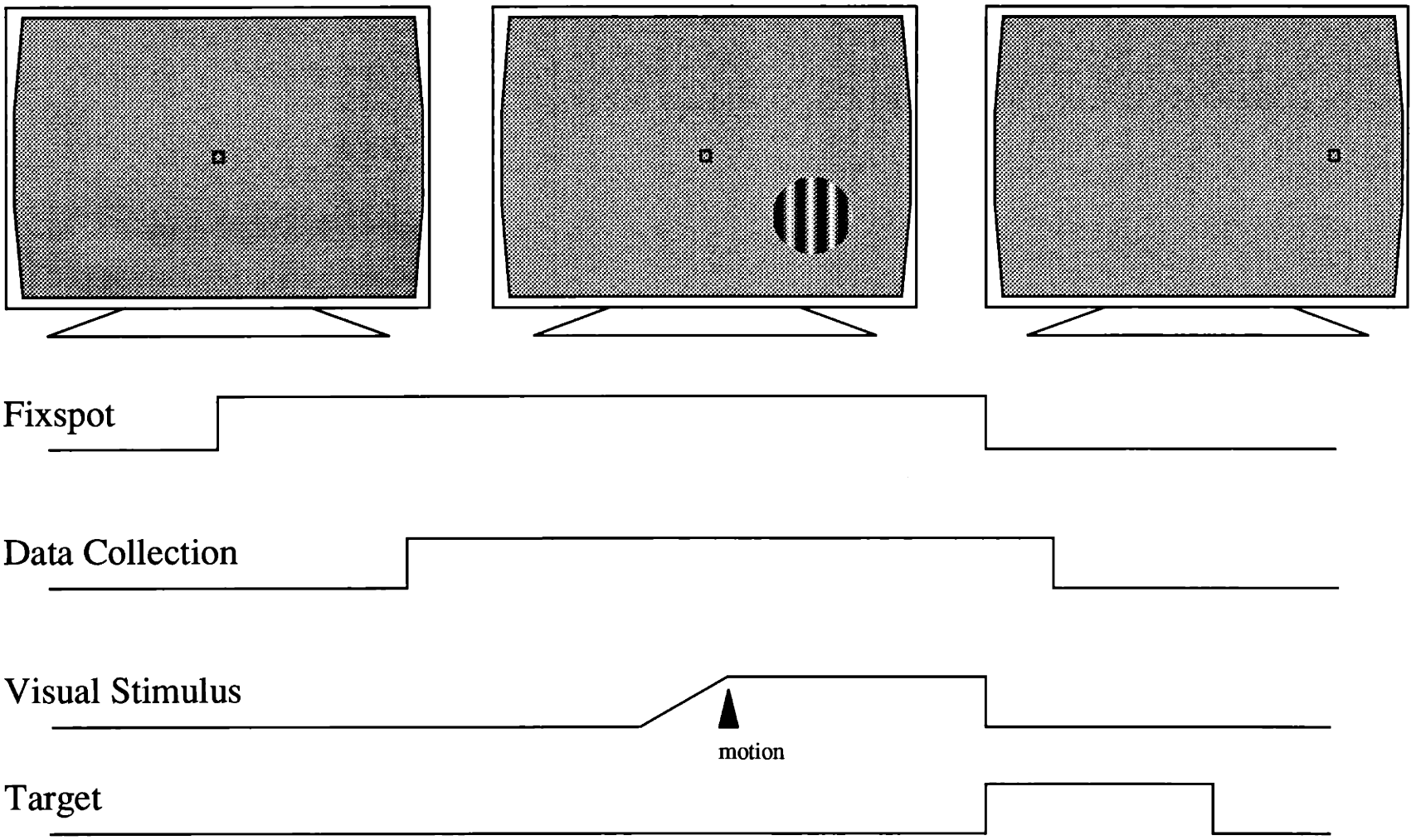

Figure 4.1

Cone Modulation Space

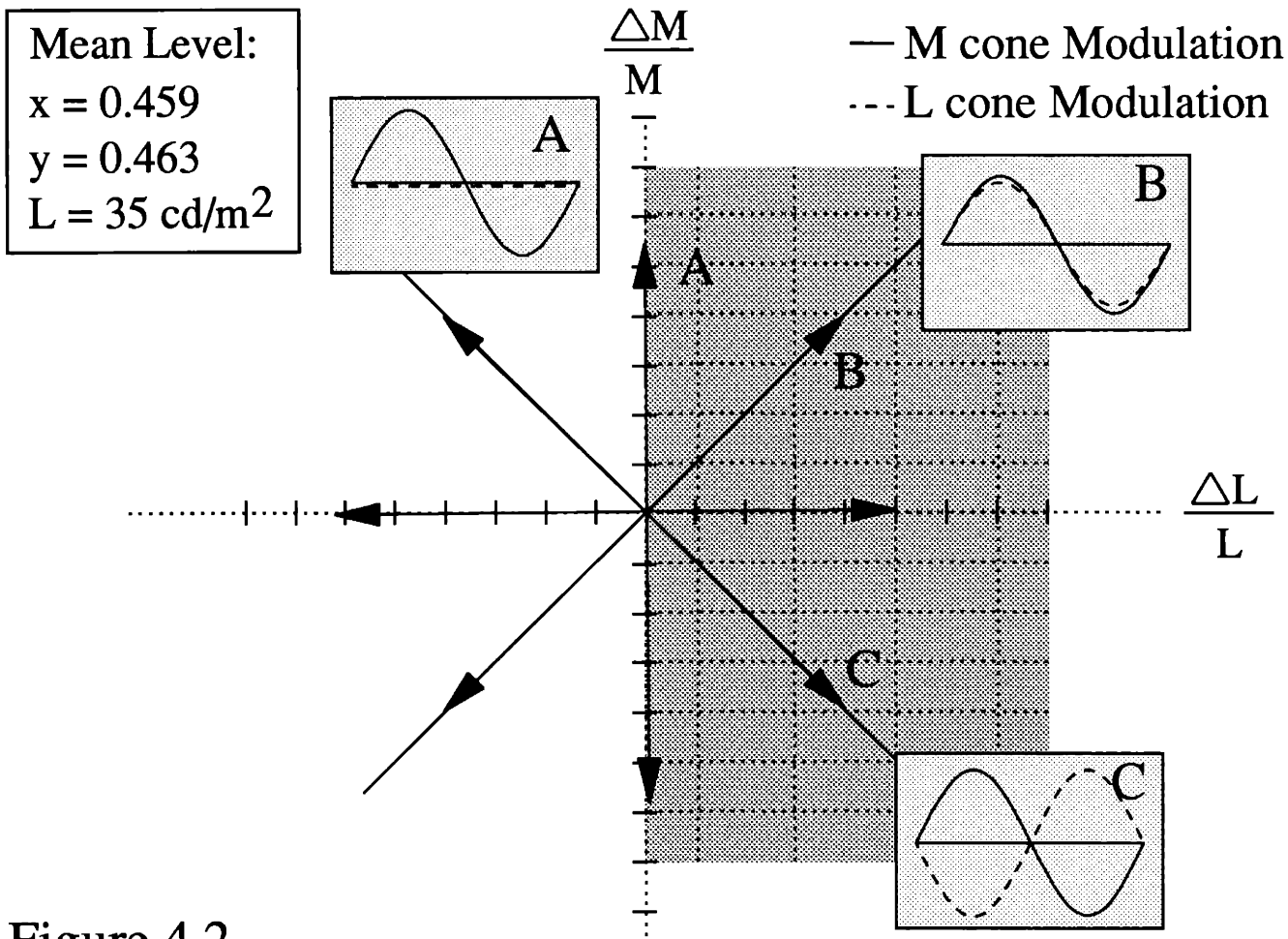

Figure 4.2

Definition of Cell Activity

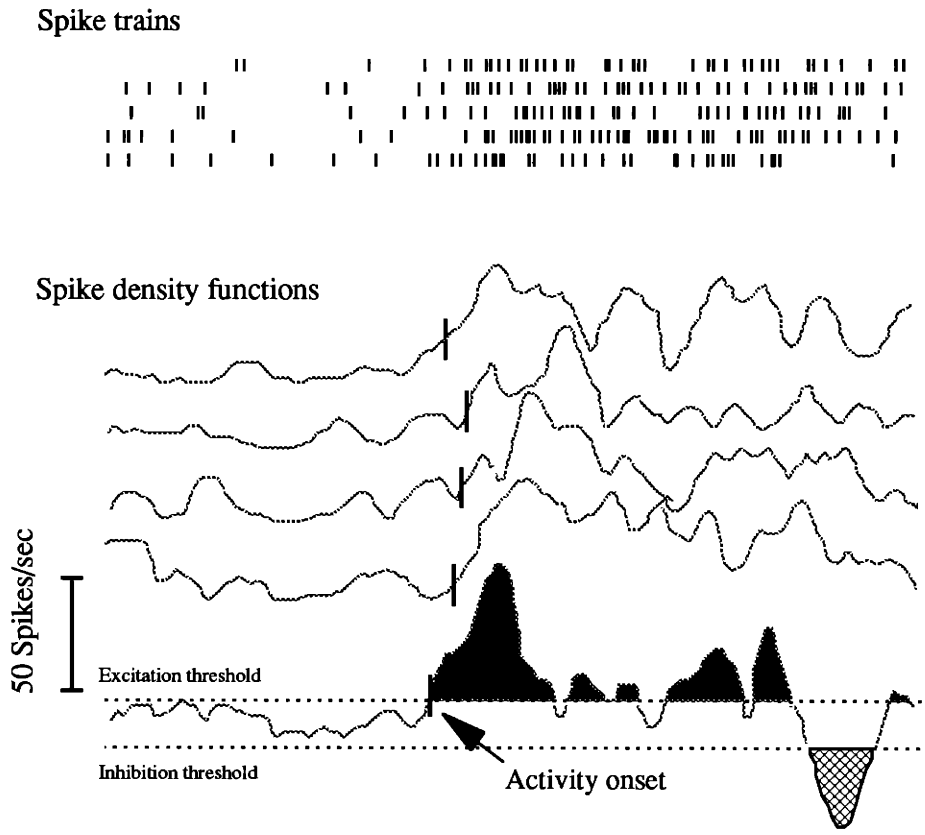

Figure 4.3

MT Cell Response: Antiphase vs. Inphase

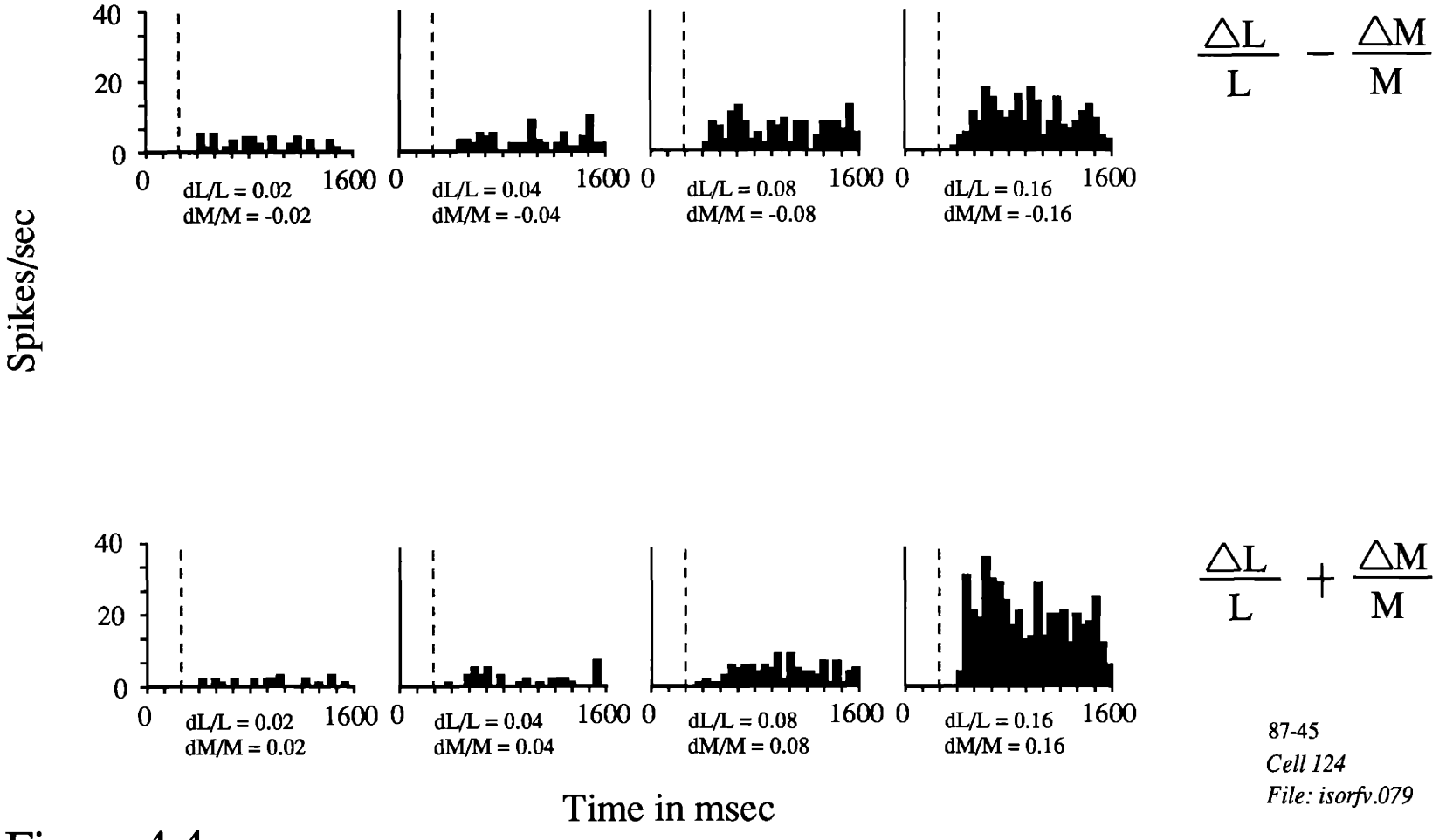

Figure 4.4

MT Cell Response: Antiphase vs. Inphase

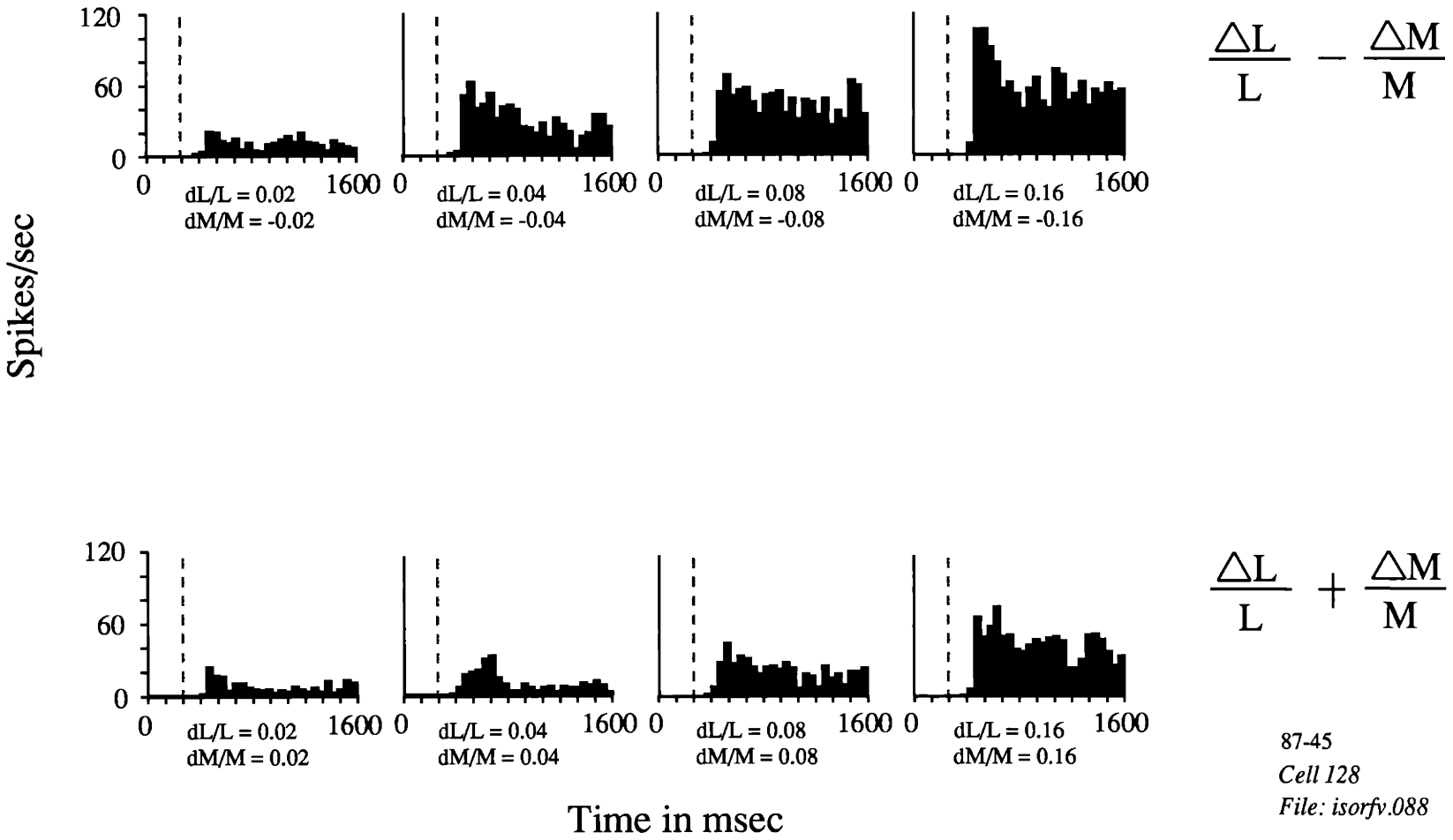

Figure 4.5

MT Cell Response: Antiphase vs. Inphase

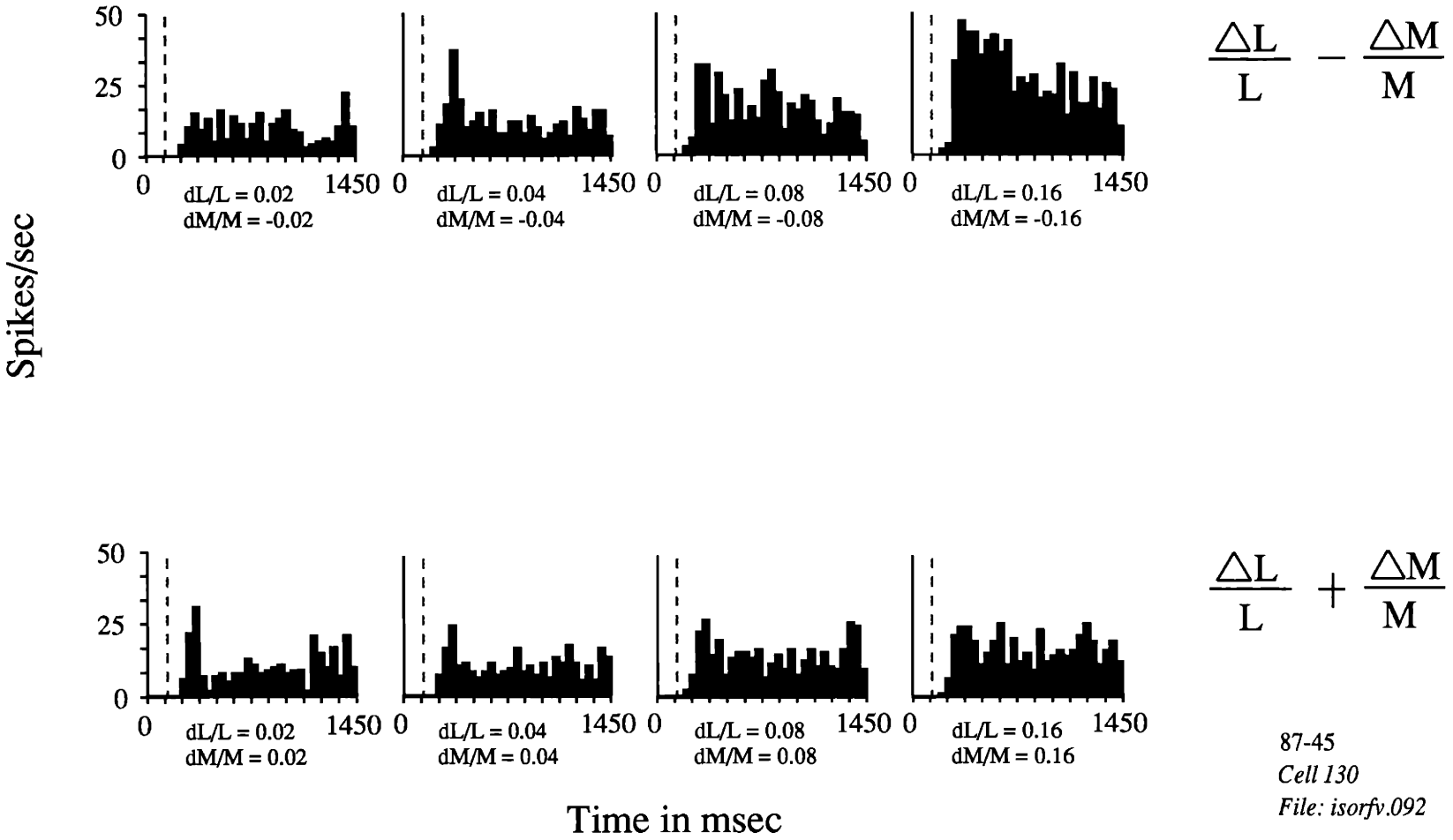

Figure 4.6

MT Cell Activity in Cone Modulation Space

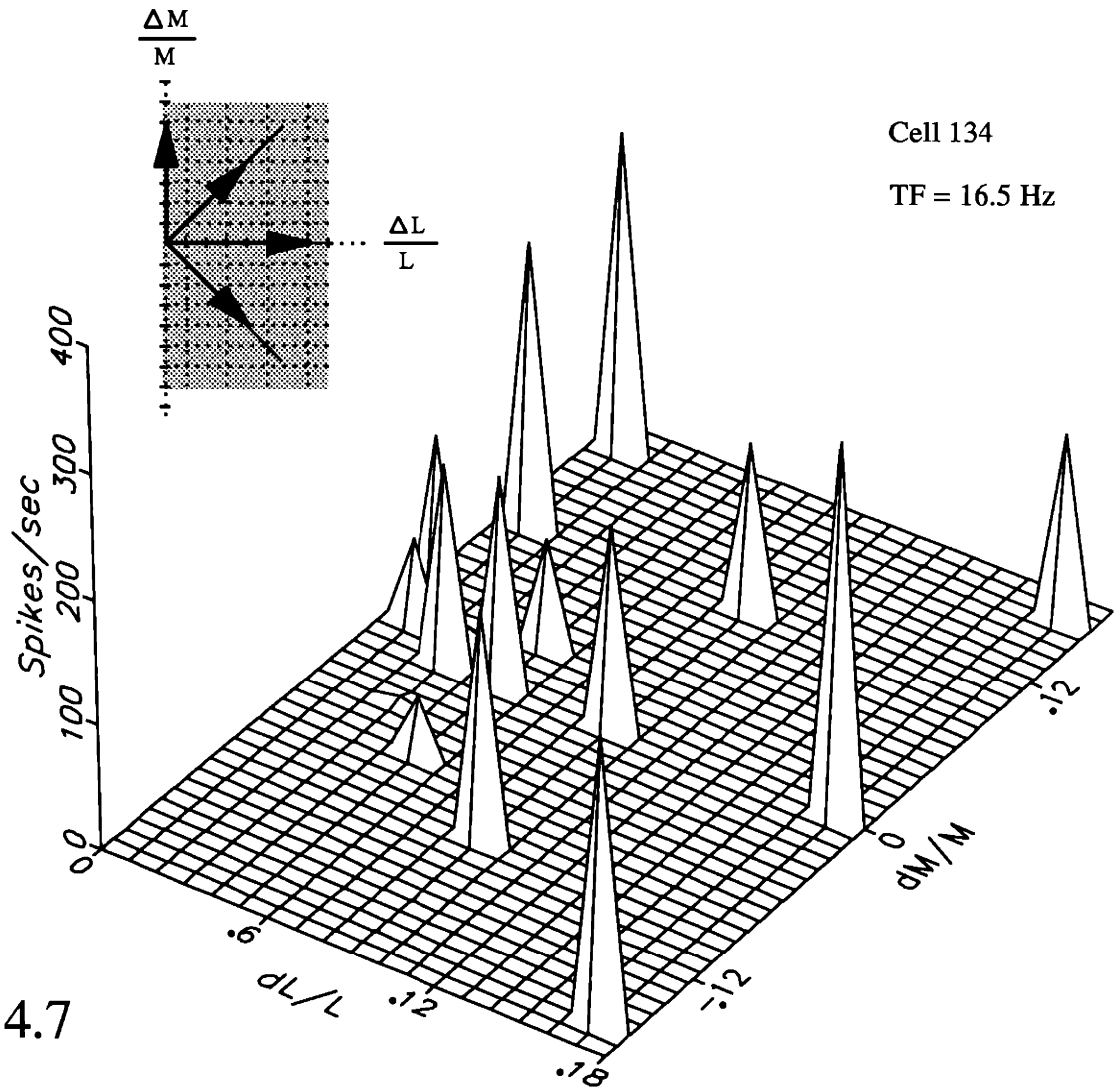

Figure 4.7

MT Cell Activity: Luminance vs. R\G Isoluminance

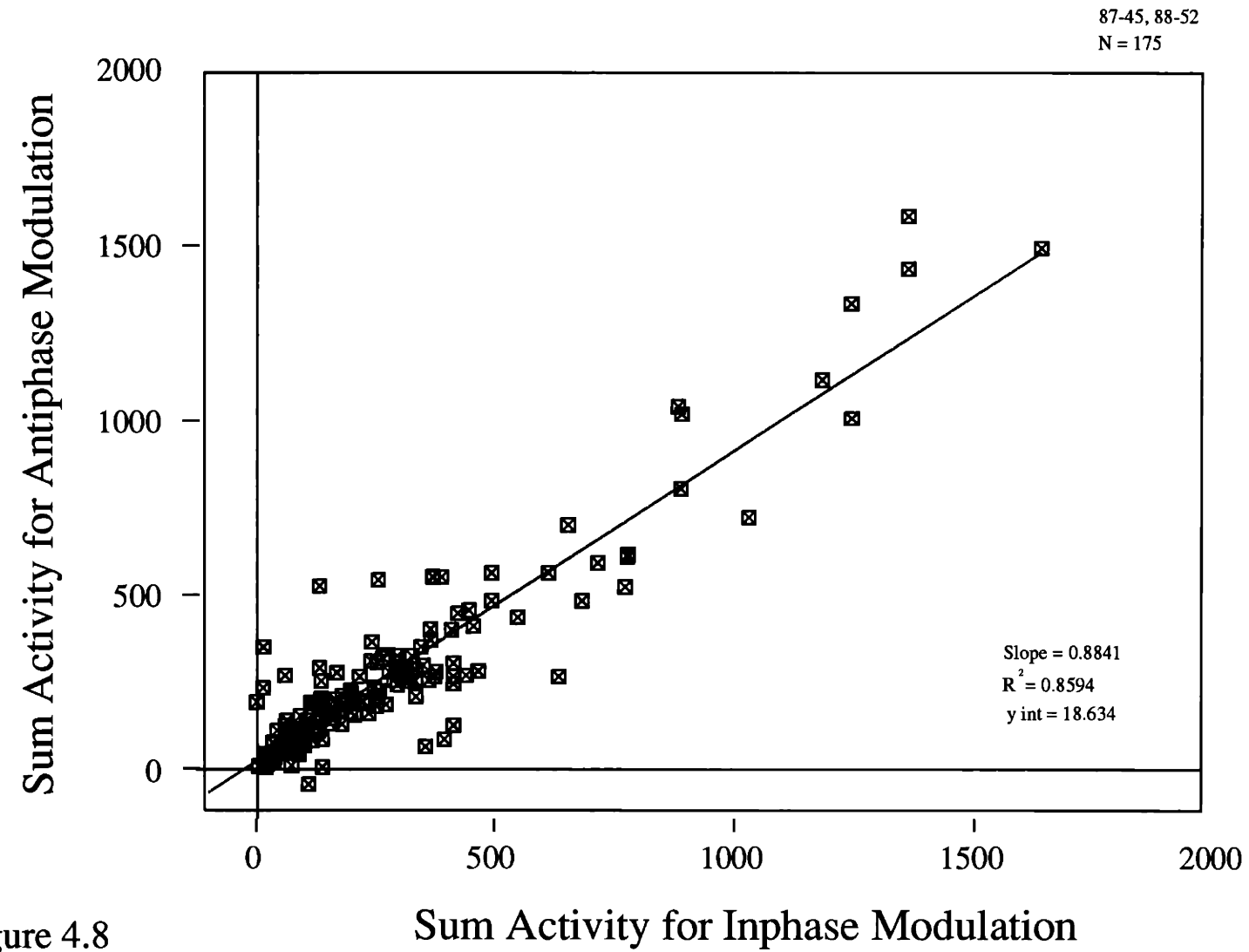

Figure 4.8

MT Cell Activity: Luminance vs. R\G Isoluminance

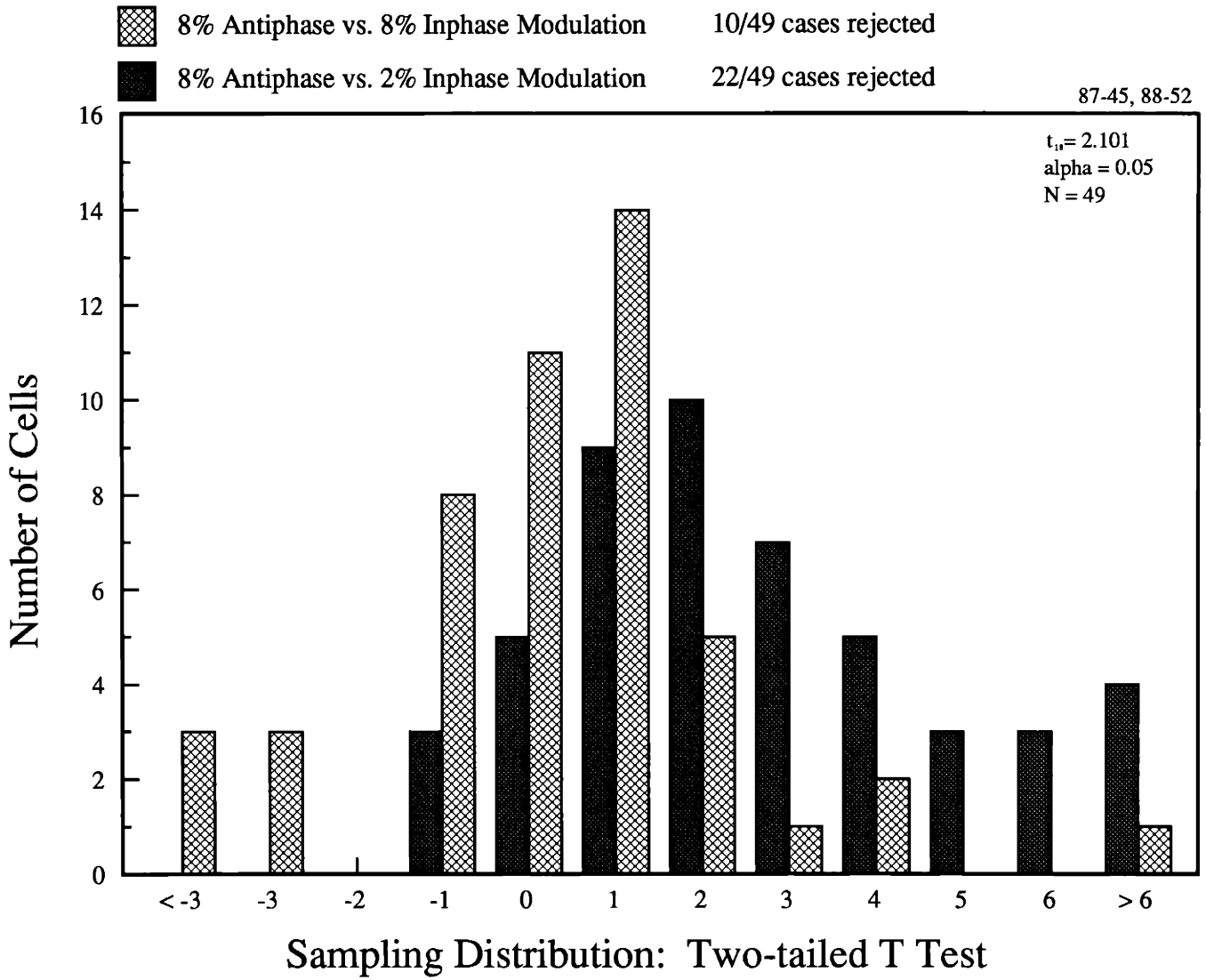

Figure 4.9

Harmonic Contribution to Activity at Isoluminance

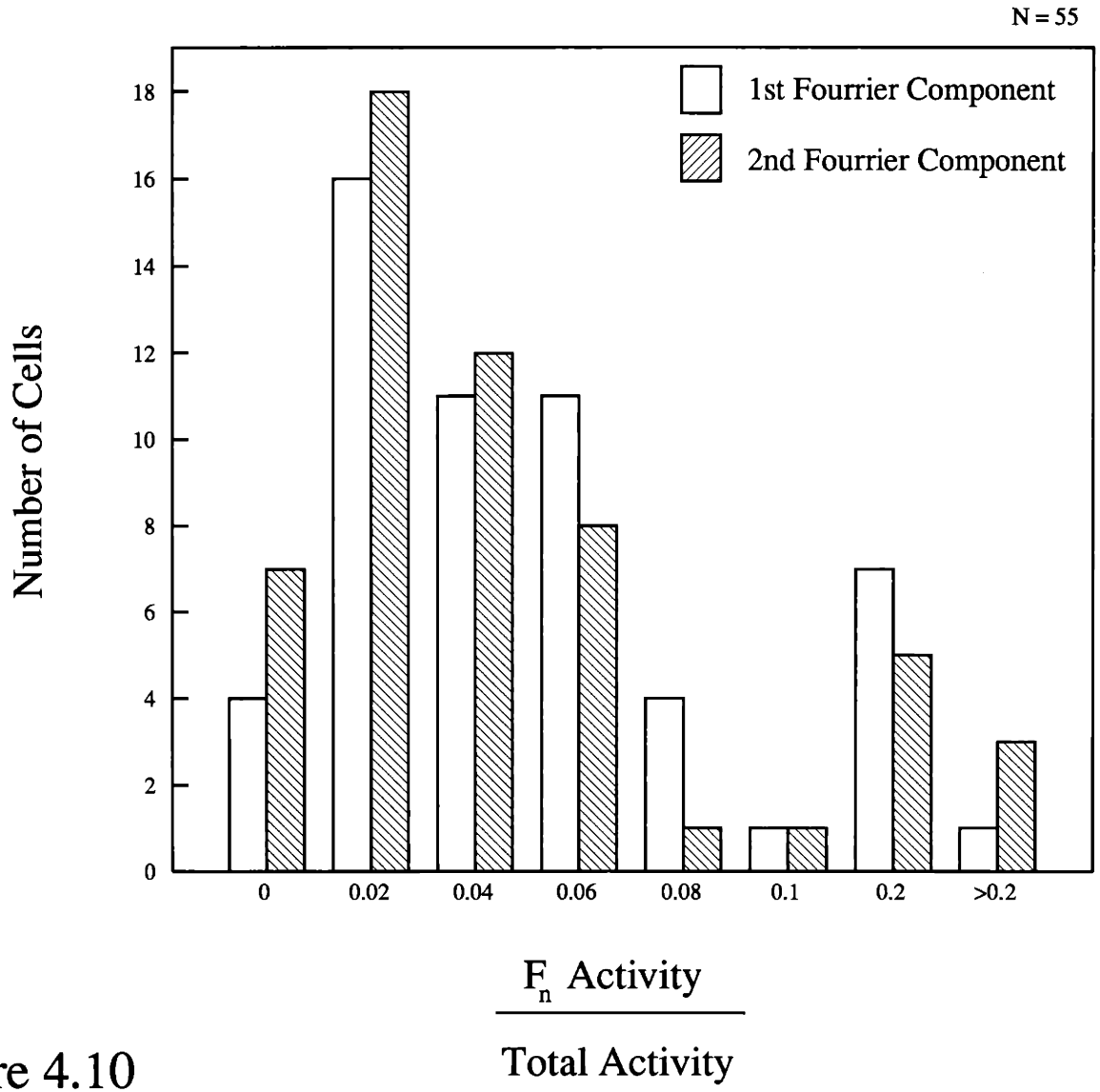

Figure 4.10

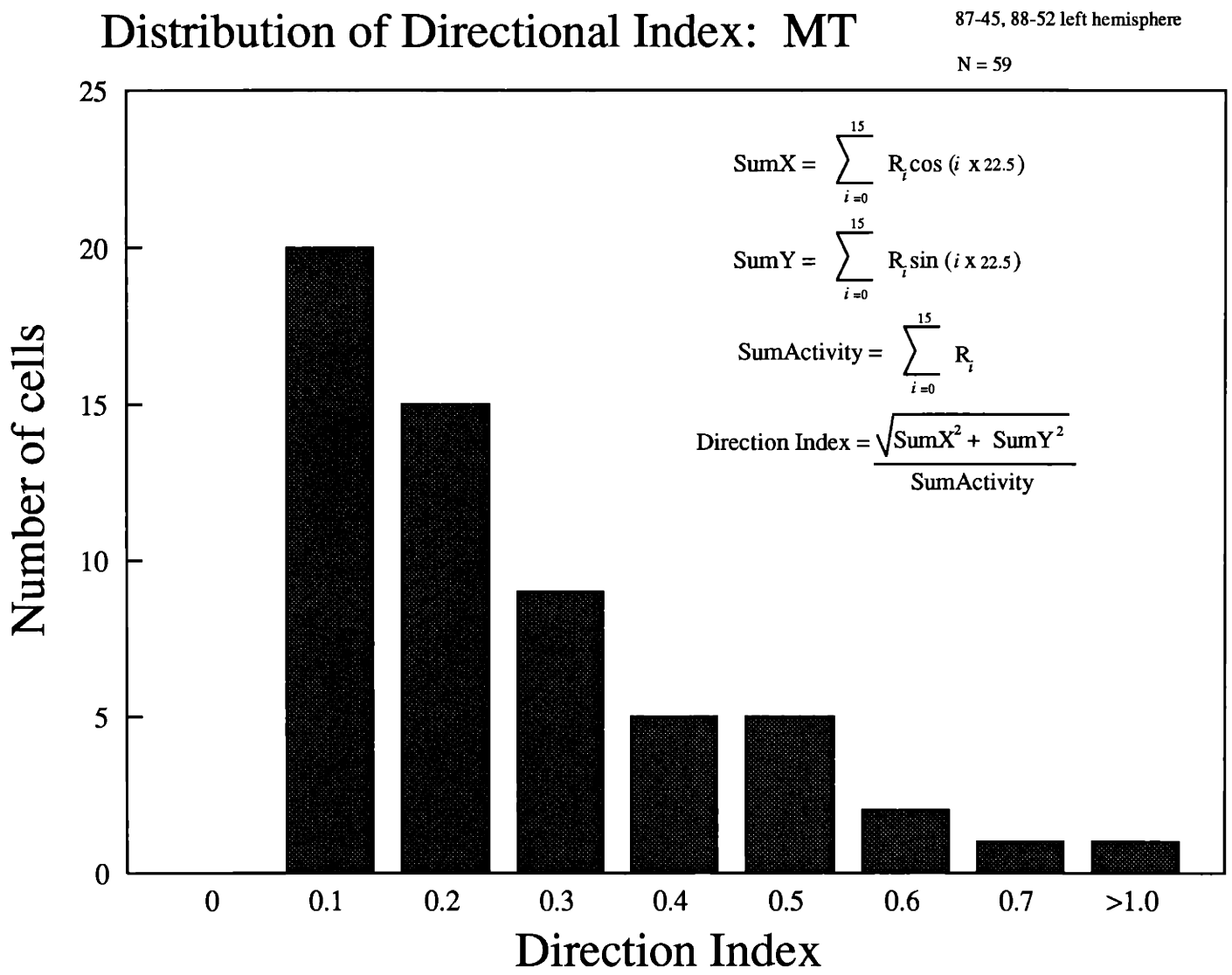
Distribution of Directional Index: MT
87-45, 88-52 left hemisphere
N = 59
SumX = $\sum_{i=0}^{15} R_i \cos(i \times 22.5)$
SumY = $\sum_{i=0}^{15} R_i \sin(i \times 22.5)$
SumActivity = $\sum_{i=0}^{15} R_i$
Direction Index = $\frac{\sqrt{SumX^2 + SumY^2}}{SumActivity}$
Number of cells
25
20
15
10
5
0
0
0.1
0.2
0.3
0.4
0.5
0.6
0.7
>1.0
Direction Index

Figure 4.11

A.

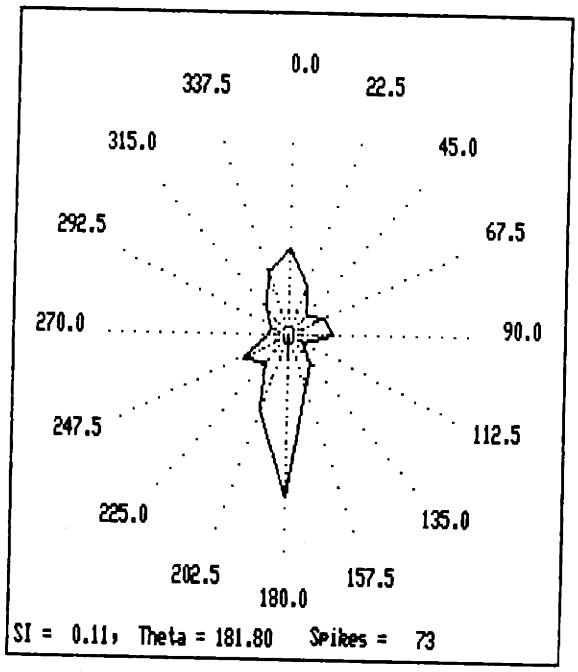
0.0
22.5
45.0
67.5
90.0
112.5
135.0
157.5
180.0
202.5
225.0
247.5
270.0
292.5
315.0
337.5
SI = 0.11, Theta = 181.80 Spikes = 73
direction

B.

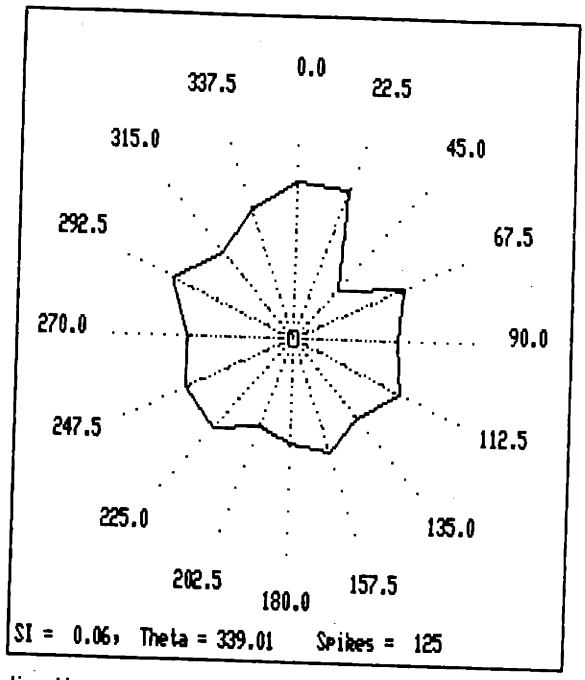
0.0
22.5
45.0
67.5
90.0
112.5
135.0
157.5
180.0
202.5
225.0
247.5
270.0
292.5
315.0
337.5
SI = 0.06, Theta = 339.01 Spikes = 125
direction

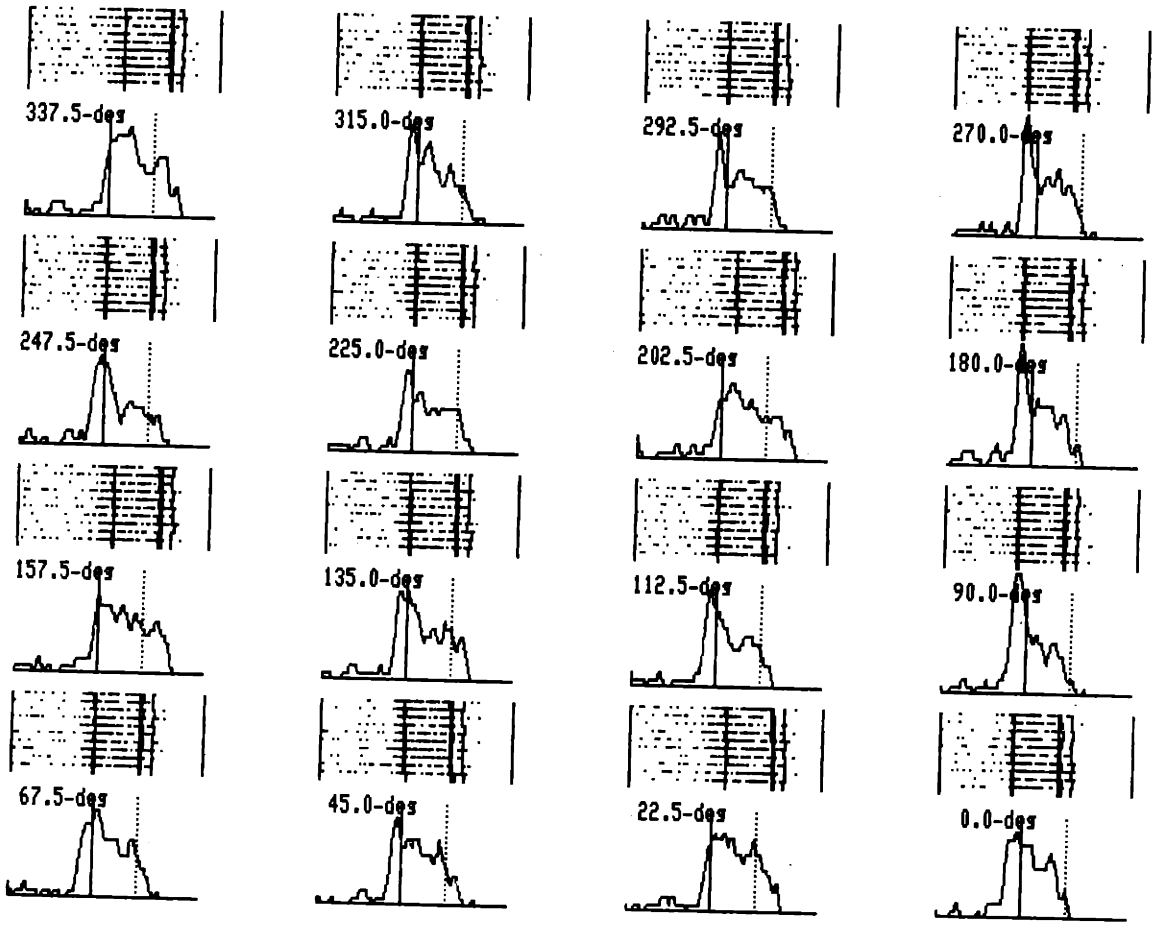
337.5-deg
315.0-deg
292.5-deg
270.0-deg
247.5-deg
225.0-deg
202.5-deg
180.0-deg
157.5-deg
135.0-deg
112.5-deg
90.0-deg
67.5-deg
45.0-deg
22.5-deg
0.0-deg

Direction Tuning: MT

Antiphase

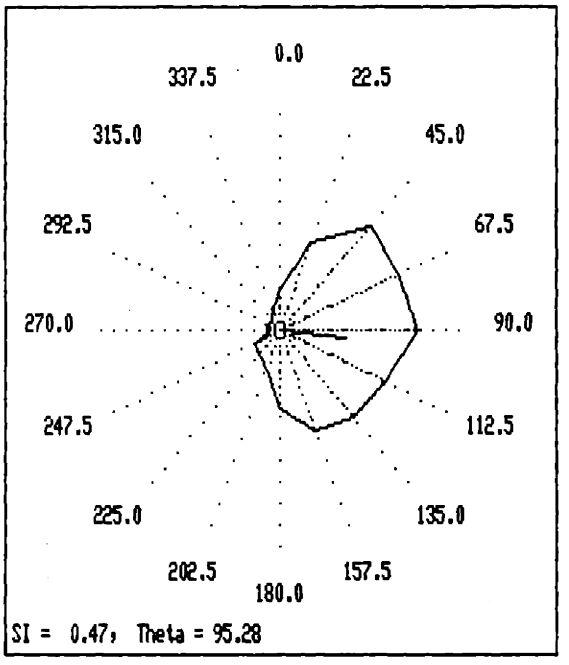

Inphase

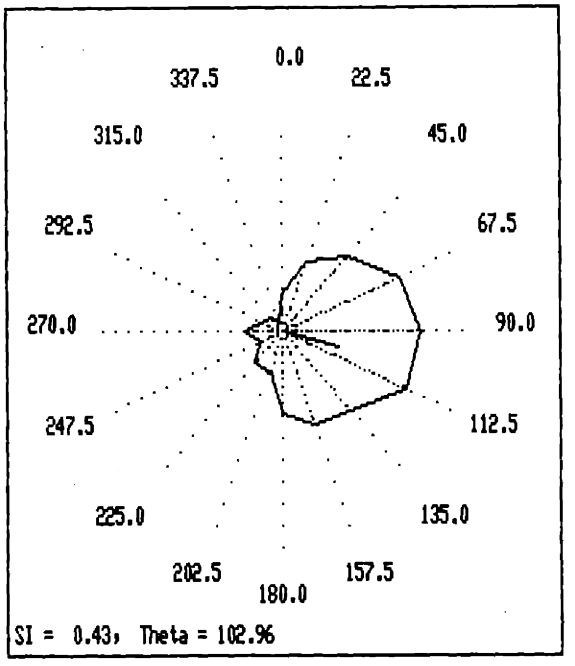

Penetration	: 0	Preferred orientation	: 0.0	Spikes =	0
Pass	: 44	Preferred direction	: 90.0	Spikes =	87
S Coord (x)	: -153	Preferred velocity	:	Spikes =	69
L Coord (y)	: 21	Preferred color contr	:	Spikes =	86
Initial Depth	: -33	Preferred spatial frq	:	Spikes =	0
Current Depth	: 141	Preferred disparity	:	Spikes =	0
Cell #	: 191	Background colors	: 57 58 0		

MT Direction Index: Luminance vs. R\G Isoluminance

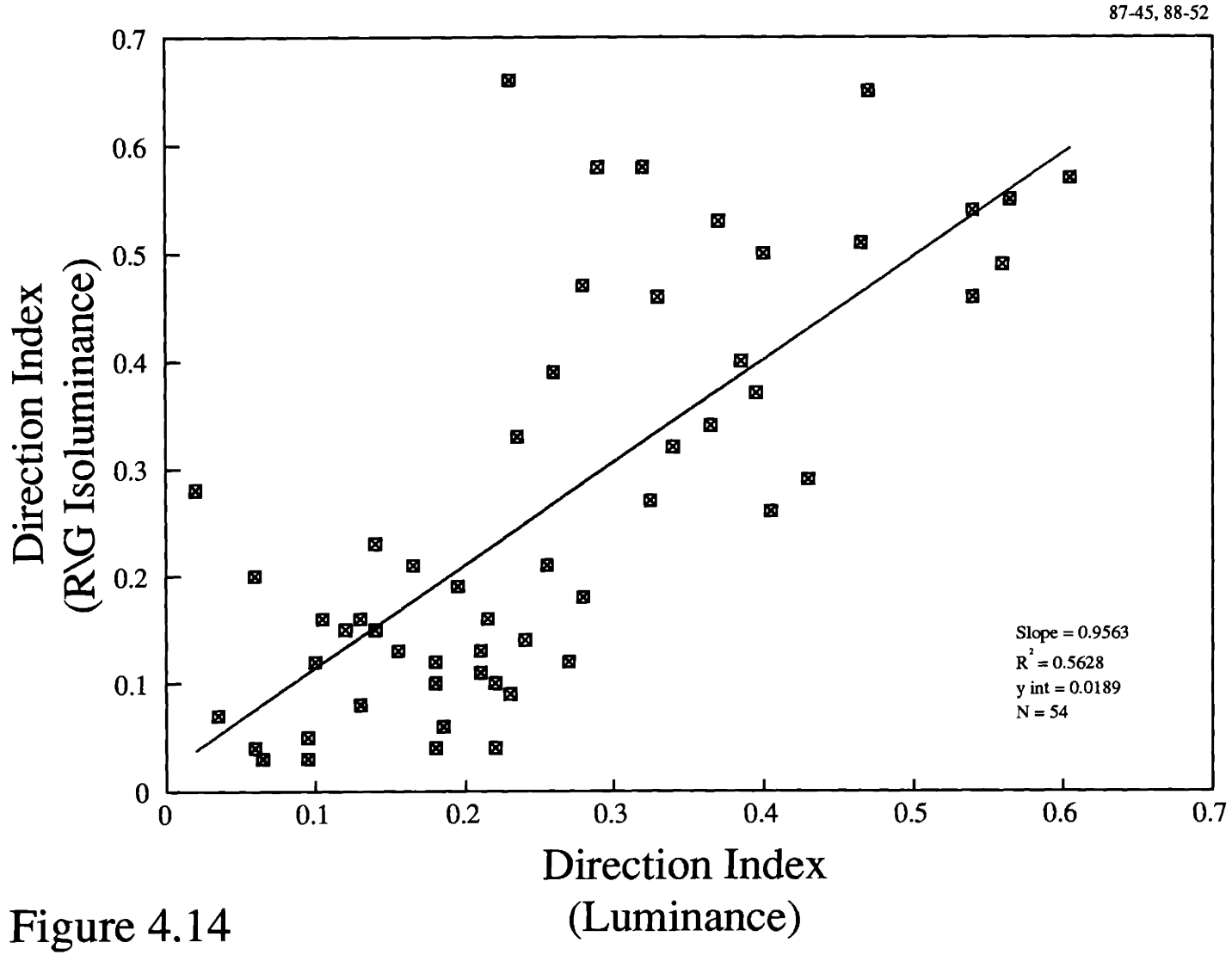

Figure 4.14

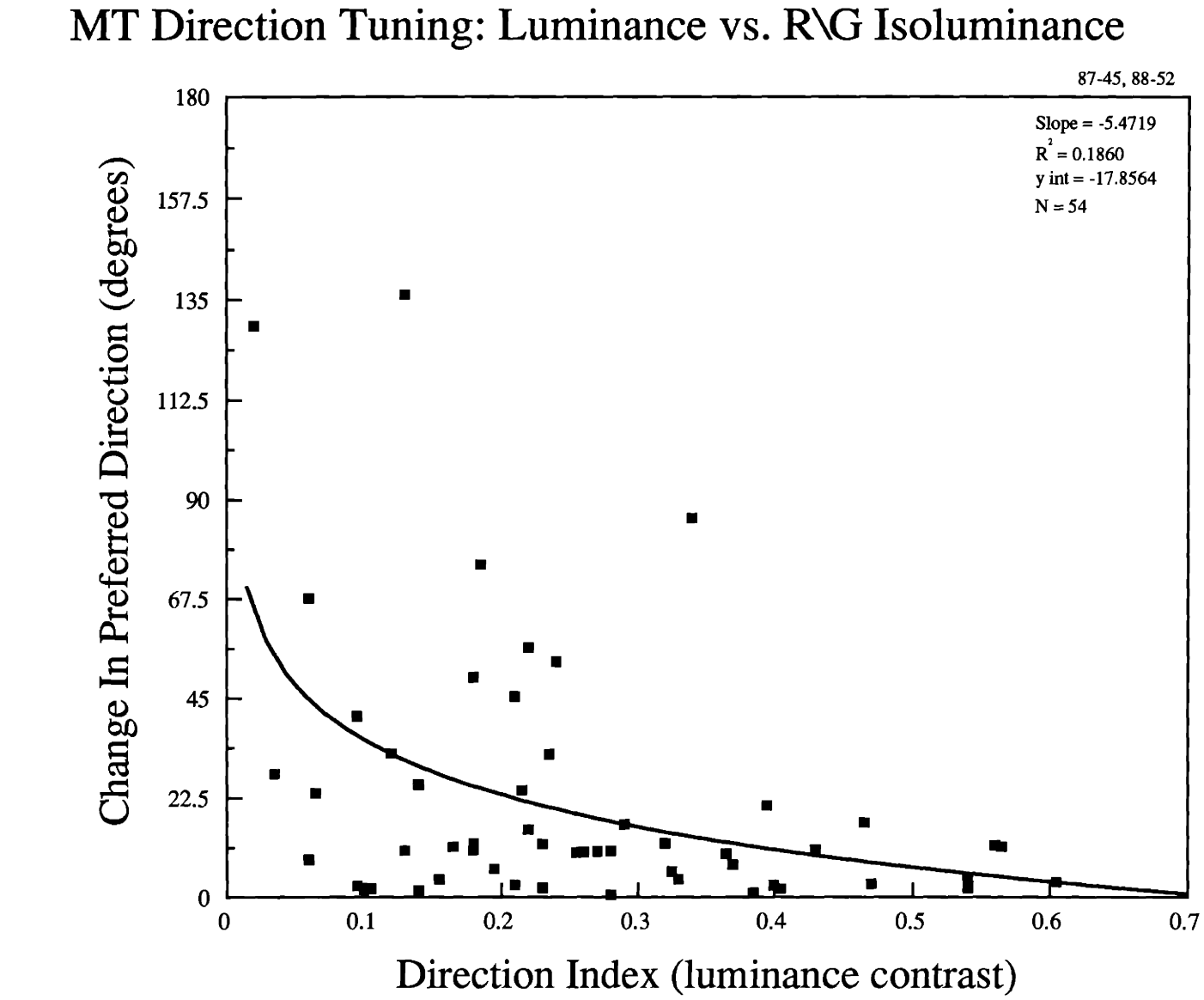
MT Direction Tuning: Luminance vs. R\G Isoluminance
87-45, 88-52
Slope = -5.4719
R² = 0.1860
y int = -17.8564
N = 54
Change In Preferred Direction (degrees)
180
157.5
135
112.5
90
67.5
45
22.5
0
0
0.1
0.2
0.3
0.4
0.5
0.6
0.7
Direction Index (luminance contrast)

Figure 4.15

Direction Tuning at Various Luminance Contrasts

(Color Modulation = 100%)

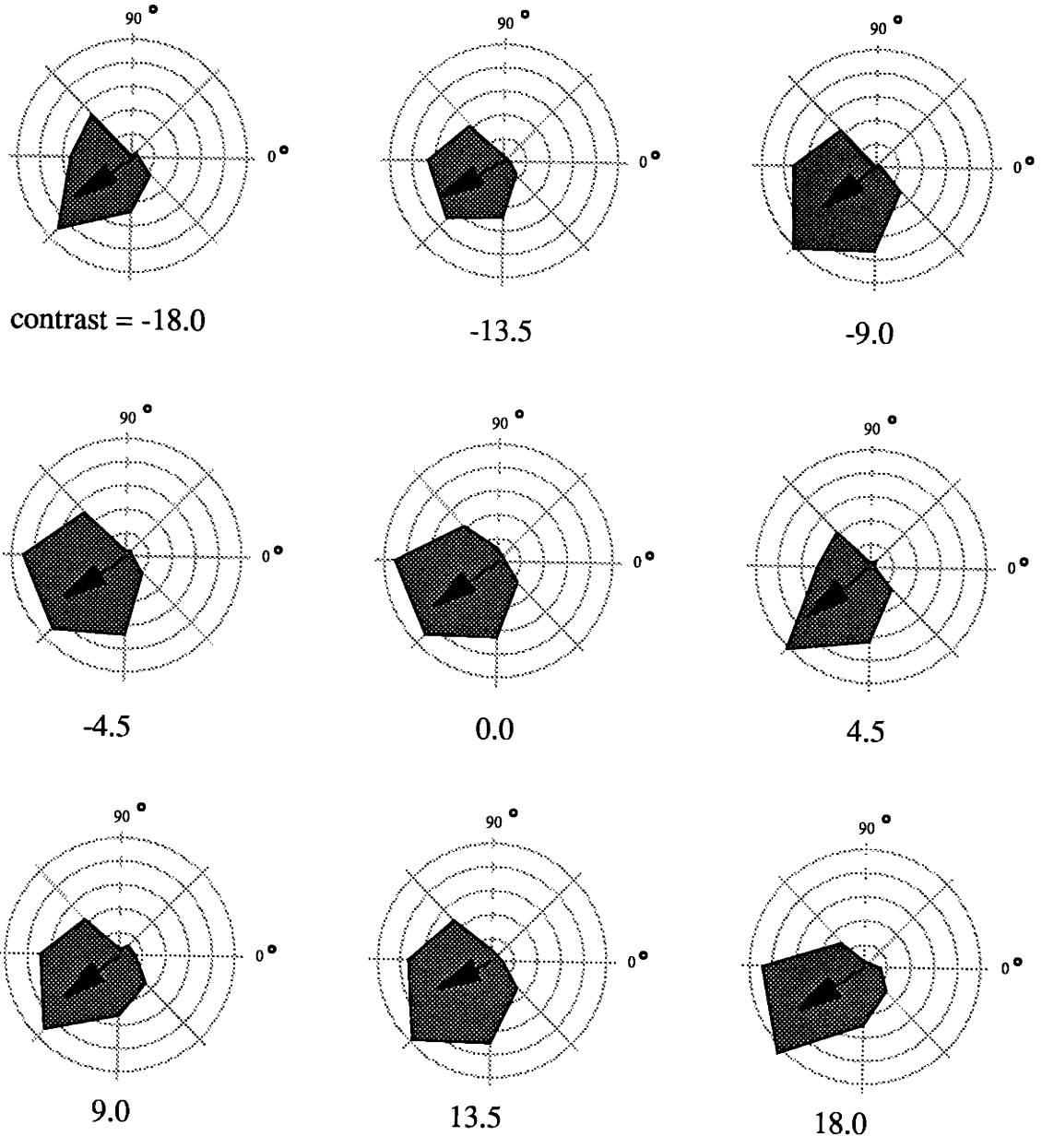

Figure 4.16

Velocity Tuning: MT

Luminance

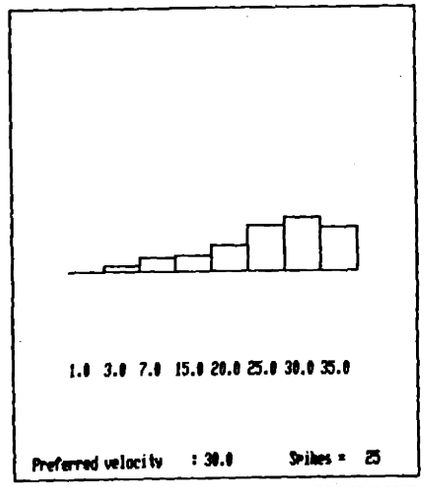

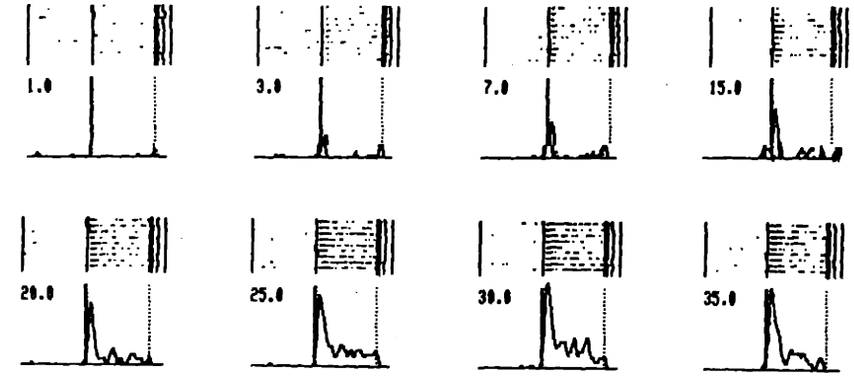

Red\Green

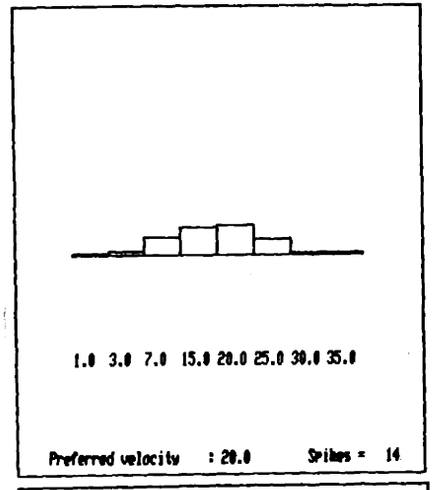

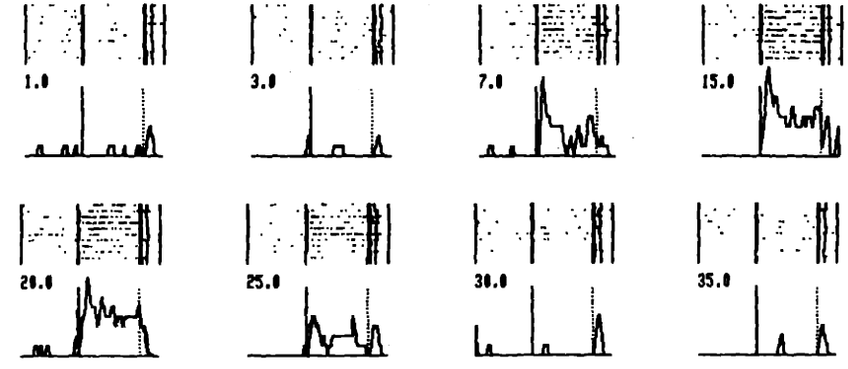

Blue\Yellow

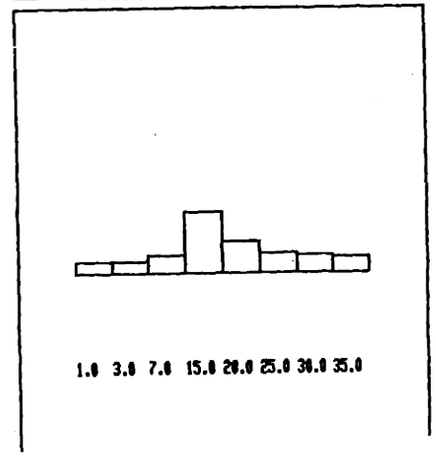

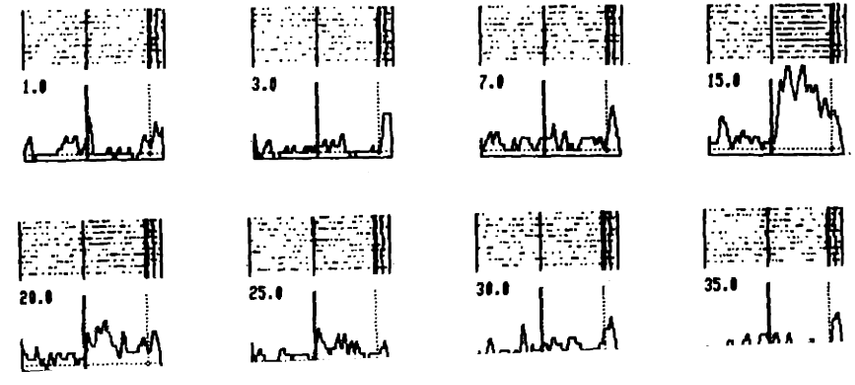

MT Cell Activity in Cone Modulation Space

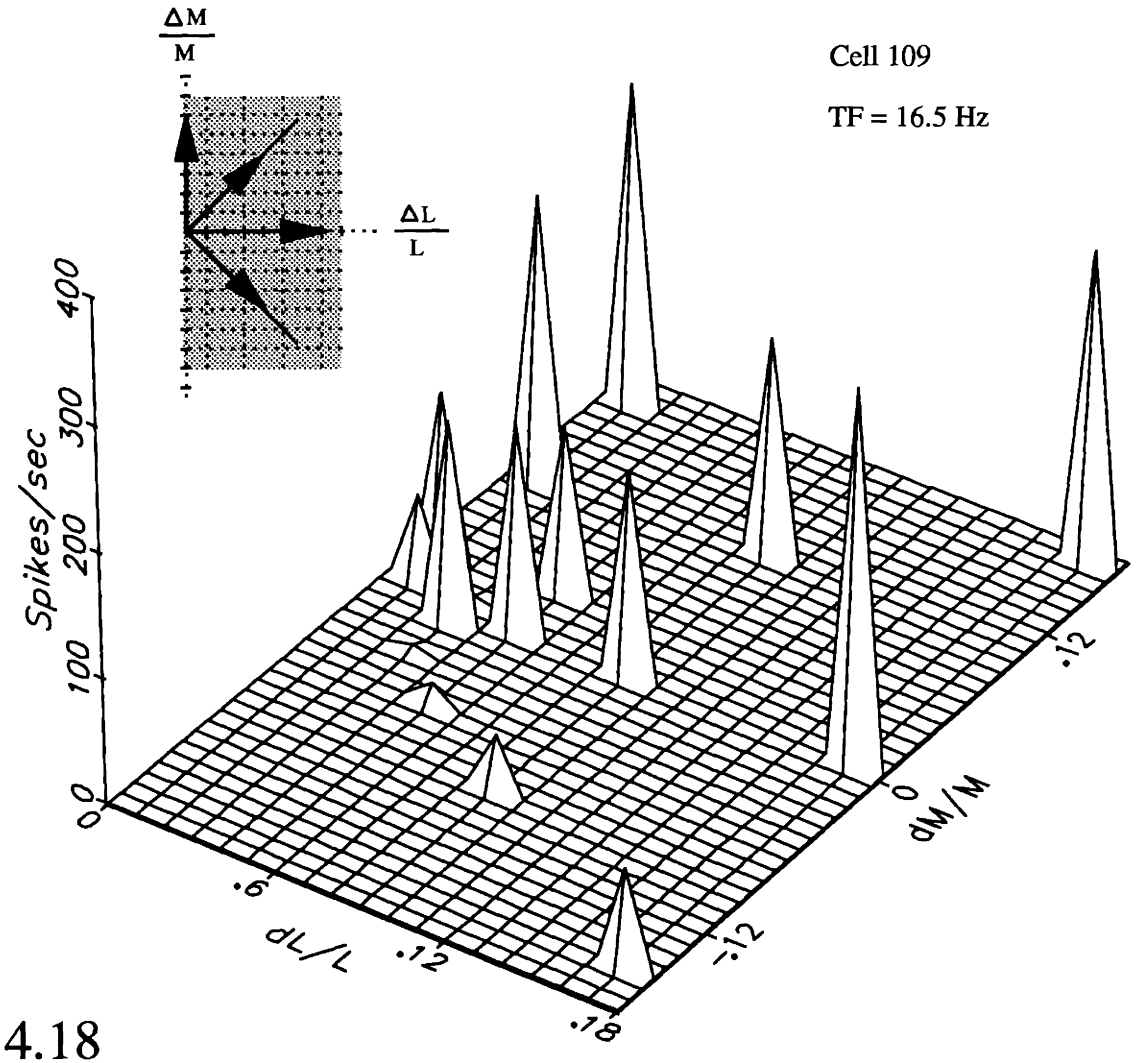

Figure 4.18

MT Cell Activity in Cone Modulation Space

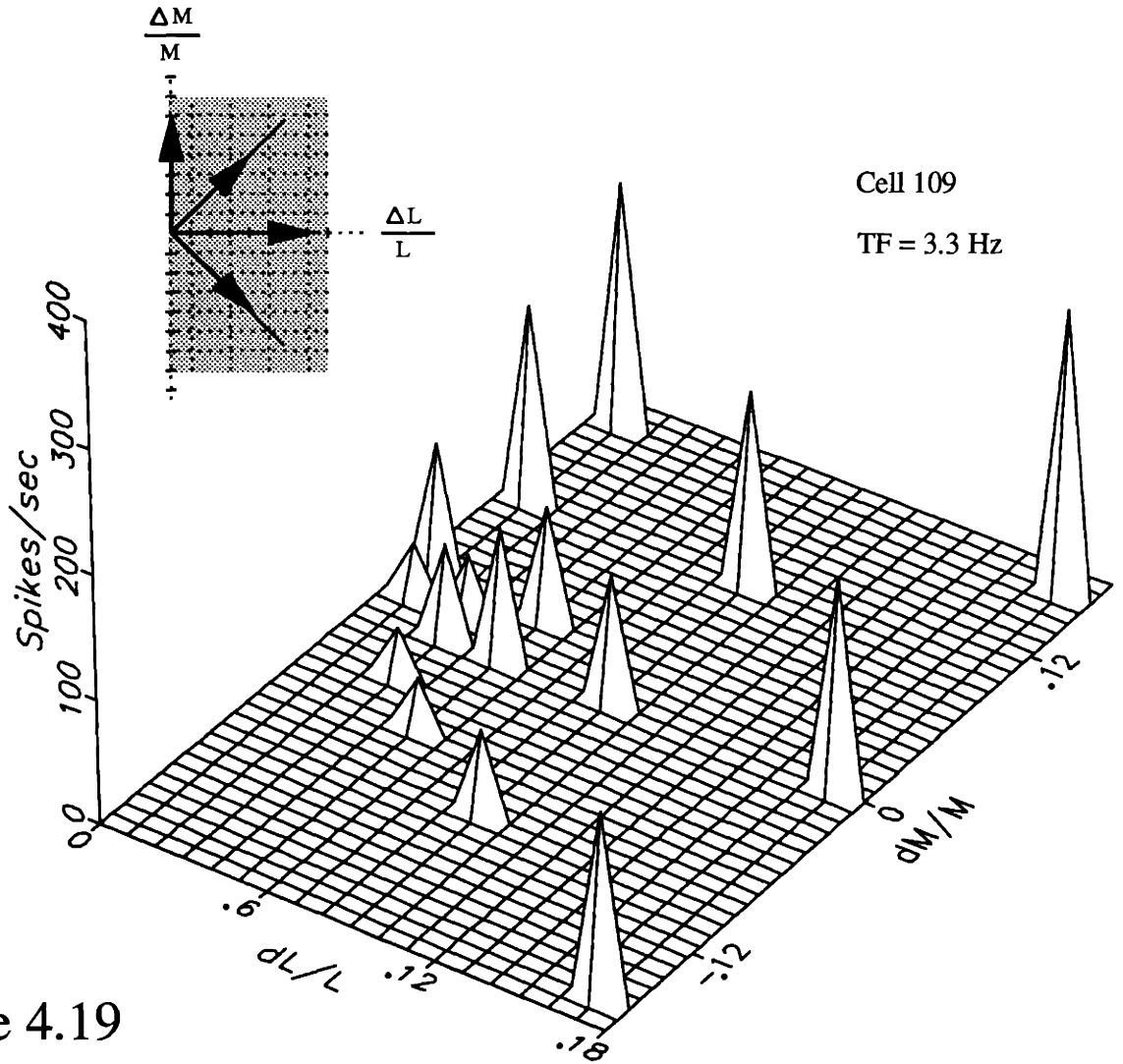

Figure 4.19

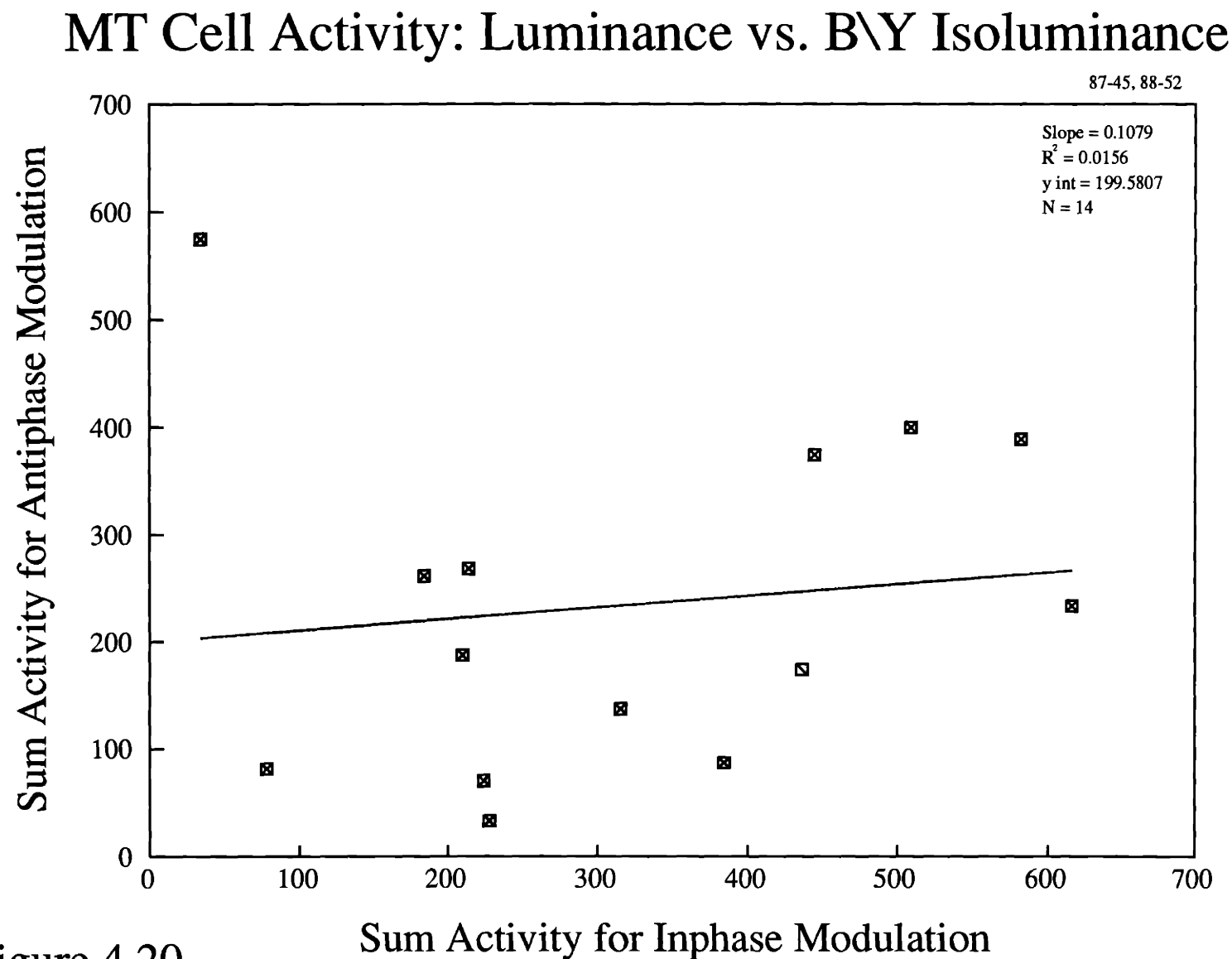
MT Cell Activity: Luminance vs. B\Y Isoluminance
87-45, 88-52
Slope = 0.1079
R² = 0.0156
y int = 199.5807
N = 14
Sum Activity for Antiphase Modulation
Sum Activity for Inphase Modulation
0
100
200
300
400
500
600
700

Figure 4.20

MT Direction Index: Luminance vs. B\Y Isoluminance

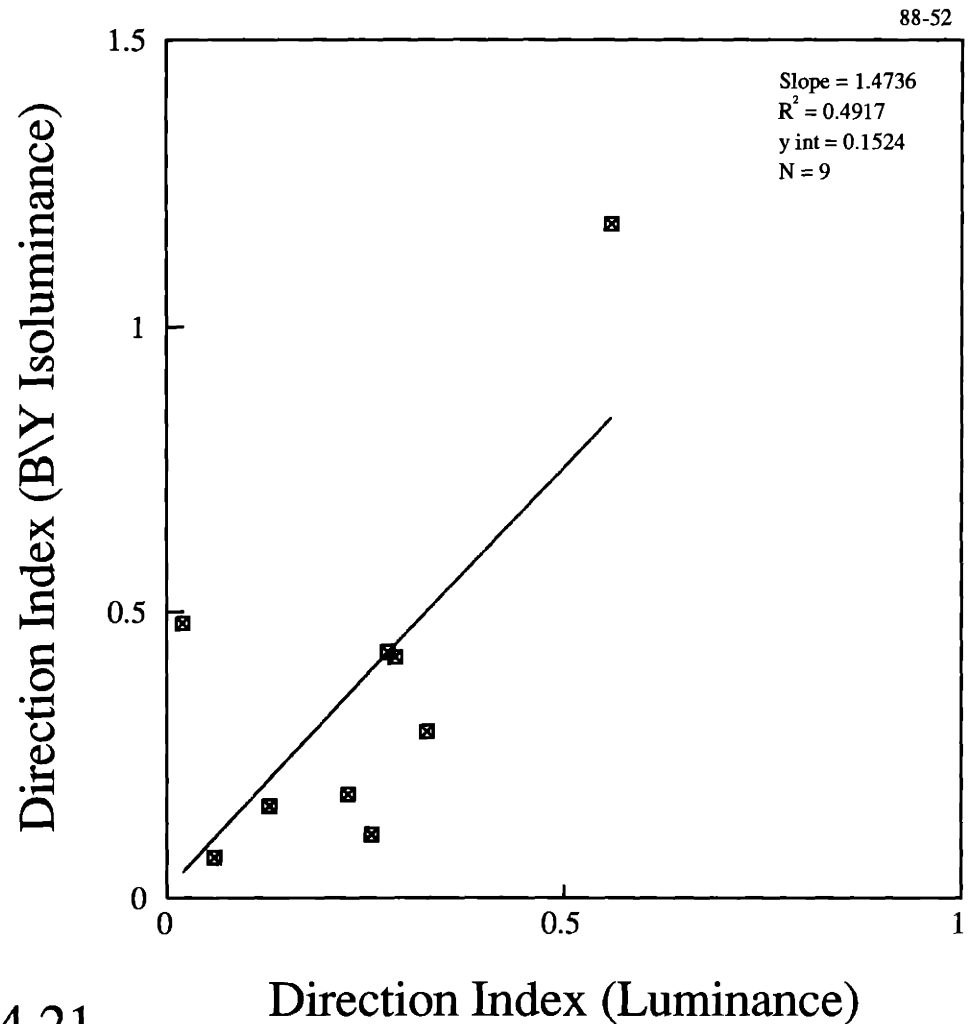

Figure 4.21

MT Direction Tuning: Luminance vs. B\Y Isoluminance

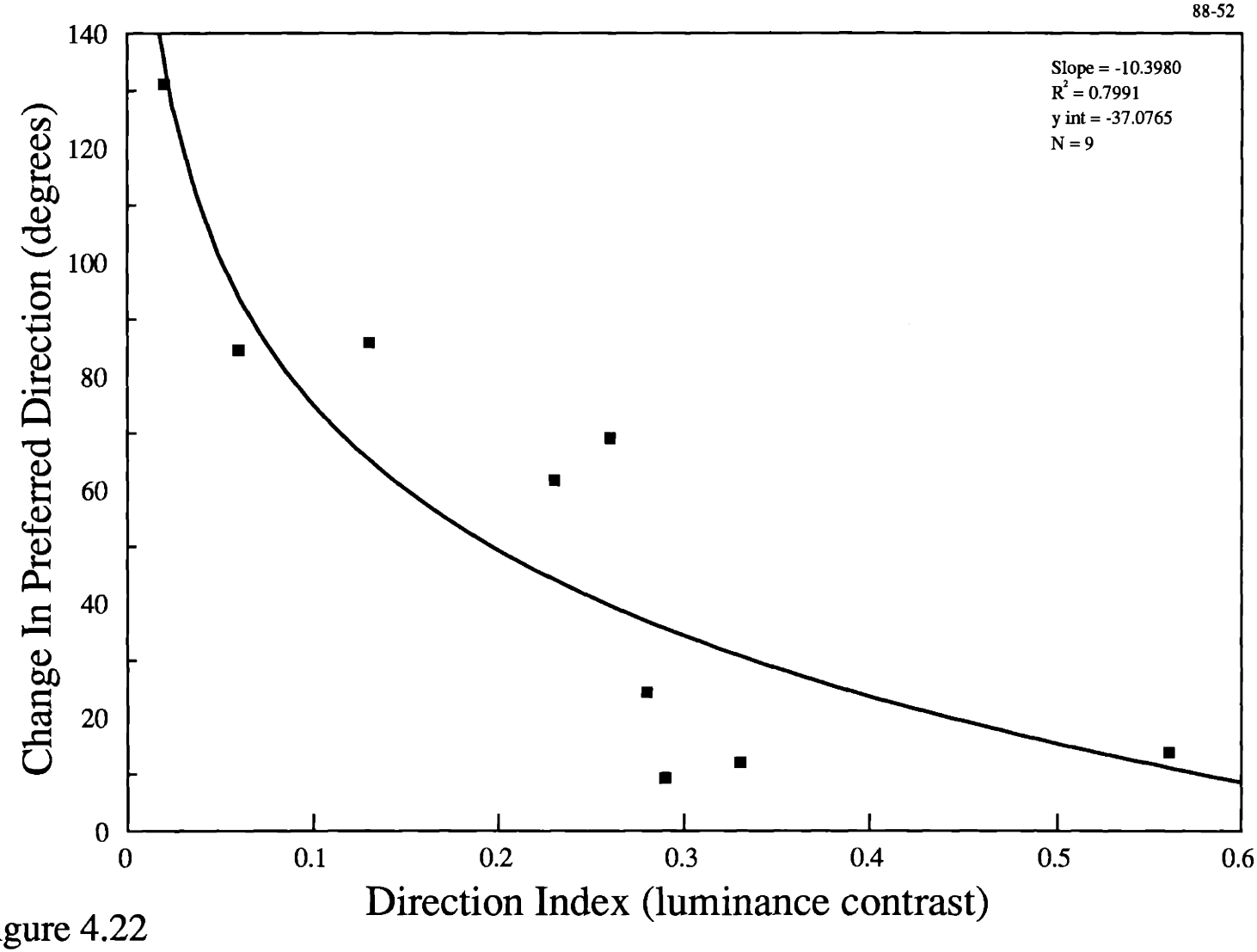

Figure 4.22

Contrast:

Luminance

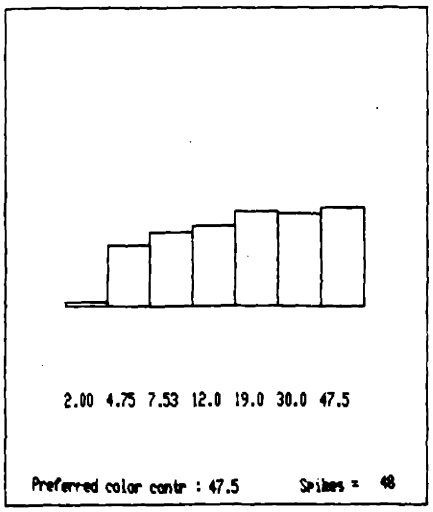

R\G

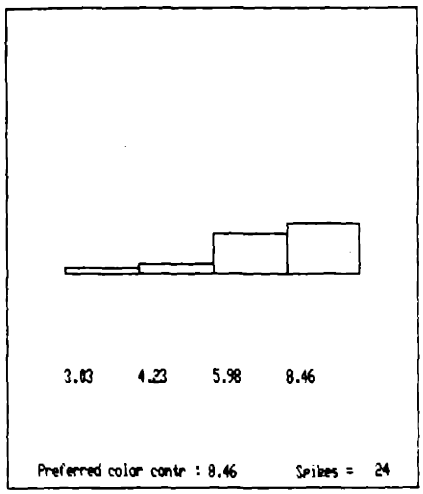

Velocity:

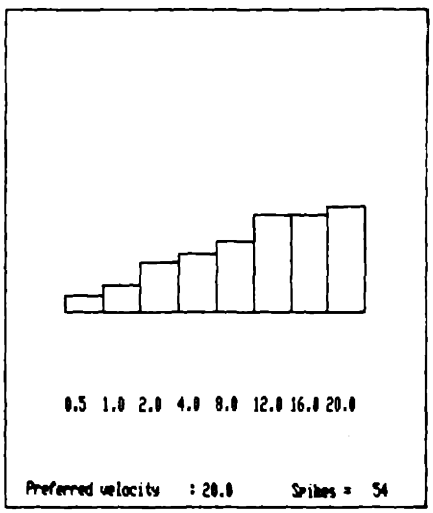

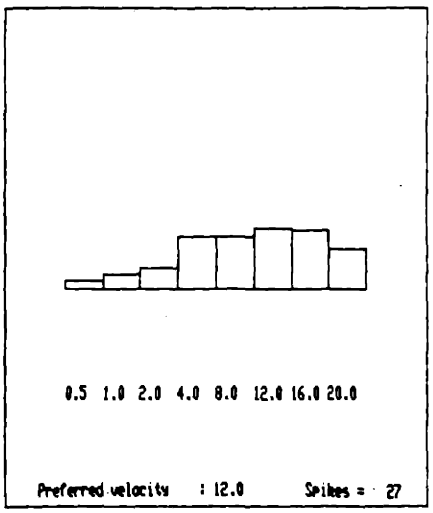

Direction:

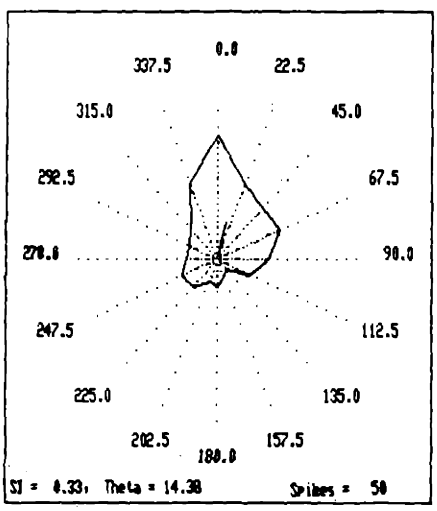

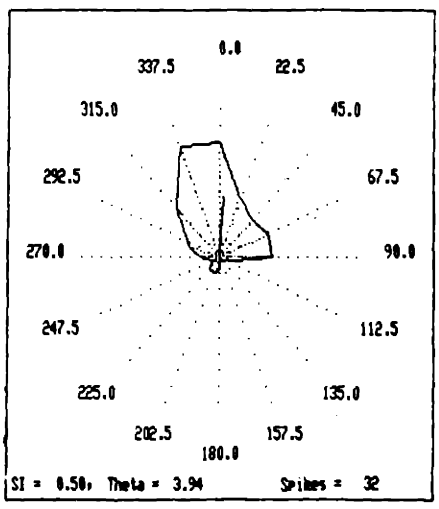

Contrast: B\Y

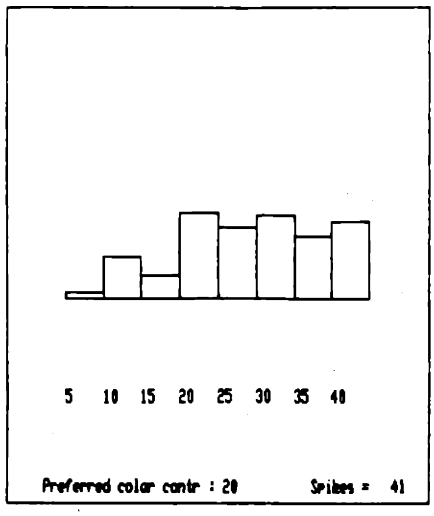

Luminance

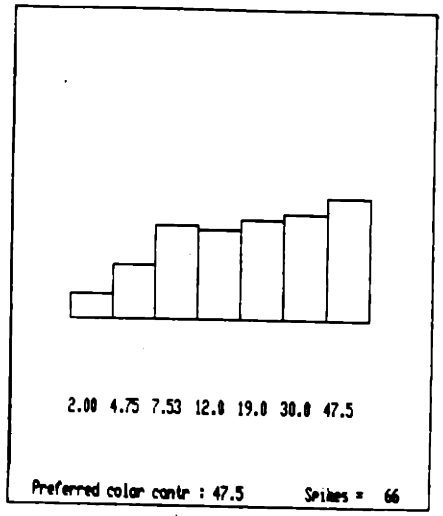

R\G

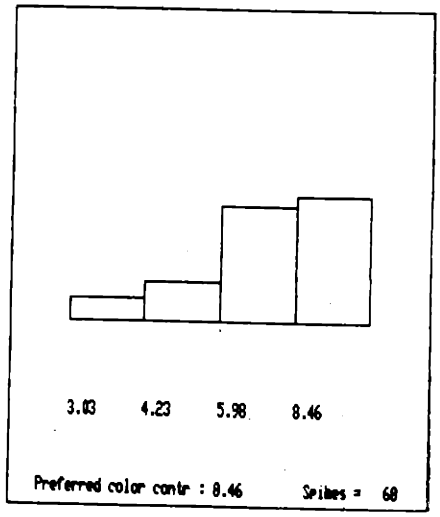

Velocity:

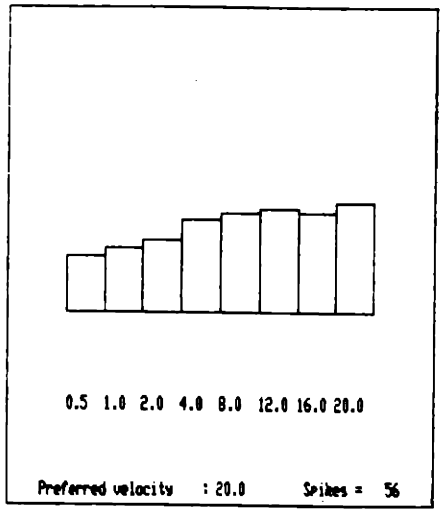

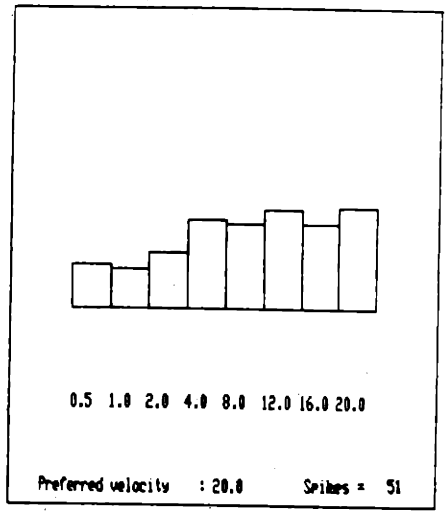

Direction:

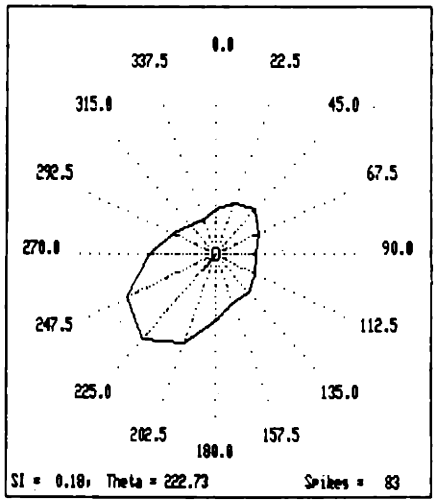

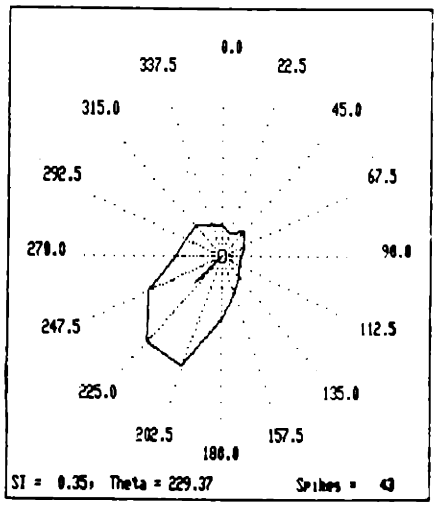

Contrast: B\Y

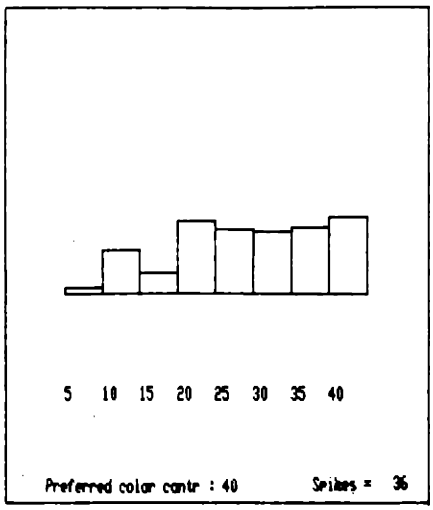

Luminance

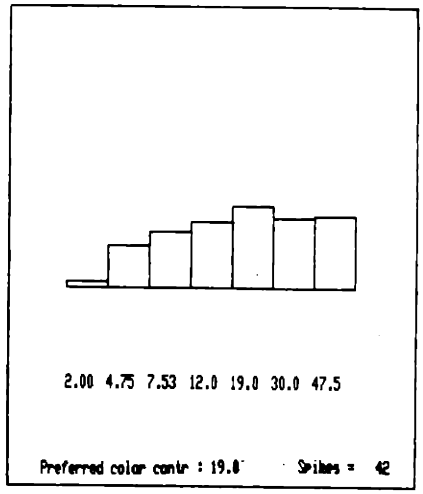

R\G

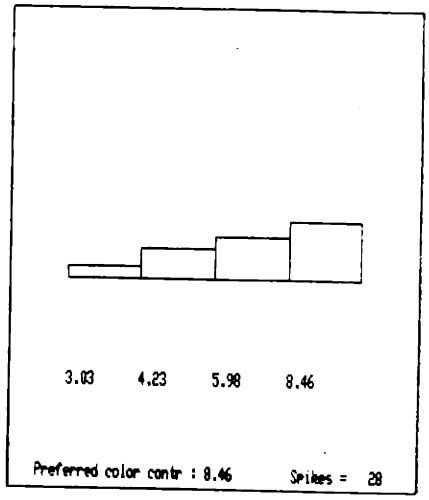

Velocity:

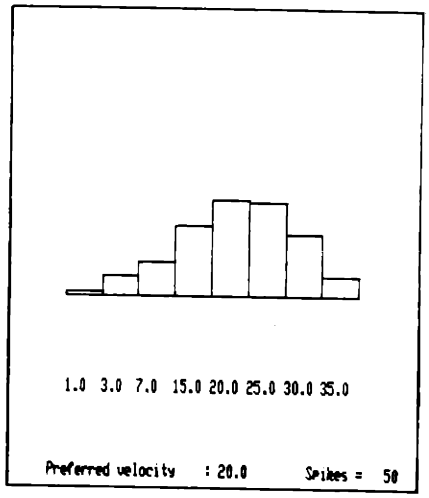

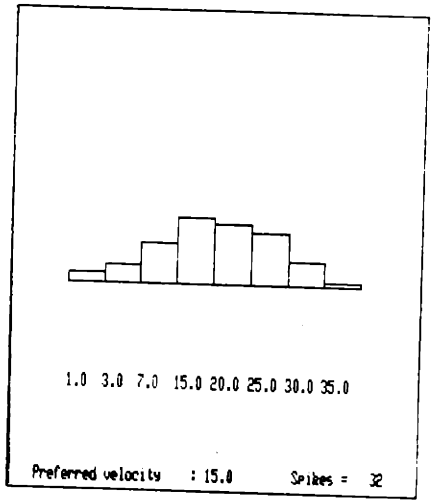

Direction:

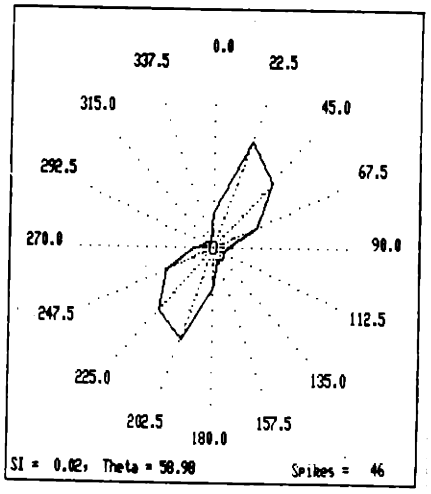

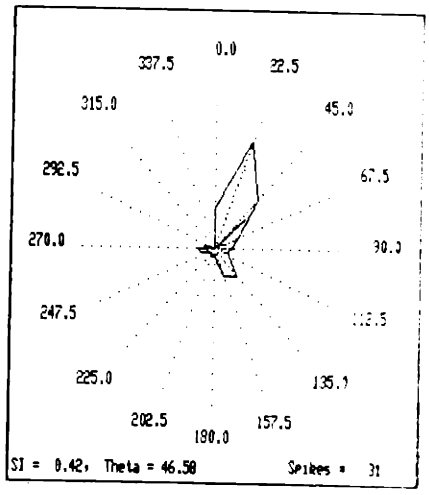

CHAPTER FIVE

TUNING PROPERTIES OF CELLS IN AREA V_4 USING STIMULI DEFINED BY LUMINANCE, CHROMINANCE AND MOTION

Summary

Cells in the proposed color/form pathway were tested to determine their responses to luminance-, color-, and motion-defined stimuli. Single-unit recordings were made in extrastriate area V_4 of the alert rhesus monkey. The stimulus configurations were identical to those used for recordings in area MT. Tuning properties were obtained for contrast, orientation and velocity using the different stimulus configurations.

V_4 cells exhibited a broad range of selectivities for wavelengths. As a result, V_4 as a whole responded worse to red/green isoluminant gratings than area MT, even when L and M cone modulations were equivalent for the luminance and chrominance conditions. Cells that were tuned for orientation using a luminance grating retained this orientation tuning for the isoluminant stimuli as long as the cell responded to the red/green gratings. Some cells showed some degree of velocity tuning, exhibiting low-, band- and high-pass tuning. A few cells showed a clear band-pass tuning for luminance contrast, unlike the majority of cells which increased monotonically with contrast. Many cells in area V_4 also responded to a motion-defined stimulus. These cells retained the same orientation tuning as luminance- and chrominance-defined stimuli. The results indicate that V_4 is not specialized for processing one quality of the visual scene, such as color, but is instead able to operate on a large set of features. In addition, notions of independent processing based on psychophysical observations using isoluminant stimuli are not supported by the physiological responses at the level of extrastriate cortex.

1.0 INTRODUCTION

The primate visual system is believed to be composed of two distinct streams that diverge early and process fundamentally different types of information (Ungerleider and Mishkin, 1982). One stream, leading to parietal cortex, performs a detailed motion analysis of the visual scene, leading to proposed function of the pathway: the identification of spatial relations between objects. Cells in the superior temporal sulcus, an extrastriate region within the pathway leading to the parietal lobe, are selective for the direction of motion, yet unselective for color or form (Dubner and Zeki, 1971; Zeki, 1974). The second or temporal pathway, central to object recognition, is involved with the processing of color and form.

Extrastriate area V_4 is a visuotopically organized area that provides the major input into the inferior temporal lobe (Gattass *et al.*, 1990; Rockland and Pandya, 1979; Desimone *et al.*, 1980). Zeki also pioneered physiological studies of this area and proposed that it was specialized for color (Zeki, 1973; 1977; 1983a; 1983b). Other studies have confirmed the involvement of V_4 with color but suggest that it may also be involved with the analysis of shape (Zeki, 1973; Desimone *et al.*, 1985; Logothetis *et al.*, 1987; Desimone and Schein, 1987).

There has been the suggestion that these two pathways, because they are involved with fundamentally distinct perceptions, operate on different types of information (Livingstone and Hubel, 1987; 1988). As the motion system is believed to be unresponsive to color cues, the color/form pathway is also believed to be incapable of motion analysis. Indeed, the foundation of many

arguments for segregated information processing are based on psychophysical experiments that conclude that the deficits observed at isoluminance (*i.e.* when only color information is present) are due to an inability of the motion pathway to exploit wavelength cues. As demonstrated in the previous chapter, cells in the motion pathway, although unable to discriminate color, are able to use wavelength information in a manner that suggests that motion processing within area MT is not wholly compromised by isoluminant color conditions. We now investigate the responses of cells in V_4 as a function of luminance and chrominance using stimuli that are identical to those used for recordings in area MT. In addition, motion-defined stimuli are also presented to determine if cells in V_4 are unable to use motion cues.

2.0 MATERIALS AND METHODS

2.1 Subjects

One juvenile (88-52) and one adult (87-45) male rhesus monkeys weighing 3.0 and 8.5 kg at the time of recordings were used for this study. Both animals were used for the psychophysical experiments described in chapter two and as a result, isoluminance was well established for each animal. The animals were cared for in accordance with the National Institutes of Health Guide for the Care and Use of Laboratory Animals and the guidelines of the Massachusetts Institute of Technology Committee on Animal Care.

2.2 Training and Recording

The methods for training and recording were almost identical to procedure described in the previous chapter. Briefly, the animals were fitted with collars and restrained in primate chairs prior to an eye-coil and head-post implantation surgery (Judge *et al.*, 1980; Robinson, 1963). The animals were then trained to perform the fixation task described previously in section 2.2 of chapter 4. To receive an apple juice reward, the animal had to maintain fixation on a small spot in the center of the monitor for a period of two to three seconds (figure 5.1). During this fixation period, a visual stimulus, either a bar or sinusoidal grating, would appear in the visual field for receptive field plotting or data collection. Data was collected prior to the appearance of the stimulus to determine the spontaneous level of activity. To keep conditions identical to the MT recordings, the transient response to onset of the stimulus was reduced by ramping the grating on over a period of 100 msec. After the period of plotting the stimulus would disappear and the monkey would then make a saccade to a laterally displaced target, signifying the end of the trial.

When the animals were sufficiently trained, they underwent a recording chamber implantation surgery. Both animals received an open cylinder chamber (Evarts, 1966). Etched platinum\iridium wires coated in glass were used for these recordings. Signals were amplified (BAK Electronics, Inc., A-1B) and band-pass filtered (Krohn-Hite, 3750) before being sent to a window discriminator (Mentor, N-750) to isolate individual cells. The signal was then split and sent to a PDP 11/73 for data collection, an oscilloscope (Hitachi, VC-6020) and an audio monitor (Grass, AM8). Recording sessions typically lasted

four to six hours.

2.3 Stimulus Presentation

The entire experiment with the exception of stimulus presentation was controlled by a PDP 11/73 (Digital). The stimuli were generated by an Adage 3000 raster display system and, in later experiments by an IBM/Pepper SGT Plus graphics system (Number Nine Computer Corp.).

When an individual V_4 cell was isolated, the receptive field was hand-plotted with a high contrast white bar using a computer-controlled joystick. The extent of the receptive field was delineated and stored using the bar stimulus. All of the subsequent stimuli consisted of sine wave gratings that were confined to the excitatory receptive fields. Brief tuning curves (2-3 trials per condition) were taken but not saved to get an indication of the degree of tuning for contrast, orientation and velocity. Most of the data files varied along one of these parameters while the others were optimized. Typically ten trials were taken for each condition within a file unless the isolation was compromised. In some cases the files varied along two parameters (i.e. contrast and velocity or contrast and orientation) and the results were consistent with tuning files presented in sequential order.

To avoid chromatic aberration artifacts at higher spatial frequencies, the majority of sinusoidal gratings had spatial frequencies below 4 cycles/degree (see chapter 2, section 2.2). For stimuli of 2 cycles/degree or higher, a spatial frequency filtered version of the stimulus (Ozolith neutral paper no. 3) was

used in order to remove high spatial frequencies that may have been introduced by errors in the calculations. As in MT, the majority of cells in V_4 did not respond to luminance gratings of contrast equivalent to the calculated worst-case artifact for a 4 cyc/deg grating.

2.4 Von Kries Color Space

The same color space was used to generate and represent the contrast of the stimuli as was used for the MT recordings (Von Kries, 1899; Stromeyer *et al.*, 1985; Stromeyer *et al.*, 1987). The stimuli are expressed as a function of individual cone class modulation (AC component), normalized to the excitation due to the steady state, background illuminant (DC component).

Figure 5.2 illustrates the configuration of the stimuli used for one animal (87-45) in this space. The horizontal, or 0 degree axis represents the rate of quantal absorption of the L cones to the stimulus (ΔL) normalized to the rate of quantal absorption due to the background adaptation level (L). The vertical, or 90 degree axis similarly represents the rate of quantal absorption for the M cones normalized to the adaptation level. The vectors represent the spatial (or temporal) modulation of the drifting sinusoidal gratings. For these experiments the modulation was constant around the mean so the vectors are symmetric. The mean level for M- and L-cone modulation was a yellow with a luminance level of 35 cd/m^2. The CIE coordinates were x = 0.459 and y = 0.463. Vectors along the vertical axis stimulate the M cone without affecting the L cones. Inset A shows the modulation of cone excitation (M cones, solid

line; L cones, broken line) along this axis over space. In this case the M cones are modulated sinusoidally while the rate of quantal absorption of the L cones remains constant. For both the M and L cones the mean rate of quantal absorption is the same and equivalent to the rate at the background illumination. An identical profile would be seen for vectors along the horizontal axis if the solid line referred to the L cones.

For this particular animal, modulation along the 45 degree axis shown in inset B produces an equivalent rate of quantal absorption at all spatiotemporal points forming a light/dark yellow luminance grating. For each cone class the cone excitation is varying sinusoidally and with the same phase with respect to the other. Stimuli presented along this axis will be referred to as "inphase" or "luminance" modulation. The representation in cone excitation space can be converted to standard Michelson contrast by dividing the 45 degree vector by the square root of two. Vectors along the -45 degree axis shown in inset C also create sinusoidally varying absorption rates of equal amplitude but the modulation is 180 degrees out of phase. For these stimuli the net quantal catch is constant and the same as the adaptation level. Thus, the luminance is constant and the stimuli appear as red/green sinusoidal gratings. These stimuli will be referred to as "antiphase" or "chrominance" modulation or "isoluminant" stimuli when relevant.

2.5 Motion-defined stimulus

The motion of sinusoidal gratings can be described in terms of an energy

distribution in the spatiotemporal frequency domain. The speed and direction of these gratings can be derived from activity in channels tuned for spatial and temporal frequencies. Non-fourier motion (Chubb and Sperling, 1988) however cannot be described in terms of power spectra within the frequency domain. This form of motion contains no orderly spatial or temporal frequency components in any given direction and is thus more appropriate for determining if cells that are tuned to specific spatial and temporal frequencies, are capable of responding to motion cues.

After determining the location of the receptive field and optimal spatial frequency for a cell, a field of random dots that could be varied in size were displayed on the monitor. Using these stored values of location and spatial frequency, we assigned sets of dots to move with uncorrelated random motion or remain stationary. These two sets corresponded to the bars of a square wave grating within the receptive field. The perceptual result was a "shape-from-motion" grating that could have one of four orientations. The contrast of the dot elements were typically set to 100% luminance contrast. As controls, data was also collected for whole field uncorrelated motion or stationary dots. Few cells responded under these conditions and no orientation tuning was observed.

2.6 Data analysis

Figure 5.3 describes how cell activity was defined for the majority of analysis. For each trial the spike train was convolved with a gaussian function

generating a spike density function (MacPherson and Aldridge, 1979). The mean level of activity, or spontaneous rate, was computed during the time period in which the monkey was fixating prior to the appearance of the stimulus. Excitation and inhibition levels were taken as the activity that was two standard deviations above or below this mean level of activity. Integration of these shaded portions of the curve then represent the total excitation and inhibition of the cell.

Orientation tuning was measured at 22.5 degree intervals for 0 to 180 degrees beginning with the vertical axis. To obtain a measure of orientation selectivity, cell activity is represented in polar coordinates with the sum of the vectors having a length equal to the cell activity (either excitation or inhibition) and a orientation equal to the tested stimulus orientation over a block of trials. Let us assume that R_i represents the spike activity value for a given stimulus direction, θ_i, where $\theta_i = (i \times 22.5)$. These vectors can be decomposed into x and y components:

$$SumY = \sum_{i=0}^{7} (R_i \cos 2\theta_i)$$

$$SumX = \sum_{i=0}^{7} (R_i \sin 2\theta_i)$$

The vector length is also normalized to the cell activity:

$$SumAct = \sum_{i=0}^{15} R_i$$

To obtain the orientation index, SI, then:

$$DI = \frac{\sqrt{SumX^2 + SumY^2}}{SumAct}$$

This represents the sum of cell activity for the tested orientations. Note that because inhibition of the firing rate is assigned a negative value, the direction index can have a value greater than one.

The preferred orientation (θ_m), of the cell in degrees is calculated as:

$$\theta_m = ArcTan\left(\frac{SumY}{SumX}\right) x \frac{180}{\Pi}$$

Thus, the preferred orientation, like SI, is a weighted sum of the responses in all tested directions, and does not necessarily correspond to the tested direction giving the maximal response. Unlike direction tuning, θ_m for orientation will have a value that is perpendicular to the best orientation.

Two ranges of values were used to determine the velocity tuning for each cell depending on the optimal spatial frequency. For higher spatial frequencies, velocities of 0.5, 1, 2, 4, 8, 12, 16, and 20 degrees/sec were used. For lower spatial frequencies 1, 3, 7, 15, 20, 25, 30, and 35 degrees/sec were used.

3.0 RESULTS

Data was collected from 197 cells from 2 hemispheres of 2 monkeys.

Due to the duration of stimulus presentation, however, not all conditions are tested in each cell.

3.1 Response to Isoluminant Color Stimuli

Responses to isoluminant color gratings were variable in V_4. Figure 5.4 shows the responses of cells in V_4 to luminance (inphase) and red/green isoluminant (antiphase) gratings. The data for each cell is taken at either 8% (triangles) or 16% (squares) L and M cone modulation and represented as the sum activity for the duration of the stimulus. Because ten trials were taken for each condition, dividing the sum activity by ten will give an estimate of the mean firing rate. As seen in the figure, cells are highly variable in their responses to both the luminance and red/green isoluminant gratings (R^2 = 0.36). While most cells respond well to the luminance gratings, many had poor responses to the red/green isoluminant gratings. Cells lying on the X axis gave responses to luminance gratings but did not respond to the red/green isoluminant gratings. Three cells were actually inhibited by the isoluminant color gratings. It was noted during the hand-plotting that many cells only responded to specific color combinations not necessarily corresponding to the cardinal directions of color space (Derrington *et al.*, 1984). The slope of the linear regression (0.61) reveals that as a whole, V_4 does not respond nearly as well to isoluminant color gratings as to luminance gratings, even in conditions where L and M cone modulations are equivalent in both cases. Fourteen additional cells are not represented in this figure because it was noted that

they gave no response to the red/green gratings and no files were taken. This would reduce the slope of the regression and increase the R^2 value further.

Some cells were also tested using blue/yellow isoluminant grating that is previously described in chapter 4, section 3.4. Like the results using the red/green isoluminant grating, responses varied from cell to cell. Although cells were not analyzed quantitatively, fewer cells were responsive to the blue/yellow stimuli than the red/green isoluminant gratings.

3.2 Orientation Tuning in area V_4

Figure 5.5 shows the distribution of orientation tuning for 146 cells using the index described in section 2.6 and summarized in the inset. Orientation tuning was determined using the optimal spatial frequency with either a high contrast luminance grating (65% Michelson contrast) or a red/green isoluminant grating, depending on the one that produced a larger response. Orientation tuning (SI) is centered on values near 0.2 although the whole range of tuning is represented. Many cells responded well to the gratings irrespective of the orientation while others exhibited very sharp tuning, firing to only one of the tested directions. Some sharply tuned cells had an SI greater than one because of inhibition, which carries a negative value, at orthogonal directions.

Figure 5.6 shows the orientation tuning of one cell in V_4. On the left are polar plots, representing the mean spike activity (r) as a function of the orientation of the grating (θ). Because orientations greater than 180 degrees

were not tested, the responses from 0 to 180 are reflected in this portion of the graph. The solid lines represent the calculated orientation: The length of the vector depicts the selectivity index (SI) and the angle represents the preferred orientation (θ_m). To the right are the raster displays for each orientation tested. Underneath are the corresponding spike density functions. The top row shows the cell's response to a luminance modulated grating (inphase). This cell displays good orientation tuning (SI = 0.51) with a preferred orientation along the 65 degree axis (Theta = 155). The bottom row shows the cell's response to a grating in which L and M cones are modulated in antiphase. Although the cell does not respond as well to the red/green isoluminant grating (mean spikes/sec = 11), orientation tuning is preserved (SI = 0.69, Theta = 158).

3.3 Direction Tuning in V_4

A subpopulation of cells were tested for direction tuning as described in chapter 4, section 2.5. Figure 5.7 shows the distribution of the indices for direction with a description of the index in the inset. Most of the cells show no directional tuning. A small percentage (DI > 0.2: 15%) did show directional responses. This agrees with previous findings by Desimone and Schein (1987).

3.4 Velocity Tuning in V_4

While the majority of cells in V_4 were not tuned for velocity, many cells had a degree of velocity tuning. Figure 5.8 shows the velocity tuning of four of these cells to a 47.5% luminance contrast grating. Low-, band-, and high-pass

(to the limits of our system) tuning was present in V_4. In the previous chapter many cells in area MT exhibited a shift towards lower preferred velocities when using isoluminant color gratings. These results were most often observed for the higher values tested. Because few cells had responses at the highest velocities, the shift in preferred velocity is not obvious in the population data. Figure 5.9 is however suggestive that the same results may be found in V_4 as were found in MT. The top row shows the response to an L and M cone inphase-modulated grating (luminance). The cell fires well to the moving grating with the response increases monotonically. For the L and M cone antiphase-modulated grating (red/green), the cell is active at all velocities, though the response does appear to drop some at velocities above 20 degrees/second.

3.5 Band-pass Luminance Contrast Tuning in V_4

The majority of cells in V_4 responded to luminance contrast with a monotonic increase in firing up to a maximum in activity as contrast was increased. A few cells however, showed a definite band-pass response to contrast tuning. Three cells exhibiting this behavior are seen in figure 5.10. On the left are histograms representing the mean spike rate of responses to L and M cone inphase-modulated gratings with contrast listed underneath. To the right are the corresponding raster displays and spike density functions. The cell in 5.10a has no response to a 2% luminance contrast grating but fires vigorously to a 4.75% grating. For higher contrasts the response decreases

with increasing contrast. No response is seen at the highest contrast level (47.5%). Histograms for the next cell (5.10b) indicate similar tuning however the raster displays and spike density functions show a somewhat different behavior. This cell also has no response to a 2% contrast grating. For the 4.75% grating, the cell fires when the grating achieves the full contrast and continues to fire for the duration of the stimulus presentation. For higher contrasts the cell is active when the stimulus is ramped on and increasing in contrast. At contrasts of 12% or higher, there is no sustained response to the stimulus and all activity occurs during the period when the stimulus is ramped on and increasing in contrast. Because the stimulus is initially ramped on over a 100 msec period, the rate at which the contrast is increased will depend on the final contrast of the grating. Thus, a grating of 4.75% contrast will be reached after 100 msec if the final contrast is 4.75% (solid vertical line in the spike density functions) but at 10 msec after the onset of the stimulus if the final contrast is 47.5%. This cell's preference for low contrast is reflected by the shift in the peak of the spike density function. For a final contrast of 4.75%, the peak is near the end of the ramping period and the cell continues to fire. As contrast is increased, the peak in response shifts towards the beginning of the ramping period when the contrast of the grating is low. The histograms do not reflect this activity because the ramping period is not used in either the determination of the spontaneous activity or for the response to the stimulus. Figure 5.10c shows another cell whose activity declines at higher luminance contrast values (30 and 47.5%).

Figure 5.11 shows the other tuning characteristics of the cell in figure 5.10a, seen again in the top row, middle. While the cell is band-pass tuned for luminance contrast, it responds optimally to the highest levels of color contrast for both blue/yellow and red/green isoluminant gratings[1]. Velocity tuning for this cell uses a 4.75% luminance contrast grating and a 8.56% cone modulation red/green isoluminant grating in the middle row of figures. In both cases the cell has an increase in response as the velocity of the drifting grating is increased. The cell, although not responding well to a stationary stimulus, does appear to be tuned to horizontal gratings. No shift in orientation is seen between the luminance and red/green isoluminant grating conditions. Thus, other than the band-pass tuning characteristics for luminance contrast, the cell behaves in much the same way as other cells in V_4.

3.6 V_4 Cell Responses to Motion-Defined Gratings

A subset of V_4 cells (N = 88) were tested with the motion-defined grating described in section 2.5. A wide range of responses were seen within V_4. Figure 5.12 is an example of a cell responding only to the luminance grating. Raster displays are presented for four orientations at 45 degree intervals (0-135 degrees). Underneath are histograms with spike activity distributed in bins of 20 msec; not spike density functions. The ordinate is the firing rate; the abscissa is the time in milliseconds. The horizontal bars under each histogram indicates the onset and duration of the stimulus presentation. This cell responds well to a luminance grating oriented along the 45 degree axis and

poorly to the other three orientations. This cell does not respond to the motion-defined grating. Figure 5.13 shows the orientation tuning curves for the two types of gratings for this cell. The filled squares represent the cell activity above the spontaneous activity for each of the orientations of the luminance gratings. The empty squares represent the activity of the motion contrast gratings. Orientation indices for the luminance and motion contrast gratings, SI_L and SI_M, confirm that the cell is tuned for the luminance grating but not for the motion-defined grating. Because the cell is poorly tuned for the motion contrast grating, preferred orientation, θ_L and θ_M listed in parentheses, is only reliable for the luminance grating condition.

Figure 5.14 shows a cell that fires not only to the luminance-defined grating but also the motion-defined grating. While the response to the motion grating is somewhat lower than the luminance contrast grating, it shows the same orientation tuning as the luminance contrast grating. Figure 5.15 shows the orientation tuning for this cell is similar for both the selectivity index (SI_L = 0.28 and SI_M = 0.22) and the preferred direction (θ_L = 93.6 and θ_M = 103.3 degrees). To insure that cells were not simply responding to flickering dot patterns that coincidentally stimulated subregions of the receptive field, uncorrelated motion or stationary dots were presented within the excitatory receptive field. Most cells gave poor responses to this control, as no gratings could be perceived in these conditions, no orientation tuning was observed for any cell.

Figure 5.16 displays the response of a cell to luminance contrast,

luminance plus color (red/green) contrast, and motion contrast gratings. In the luminance plus color contrast condition, the luminance contrast was the same as the luminance contrast only condition, but the red and green phosphors were modulated in antiphase to provide 100% color contrast. Luminance (black) and luminance plus color (shaded) are represented in the upper panel. The cell is more active for the luminance plus color grating condition at all orientations, demonstrating wavelength selectivity for the cell. This cell also fires to the motion grating that is oriented along the 45 degree axis. Figure 5.17 shows that the orientation tuning is sharpest (SI_M = 0.62) for the motion-defined grating condition and broadest for the luminance plus color condition (SI = 0.31) primarily due to the response to the vertical grating. As with the previous cell, the preferred orientation does not vary much for the different conditions.

Figure 5.18 compares the orientation tunings to luminance- and motion-defined gratings for the population. The distribution of orientation indices (SI_L) for luminance gratings are on the left and indices for motion contrast gratings (SI_M) are on the right. The black histogram at 0.0 for the motion contrast grating signifies that cells were unresponsive to the motion-defined stimulus. Over half the cells were responsive, however, and exhibited selectivity indices similar to those using the luminance contrast grating. The majority of the cells that responded were within 10 degrees of the fovea. Upon casual inspection, cells only seemed to respond to the motion-defined grating if the grating could be perceived however this was not tested in the monkeys.

Figure 5.19 compares the preferred orientations and selectivity indices for the luminance and motion contrast conditions. Only cells that exhibited tuning for the luminance contrast gratings (SI > 0.2) were included in this analysis. The linear regression analysis shows that cells retain orientation selectivity although the cells are somewhat more broadly tuned for the motion-defined stimulus (r = 0.85). The graph on the right show that these cells do not change the preferred orientation however (r = 0.97).

The next two figures summarize the responses seen in area V_4. Figure 5.20 illustrates the tuning properties of one cell for contrast, velocity and orientation. The histogram for contrast labelled 'C0/90' represents the cells responses vectors in the color space that modulate single cone classes. The left four histograms show responses to gratings that modulate along the 0 degree or L cone axis. The cell only responds to a 16% L cone modulation. The right four histograms of this figure represent the activity to M cone modulation. In this case the cell responds to all but the 2% M cone modulation. A differential response to individual cone class modulations seemed to be common in V_4 cells. The histogram labelled 'C45/135' represents inphase (right four histograms) and antiphase (left four histograms) L and M cone modulated gratings. For this cell, responses were nearly the same for the luminance and isoluminant red/green gratings. Unlike the cells described in section 3.5, cell activity increased monotonically with increased contrast for all conditions. While this cell responded well to moving gratings, it showed little velocity tuning. Like some V_4 cells tested, there was a sharper decline in response for the higher

velocities. The bottom row shows orientation tunings using inphase (luminance) and antiphase (R/G) L and M cone modulated gratings. For this cell the orientation tuning is somewhat sharper for the luminance grating but the preferred orientation remains unchanged.

Figure 5.21 shows the response of one cell to a 100, 4, and 2% luminance contrast grating as well as a motion-defined grating. The best response for this cell is to the 4% luminance contrast grating although the best orientation tuning is seen in the 100% luminance contrast condition. The cell appears to lose orientation selectivity at the lower (4%) contrast condition. This cell also has a response to the motion contrast stimulus and this response exhibits the same preferred orientation as the luminance conditions.

4.0 DISCUSSION

4.1 Response to Isoluminant Stimuli

While many of the cells responded well to the luminance gratings, the responses to either red/green or blue/yellow isoluminant gratings varied from cell to cell. Many cells did not respond to the isoluminant stimuli even though the L and M cone modulations were equivalent to those of the luminance gratings which produced responses. The regression analysis suggests that V_4 as a whole is compromised at isoluminance (slope = 0.61). This heterogeneity is a result of the spectral sensitivity in area V_4 (Zeki, 1973; 1977; 1983a; 1983b; De Monasterio and Schein, 1982; Schein *et al.*, 1982; Schein and De Monasterio, 1990). In figure 5.20 the graph labelled 'C0\90' indicates that the

weights of L and M cones are not equivalent suggesting that the preferred color may not fall along cardinal directions. Cells that are tuned to short wavelengths of the visible spectrum will not respond to L and M cone antiphase-modulated gratings. On the other hand, cells tuned to either red or green may fire more vigorously to the isoluminant grating than the luminance grating. Because of this variability in response, population analysis comparing luminance and isoluminant color gratings was difficult.

4.2 Tuning Properties of cells in V_4

V_4 cell activity usually increased monotonically with increased contrast, as was seen in area MT. Some cells did however exhibit a band-pass tuning response to luminance contrast (figures 5.10 and 5.21). This type of cell may contribute to determining the contrast of objects. These cells behaved like cells whose activity rose with increased contrast in all other respects. As was mentioned in the previous chapter, if cells are carrying a multiplexed signal, *e.g.* contrast and orientation, it is necessary to carry a separate measure of contrast in order to recover orientation independently. Figure 5.21 suggests that these cells may fire more at low contrasts because inhibitory mechanisms are less sensitive to luminance contrast than the excitatory mechanisms. Because the cells in figure 5.10 are tested at the preferred orientation, this would require that the inhibition be present at the preferred orientation. Further investigation of band-pass tuned cells would be necessary before determining the basis of this tuning. While these cells were rarely encountered

(2%), it is likely that many were missed due to the method used to plot the receptive fields in V_4. Figure 5.11 indicates the difficulties in driving these cells. While the cell responds quite well to a 4.75% luminance contrast grating (52 spikes/sec), there is no response to the 47.5% contrast grating (top row, middle). Since V_4 cells were isolated and plotted using a high contrast luminance bar, only very diligent plotting revealed these cells. In addition, the cell in figure 5.11 gave poor responses to low velocities (middle row). This is reflected by the poor responses seen in the orientation tuning curves (bottom).

When cells would respond to the red/green isoluminant grating and were orientation tuned, orientation tuning was not greatly affected. The preferred orientation for the cell did not change at isoluminance (figures 5.6, 5.20). Changes in the degree of tuning were seen for many cells however. The cell in figure 5.6 had an orientation tuning index of 0.51 for the luminance grating while the index for the isoluminant color grating was somewhat higher (SI = 0.69). The firing rate for the red/green grating (11 spikes/sec) is much lower than the luminance grating (28 spikes/sec) which may explain the differences in tuning. The cell in figure 5.20 also shows differences in the sharpness in tuning. In this case the cell is more sharply tuned to the luminance grating but the average response is comparable (48 spikes/sec and 46 spikes/sec) for the two gratings. These findings support psychophysical work (Bradley, *et al.*, 1988; Cavanagh, 1989; Flanagan *et al.*, 1990) which suggests that orientation mechanisms are coupled to the colors of the contours. Bradley *et al.* find elevations in thresholds that are orientation dependent after adapting to

isoluminant gratings. Cavanagh and Flanagan *et al.* make use of tilt aftereffects to conclude that orientation can be supported by chromatic mechanisms. Further it was determined that orientation selectivity occurs independently in the cardinal directions of color space (Flanagan *et al.*, 1990). While the physiological evidence at the level of V_4 does not support orientation tuning falling on the cardinal axes of color space, it does suggest that units in area V_4 are specific for both wavelength and orientation, permitting differential adaptation.

Many of the cells in area V_4 exhibited some degree of velocity tuning. Examples of cells that were tuned to low, intermediate and high velocities are displayed in figure 5.8. While the low-pass velocity tuned cells may be a result of the spatial separation of On- and Off-cell subregions of the receptive fields which occurs for a fraction of V_4 cells (Desimone *et al.*, 1985; Desimone and Schein, 1987), band-pass tuning must be a result of cortical inhibitory mechanisms (Worgotter and Koch, 1991). When using gratings in which L and M cones were modulated in antiphase, cells do not respond as well to high velocities (figure 5.10). While only a few cells responded well to high velocities and the red/green gratings, the data is suggestive that a shift towards lower velocities may be occurring in V_4 like the change in preferred velocity observed in area MT (chapter 4, section 3.3). In addition, a low percentage of cells in V_4 were direction tuned (figure 5.7). This is in agreement with Desimone and Schein (1987) who found about 8% of the cells to be tuned to direction. If area V_4 is not involved in motion processing, it is difficult to explain the presence of

velocity and direction tuned cells with properties similar to those of cells in area MT.

4.3 Response to Motion-defined Stimuli

Many cells in V_4 respond to gratings defined by non-fourier random dot motion (figures 5.14-5.17, 5.21). Because the power spectra for these stimuli are randomly distributed in the spatial and temporal frequency domains, these responses represent a true motion response. If these cells are orientation tuned using luminance gratings, the cells are similarly tuned for the motion contrast gratings both in terms of the preferred direction and selectivity index (figure 5.21). Although orientation selectivity is constructed prior to V_4, persistence of tuning in the motion-defined stimulus indicate that cells within the proposed color/form pathway are using of motion information in a meaningful way. This is also supported by the observation that cells that did respond to the motion contrast stimulus required stimulus configurations that produced a perceptible grating. If cells in V_4 were responding nonspecifically to the motion stimulus, one might expect cells outside of the central 10 degrees to respond. One might also predict that a nonspecific response driving inputs to V_4 should produce responses in all cells. In addition, specific spatial frequencies and dot sizes were necessary to elicit responses arguing further that the signal is relevant. The source of this activity is not clear. V_4 receives input through both the parvocellular and magnocellular LGN (Ferrera *et al.*, 1990) and also has a reciprocal connection with area MT (Rockland and

Pandya, 1979; Maunsell and Van Essen, 1983; Ungerleider and Desimone, 1986). These stimuli have not been tested at the level of LGN yet to determine if one population selectively responds to the motion-defined stimulus.

1) In figure 5.11, the top left figure labelled "B/Y" is a cell's response to blue/yellow isoluminant gratings. The labels refer to the S/L+M cone modulation. Modulation along this blue/yellow axis however, affects all three cone types.

REFERENCES

Bradley, A., Switkes, E. and De Valois, K. Orientation and spatial frequency selectivity of adaptation to color and luminance gratings. Vision Research 28:841-856, 1988.

Cavanagh, P. "Multiple analyses of orientation in the visual system." In: Neural Mechanisms of Visual Perception, eds D.M.K. Lam and C.D. Gilbert. Gulf Publishers, Houston, 1989.

Chubb, C. and Sperling, G. Drift-balanced random stimuli: A general basis for studying non-fourier motion perception. Journal of the Optical Society of America A 5:1986-2007, 1988.

De Monasterio, F.M. and Schein, S.J. Spectral bandwidths of color-opponent cells of geniculostriate pathway of macaque monkeys. Journal of Neurophysiology 47:214-224, 1982.

Derrington, A.M., Krauskopf, J. and Lennie, P. Chromatic mechanisms in lateral geniculate nucleus of macaque. Journal of Physiology 357:241-265, 1984.

Desimone, R., Fleming, J. and Gross, C.G. Prestriate afferents to inferotemporal cortex: An HRP study. Brain Research 184:41-55, 1980.

Desimone, R. and Schein, S.J. Visual properties of neurons in area V_4 of the macaque: Sensitivity to stimulus form. Journal of Neurophysiology, 57:835-868, 1987.

Desimone, R., Schein, S.J., Moran, J., and Ungerleider, L.G. Contour, color and shape analysis beyond the striate cortex. Vision Research 25:441-452, 1985.

Dubner, R. and Zeki, S.M. Response properties and receptive fields of cells in an anatomically defined region of the superior temporal sulcus. Brain Research, 35:528-532, 1971.

Evarts, E.V. Methods for recording activity of individual neurons in moving animals. Methods in Medical Research 11:241-250, 1966.

Ferrera, V.P., Nealey, T.A. and Maunsell, J.H.R. Magnocellular and parvocellular inputs to macaque area V_4. Investigative Ophthalmology and Visual Sciences Supplement 32:1117, 1991.

Flanagan, P., Cavanagh, P. and Favreau, O.E. Independent orientation-selective mechanisms for the cardinal directions of colour space. Vision

Research 30:769-778, 1990.

Gattass, R., Sousa, A.P.B., and Gross, C.G. Visuotopic organization and extent of V_3 and V_4 of the macaque. Journal of Neuroscience 8:1831-1845, 1988.

Heywood, C.A. and Cowey, A. On the role of cortical area V_4 in the discrimination of hue and pattern in macaque monkeys. Journal of Neuroscience 7:2601-2617, 1987.

Livingstone, M.S. and Hubel, D.H. Psychophysical evidence for separate channels for the perception of form, color, movement, and depth. Journal of Neuroscience 7:3416-3468, 1987.

Livingstone, M. and Hubel, D. Segregation of form, color, movement, and depth: Anatomy, physiology, and perception. Science 240:740-749, 1988.

Logothetis, N.K., Voegels, R., and Schiller, P.H. Neuronal activity in V_1, V_2, and V_4 in Macaque Monkey Performing a Visual Matching Task. Society of Neuroscience Abstracts 13:624, 1987.

Maunsell, J.H.R. and Van Essen, D.C. The connections of the middle temporal visual area (MT) and their relationship to a cortical hierarchy in the macaque monkey. Journal of Neuroscience 3:2563-2586, 1983.

Rockland, K.S. and Pandya, D.N. Laminar origins and terminations of cortical connections of the occipital lobe in the rhesus monkey. Brain Research 179:3-20, 1979.

Schein, S.J. and Desimone, R. Spectral properties of V_4 neurons in the macaque. Journal of Neuroscience, 10:3369-3389, 1990.

Schein, S.J., Marrocco, R.T., and De Monasterio, F.M. Is there a high concentration of color-selective cells in area V_4 of monkey visual cortex? Journal of Neurophysiology 47:193-213, 1982.

Schiller, P.H., Charles, E.R. and Logothetis, N.K. The effect of V_4 and parvocellular lesions on primate vision. Investigative Ophthalmology and Visual Science Supplement 29:328, 1988.

Shipp, S. and Zeki, S. Segregation of pathways leading from area V_2 to areas V_4 and V_5 of macaque monkey visual cortex. Nature 315:322-325, 1985.

Ungerleider, L.G. and Desimone, R. Cortical connections of visual area MT in the macaque. Journal of Comparative Neurology 248:190-222, 1986.

Ungerleider, L.G. and Mishkin, M. Two cortical visual systems. In: Analysis

of Visual Behavior, eds. D.J. Ingle, M.A. Goodale, and R.J.W. Mansfield. MIT Press, Cambridge, MA (1982).

Worgotter, F. and Koch, C. A detailed model of the primary visual pathway in the cat: Comparison of afferent excitatory and intracortical inhibitory connection schemes for orientation selectivity. Journal of Neuroscience 11:1959-1979, 1991.

Zeki, S.M. Colour coding in the rhesus monkey prestriate cortex. Brain Research 53:422-427, 1973.

Zeki, S.M. Colour coding in the superior temporal sulcus of rhesus monkey visual cortex. Proceedings of the Royal Society of London, Series B 197:195-223, 1977.

Zeki, S. Colour coding in the cerebral cortex: The reaction of cells in monkey visual cortex to wavelengths and colours. Neuroscience 9:741-765, 1983a.

Zeki, S. Colour coding in the cerebral cortex: The responses of wavelength-selective and colour-coded cells in monkey visual cortex to changes in wavelength composition. Neuroscience 9:767-781, 1983b.

Zeki, S. and Shipp, S. The functional logic of cortical connections. Nature 335:311-317, 1988.

FIGURES

Figure 5.1. Description of a trial during V_4 recordings. Time progresses from left to right. The trial begins with the appearance of a small fixation spot in the center of the monitor which the animal must foveate. Data collection begins after foveation and spontaneous activity is recorded. A sinusoidal grating is then ramped on over a period of 100 msec within the receptive field and then begins drifting with a fixed velocity. After the data collection period, a laterally displaced target appears to signal the end of the trial. If the animal fails to hold fixation during any point during the trial is aborted.

Figure 5.2 Description of the color space used to define the luminance and chrominance stimuli. The sinusoidal gratings are modulated around a mean level defined in CIE coordinates in the upper left. This is a saturated yellow background. Axes of the space are changes in individual cone excitation normalized to the cone excitation due to the mean level. M cone modulation is represented on the Y axis and L cone modulation is on the X axis. All modulation vectors used in these experiments were equal around the mean. Inset A represents modulation of the M cones while the excitation of the L cones remains constant at the mean level. Inset B represents equal modulation of both M and L cones with the same phase (inphase modulation). Modulation approximately along this 45 degree axis represents luminance modulation of the stimulus. Modulation along the -45 degree axis (inset C) represents excitation of M and L cones 180 degrees out of phase (antiphase modulation). In one animal modulation along this axis represented isoluminance. Individual variation in isoluminance determined behaviorally will shift the angle of this axis slightly.

Figure 5.3 Definition of cell activity. Individual spike trains were convolved with a gaussian function to produce spike density functions. Spike density functions were aligned to the onset of the stimulus and summed. The portion of the function prior to the onset determined the mean spontaneous activity level. We defined excitation as the area under the curve that was two standard deviations above the mean level (shaded area). Similarly, inhibition is the area integrated under the curve two standard deviations below the mean level (cross-hatched area). Inhibition was assigned negative values.

Figure 5.4 Responses of V_4 cells to luminance and isoluminant color gratings. Gratings were composed of either 8% (triangles) or 16% (squares) L and M cone modulated inphase (luminance) or antiphase (isoluminance). The solid line represents the linear regression. The slope of the regression (0.61) shows that V_4 as a whole does not respond as well to isoluminant color gratings even when cone modulation is equated. Further, the response of V_4 cells is highly variable ($R^2 = 0.36$); Some cells prefer the isoluminant red/green grating to the luminance grating while others give no response or are inhibited to the color

grating.

Figure 5.5 Distribution of the orientation index for V_4 cells. The inset describes the circular statistics used to derive the index. A few cells had an index greater than one due to inhibition (negative values) at the orthogonal orientations.

Figure 5.6 Orientation tuning for one cell in V_4 using a luminance and isoluminant color grating. The left column contains polar plots of orientation (θ) plotted against spike activity (r). On the right are the corresponding raster displays. The top row shows the orientation tuning of the cell using the luminance grating. The cell prefers gratings oriented along the 67.5 axis (Theta = 155) and responds poorly in the orthogonal direction (SI = 0.51). The bottom row shows the response to a red/green isoluminant grating using the same degree of L and M cone modulation. Although the cell does not respond as well to the color grating, the orientation tuning is preserved (SI = 0.69, Theta = 158 degrees).

Figure 5.7 Direction tuning indices for a population of V_4 cells. The inset gives a description of the circular statistics used to derive the direction index. Most cells do not produce directional responses however a small percentage (15%) are clearly tuned.

Figure 5.8 Velocity tuning of four cells in area V_4. Histograms plot the firing rate of each cell in response to a drifting sinusoidal luminance grating at the velocities listed underneath. For cells that exhibited tuning, low-pass, band-pass and high-pass (to the limits of our system) were seen.

Figure 5.9 Velocity tuning of one cell in V_4 using a luminance and isoluminant color grating. On the left are histograms of the spike activity over the range of velocities tested. On the right are the corresponding raster displays and spike density functions. The solid lines in the spike density functions show when the stimulus achieves full contrast and begins moving and the dotted line signifies the offset of the stimulus. The top row shows the responses to an L and M cone inphase-modulated grating. The cell responds well when the stimulus is ramped on and is stationary. This response is constant for each of the stimulus conditions. At high velocities in the luminance condition, the cell responds better to the moving grating whereas in the color condition the cell responds worse than the initial burst. To some extent the cell shows differences in velocity tuning.

Figure 5.10 Three V_4 cells that exhibit band-pass tuning for luminance contrast. Displayed are histograms of spike activity, raster displays and spike density functions as a function of luminance contrast. The first two cells (5.10a, 5.10b) respond optimally to the 4.75% luminance contrast and all three fire poorly to the gratings of the highest luminance contrast.

Figure 5.11 Tuning curves for the cell displayed in figure 5.10a. Although the cell does show band-pass tuning to luminance contrast (top row, middle), it behaves like other V_4 cells in other respects. The cells increases in firing rate as color contrast is increased (top row). In addition, has comparable tunings for velocity and orientation for both luminance and isoluminant color conditions.

Figure 5.12 Histogram activity of a V_4 cell using luminance- and motion-defined stimuli. Spike activity is plotted as a function of orientation. Orientation is tested in 45 degree intervals. The cell is tuned to luminance gratings oriented along the 45 degree axis. This cell does not respond to the motion contrast stimulus.

Figure 5.13 Orientation tuning of the cell described in figure 5.11. Spike activity is again plotted as a function of orientation. Orientations indices are given for the luminance (SI_L) and the isoluminant color (SI_M) gratings as well as the preferred orientations, given in parentheses.

Figure 5.14 Histogram activity of another V_4 cell using luminance- and motion-defined stimuli. This cell responds to both the luminance contrast and motion contrast.

Figure 5.15 Orientation tuning of the cell described in figure 5.12. The orientation of this cell is similar for both conditions $SI_L = 0.28$, $SI_M = 0.22$; $theta_L = 93.6$, $theta_M = 103.3$).

Figure 5.16 Histogram activity of a cell similar to figures 5.11 and 5.13. This cell was also tested using a grating in which color (100% r/g modulation) was added to the luminance contrast. The cell responded much better to the luminance plus color contrast condition, but still fired to both the luminance only and motion contrast gratings also.

Figure 5.17 Orientation tuning for the cell in figure 5.15. With the exception of the cell's response to the luminance plus color grating at 0 degrees, the tuning curves are similar for all three conditions.

Figure 5.18 Orientation selectivity indices measured using the luminance contrast grating (left) and the motion contrast grating. The dark histogram in the motion-defined stimulus condition represents the cells that did not respond to the motion stimulus. Other cells did exhibit orientation tuning to the motion-defined stimulus.

Figure 5.19 Comparison of orientation tunings for different stimulus conditions. Orientation indices (right) and preferred orientations (left) are compared for the luminance contrast and motion contrast stimuli. Since some cells did not respond to the motion-defined stimulus, only cells having a

luminance-defined selectivity index greater than 0.2 were included in the analysis. Cells exhibit better orientation tuning to luminance-defined gratings than the motion-defined gratings (slope = 0.85, R^2 = 0.72). The preferred orientation of the gratings, however, changes little between the two stimulus conditions (slope = 0.97, R^2 = 0.94).

Figure 5.20 Contrast, velocity and orientation tuning curves for a cell in V_4. The top row represents modulations along different axes in color space. The histogram labelled 'C0\90' shows the cell's responses to L cone modulation (left four histograms) and M cone modulation (right four). This cell fires better to M cone modulation, showing the best response to a 16% M cone modulation. The figure labelled 'C45\135' shows the responses to modulation along the 45 degree axis (luminance) and 135 degree axis (red/green isoluminance). Although the cell responds differentially to L and M cones, tunings are similar for the inphase (right four histograms) and antiphase (left four) conditions, peaking at 16% modulation in both cases. The cell is tuned slight better for velocity in the isoluminant color condition (R/G) by virtue of the reduced responses at the higher velocities. Orientation tuning is a little broader for the isoluminant color condition but still well-tuned (SI = 0.48 vs. SI = 0.77). The preferred orientation, however, remains unchanged (Theta = 180 degrees in both cases).

Figure 5.21 Orientation tuning of a V_4 cell using various luminance contrasts and a motion-defined grating. The cell fires best to a 4% luminance contrast grating, similar to the cells seen in figure 5.10. Interestingly, the cell's best tuning is at 100% luminance contrast, suggesting that the inhibitory mechanisms are not present at low contrasts. This cell also responds to the motion-defined grating and exhibits orientation tuning that similar to the high luminance contrast condition.

Trial Description

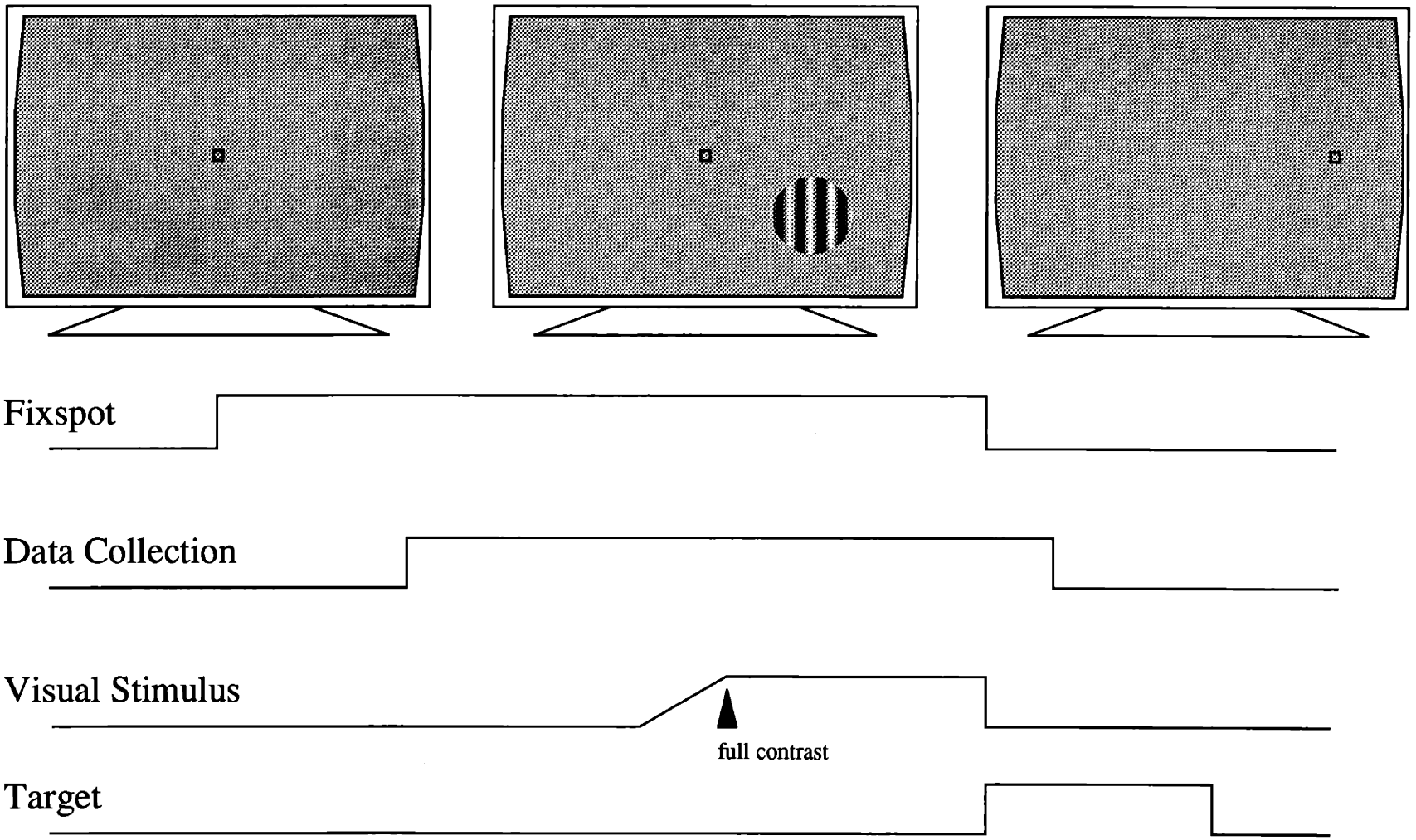

Figure 5.1

Cone Modulation Space

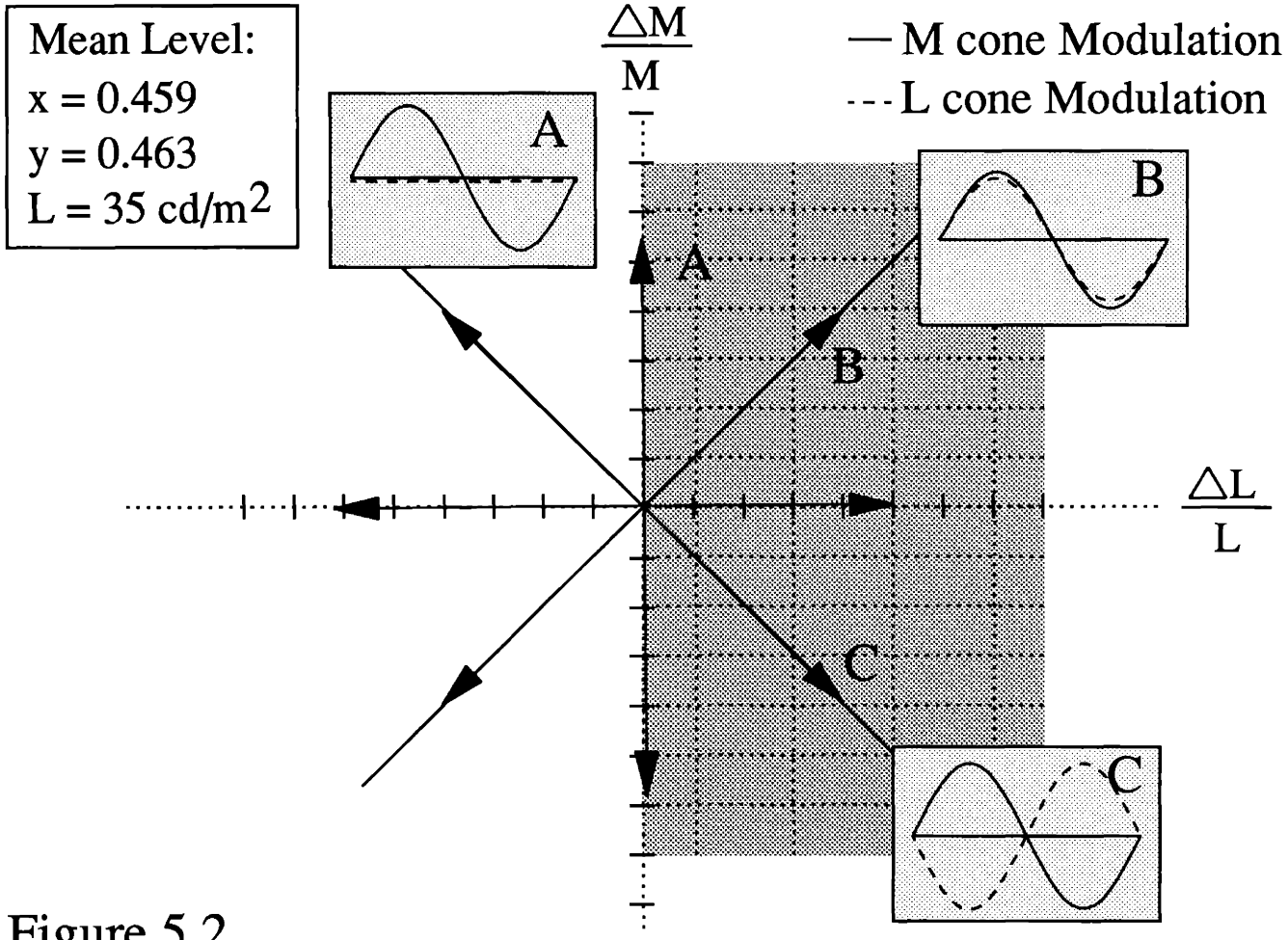

Figure 5.2

Definition of Cell Activity

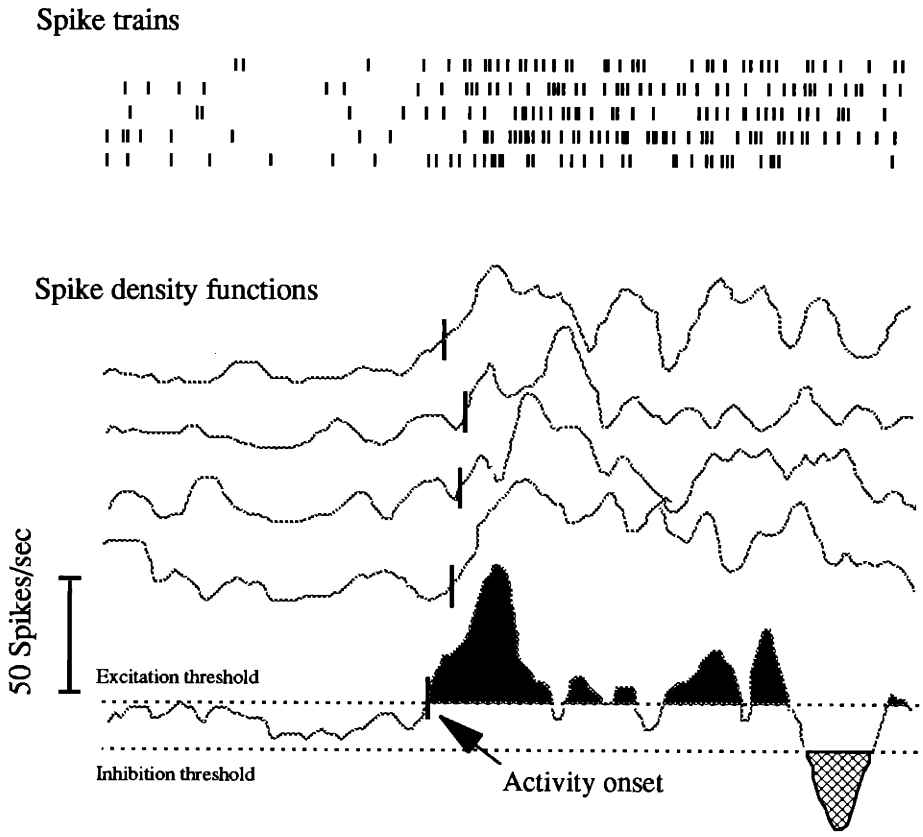

Figure 5.3

V4 Cell Activity: Luminance vs. R\G Isoluminance

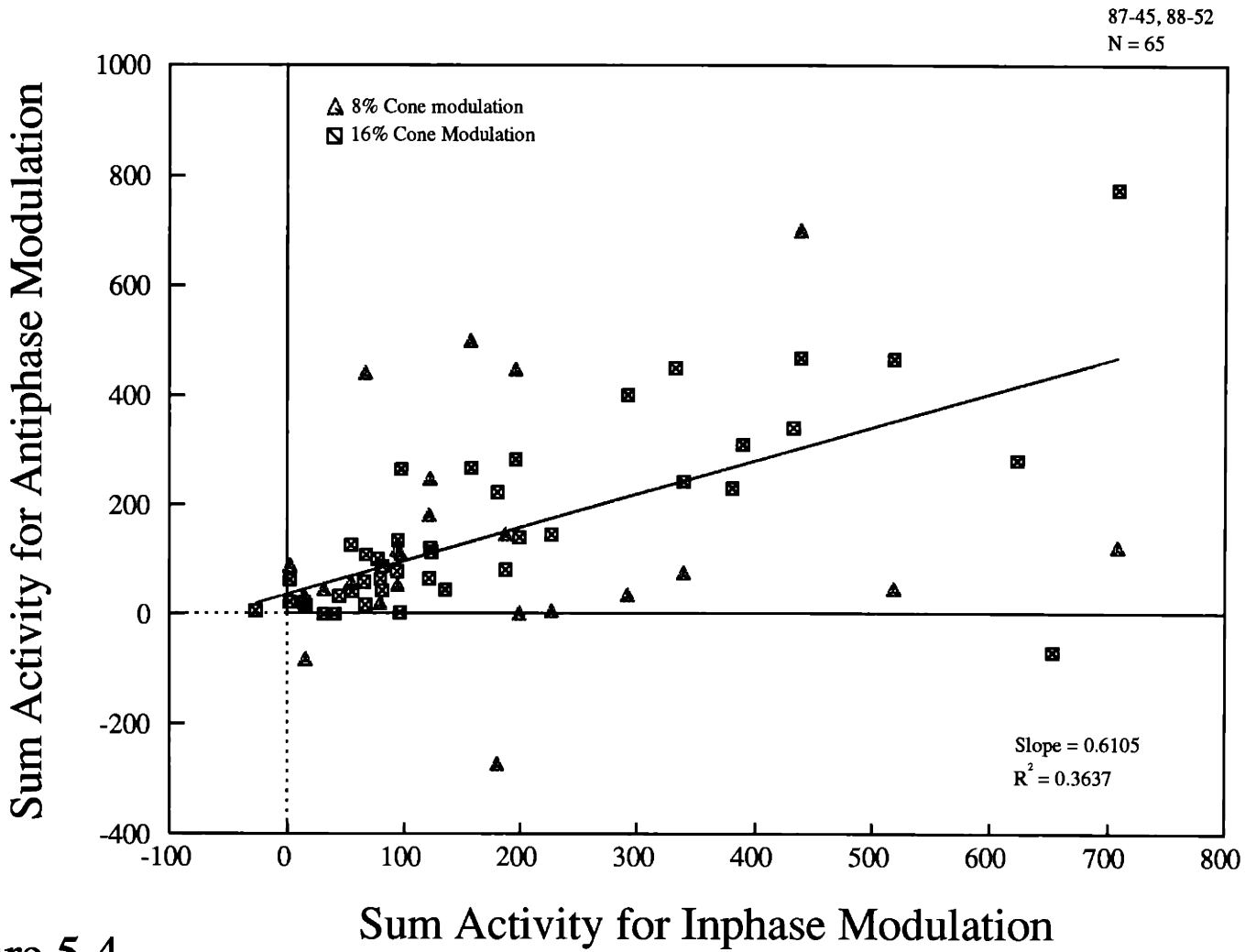

Figure 5.4

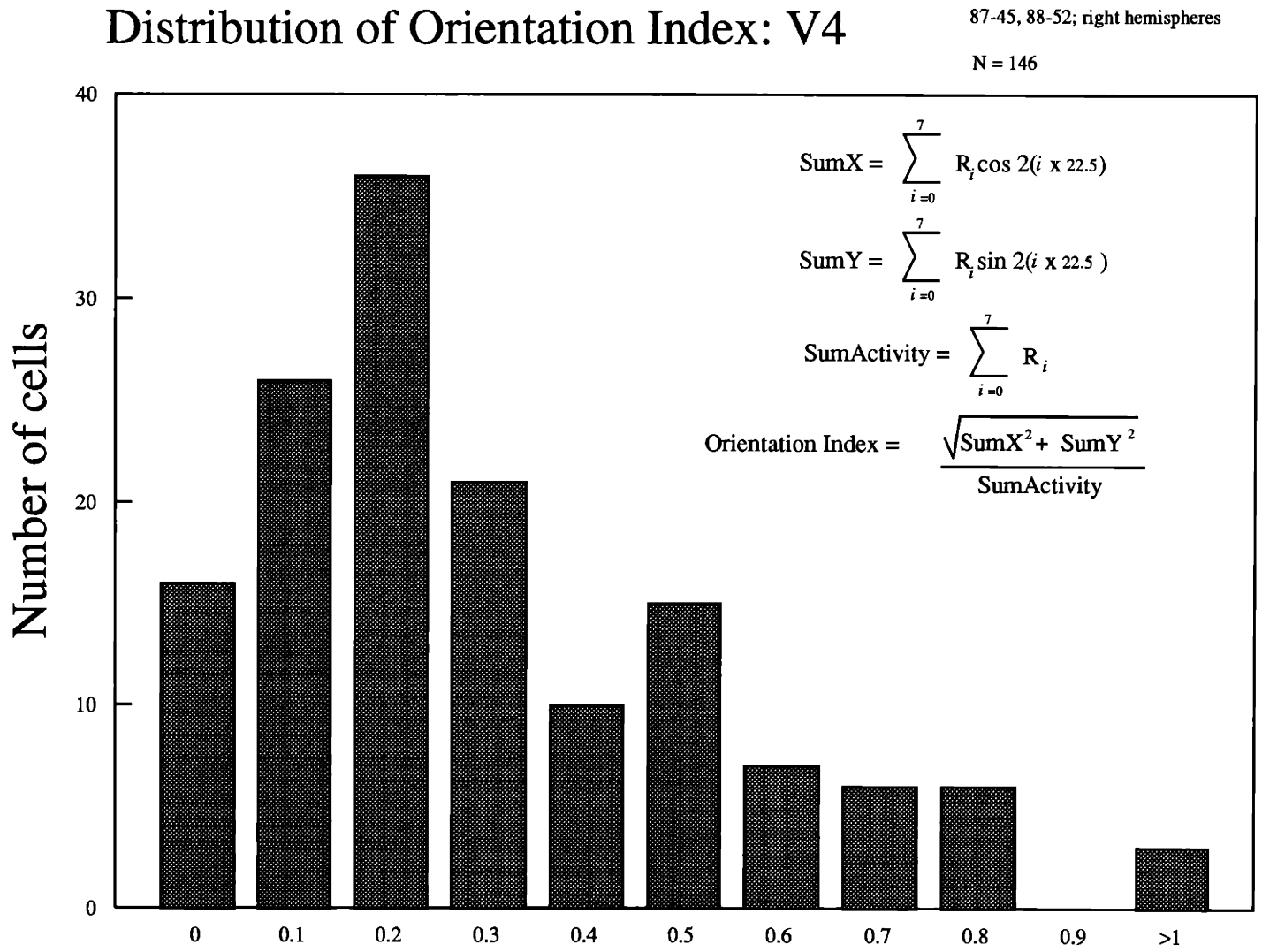
Distribution of Orientation Index: V4
87-45, 88-52; right hemispheres
N = 146
SumX = $\sum_{i=0}^{7} R_i \cos 2(i \times 22.5)$
SumY = $\sum_{i=0}^{7} R_i \sin 2(i \times 22.5)$
SumActivity = $\sum_{i=0}^{7} R_i$
Orientation Index = $\frac{\sqrt{SumX^2 + SumY^2}}{SumActivity}$
Number of cells
40
30
20
10
0
0
0.1
0.2
0.3
0.4
0.5
0.6
0.7
0.8
0.9
>1
Orientation Index

Figure 5.5

Orientation Tuning: V4

Inphase

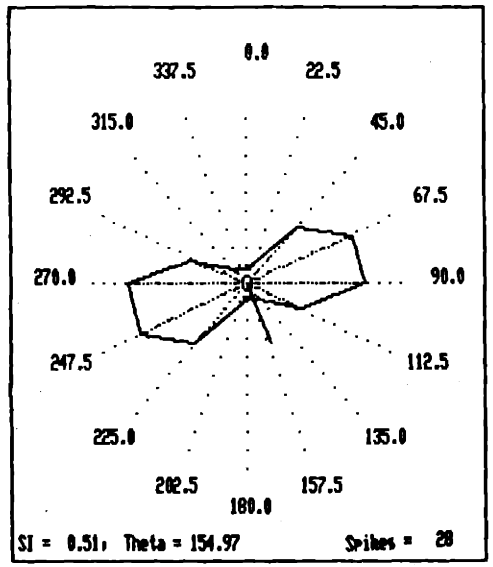

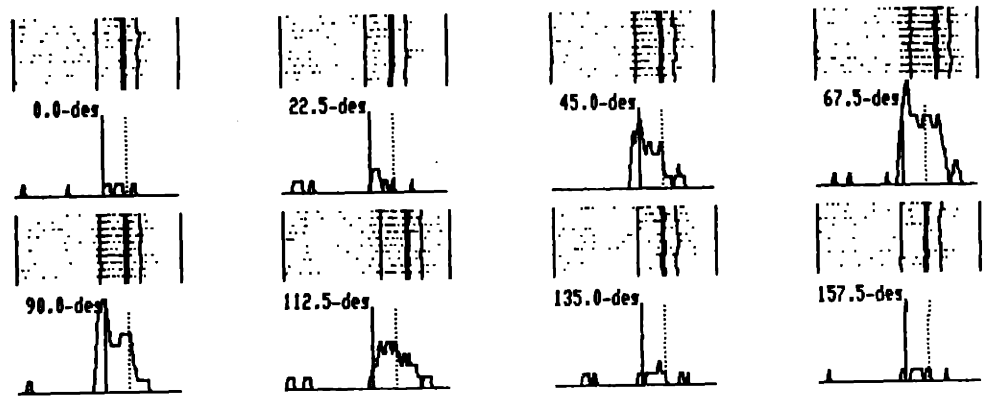

Antiphase

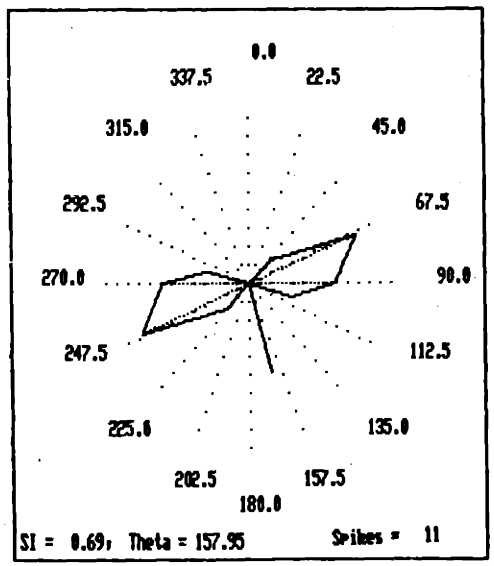

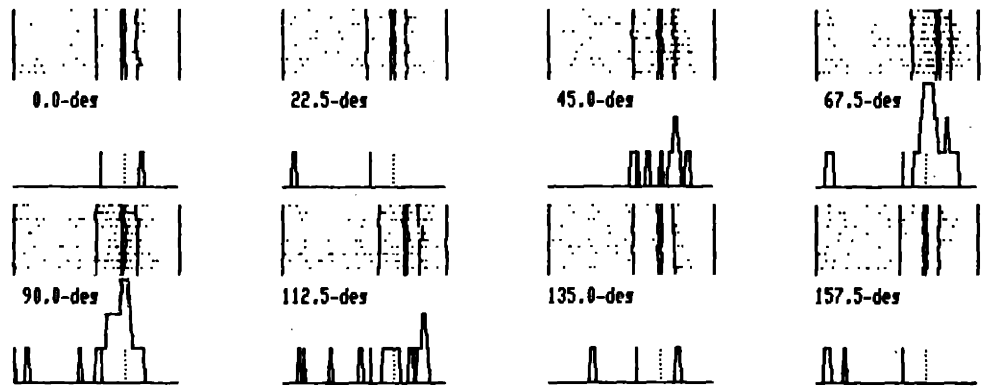

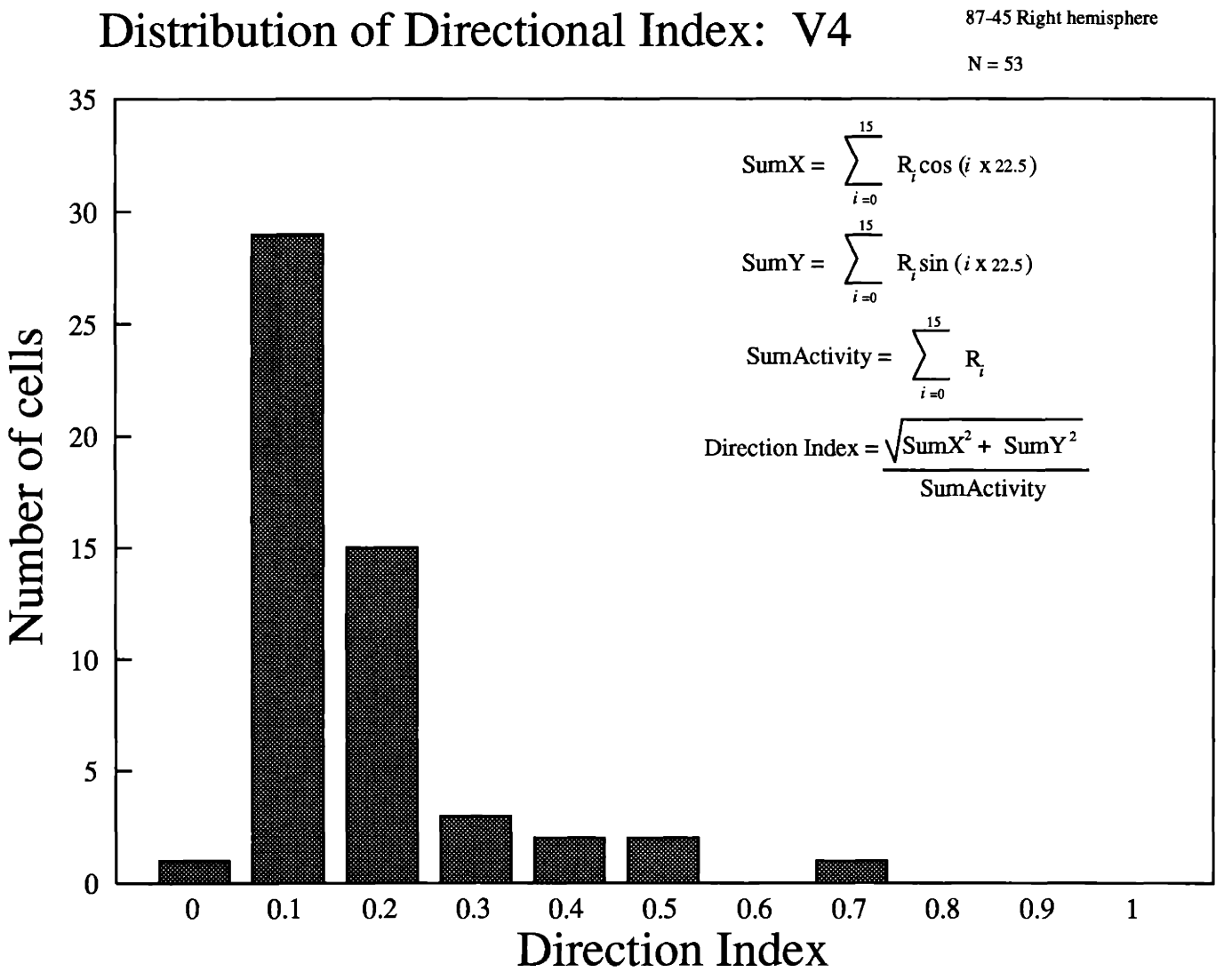
Distribution of Directional Index: V4
87-45 Right hemisphere
N = 53
SumX = $\sum_{i=0}^{15} R_i \cos(i \times 22.5)$
SumY = $\sum_{i=0}^{15} R_i \sin(i \times 22.5)$
SumActivity = $\sum_{i=0}^{15} R_i$
Direction Index = $\frac{\sqrt{SumX^2 + SumY^2}}{SumActivity}$
Number of cells
0
5
10
15
20
25
30
35
0
0.1
0.2
0.3
0.4
0.5
0.6
0.7
0.8
0.9
1
Direction Index

Figure 5.7

Velocity Tuning: V4

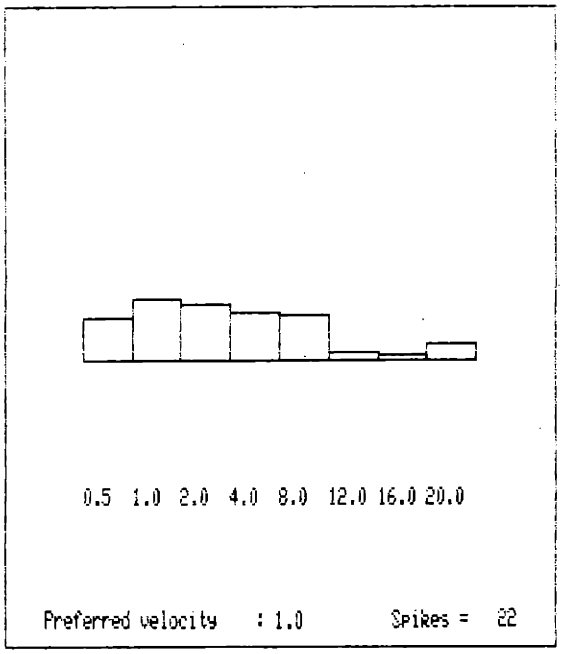

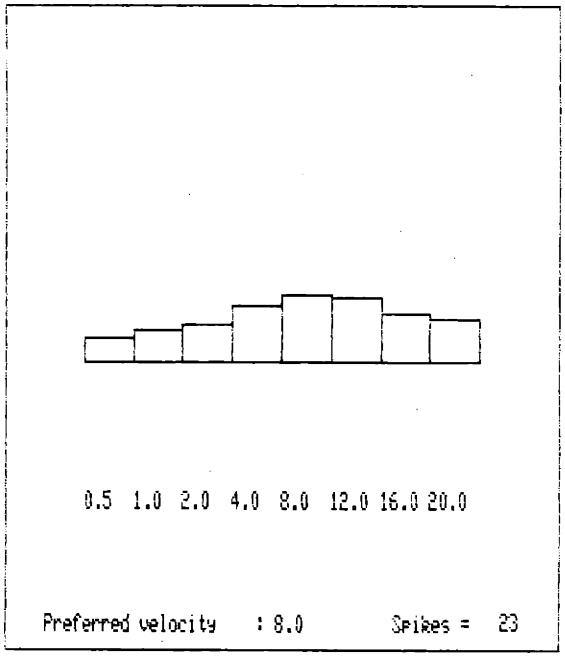

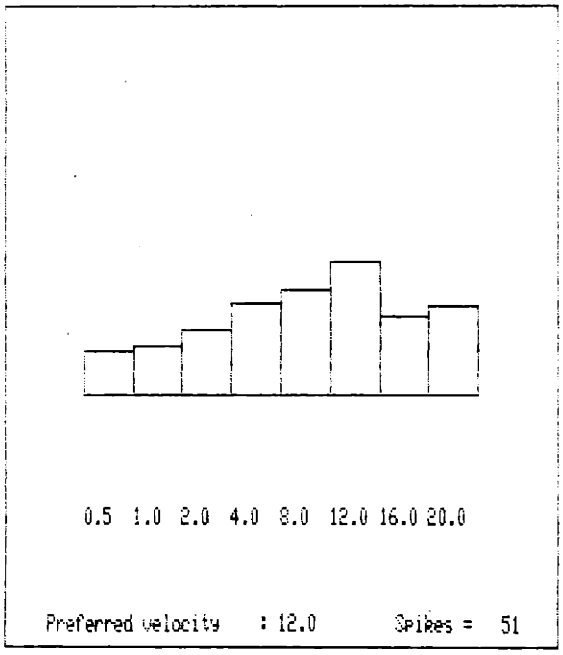

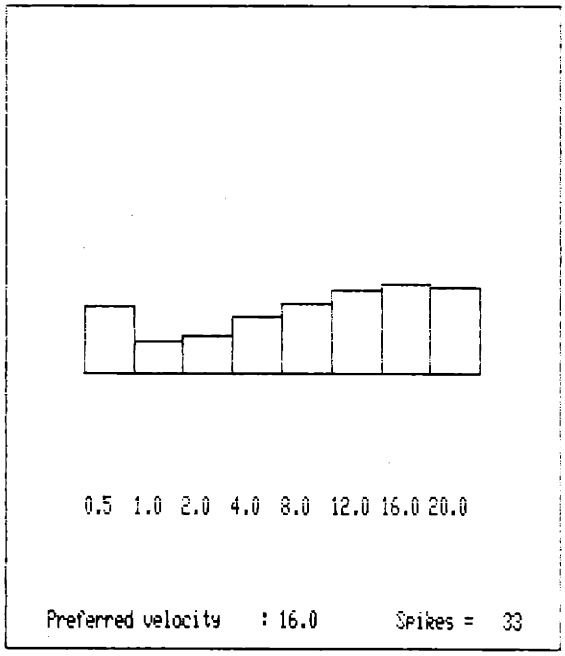

Velocity Tuning: V4

Luminance

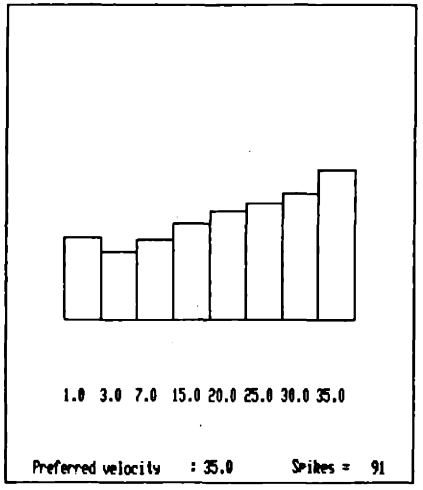

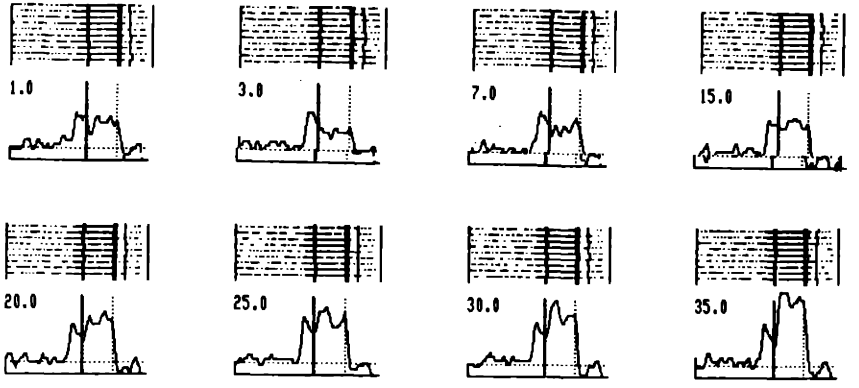

Red\Green

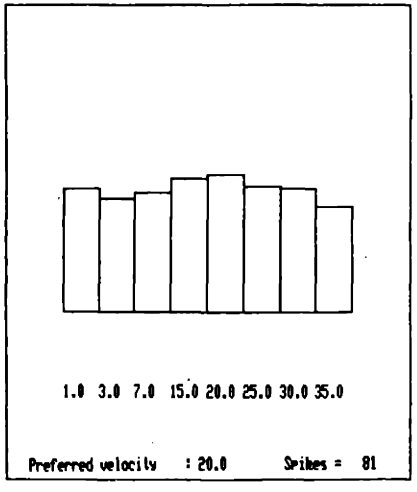

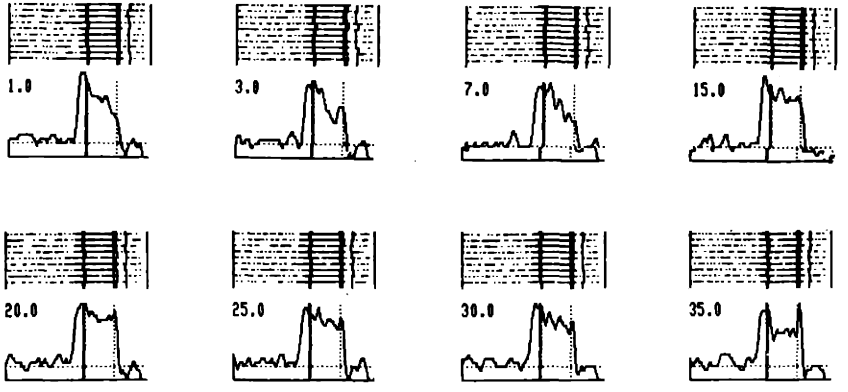

Luminance Contrast Tuning: V4

A.

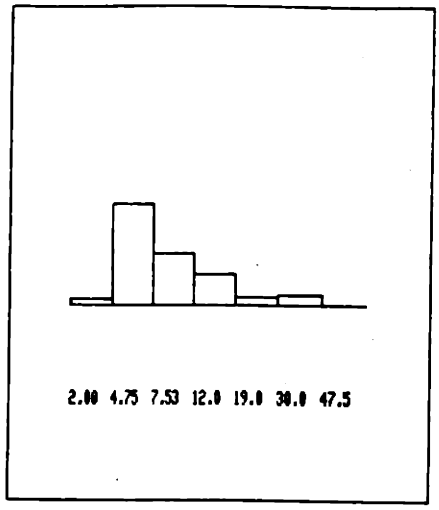

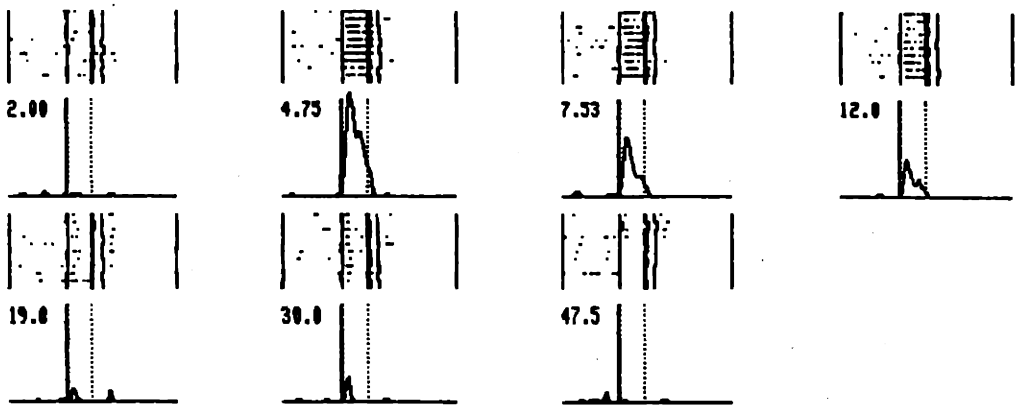

B.

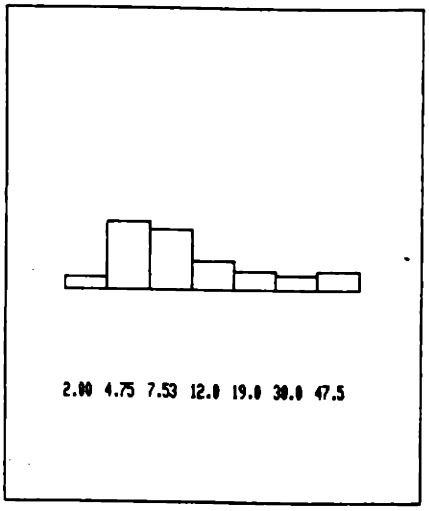

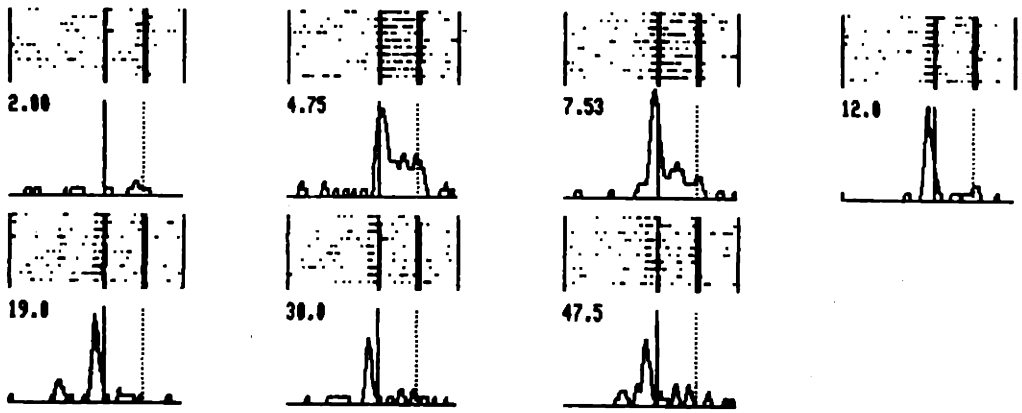

C.

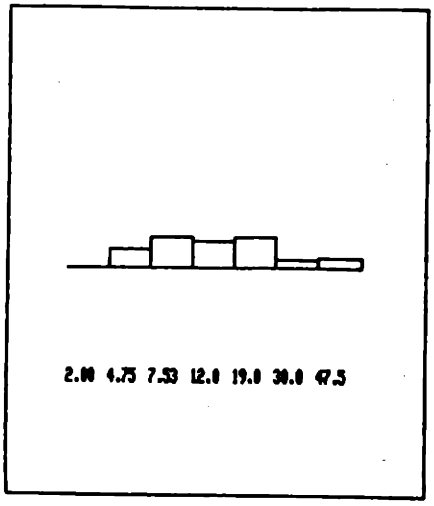

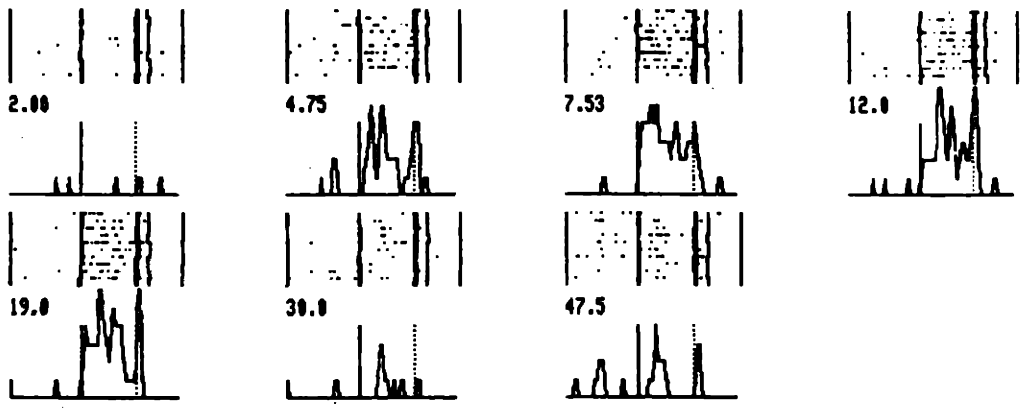

Contrast: B\Y

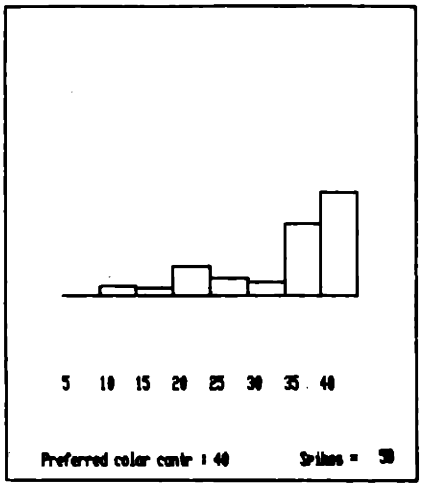

Luminance

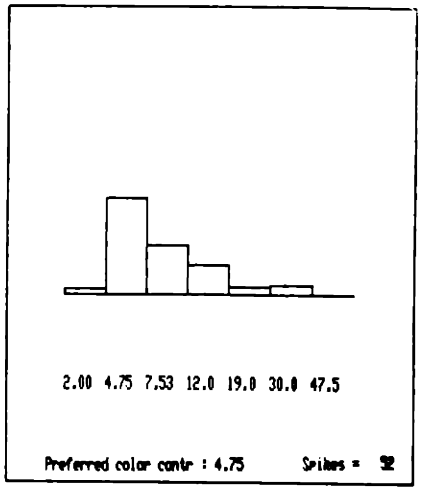

R\G

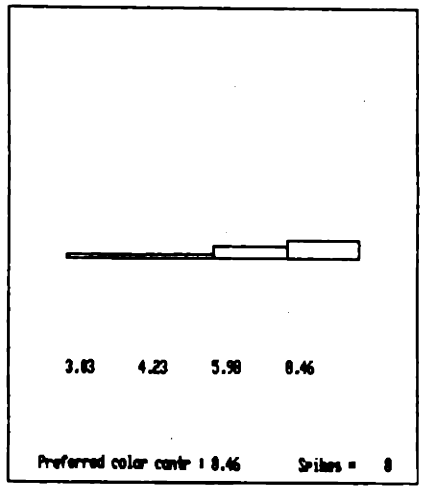

Velocity:

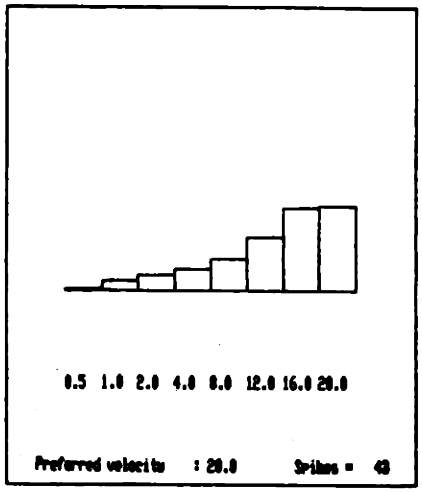

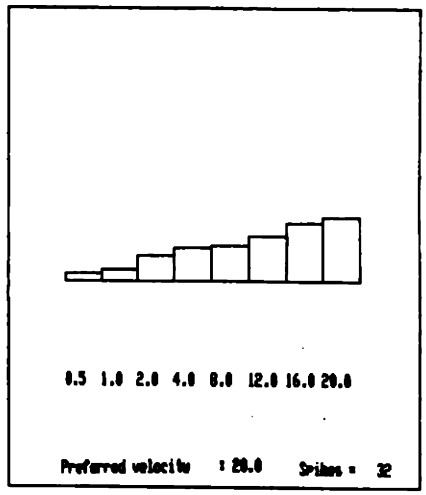

Orientation:

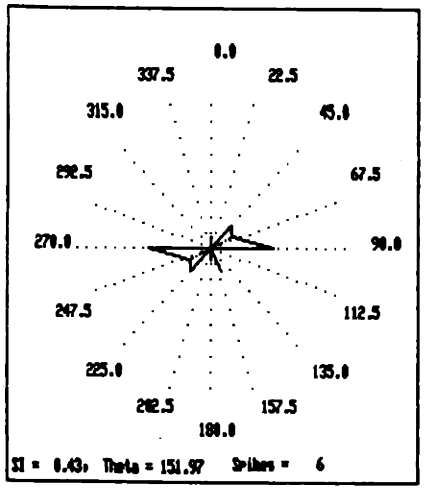

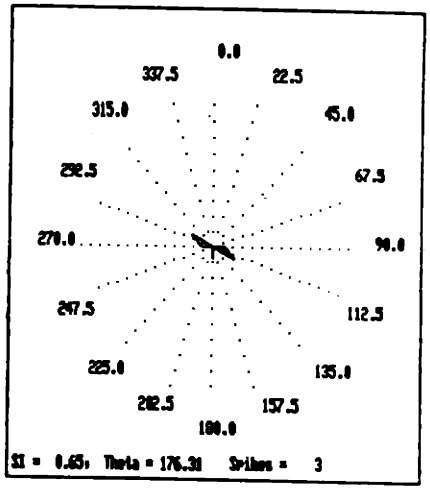

Orientation Tuning: V4

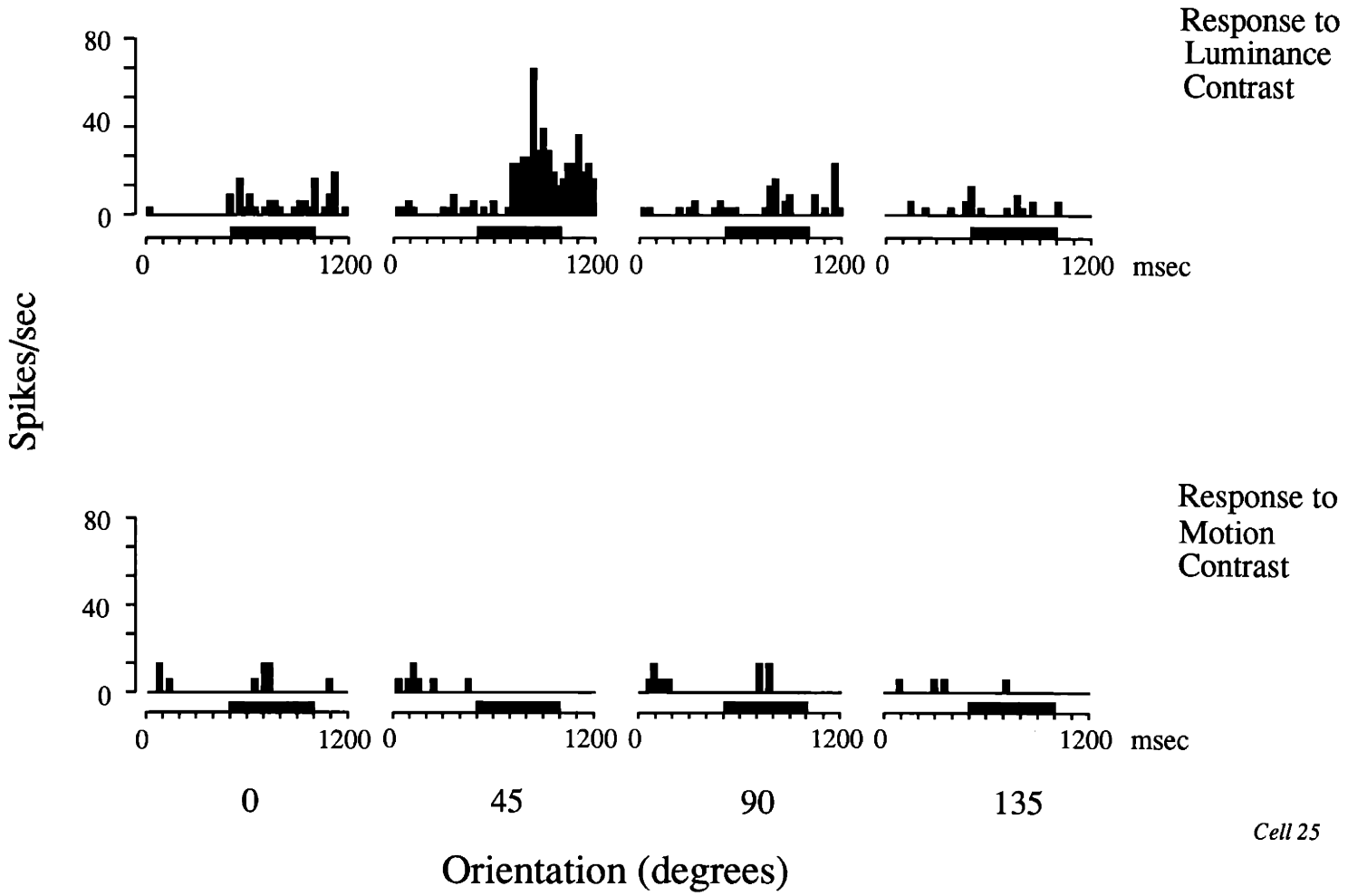

Figure 5.12

Orientation Tuning: V4

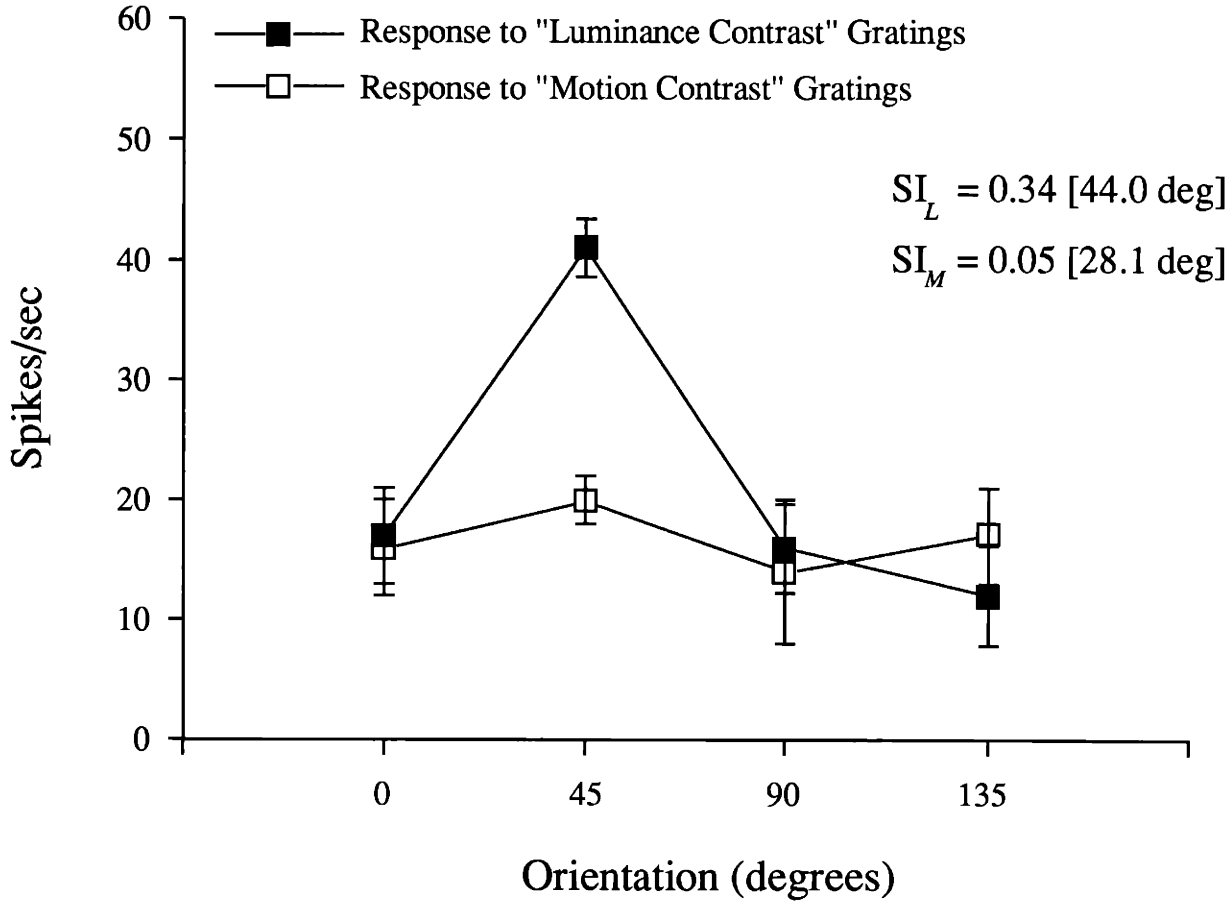

Figure 5.13

Orientation Tuning: V4

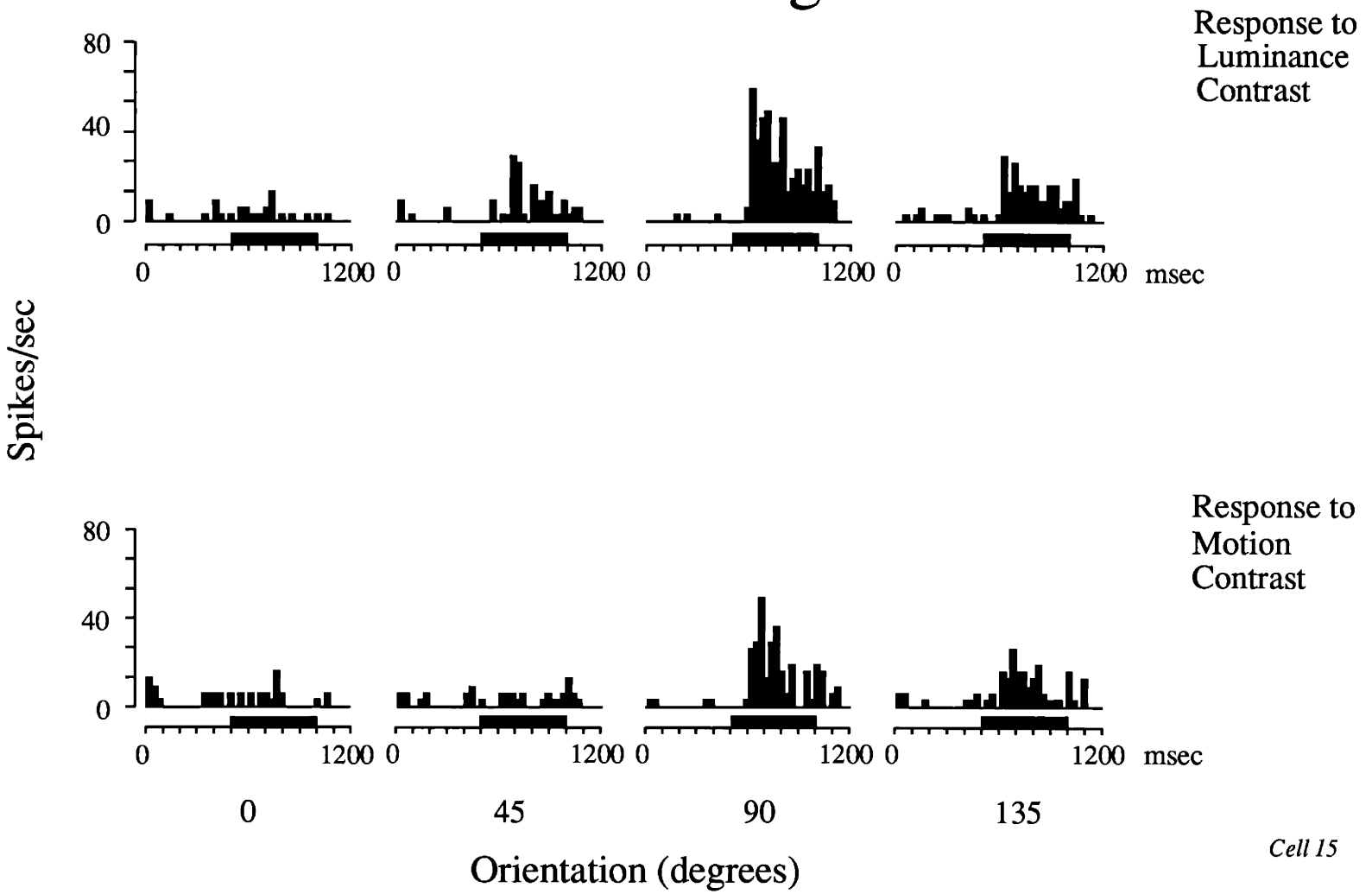

Figure 5.14

Orientation Tuning: V4

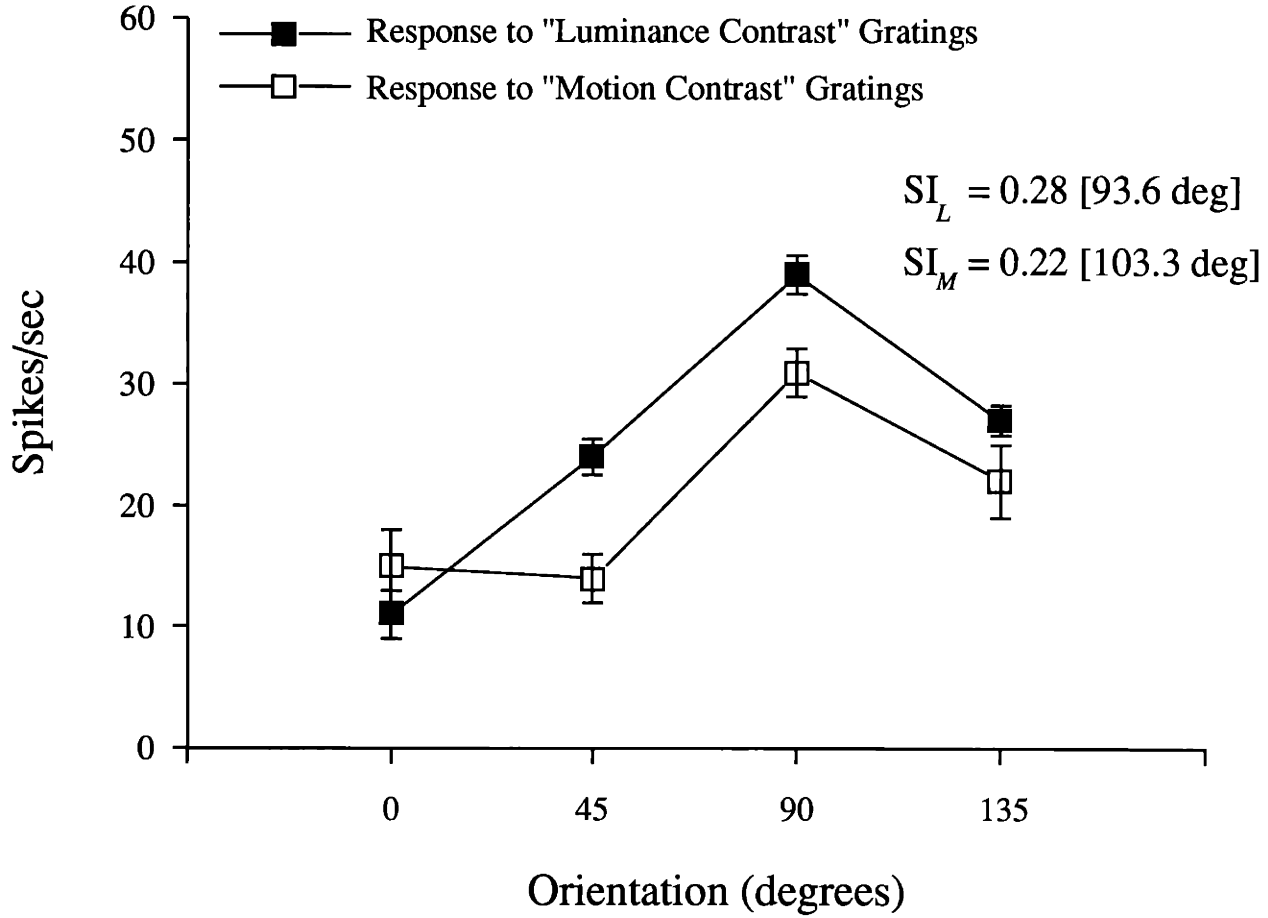

Figure 5.15

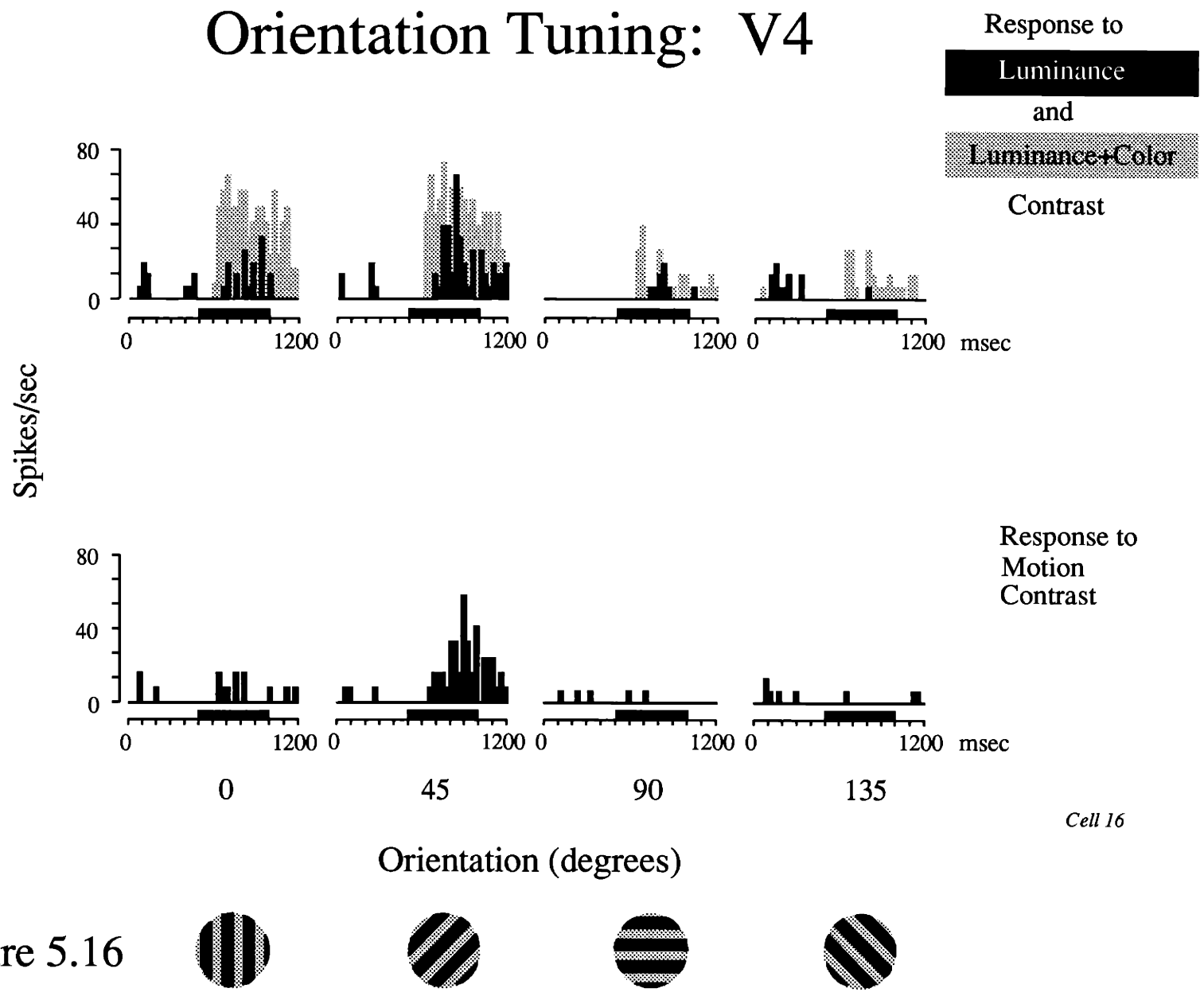
Orientation Tuning: V4
Response to
Luminance
and
Luminance+Color
Contrast
80
40
0
0
1200
msec
Spikes/sec
Response to
Motion
Contrast
0
45
90
135
Cell 16
Orientation (degrees)

Figure 5.16

Orientation Tuning: V4

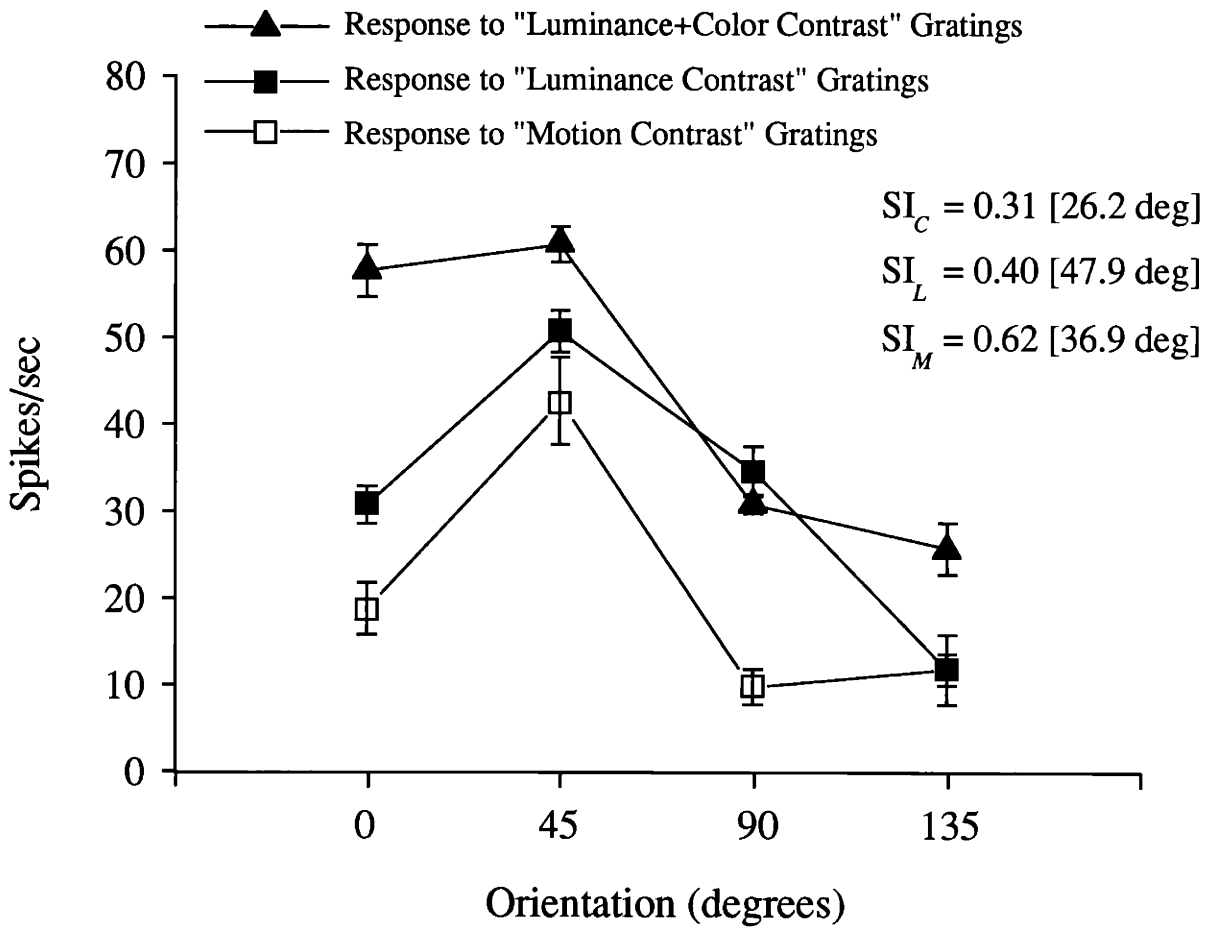

Figure 5.17

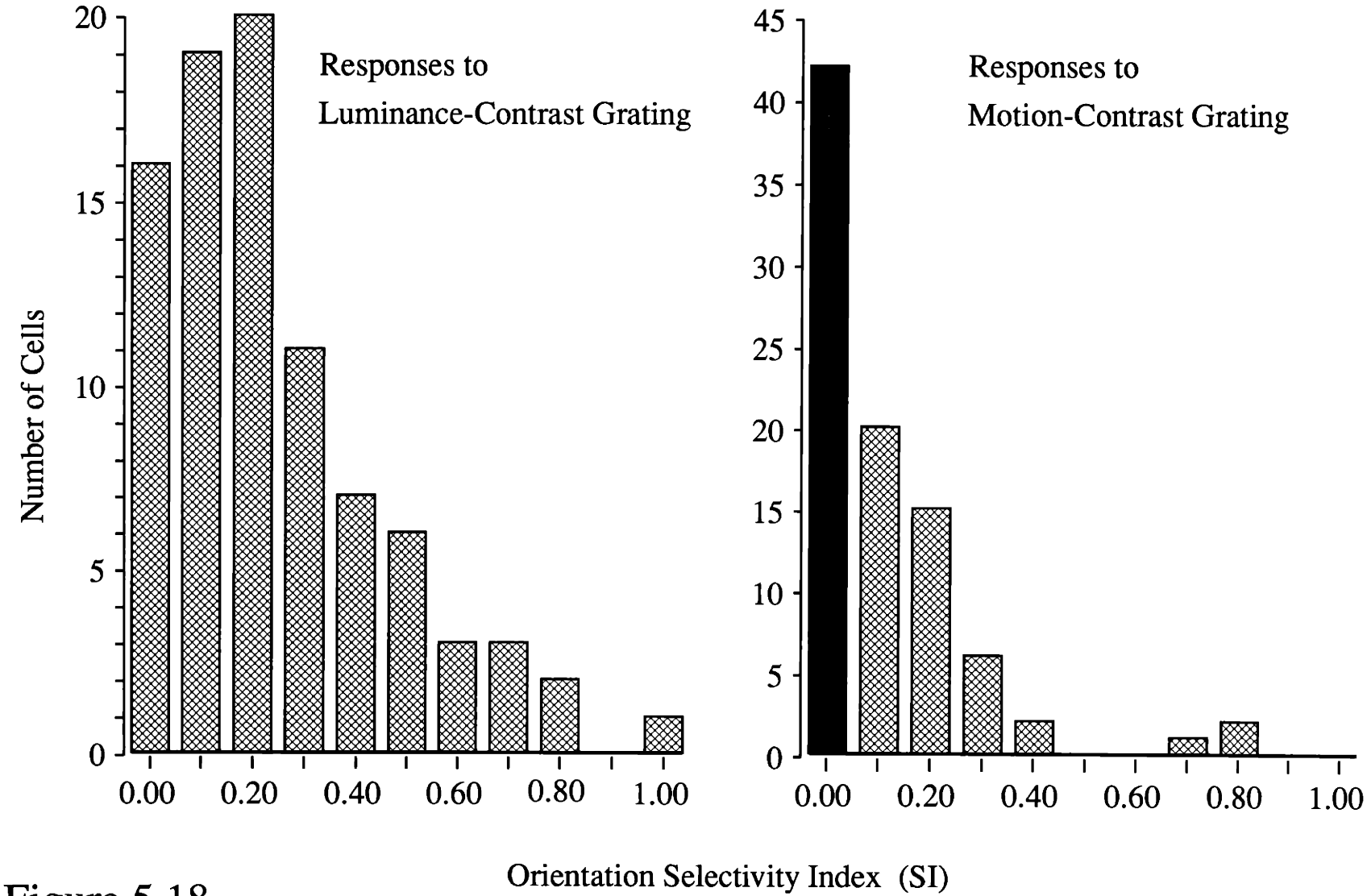
Responses to
Luminance-Contrast Grating
Responses to
Motion-Contrast Grating
Number of Cells
20
15
10
5
0
45
40
35
30
25
20
15
10
5
0
0.00
0.20
0.40
0.60
0.80
1.00
Orientation Selectivity Index (SI)

Figure 5.18

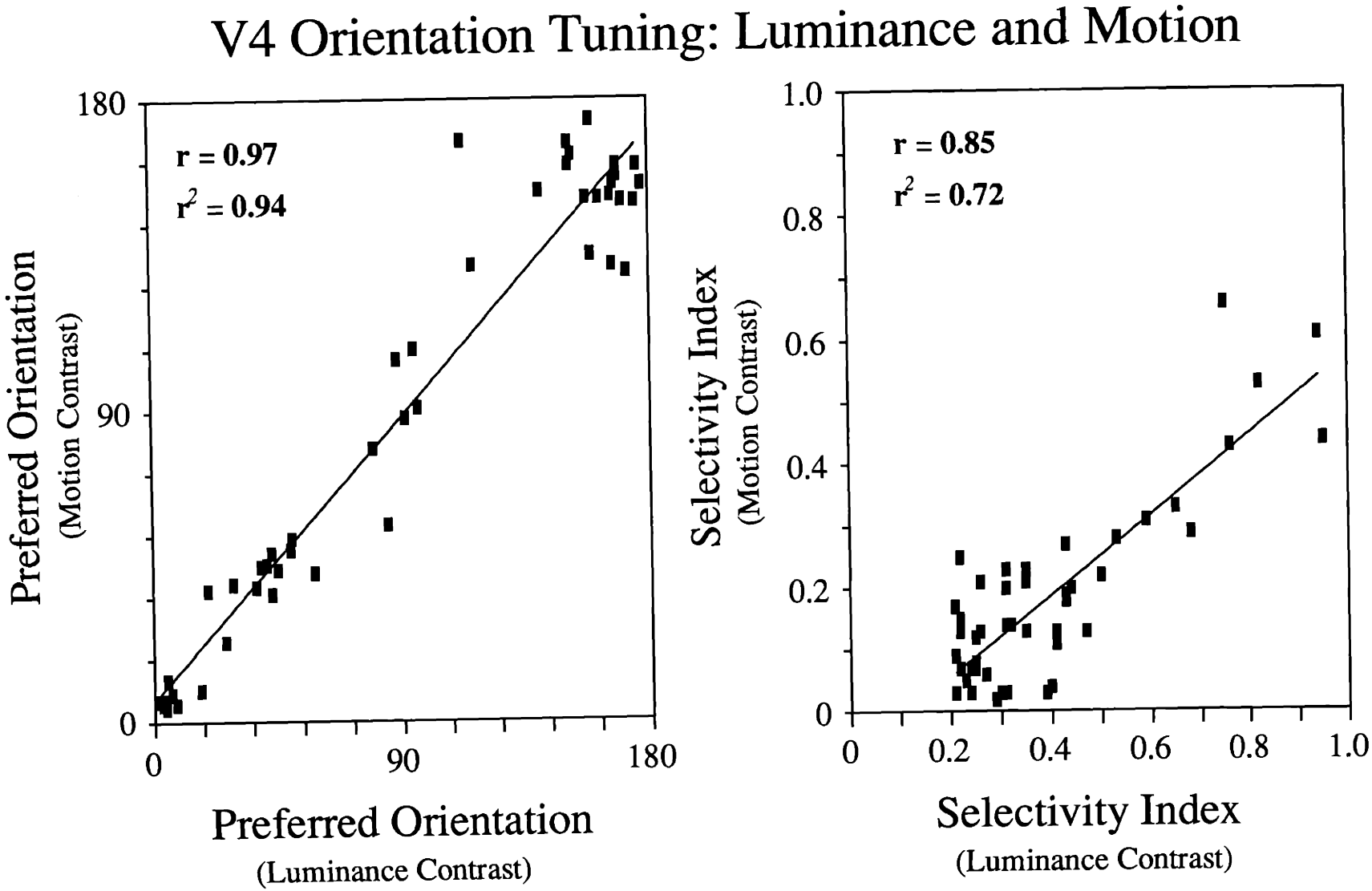
V4 Orientation Tuning: Luminance and Motion
r = 0.97
r² = 0.94
Preferred Orientation
(Motion Contrast)
180
90
0
0
90
180
Preferred Orientation
(Luminance Contrast)
r = 0.85
r² = 0.72
Selectivity Index
(Motion Contrast)
1.0
0.8
0.6
0.4
0.2
0
0
0.2
0.4
0.6
0.8
1.0
Selectivity Index
(Luminance Contrast)

Figure 5.19

Contrast:

C0\90

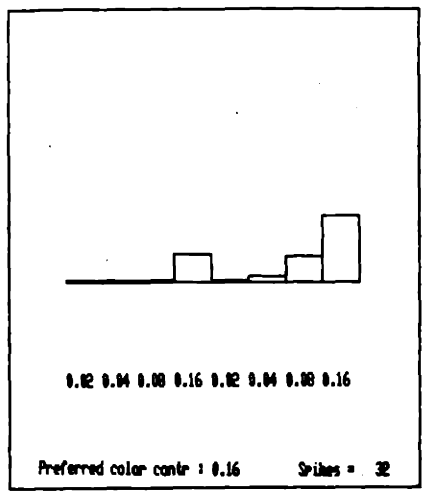

C45\135

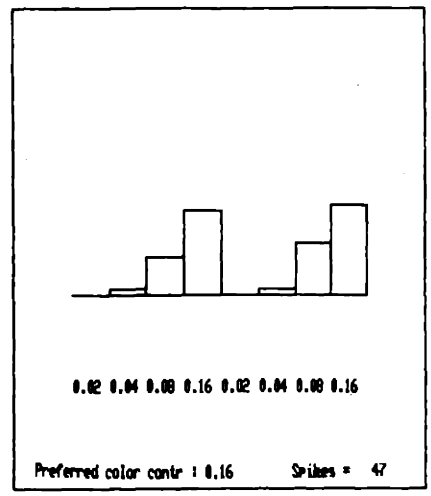

Velocity:

Luminance

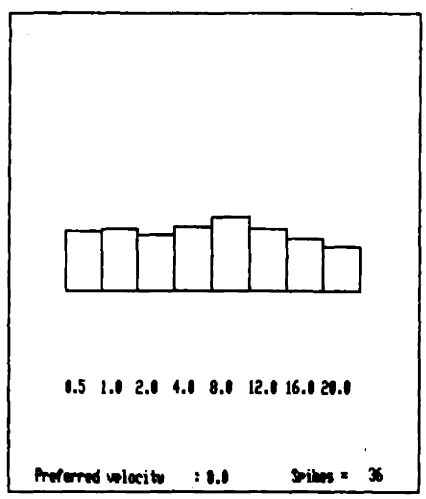

R\G

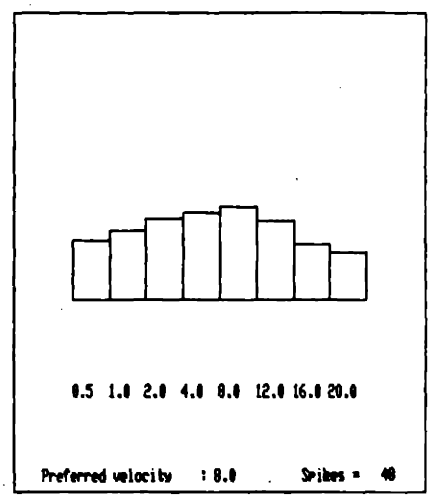

Orientation

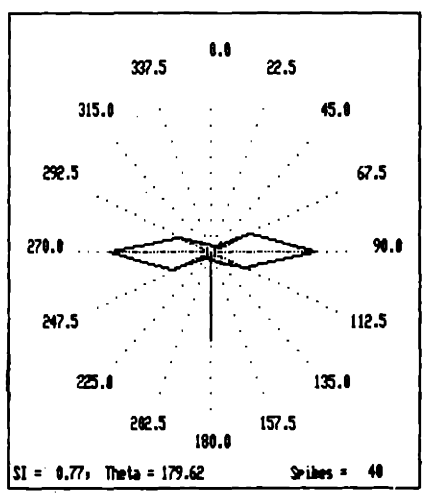

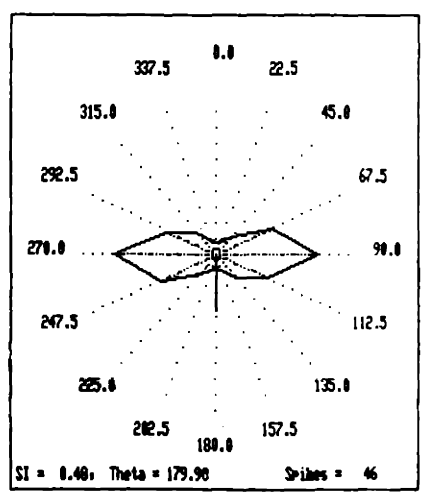

Orientation Tuning: V4

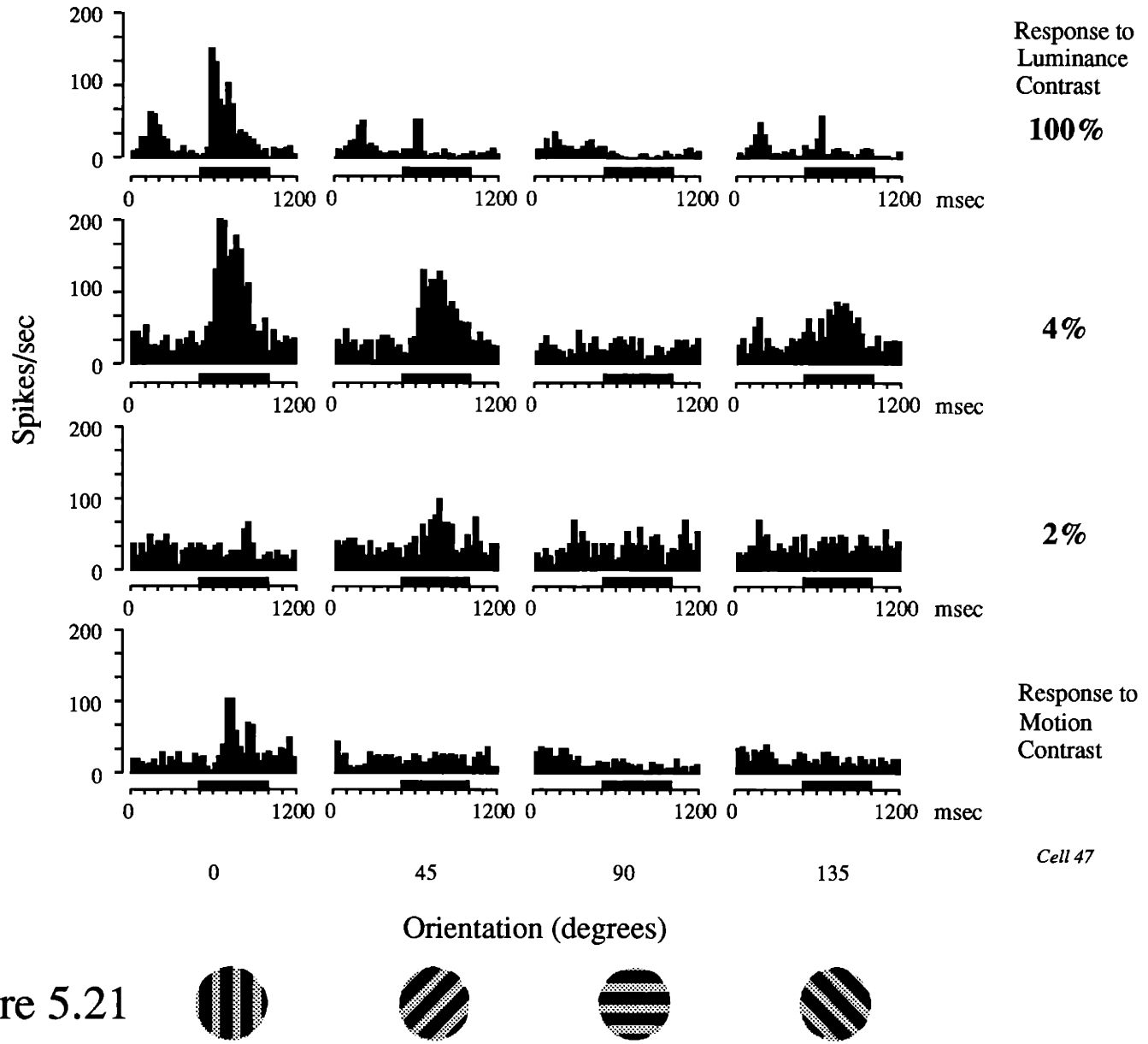

Figure 5.21

CHAPTER SIX

GENERAL DISCUSSION

1.0 Summary of Results

In this dissertation I have provided evidence that information from different perceptual attributes, specifically luminance, motion and color, are integrated early within the visual system. Combining information from fundamentally different attributes offers a more reliable segmentation of the visual scene. In chapter 2, I described the establighment of isoluminance using a variety of psychophysical methods in both rhesus monkeys and humans. The results indicated that color vision is similar between the two species allowing one to draw comparisons between human psychophysics and animal physiology. Two psychophysical measures, heterochromatic flicker photometry and the minimum-motion technique, proved to be accurate and reliable indicators of isoluminance in other tasks such as depth and motion perception. These psychophysical measures have the added advantage that they are simple tasks for the animals and are excellent stimulus configurations for driving cells at the level of the lateral geniculate nucleus and extrastriate cortex. In addition,

a color contribution to motion and stereoscopic depth perception was demonstrated: performance was measured in stereoscopic depth and motion tasks for a fixed set of luminance contrasts. Although the luminance values remained the same, as color information was introduced, the performance of a given task increased. For another task that required matching the velocity of the stimulus, no deficits were seen at isoluminance suggesting that color alone was sufficient to drive the motion signal.

In chapter three I recorded from the two divisions of the LGN in paralyzed, anesthetized monkeys. Both magno- and parvocellular subdivisions were compromised at values near isoluminance. Responses of cells in the magnocellular LGN were reduced in overall activity, but exhibited a frequency-doubled response at isoluminance and were never silenced. Parvocellular LGN cells varied a great deal depending on wavelength selectivity. For cells that were not very selective, the relative red and green luminances of the stimulus could be adjusted to a point where the cell would no longer signal the wavelength exchange. Strongly wavelength-selective cells on the other hand, would always respond to their preferred wavelength irrespective of the luminance differences and could not be nulled. Luminance ratios where cells exhibited either second harmonic responses (mLGN) or nulls (pLGN) varied from cell to cell but were centered on behavioral isoluminance.

I discussed recordings from cells in area MT of the alert rhesus monkey in chapter 4. The luminance and chrominance of the stimuli could be varied while holding the modulation of different cone classes constant producing

gratings of luminance or isoluminant color contrast. When cone modulations were equivalent in the two conditions, the cells responded nearly as well to the isoluminant color gratings. In addition, direction tuning was unaffected by the use of isoluminant color stimuli. For some cells, however, velocity tuning shifted downwards when using isoluminant stimuli.

Using the same stimulus configurations, I also recorded from cells in area V_4. Cells in this extrastriate region were more variable in their responses to the isoluminant color stimuli. Like cells in the pLGN, the response was dependent on the wavelength selectivity of the cell: Cells that preferred red and green wavelengths responded well to the isoluminant stimulus. Cells that preferred short wavelengths or color combinations other than the ones used did not respond well. If cells did respond to the red/green isoluminant gratings, the preferred orientation did not change but there was some variability in the degree of tuning. I also tested cells using a motion-defined grating and found that about half of the cells responded to this stimulus. If the cells exhibited orientation tuning to a luminance grating, they would retain this tuning for the motion contrast stimulus.

2.0 Integration of Attributes

Cavanagh (1989) proposed that visual attributes such as luminance, color, texture, motion and binocular disparity are all coded similarly into size and orientation. A standardized image representation allows the system to combine information from different attributes and increase reliability.

Combining information from different attributes implies that at some level there will be an invariant representation that is not dependent on stimulus attributes. Evidence for this comes from examining tilt aftereffects using combinations of the five visual attributes as both adaptation and test stimuli. Cavanagh finds a significant aftereffect for many of the combinations suggesting both multiple descriptions and integration of these descriptions.

The color contribution to motion and stereoscopic depth discussed in chapter 2 indicates that luminance and chrominance information are combined prior to movement and depth perception. From the psychophysical experiments however, we do not know when this information is combined. At the level of the LGN we know that both magno- and parvocellular LGN respond to luminance as well as isoluminant color stimuli although the magnocellular subdivision is not believed to provide much information about the specific wavelength. Thus, it is unclear if responses at isoluminance seen in the mLGN are responsible for activity in area MT (see chapter 4, section 4.6). Perhaps for reasons of economy, information is segregated, but this is by no means complete, at the next stages of processing. In striate cortex, color, form and motion information appear to be segregated into the blobs, interblobs, and layer 4B. This segregation is continued in V_2 in the thin, pale and thick stripes, respectively (see chapter 1). In the next stages of extrastriate cortex, V_4 and MT, cells respond to stimuli defined by luminance, chrominance and motion (chapters 4 and 5; Albright, 1987). In addition, tuning properties for orientation and direction do not vary between the different stimulus attributes.

This suggests that luminance-, chrominance- and motion-defined stimuli are all contributing to the processing that occurs in V_4 and MT. This work is consistent with a notion of an invariant representation at the level of MT and V_4.

3.0 Using Isoluminance to Dissect the M and P Pathways

The preceding evidence demonstrates that it is inappropriate to use psychophysical experiments at isoluminance to determine the functions of the M and P pathways. The validity of this 'psychophysical dissection' rests on the assumption that the M pathway is silenced because M cells in the retina and LGN show no overt color-opponency (Ramachandran and Gregory, 1978; Livingstone and Hubel, 1988). Clearly, this assumption is erroneous. Physiology at the level of the LGN shows that the cells in the magnocellular layers are responsive at isoluminance. It turns out that activity in both the mLGN and pLGN are affected at isoluminance. If one instead investigates the M and P pathways at a level where function is believed to be more segregated, one still finds the M pathway active. All cells in extrastriate area MT respond very well to isoluminant color stimuli and the data suggest that the activity is used in a meaningful way. On the other hand, an extrastriate area in the P pathway, V_4, is more affected at isoluminance. A range of responses are seen, some cells firing better to an isoluminant stimulus than a luminance one, others not at all.

Another premise of segregated processing is that color information is not

used in motion or stereoscopic depth processing. Psychophysical experiments presented in chapter two show that this too is false. Introduction of color information was shown to improve perception on stereo and motion tasks. In addition, the performance on the motion task measuring the velocity of the slow phase of the optokinetic nystagmus showed no deficit whatsoever at isoluminance. This is not to suggest that deficits do not exist at isoluminance, only that to conclude that color cannot support motion processing by testing one specific set of conditions may be premature. Indeed, even the motion detection task described in chapter 2 (section 2.43) required very specific spatial and temporal conditions to achieve a minimum at isoluminance. In any case, a color contribution to motion has been clearly established (Cavanagh *et al.*, 1984; Dobkins and Albright, 1990; Cavanagh and Anstis, 1991). Further, others have found deficits at isoluminance for tasks believed to be carried by the P pathway (Schiller *et al.*, 1990) indicating that isoluminance experiments may not be suitable for dissecting the two pathways.

Just as the term "motion" encompasses a broad set of percepts related to displacements over time, "isoluminance" is equally ill-defined. In the strict sense, this indicates that the luminance does not vary over space or time. No indication of the degree of color content, if any, is conveyed by this term. Isoluminant stimuli are often poorly characterized and then compared to high contrast luminance stimuli. This comparison then cannot be investigated in any meaningful way (see chapter 4; Cavanagh and Anstis, 1991). The experiments in this dissertation as well as others (Lee *et al.*, 1989) demonstrate

that isoluminant stimuli that modulate L and M cones in antiphase may be the most appropriate for physiological investigations. Thus, it is not surprising that in isoluminant conditions with small degrees of antiphase modulation perception is weak; for example, poor figure/ground segregation with a yellow bicycle on an isoluminant grey background. Expressing the stimuli in terms of cone modulations further allows a direct comparison between luminance- and chrominance-defined stimuli. In fact, if luminance and chromatic stimuli are compared in other relevant terms, multiples of contrast threshold, chromatic mechanisms are more sensitive to motion than luminance mechanisms (Stromeyer *et al.*, 1990).

4.0 Functions of the M and P Pathways

At the outset I stated that the experiments presented here could not determine the roles of these two channels. Given the limitations of single unit recordings, lesion studies may be more appropriate for elucidating the roles of these two channels. The physiological properties of cells in these pathways however, may better suggest what these roles might be. Recent lesion studies of the LGN confirm that the parvocellular layers are essential for hue discrimination (Merigan, 1989; Schiller *et al.*, 1990a; 1990b) and high spatial and low temporal form vision (Schiller *et al.*, 1990a; 1990b; Merigan *et al.*, 1990). The magnocellular layers are involved with motion and high temporal and low spatial form vision (Schiller *et al.*, 1990a, 1990b; Merigan and Maunsell, 1990). Lesion studies in extrastriate cortex (see chapter one for a

review) strongly implicate MT as the primary cortical area specialized in motion processing. Area V_4 appears to be involved in both color and form vision, though recent work brings the central role of V_4 in color vision into question (Schiller and Logothetis, 1990).

The lesion studies cannot exclude the M pathway from participating in color analysis. Physiological recordings mLGN and area MT show that these areas do respond to differences in wavelength although they are not coded for specific wavelengths. While arguments are made that these differences are used for segmentation of the image for motion analysis, this does not suggest that they cannot be used for other purposes as well. There is evidence that edge information is crucial for the computation of color (Land and McCann, 1971; Brou *et al.*, 1986). Both the mLGN and area MT seem to be more reliable in signalling chromatic borders than pLGN and V_4 respectively. In addition, brightness and saturation are fundamental components of color. Responses in both mLGN and MT can be modulated by changes in brightness and saturation. Further experiments are necessary to determine if the M pathway participates in color vision.

As mentioned previously, lesion studies implicate MT as an area central to motion analysis. Few studies of V_4 test for deficits in motion perception though. Chapter 5 demonstrates that there are velocity and direction tuned cells in V_4, whose existence in MT provided the initial arguments for a specialized area for motion processing. Cells in area MT seem to be optimally tuned to relatively high velocities, centered on about 30 deg/sec (Maunsell and

Van Essen, 1983; Mikami *et al.*, 1986) and cells in mLGN are responsible for high temporal frequency flicker. It is possible that lower velocities are represented in the P pathway. Parvocellular LGN cells feed into cells with spatially segregated On and Off subregions which, by this structure, have low pass velocity tuning characteristics (Worgotter and Koch, 1991).

Schiller and Logothetis (1990) argue that the different subdivisions of the LGN cooperatively extend the range of vision in spatial, temporal and wavelength domains. One may speculate that similar interactions are occurring at the level of extrastriate cortex, or as mentioned, these areas are performing different operations that contribute to either motion or color perception and are not tied to specific stimulus attributes.

REFERENCES

Albright, T.D. Isoluminant motion processing in macaque visual area MT. Society of Neuroscience Abstracts 13:1626, 1987.

Brou, P., Sciascia, T.R., Linden, L., and Lettvin, J.Y. The colors of things. Scientific American 225:84-91, 1986.

Cavanagh, P. "Multiple analyses of orientation in the visual system." In: Neural Mechanisms of Visual Perception, eds D.M.K. Lam and C.D. Gilbert. Gulf Publishers, Houston, 1989.

Cavanagh, P. and Anstis, S. The contribution of color to motion in normal and color-deficient observers. Vision Research (in press).

Cavanagh, P., Tyler, C.W. and Favreau, O.E. Perceived velocity of moving chromatic gratings. Journal of the Optical Society of America, A, 1:893-899, 1984.

Dobkins, K.R. and Albright, T.D. What happens if it changes color when it moves? Investigative Ophthalmology and Visual Science Supplement 32:823, 1991.

Land, E.H. and McCann, J.J. Lightness and retinex theory. Journal of the Optical Society of America 61:1-11, 1971.

Lee, B.B., Martin, P.R., and Valberg, A. Nonlinear summation of M- and L-cone inputs to phasic retinal ganglion cells of the macaque. Journal of Neuroscience 9:1433-1442, 1989.

Livingstone, M.S. and Hubel, D.H. Psychophysical evidence for separate channels for the perception of form, color, movement, and depth. Journal of Neuroscience 7:3416-3468, 1987.

Merigan, W.H. Chromatic and achromatic vision of macaques: Role of the P Pathway. Journal of Neuroscience 9:776-783, 1989.

Merigan, W.H., Katz, L.M. and Maunsell, J.H.R. The effects of parvocellular lateral geniculate lesions on the acuity and contrast sensitivity of macaque monkeys. Journal of Neuroscience 11:994-1001, 1991.

Merigan, W.H. and Maunsell, J.H.R. Macaque vision after magnocellular lateral geniculate lesions. Visual Neuroscience 5:347-352, 1990.

Ramachandran, V. and Gregory, R. Does colour provide an input to human motion perception? Nature, 275:55-56, 1978.

Schiller, P.H. and Logothetis, N.K. The color-opponent and broad-band channels of the primate visual system. Trends in Neuroscience 13:392-398, 1990.

Schiller, P.H., Logothetis, N.K. and Charles, E.R. Functions of the colour-opponent and broad-band channels of the visual system. Nature 343:68-70, 1990a.

Schiller, P.H., Logothetis, N.K. and Charles, E.R. Role of the color-opponent and broad-band channels in vision. Visual Neuroscience 5:321-346, 1990b.

Stromeyer III, C.F., Eskew, Jr., R.T., and Kronauer, R.E. The most sensitive motion detectors in humans are spectrally-opponent. Investigative Ophthalmology and Visual Sciences Supplement 31:240, 1990.